https://doi.org/10.15388/vu.thesis.425
https://orcid.org/0000-0002-1518-5891

VILNIUS UNIVERSITY

Gitana Mickienė

Generation, purification and characterization of homo- and heterodimers of granulocyte colony-stimulating factor (G-CSF) and stem cell factor (SCF)

DOCTORAL DISSERTATION

Technological Sciences,
Chemical Engineering (T 005)

VILNIUS 2022

The work presented in this doctoral dissertation has been carried out at the Institute of Biotechnology, Life Sciences Center, Vilnius University and UAB Profarma in 2012–2019. The research was partially supported by the Lithuanian Science and Studies Foundation (Grant No. N-07006).

The dissertation is defended on an external basis.

Scientific supervisor:
Dr. Milda Plečkaitytė (Vilnius University, Technological Sciences, Chemical Engineering – T 005).

This doctoral dissertation will be defended in a public meeting of the Dissertation Defence Panel:

Chairman – Prof. Dr. Rolandas Meškys (Vilnius University, Technological Sciences, Chemical Engineering – T 005).
Members:
Dr. Alma Gedvilaitė (Vilnius University Technological Sciences, Chemical Engineering – T 005),
Dr. Saulius Kulakauskas (Micalis University, France, Natural Sciences, Biochemistry – N 004, Biology – N 010),
Prof. Habil. Dr. Audrius Maruška (Vytautas Magnus University, Natural Sciences, Chemistry – N 003),
Prof. Dr. Rimantas Daugelavičius (Vytautas Magnus University, Natural Sciences, Biochemistry – N 004, Biology – N 010).

The dissertation shall be defended at a public meeting of the Dissertation Defence Panel at 13:00 on 22th December 2022 in the hall R-401 of Vilnius University Life Sciences Center and/or meeting room.
Address: Saulėtekio al., 7, LT-10257 Vilnius, Lithuania.

The text of this dissertation can be accessed at the libraries of Vilnius University, as well as on the website of Vilnius University:
www.vu.lt/lt/naujienos/ivykiu-kalendorius

https://doi.org/10.15388/vu.thesis.425
https://orcid.org/0000-0002-1518-5891

VILNIAUS UNIVERSITETAS

Gitana Mickienė

Granuliocitų kolonijas stimuliuojančio veiksnio (G-CSF) ir kamieninių ląstelių veiksnio (SCF) homo- ir heterodimerų sukūrimas, gryninimas ir charakterizavimas

DAKTARO DISERTACIJA

Technologijos mokslų kryptis,
Chemijos inžinerija (T 005)

VILNIUS 2022

Disertacija rengta 2012–2019 m. Vilniaus universiteto Gyvybės mokslų centro Biotechnologijos institute ir UAB Profarma. Šis darbas iš dalies buvo finansuotas Lietuvos valstybinio mokslo ir studijų fondo (sutarties Nr. N-07006) lėšomis.

Disertacija ginama eksternu.

Mokslinė konsultantė:
Dr. Milda Plečkaitytė (Vilniaus universitetas, technologijos mokslai, chemijos inžinerija – T 005).

Gynimo taryba:
Pirmininkas – prof. dr. Rolandas Meškys (Vilniaus universitetas, technologijos mokslai, chemijos inžinerija – T 005).
Nariai:
Dr. Alma Gedvilaitė (Vilniaus universitetas, technologijos mokslai, chemijos inžinerija – T 005),
Dr. Saulius Kulakauskas (Micalis institutas, Prancūzija, gamtos mokslai, biologija – N 010),
Prof. habil. dr. Audrius Maruška (Vytauto Didžiojo universitetas, gamtos mokslai, chemija – N 003),
Prof. dr. Rimantas Daugelavičius (Vytauto Didžiojo universitetas, technologijos mokslai, chemijos inžinerija – T 005).

Disertacija ginama viešame Gynimo tarybos posėdyje 2022 m. gruodžio mėn. 22 d. 13:00 val. Vilniaus universiteto Gyvybės mokslų centre R-401 auditorijoje ir/arba nuotoliniu būdu.
Adresas: Saulėtekio al. 7, LT-10257 Vilnius, Lietuva.

Disertaciją galima peržiūrėti Vilniaus universiteto bibliotekose ir VU interneto svetainėje adresu:
https://www.vu.lt/naujienos/ivykiu-kalendorius

LIST OF ABBREVIATIONS

11-MUA	11-mercaptoundecanoic acid
AD	Alzheimer's disease
aFGF	Acidic fibroblast growth factor
AIDS	Acquired immune deficiency syndrome
ANC	Absolute neutrophil count
BFGH	Basic fibroblast growth factor
BMP	Bone morphogenetic proteins
CD	Cluster of differentiation
CHO	Chinese hamster ovary cells
c-KIT	SCF receptor
CLP	Common lymphoid progenitor
CMP	Common myeloid progenitor
CNTF	Ciliary neurotrophic factor
COVID-19	Coronavirus disease 2019
CRH	Cytokine receptor homologous
CSF-1	Colony stimulating factor-1
CSF3	Colony stimulating factor 3
CTAP	Connective tissue activating peptide
CTCL	Cutaneous T-cell lymphoma
CTP	Carboxyterminal peptide
DOT	Dissolved oxygen tension
DPPC	Dipalmitoyl phophatidylcholine
DTT	1,4-dithiothreitol
E. coli	*Escherichia coli*
ECGF	Endothelial cell growth factor
EDC	N-(3-dimethylaminopropyl)-N'-ethyl-carbodiimide hydrochloride
ELISA	Enzyme linked immunosorbent assay
ELISPOT	Enzyme linked immuno spot
EMA	European Medicines Agency
EPO	Erythropoietin
ERK	Extracellular signal–regulated kinase
EU	European Union
FA	Formic acid
FAsL	Fas ligand

Fc	Fragment crystallizable
FDA	Food and Drug Administration
FF	Fast flow
FL	Flt ligand
GCP-2	Granulocyte chemotactic protein-2
G-CSF	Granulocyte colony-stimulating factor
GCSF-R	Granulocyte colony-stimulating factor receptor
GdnHCl	Guanidine hydrochloride
GH	Growth hormone
GLP	Glucagon like peptide
GM-CSF	Granulocyte-macrophage colony-stimulating factor
GSSG	Oxidized glutathione
HPC	Hematopoietic progenitor cell
HPLC/ESI-MS	High-performance liquid chromatography/electrospray ionization mass spectrometry
HSA	Human serum albumin
HSC	Hematopoietic stem cell
HSPCs	Hematopoietic stem/progenitor cells
HTF	Human transferrin
IBs	Inclusion bodies
IFN	Interferon
IgG	Immunoglobulin G
IgG1	Immunoglobulin G1
Ig-like	Immunoglobulin-like
IL	Interleukin
IPTG	Isopropyl β-D-1-thiogalactopyranoside
LIF	Leukemia inhibitory factor
LPS	Lipopolysaccharide
LT	Lymphotoxin
Lα	Alpha-helix-forming peptide linker
mAbs	Monoclonal antibodies
MAPK	Multiple mitogen-activated protein kinase
MCP	Monocyte chemoattractant
M-CSF	Macrophage colony-stimulating factor
MIG	Monokine induced by interferon γ
MIP	Macrophage inflammatory protein

mSCF	Membrane-bound form of SCF
MTS	Tetrazolium salt solution
NAP-2	Neutrophil activating protein-2
NHS	N-hydroxysuccinimide
OPG	Osteoprotegerin
OSM	Oncostatin M
PB	Peripheral blood
PBPC	Peripheral blood progenitor cells
PCR	Polymerase chain reaction
PDGF	Platelet-derived growth factor
PEG	Polyethylene glycol
PF	Platelet factor
PI3K	Phosphatidyl inositol 3'Kinase
PLGA	Poly(lactic-co-glycolic) acid
PMDA	Pharmaceuticals and Medicals Devices Agency
PMSF	Phenylmethylsulfonyl fluoride
PTSD	Post-traumatic stress disorder
RA	Rheumatoid arthritis
rcSCF	Recombinant canine SCF
RH	Relative humidity
rhG-CSF	Recombinant human G-CSF
rhSCF	Recombinant human SCF
RP-HPLC	Reverse-phase high-performance liquid chromatography
rrSCF	Recombinant rat SCF
RT	Room temperature
RTK	Receptor tyrosine kinase
SAM	Self-assembled monolayer
SCF	Stem cell factor
SCN	Severe congenitial neutropenia
SD	Standard deviation
SDS-PAGE	Sodium dodecyl sulfate-polyacrylamide gel electrophoresis
SEM	Standard error of mean
Sl	Steel
SPR	Surface plasmon resonance
sSCF	Soluble form of SCF

STAT	Signal transducer and activator of transcription
TFA	Trifluoroacetic acid
TGF	Transforming growth factor
TIRE	Total internal reflection ellipsometry
TNF	Tumor necrosis factor
TPO	Thyroperoxidase

CONTENTS

INTRODUCTION

Biopharmaceuticals have become key players in the drug market for the treatment of a variety of diseases. Diabetes, cancer, inflammatory diseases, and hemophilia have already been targeted by biological drugs (Walsh, 2014). Biopharmaceuticals, which are mainly based on polypeptides and proteins, face several drawbacks, such as physicochemical instability, susceptibility to proteolytic degradation, and short circulation times.

Many technologies have been developed to enhance the biopharmaceutical properties of the administered drugs (Metzner et al., 2013; Pasut, 2014; Strohl, 2015; Witteloostuijn et al., 2016). Amino acid replacement targets mainly proteolytic instability and immunogenicity. Half-life extension strategies include chemical modification by the attachment of polyethylene glycol (PEGylation) and carbohydrate polymers (HESylation, polysialylation), glycosylation, and chemical lipidation (Pasut, 2014; Witteloostuijn et al., 2016). Fusion of the target proteins to human serum albumin (e.g. Albiglutide) results in prolonged circulation time due to a large size that prevents renal clearance (Rogers et al., 2015). A decreased susceptibility to intracellular degradation can be achieved by fusion with the fragment crystallizable (Fc) portion of immunoglobulin G (IgG) (Czajkowsky et al., 2012). Novel fusion partners for therapeutic proteins include human transferrin and highly sialylated carboxyterminal peptide (CTP). CTP fusion to erythropoietin (Fares et al., 2007) and follicle-stimulating hormone (Duijkers et al., 2002) results in recombinant proteins with increased half-live.

A cytokine granulocyte colony-stimulating factor (G-CSF) used intensively for treatment of cancer therapy-induced neutropenia and other neutropenic conditions, has found widespread clinical application, and modified forms with improved biopharmaceutical properties have been marketed as well. Besides the first-generation drugs of G-CSF, filgrastim and lenograstim, an improved second-generation therapeutic form, nartograstim and pegfilgrastim, have been used. In nartograstim, the amino acid sequence manipulation results in increased granulopoiesis activity (Maruyama et al., 1998; Okabe et al., 1990; Suzuki et al., 1992). Protein modification of filgrastim by PEGylation gives in a substantially reduced renal clearance that allows for less frequent dosing during administration (Molineux, 2004). However, there are concerns connected to the immunogenicity of PEGylated compounds and bioaccumulation of the synthetic polymer (Baumann et al., 2014). Therefore, to improve the therapeutic properties of G-CSF and to overcome challenges connected with chemical modifications, the development of new G-CSF forms is still ongoing and needed.

The interaction between the G-CSF molecule and its G-CSF receptor (GCSF-R) results in a stoichiometric ratio of 2:2 (Tamada et al., 2006), meaning that binding of two G-CSF molecules is needed for receptor homodimerization and subsequent signal transduction. Therefore, G-CSF dimers acting as protein dimerizer represent a promising option for the design of improved therapeutic forms of G-CSF. To test this hypothesis, several dimeric G-CSFs were created in other studies at the beginning of this research (Hu et al., 2010; Fidler et al., 2011). The F-627 protein, consisting of two molecules of recombinant human G-CSF that are covalently connected through disulfide bridges forged between the Fc fragment of the IgG molecule, generated a faster increase of neutrophils in cyclophosphamide-treated monkeys compared to G-CSF monomer (Hu et al., 2010). However, the other G-CSF dimer constructed by joining two G-CSF molecules via disulfide bridges between non-paired cysteines had the lower biological activity and the same circulation half-life as the G-CSF monomer (Fidler et al., 2011).

Many studies confirmed that linkers are an indispensable tool in recombinant fusion protein technology, because their type, length, and flexibility can have a crucial effect on the physical and biological characteristics of fusion proteins. Linkers can offer some advantages such as improved biological activity, improved pharmacokinetic profiles and expression yields. Therefore, the rational design of linkers remains a challenging, but important issue.

Although several therapeutic forms of G-CSF have been developed and approved, there is a need for more effective and cheaper medications to treat neutropenia.

The aim of this work was to develop and characterize novel human G-CSF homo- and heterodimers by genetical fusion of G-CSF and SCF molecules via specific structured and non-structured linkers.

The main tasks of this study were:

1. To produce in *E. coli* dimeric G-CSF connected by a covalent fusion of two G-CSF molecules using three types of linkers.
2. To purify and characterize dimeric G-CSF proteins using a set of analytical methods.
3. To determine the biological activity and circulation half-life of dimeric G-CSF proteins *in vivo*.

4. To optimize the purification protocol of the most promising dimeric G-CSF drug candidate and to show the stability of the protein in the formulation buffer.
5. To produce in *E. coli* heterodimeric fusion proteins composed of human SCF and G-CSF connected via a peptide linker, which ensures the improved characteristics of the G-CSF homodimer.
6. To purify and charaterize heterodimeric proteins using a set of analytical methods.

Scientific novelty and relevance

Various strategies have been used to improve the characteristics of biopharmaceuticals. Fusion proteins result in longer circulation half-lives and/or targeting moieties. In this work, the development of homodimers composed of two G-CSF molecules and heterodimers composed of G-CSF and SCF has been described. For the first time, three types of linkers were used to connect two G-CSF molecules to examine the effect on the physical characteristics and activity of G-CSF dimeric proteins. An alpha-helix-forming peptide Lα linker provided the best characteristics of G-CSF homodimers. The G-CSF dimer having Lα had a more than seven-fold longer half-life in blood serum and produced a stronger neutrophil response than that of monomeric G-CSF. The total internal reflection ellipsometry (TIRE) data demonstrated that GCSF-Lα-GCSF and GCSF-L7-GCSF may activate the receptor with higher efficiency than GCF-L2-GCSF protein, supporting the 1:2 stoichiometry between the dimeric G-CSF protein and its G-CSFR receptor.

The fusion of two G-CSF molecules into a homodimer has competitive advantages over other marketed second-generation G-CSFs, as dimer generation was obtained by more simple technology than PEGylation. The developed GCSF-Lα-GCSF purification scheme, which consists of protein oxidative refolding by dilution and three chromatography steps (ion-exchange followed by gel-filtration), allowed to get high purity (≥95%) and yield (≥14%) of the dimer. The optimized purification procedure exhibits advantages such as ease of scale-up, low overall cost and time of purification.

Further studies of GCSF-Lα-GCSF are needed to consider this protein as a potentially new G-CSF drug, which is structurally novel compared to currently commercially available G-CSF analogs. In addition, the Lα linker can be applied for the development of structurally similar receptor/ligand systems.

To demonstrate the effectiveness of the Lα-type linker in separating individual domains of bifunctional fusion proteins and to overcome challenges connected with the administration of two cytokines, in the second part of this work, we generated fusion proteins composed of human SCF and human G-CSF interspaced by an alpha-helix-forming peptide linker. Many studies have demonstrated the SCF synergy with G-CSF resulting in important biological responses. The fusion of these cytokines is attractive for therapeutic applications because their concerted activity can enhance the effect of the separate moieties and even confer novel functions. The administration of a fusion protein may reduce the adverse effects of repeated injections of proteins. *In vitro* biological activity studies and TIRE data with purified SCF-Lα-GCSF and GCSF-Lα-SCF demonstrated that the Lα linker ensures spatial separation between the domains of the fusion protein at a favorable distance for their independent functioning. Purified heterodimers possessed the receptor binding activity that resulted in cell proliferation. The biological activity of SCF-Lα-GCSF protein in *vivo* is comparable to that of the mixture of SCF and G-CSF making the protein a promising candidate for further studies.

Thesis statements

1. The developed purification procedure of GCSF-Lα-GCSF results in higher purity and yield compared to other studied homodimeric G-CSFs.
2. GCSF-Lα-GCSF has a longer circulation half-life and increased biological activity *in vivo* compared to monomeric G-CSF.
3. The developed isolation and purification procedures of the dimers are suitable for small and large-scale protein production.
4. The flexible Lα linker ensures the independent functioning of monomers in the fused proteins.
5. The SCF and G-CSF moieties in the SCF-Lα-GCSF protein are biologically active.
6. Fused homo- and heterodimers might be developed as therapeutics.

1. LITERATURE OVERVIEW

1.1. Cytokines

The term cytokine is derived from the Greek words kyttaro (cell) and kines (movement) and represents a large group (more than 130) of small secreted proteins (6-70 kDa) released by cells that have a specific effect on the interactions and communications between cells (Feldmann, 2008; Zhang et al., 2009; Baldo, 2014; Stenken and Poschenrieder, 2015). There are over 100 separate genes coding for cytokine-like activities, many of these overlap with activities and many are still unexplored (Dinarello, 2011). Cytokines can be secreted by various immune cells (monocytes, macrophages, neutrophils, B-cells, and T-cells, mast cells), as well as endothelial cells, fibroblasts, and various stromal cells (Figure 1.1.), although it has been acknowledged that every nucleated cell type is capable of producing cytokines (Stenken and Poschenrieder, 2015). These proteins are widespread through mammals and interestingly have been also discovered in invertebrates (Beschin et al., 2001; Beschin et al., 2004).

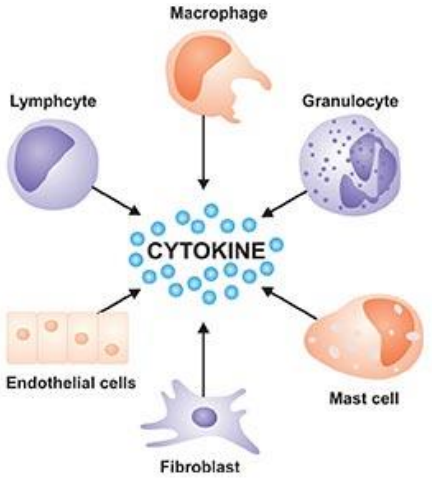

Figure 1.1. The main types of cells producing cytokines (https://www.cusabio.com/cytokines/What-Cells-Release-Cytokines.html).

1.2. Functions and properties of cytokines

Cytokines act as mediators and modulators within highly localized environments and regulate immunological responses, hematopoietic development, and cell-to-cell communication as well as host responses to infectious agents and inflammatory stimuli (Lefkowitz and Lefkowitz, 2001; Stenken and Poschenrieder, 2015). Also, they are involved in mammalian

embryonic development and implantation in the endometrium (Tabibzadeh and Babaknia, 1995; Cuenca et al., 1999). Cytokines have been found in a wide range of situations, and most of them drive various cell functions. They are often produced in a cascade, as one cytokine stimulates its target cells to make additional cytokines. Cytokines can act synergistically or antagonistically or interact with each other in complex ways that may be additive (Zhang and An, 2007). In addition, cytokines exhibit the phenomena of cytokine "pleiotropy" and "redundancy". Cytokine pleiotropy is the ability of a cytokine to exert many different types of responses, often on different cell types, whereas cytokine redundancy addresses the fact that many different cytokines can induce a similar response. Many individual cytokines are themselves pleiotropic and particularly *in vitro*, have overlapping actions. Overlapping actions and redundancy of different cytokines can be explained by similar cellular distributions of specific receptors for different cytokines as well as by the sharing of signaling pathways, which are particularly present when different receptors share similar motifs that mediate the coupling to the same pathways. Furthermore, redundancy can be at least partly explained by the ability of certain cytokines to signal via more than one type of receptor complexe sand by sharing of an individual receptor component by more than one cytokine (Paul, 1989; Leonard, 1994).

Cytokine production is often tightly and transiently regulated. Due to the high biological effect of most cytokines, their concentration in body fluids or tissues is low, e.g. picomolar concentrations (Schenk et al., 2001). However, if needed, their concentrations can increase up to 1000-fold. In healthy subjects, cytokines are not detectable or present at pg/mL concentrations, meanwhile increased concentrations of cytokines indicate activation of cytokine pathways related to inflammation or disease progression (Dinarello, 2000; Stenken and Poschenrieder, 2015).

1.3. Cytokine receptors

The cytokines transmit their biological signals through receptors present on the membrane of target cells. Cytokine receptors are mainly transmembrane proteins, consisting of extracellular, transmembrane and cytoplasmic domains (Gulati et al., 2016). The extracellular domain is the site that recognizes binding cytokines, and transmembrane and cytoplasmic domains can transmit signals and promote effector function. As shown in the scheme of Figure 1.2., on the basis of common structural features, cytokine receptors are broadly classified into six major superfamilies (O'Shea et al., 2019, Floss and Scheller, 2019).

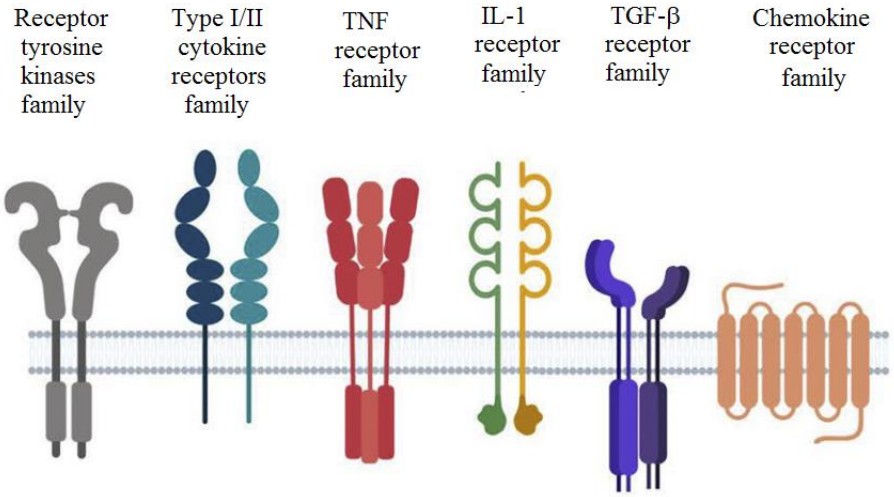

Figure 1.2. Schematic representation of major cytokine receptors superfamilies. Abbreviations: IL-1, interleukin-1; TGF-β, transforming growth factor-beta; TNF, tumor necrosis factor (O'Shea et al., 2019, Floss and Scheller, 2019).

The cytokine receptors and their cytokines exhibit very high affinity for each other and possess dissociation constants ranging from 10^{-10} to 10^{-12} M. Because of this high affinity, cytokines can mediate biological effects at picomolar concentrations (Gulati et al., 2016). A cytokine may bind to receptors on the membrane of the same cell that secretes them (autocrine action), it may bind to receptors on nearby cell (paracrine action), or in some instances, cytokines do enter the bloodstream and can act in an endocrine action (Jason et al., 2001).

1.4. Clasification of cytokines

Cytokines can be grouped according to several different schemes, all of which are somewhat arbitrary and not completely accurate. In an older nomenclature, cytokines were classified according to the type of cell responsible for their synthesis; cytokines produced by lymphocytes were called "lymphokines", while those produced by macrophages or monocytes were called "monokines". However, cytokines can be secreted from various cells, so these terms are rarely used today (Alarcon and Fink, 2008). Structural studies have allowed the classification of these proteins into families based on their similarity in amino acid sequence, and in three-dimensional structure (Table 1.1.). (1) The hematopoietins constitute a family of cytokines that form four α helices, whereas members of (2) the TNF family form a jelly-roll motif. Other important families are (3) interleukin IL-1, (4) platelet-derived growth

factor (PDGF), and (5) T-cell growth factor β (TGF-β) families. (6) Chemokine family, small cytokines with chemotactic activities, is subdivided into two major groups, the cys-x-cys (C-X-C) and the cys-cys (C-X), depending on whether the first two of four conserved cysteine residues are separated by one amino acid (Andreakos et al., 2004).

In addition, cytokines can be classified according to the type of receptor they bind (class I cytokine receptors, class II cytokine receptors, TNF receptors, tyrosine kinase receptors, chemokine receptor). Also, cytokine families can be grouped differently according to other aspects such as sharing a receptor subunit (i.e. the gp130 family) or its physiological roles (i.e. neuropoietic family, for its effects on the hematopoietic and nervous system) (Tansey and Wyss-Coray, 2008; Mousa and Bakhiet, 2013).

Table 1.1. Cytokine families classified by structural similarity

Family	Cytokines
Hematopoietins	IL-2, IL-3, IL-4, IL-5, IL-6, IL-7, IL-9, IL-11, IL-12, IL-15, IL-16, IL-17, EPO, LIF, GM-CSF, G-CSF, OSM, CNTF, GH, TPO, and SCF
TNF family	TNF-α, LT-α, LT-β, CD40L, CD30L, CD27L, 4-1 BBL, OX40, OPG, and FasL
IL-1	IL-1α, IL-1β, IL-1ra, IL-18, BFGF, aFGF, and ECGF
PDGF	PDGF A, PDGF B, and M-CSF
TGF-β	TGF-β and BMPs (1, 2, 4, etc.)
Chemokines	
C-X-C subfamily	IL-8, Gro-α/β/γ, NAP-2, ENA 78, GCP-2, PF4, CTAP-3, MIG, and IP-10
C-C subfamily	MCP-1, MCP-2, MCP-3, MIP-1α, MIP-1β, RANTES

Adapted from Andreakos et al., 2004. Abbreviations: aFGF, acidic fibroblast growth factor; 4-1 BBL, 4-1 BB ligand; BFGH, basic fibroblast growth factor; BMP, bone morphogenetic proteins; C-C, cysteine-cysteine; CD, cluster of differentiation; CNTF, ciliary neurotrophic factor; CTAP, connective tissue activating peptide; C-X-C, cysteine-x-cysteine; ECGF, endothelial cell growth factor; EPO, erythropoietin; FasL, Fas ligand; GCP-2, granulocyte chemotactic protein-2; G-CSF, granulocyte colony-stimulating factor; GH, growth hormone; GM-CSF, granulocyte-macrophage colony-stimulating factor; Gro, growth-related gene products; IL, interleukin; IP, interferon-γ inducible protein; LIF, leukemia inhibitory factor; LT, hymphotoxin; MCP, monocyte chemoattractant; M-CSF, macrophage colony-stimulating factor; MIG, monokine induced by interferon γ; MIP, macrophage inflammatory protein; NAP-2, neutrophil activating protein-2; OPG, osteoprotegerin; OSM, oncostatin M; PDGF, platelet-derived growth factor; PF, platelet factor; R, receptor; RANTES, regulated on activation; normal T cell-expressed and –secreted; TGF, transforming growth factor; TNF, tumor necrosis factor; TPO, thyroperoxidase.

Depending on the role cytokines are also classified into pro-inflammatory or anti-inflammatory cytokines (Sprague and Khalil, 2009). Pro-inflammatory cytokines (IL-1β, IL-6, IL-8, IL-12, TNF-α, and interferons) facilitate inflammatory reactions and can stimulate immunocompetent cells. Meanwhile, anti-inflammatory cytokines (IL-4, IL-6, IL-10, IL-11, IL-13, IL-1 receptor antagonist (IL-1RA), and TGF-β) inhibit inflammation and suppress immune cells. Some the cytokines (e. g. IL-6) have both pro- and anti-inflammatory effects (Liu et al., 2021).

1.5. Role of cytokines in diseases

The abnormalities in cytokines, their receptors, and the signaling pathways that they initiate are related to a wide variety of diseases. Table 1.2. represents various typical diseases related to interactions of different pro- and anti-inflamatory cytokines.

Table 1.2. Diseases related to interactions of various cytokines

Diseases	Related cytokines
Autoimmune diseases	IL-1, IL-2, IL-6, IL-12, IL-15, IL-16, IL-17, IL-18, IL-23, TNF-α, IFN-α, IFN-γ
Allergy	IL-1, IL-4, IL-5, IL-9, IL-10, IL-13
Alzheimer‘s disease	TNF-α, TGF-β, IL-1, IL-4, IL-6, IL-10
Atherosclerosis	TNF-α, IFN-γ, TGF-β, IL-1, IL-2, IL-4, IL-5, IL-6, IL-8, IL-10, IL-12, IL-17, IL-18, IL-20, IL-33, IL-37
Cardiovascular disorders	TNF-α, TGF-β, IL-1, IL-6, IL-10, IL-17, IL-18
Cancer	TNF-α, TRAIL, IL-6, IL-10, IL-12, IL-17, IL-23
Depression	TNF-α, IFN-γ, IL-1, IL-2, IL-6
Gastrointestinal diseases	TNF-α, IFN-γ, TGF-β, IL-1, IL-4, IL-6, IL-8, IL-10
Sepsis	TNF-α, IFN-γ, TGF-β, MIF, IL-1, IL-6, IL-4, IL-10, IL-12

Adapted from Liu et al., 2021.

For example, IL-1 and TNF-α are produced in excess in rheumatoid arthritis, a chronic autoimmune disease, where they are involved in inflammation and joint damage (Zhang, 2021). Inflammatory processes controlled by cytokines are important in the etiology of Alzheimer‘s disease (AD) also. A rise in the serum levels of several proinflammatory cytokines including IL-6, IL-1β, and TNF-α has been noticed in AD patients (Humpel and Hochstrasser, 2011). Increases in peripheral inflammatory cytokines have also been observed in other psychiatric disorders such as: IL-6, TNF-α, and

TGF-β in acute psychosis (Mahadevan, 2017); IL-2R (Rapaport et al., 1993) and IL-6 (Ganguli et al., 1994; Ng et al., 2018) in schizophrenia; IL-1β (Brambilla et al., 1994; Hoge et al., 2009) IL-6 and TNF-α (Hoge et al., 2009) in panic disorders; IL-1β and TNF-α in obsessive-compulsive disorders (Brambilla et al., 1997), and IL-1β, IL-6 and TNF-α in post-traumatic stress disorder (PTSD) (Lindqvist et al., 2014; Oganesyan et al., 2009).

As a topical example, with the spread coronavirus disease 2019 (COVID-19) pandemic, research has found that patients with severe COVID-19 tend to have highly elevated levels of pro-inflammatory cytokines compared to those who are mildly or moderately ill. Increasing studies revealed that the "cytokine storm", i.e. an activation cascade of auto-amplifying cytokine production due to unregulated host immune response to different triggers, can lead to apoptosis of epithelial and endothelial cells, vascular leakage and, finally, result in acute respiratory distress syndrome and other severe syndromes, or even death (Tang et al., 2020). Figure 1.3. illustrates the proposed mechanism of the cytokine release syndrome (Liu et al., 2021).

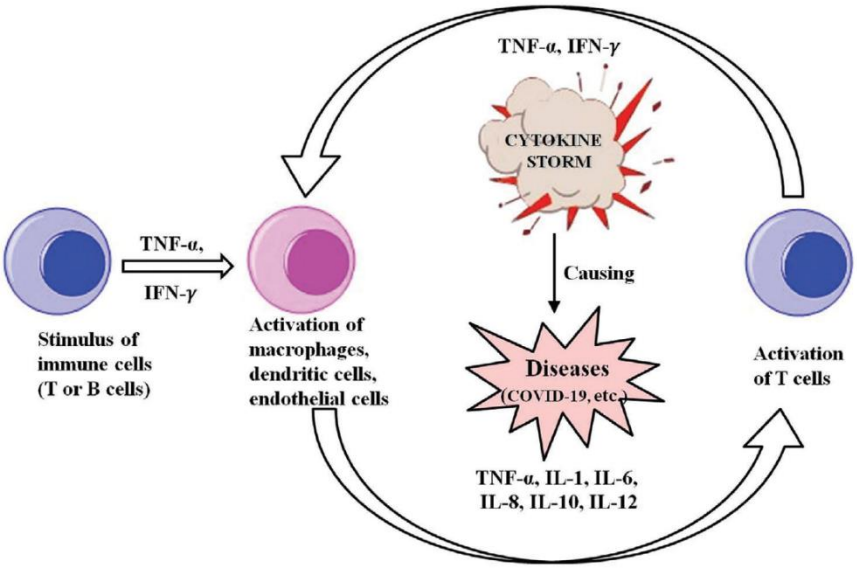

Figure 1.3. The proposed mechanism of cytokine release syndrome. In SARS-CoV-2 infection, the virus infects the respiratory epithelial tissue and activates local innate immune cells. Activation of T cells or lysis of immune cells induces the production of TNF-α or IFN-γ. Subsequently, TNF-α or IFN-γ triggers activation of macrophages, dendritic cells or other immune cells, which further release pro-inflammatory cytokines (i. e. IL-6, IL-10, IL-2, IL-8 and others) contributing to a positive feedback loop to activate T cells that can result in severe toxicity (Liu et al., 2021).

1.6. Clinical importance of cytokines

Progress in the understanding cytokine biology has led to the appreciation of the importance of cytokines in every field of medicine. Cytokines can be used as biomarkers for disease indication or monitoring, as well as therapeutic agents or targets of therapeutics.

1.6.1. Cytokines as biomarkers

Quantification of cytokines has great importance in both biology and clinical medicine biology as the levels provide an understanding of physiological and pathological processes. Usually, cytokine measurements are important to understand and predict disease progression (Bienvenu et al., 2000; Stenken and Poschenrieder, 2015). Also, an accurate quantification of cytokines provides valuable information in the clinical context for adjusting therapies in various diseases, including asthma (Berry et al., 2006), atherosclerosis (Ohta et al., 2005), cancer (Massague, 2008), depression (Dowlati et al., 2010), heart disease (Guilherme et al., 2004), acquired immune deficiency syndrome (AIDS) (Brockman et al., 2009), kidney injury (Sanz et al., 2011), sepsis (Bozza et al., 2007), rheumatoid arthritis (McInnes and Schett, 2007), and other chronic diseases (Liu et al., 2021).

Many standard assay procedures exist and are used in clinical practice to detect cytokines. The commercially available assays include enzyme-linked immunosorbent assay (ELISA) methods (determine cytokines by capturing with capture antibodies), bioassays (detect cytokines by measuring their biological activity), polymerase chain reaction (PCR) methods (determine gene expression for cytokine production) and enzyme linked-immuno spot (ELISPOT) assays (detect cytokines from single cells) (Stenken and Poschenrieder, 2015).

However, there are some challenges to *in vitro* cytokines detection. It is very difficult to evaluate cytokines' diagnostic ability due to the challenge of distinguishing "normal" versus "abnormal" cytokine levels. Cytokines can vary greatly among individuals, their release and subsequent activities can differ based upon activating signals, specific cell targets, and physiological factors including feeding state, fitness level, and stress (Zhou et al., 2010; Monastero and Pentyala, 2017). Furthermore, their short half-life or potential degradation can affect the precision of cytokine measurement and analysis (Liu et al., 2021).

To deal with these challenges, research in the area of cytokines quantification are still in its developing stages and are on the way to

developing sensitive, selective, and rapid real-time cytokine analysis platforms for quantitive analysis of cytokines from *in vitro* to *in vivo* (Liu et al., 2021).

1.6.2. Cytokines as therapeutic agents

The use of recombinant proteins as therapeutic agents has been known for the past three decades (Rider et al., 2016). Interferon-α was the first recombinant cytokine approved as therapeutic protein by the Food and Drug Administration (FDA) in two versions, concurrently in 1986: (1) IFN α-2b (Intron A; from Schering-Plough) for the treatment of hairy cell leukemia, followed by many indications, including AIDS-related Kaposi's sarcoma, hepatitis B and C, malignant melanoma, follicular lymphoma, and genital warts and (2) IFN α-2a (Roferon; from Hoffman La Roche) for the treatment of hairy cell leukemia, and chronic myelogenous leukemia and later hepatitis C (Martin-Moe et al., 2010). There are currently more than 20 cytokine preparations approved by FDA and European Medicines Agency (EMA) for human therapy, which are all in recombinant human form. The main therapeutic indications for some of them are listed below:

- Interferon beta used to treat multiple sclerosis;
- Interferon gamma used to treat chronic granulomatous disease and malignant osteopetrosis;
- IL-2 used to treat kidney carcinoma and melanoma;
- IL-11 used to treat thrombocytopenia during tumor therapy;
- EPO used to treat anemia;
- G-CSF and GM-CSF used to stimulate neutrophil production in chemotherapeutically treated tumor patients and after bone marrow transplantation.

Many other cytokines are participating in clinical studies (Baldo, 2016). It has been suggested that the pharmaco-dynamic potency of cytokine-based therapeutic could be primarily related to three factors including (1) cytokine/receptor binding affinity, (2) cytokine/receptor endocytic trafficking dynamics, and (3) cytokine/receptor signaling (Croxford et al., 1998).

1.6.3. Cytokines as targets of therapeutics

Today, anti-cytokine medicine is a rapidly growing field and some the successful biological agents, which block and control such cytokine activities, have been approved for use during the last decade (Feldman, 2008; Donnelly et al., 2009). Mainly, such biologics are composed of:

(1) monoclonal antibodies that inhibit the activity of specific cytokines, either by blocking cytokine receptors or neutralizing cytokine activity;

(2) or soluble cytokine receptor constructs that bind the cytokines and facilitate their clearance from the body (Rider et al., 2016; Donnelly et al., 2009).

The first major success of anti-cytokine therapy was reached in rheumatoid arthritis (RA), a chronic autoimmune inflammatory disease that can affect more than just your joints. RA is well characterized by the infiltration and activation of inflammatory T cells that produce proinflammatory cytokines, such as TNF-α, IL-1, and IL-6. Among them, TNF-α plays an essential role in RA: TNF-α blockade has been shown to have beneficial effects on all aspects of disease activity. Today, five biologic agents that inhibit TNF-α are approved for clinical use in the United States. Three of them are monoclonal antibodies (mAbs) against TNF-α, and the other two are soluble receptor constructs that act by binding TNF-α. Hovewer the other biologics, like IL-1 and IL-6 inhibitors, can be used, when patients with RA are refractory to anti-TNF therapy (Donnelly et al., 2009).

In addition, anti-cytokine therapy is useful for the treatment of psoriasis. In psoriasis, an immune-mediated chronic inflammatory skin disease, multiple cytokines stimulate the growth of keratinocytes. Ustekinumab, a humanized mAb that binds the shared p40 subunit of IL-12 and IL-23, was shown to be effective and was approved in 2009 for plaque psoriasis and in 2013 for psoriatic arthritis. By blocking both IL-12 and IL-23, ustekinumab inhibits inflammatory cell infiltration, decreases expression of such cytokines as IFN-γ, IL-17, and IL-22, and reduces epidermal hyperplasia (Rider et al., 2016; Donnelly et al., 2009).

1.7. Limitations of cytokine therapy

The cytokine-based therapy, besides the clinical benefits for patients, has some limitations: (1) cytokines have a very short half-life, and frequent administration may be required; (2) attaining optimal concentrations in the tumor microenvironment for cancer immunotherapy is difficult; (3) therapy with cytokines often leads to dose-dependent side effects. Being pleiotropic in nature, cytokines are able to influence more than a single cell exerting potent immune responses with unpredictable and undesirable side effects. The most common toxic effects are nausea, vomiting, fever/chills, fatigue, and headache. Rare but potentially serious side effects include anemia, thrombocytopenia, respiratory distress, shock, and coma (Dhama et al., 2013; Baldo, 2014). Blocking the bioactivity of proinflammatory cytokines has

proved to be accompanied by an increased susceptibility to infections (Van der Meer et al., 2005). During therapy with TNF-blockers, the reactivation of latent *Mycobacterium tuberculosis* was observed as the most common opportunistic infection. Other pathogens reported causing serious infections in patients using TNF blockers to include *Listeria*, *Pneumocystis*, *Histoplasma*, *Aspergillus*, systemic *Candida*, *Cryptococcus*, and *Coccidioides* (Moiton et al., 2006; Furst et al., 2006).

The last but not least limitation of cytokine-based therapy is that (4) the production and manufacturing of biologics is still an expensive process composed of many production and product purification stages which are under strict regulation of the respective authorities. Finally, compared to chemical drugs, (5) recombinant cytokines have limited shelf half-life, require special/controlled storage conditions, and are typically administrated by a physician (Rider et al., 2016).

1.8. Recombinant engineering of therapeutic cytokines

Many cytokines have been engineered to enhance their therapeutic efficacy as well as to overcome their limitations. Most important cytokines require protein engineering strategies to increase their half-life in blood serum, specific activity towards the target and to reduce toxicity. For this purpose, PEGylation, fusion with other proteins, immuno complexing, and mutagenesis have been exploited.

One of the earliest strategies used for a half-life extension of therapeutic proteins was PEGylation, which has been used in the clinic for more than 30 years (Swierczewska et al., 2015). PEGylation means the process in which the protein is covalently conjugated or non-covalently complexed with one or more chains of polyethylene glycol (PEG) (5-40 kDa) – a chemically inert, highly hydrophilic, flexible, and variable size polymer (Gupta et al., 2019; Zou and Nock, 2020). A number of cytokines have been PEGylated, but most of the published research still undergoing preclinical studies. Currently, there are around 4 FDA approved PEGylated cytokines on the market that treat a variety of diseases. (1) PEG-G-CSF is employed for the treatment of chemotherapy-induced neutropenia, (2) PEG-IFN-β1a is used to treat a multiple sclerosis, and both (3) PEG-IFN-α2a and (4) PEG-IFN-α2b are used for treating hepatitis C (Baldo, 2016; Mishra et al., 2016). The characteristics of PEGylated products are discussed in more detail in section 1.9.1.4.

Genetic fusion of cytokines to other proteins is another useful strategy for increasing the biophysical properties of cytokine therapeutics (Figure 1.4.). A fusion or chimeric protein is defined as an artificial construct

combining unrelated whole proteins or domains of those proteins. Such protein is created through the joining of two or more select protein/domain genes and it is expressed as a single polypeptide (Vazquez-Lombardi et al., 2013; Rogers et al., 2015). Therapeutic cytokine fused to a partner protein display:

- prolonged half-life (fusion to the Fc, human serum albumin (HSA), human transferrin (HTF));
- localized delivery (fusion to whole antibodies or antibody fragments);
- enhanced targeted cytotoxicity (fusion to bacterial toxins);
- increased activity (fusion to agonistic cytokine receptors).

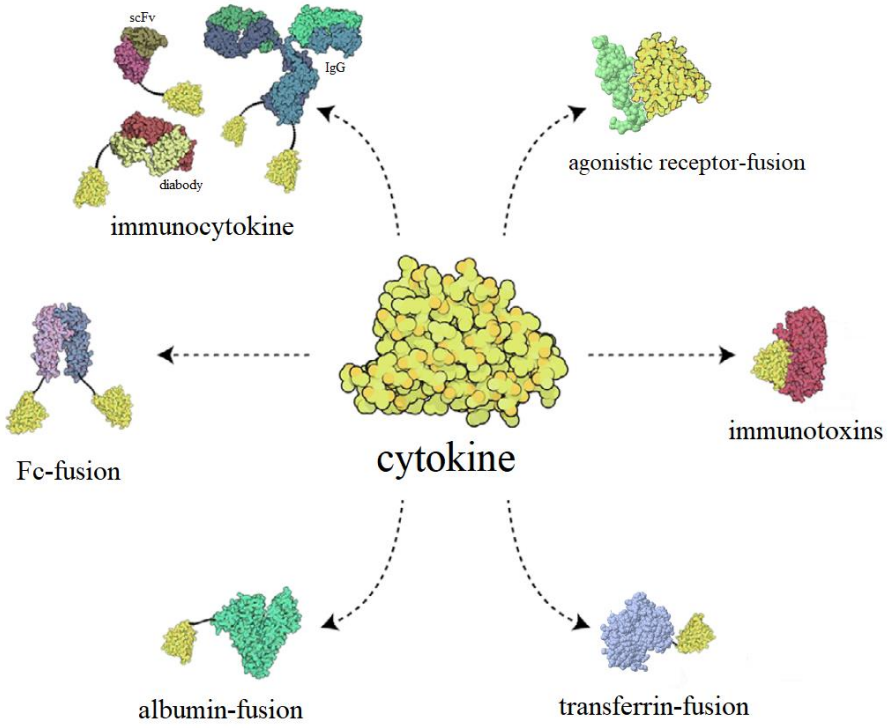

Figure 1.4. Illustration of major fusion strategies utilized for cytokine optimization (Pires et al., 2021)**.**

Among many potential fusion proteins, Fc-fusion proteins are one of the most intensively investigated groups and their therapeutic importance is growing. Fc fusion drugs, such as Enbrel (etanercept), Orencia (abatacept), and Nplate (romiplostim) have been approved and used in clinical practice (Rogers et al., 2015). IgG antibody Fc domain, a non-antigen binding part, has

been mostly used to construct cytokine fusion molecules (Jazayeri and Carroll, 2008). Usually, the half-life of Fc-fusions is typically shorter than intact antibodies (1-2 weeks) but still significantly longer than of the fused parts.

Similar to IgG antibodies, HSA displays a long circulation half-life (19 days in humans), mainly due to FcRn-mediated recycling (Anderson et al., 2006; Chang et al., 2009). The first HSA-peptide or protein fusion product has been approved for marketing in 2014 was Albiglutide (trade names Eperzan in Europe and Tanzeum in the US). Albiglutide is DPP-4-resistant glucagon-like peptide (GLP)-1-HSA fusion polypeptide that improves the half-life of pharmacologically active GLP-1 from 1-2 min for native GLP-1 to 4-7 days and allows for once-weekly dosing in patients with type 2 diabetes mellitus (Strohl, 2015). Also, albumin fusion technology has been adapted to various cytokines such as G-CSF, IL-2, $IFN_{\alpha 2a/\alpha 2b}$, EPO, GM-CSF. Still, none has been approved, but some of them are now or were in development, early and late-stage clinical trials (Rogers et al., 2015; Strohl, 2015).

Genetic fusion to HTF, a naturally abundant blood plasma glycoprotein, represents another promising strategy that results primarily in a longer half-life of cytokines. A half-life of the glycosylated form of HTF is reported being to be 7-12 days (Kontermann, 2009; Kim et al., 2010). Fusion of peptide and proteins to TF or TFR-binding antibodies has been applied in some applications, including half-life extension and targeting of cancer cells expressing high levels of TFRs and targeting of the brain capillary endothelium for transport of therapeutics across the brain-blood barrier (Chang et al., 2009; Daniels et al., 2006; Kim et al., 2010). The relative resistance of TF to gastrointestinal digestion (Azari and Feeney, 1958) and the high expression of TFR in the human gastrointestinal epithelium (Banerjee et al., 1986) also provide the potential for oral delivery of TF-associated drugs (Gillies et al., 1998).

Other cytokine fusion proteins include immunocytokines (List and Neri, 2013; Weide et al., 2019), cytokines fusion to bacterial toxins (Schmidt, 2009; Vazquez-Lombardi et al., 2013), and fusion to cytokine agonists (Jones and Rose-John, 2002). Although a number of such chimeric cytokines have been developed and tested as potential therapeutics, only diphtheria-toxin–based fusion protein (denileukindiftitox, DAB-IL-2) received FDA approval in 1999 for the treatment of patients with cutaneous T-cell lymphoma (CTCL), a rare cancer of T-lymphocytes that involves the skin (Cheung et al., 2019).

1.9. Granulocyte colony stimulating factor and stem cell factor

G-CSF and SCF are essential members of the hematopoietin cytokine family (Figure 1.5.). They are critically involved in the regulation of hematopoietic stem cells or hematopoietic progenitor cells (HSCs/HPC) proliferation and differentiation (McNiece and Briddel, 1995; Greenbaum and Link, 2011).

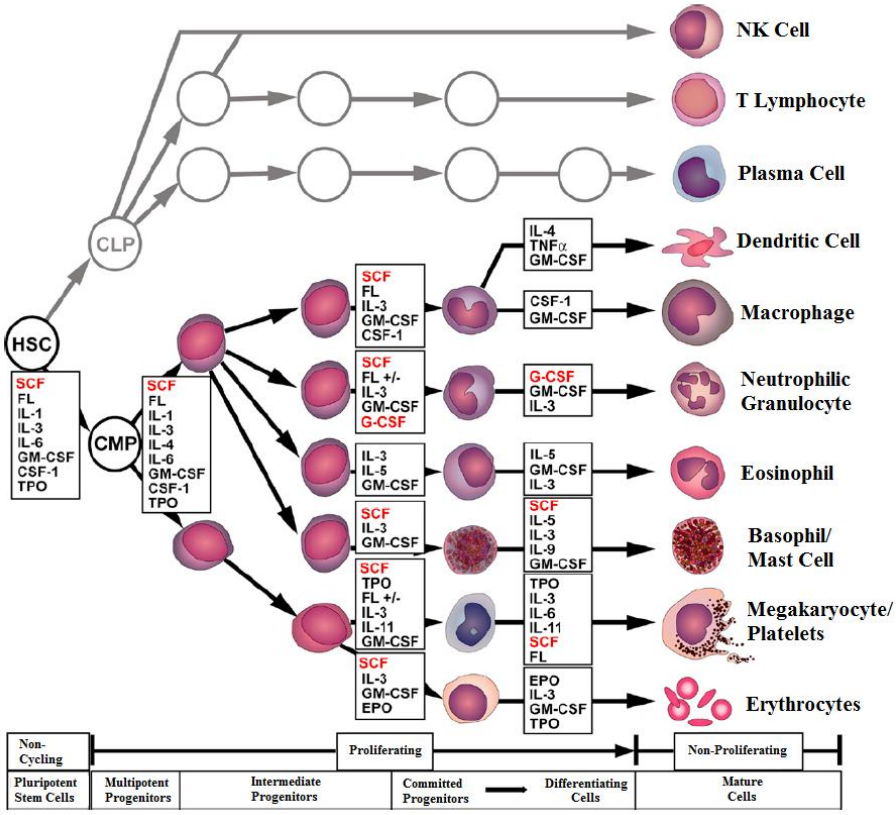

Figure 1.5. Hematopoietic tree. Diagram depicting the effects of SCF and G-CSF (color in red) and some other cytokines on formation of different blood cells (Pixley and Stanley, 2003). Abbreviations: HSC, hematopoietic stem cell; CLP, common lymphoid progenitor; CMP, common myeloid progenitor; FL, Flt ligand; IL, interleukin; GM-CSF, granulocyte-macrophage colony-stimulating factor; CSF-1, colony stimulating factor-1; TPO, thrombopoietin; EPO, erythropoietin; TNF, tumor necrosis factor.

1.9.1. Granulocyte colony stimulating factor

1.9.1.1 Biology of G-CSF

G-CSF, also known as colony-stimulating factor 3 (CSF3), was originally identified and characterized by its ability to support the proliferation and maturation of bone marrow-derived myeloid progenitor cells in semisolid culture media. The colonies formed in response to this factor consisted primarily of granulocytes, hence the name G-CSF (Metcalf, 2013).

The importance of G-CSF to granulopoiesis is well established. G-CSF is an endogenous hematopoietic factor that promotes the proliferation and differentiation of neutrophil granulocyte precursors and stimulates their release from the bone marrow (Anderlini et al., 1996). It also regulates the function and survival of mature neutrophils (Basu et al., 2002). Studies with G-CSF-deficient mice revealed that these mice have chronic neutropenia and impaired neutrophil mobilization from the bone marrow: had a 70-80% reduction in peripheral neutrophil counts compared to wild-type mice, and a 50% reduction in neutrophil granulocyte precursors in the bone marrow (Lieschke et al., 1994).

In normal cells, G-CSF production is strictly regulated. Although healthy individuals express low G-CSF levels in serum (30-163 pg/mL), however its aberrant production greatly increases upon inflammation or infection (until 3,199 pg/mL) (Watari et al., 1989; Cheers et al., 1988). G-CSF is produced in a response to inflammatory stimuli such as bacterial lipopolysaccharide (LPS), IL-17, TNF-α, and IL-1β by different of cell types, including mainly macrophages and monocytes (Kim et al., 2006, Lee et al., 1990), bone marrow stromal cells (Fibbe et al., 1988), endothelial cells (Zsebo et al., 1988) and fibroblasts (Koeffler et al., 1987). Overexpression of G-CSF has also been reported in various tumors and is frequently associated with aggressive tumor cell growth and a poor clinical outcome (Hirasawa et al., 2002; Shojaei et al., 2009; Kowanetz et al., 2010; Waight et al., 2011). Usually, patients with G-CSF-producing tumors have a fever and severe leukocytosis without evidence of infection (Kitadele et al., 2015).

1.9.1.2 G-CSF receptor structure and activation

Various biological effects of G-CSF occur as a consequence of the activation of a specific high-affinity receptor, located on the surface of target cells (G-CSF receptor). The GCSF-R is expressed mainly on neutrophils, monocytes/macrophages (Kim et al., 2006), hematopoietic stem/progenitor

cells (HSPCs) (Lieschke et al., 1994; Liu et al., 1996), and a subset of B lymphocytes (Franzke et al., 2003). The receptor is also expressed on endothelial cells (Bussolino et al., 1989) and placenta (Nicola and Metcalf, 1985).

The GCSF-R is a transmembrane glycoprotein, 100-150 kDa in size, which belongs to the class I family of hemopoietic cytokine receptors. Its single polypeptide chain is composed of three distinct components (Figure 1.6.). A large glycosylated extracellular region contains an immunoglobulin-like (Ig-like) domain, a cytokine receptor homolog (CRH) domain, and three fibronectin-type III-like domains. Four conserved cysteine residues and a Trp-Ser-X-Trp-Ser motif of the CRH domains are required for ligand binding and receptor activation (Fukunaga et al., 1991; Touw and Geijn, 2007). It was reported that the Ig-like domain also mediates intermolecular interactions with G-CSF (Layton et al., 1999). The extracellular region is separated from the intracellular cytoplasmic region by a short transmembrane sequence. The cytoplasmic domain of G-CSF is considered the signal transduction domain of the receptor. It contains three distinct motifs termed boxes 1 – 3 and four tyrosine (Y) residues, which function as docking sites for the phosphorylation of a variety SH2-containing signaling molecules. A conserved Boxes 1 and 2 and a tyrosine residue (Y704) are essential for proliferative signaling (Liongue et al., 2009). A less concerved Box 3 is related to receptor trafficking (Ward et al., 1999) and three other tyrosine residues (Y729, Y744, and Y764) are required for proliferation, differentiation, and survival (Ward et al., 1999; Liongue et al., 2009).

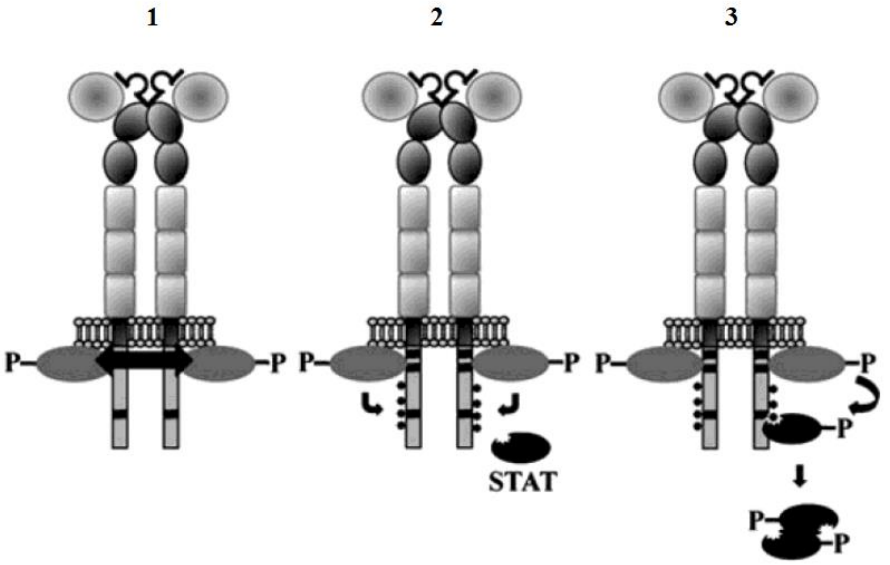

Figure 1.6. Schematic illustration of G-CSF induced activation of JAK-STAT signal transduction pathway. (1) The formation of G-CSF and GCSF-R complex induces activation of members of Janus kinase family (JAK1, JAK2, and TYK2). (2) Phosphorylated JAKs subsequently phosphorylate four tyrosine residues (Y704, Y729, Y744, Y764) in G-CSF receptor, creating docking sites for signal transducer and activator of transcription (STAT) proteins in the cytoplasm. (3) STAT protein binds to the phosphorylated G-CSF through its SH2 domain and phosphorylates. Activated STAT dimerizes and translocates to the nucleus where they bind DNA and activate the transcription of responsive genes (Nguyen-Jackson et al., 2012).

Previous studies have shown that the G-CSF receptor has a weak tendency to self-associate into a dimer in the absence of G-CSF (Horan et al., 1996). G-CSF binding to G-CSF receptor monomer occurs with high affinity. The binding of G-CSF also enhances the GCSF-R dimerization: when one G-CSF molecule is bound to GCSF-R:GCSF-R complex, dimerization is enhanced 80-fold, meanwhile the dimerization of 2:2 G-CSF:GCSF-R complex is increased even ~2000-fold (Horan et al., 1996). The G-CSF:GCSF-R formed a 2:2 stoichiometry, resulting in a crossover homodimeric complex (Tamada et al., 2006).

The resulting GCSF-R homodimer activates multiple signaling pathways. The cytoplasmic domain of GCSF-R lacks intrinsic tyrosine kinase activity, therefore, it is associated with various non-receptor tyrosine kinases (Corey et al., 1994; Nicholson et al., 1994; Yoshikawa et al., 1995; Nicholson et al., 1995; Matsuda et al., 1995; Ward et al., 1998). Besides the well-known JAK-STAT signal transduction (Figure 1.6.), G-CSF also activates other downstream signaling pathways such as phosphatidylinositol 3'Kinase

(PI3K)/AKT and multiple Mitogen-Activated Protein kinase (MAPK)/extracellular signal-regulated kinase (ERK) (Avalos, 1996; Dwivedi et al., 2017). Specific intracellular signaling pathways appear conserved in many tissues and contribute to the different target cells responses (Chakraborty et al., 1996; Rausch and Marshall, 1997; Dong and Larner, 2000, Dong et al., 2001; Naito et al., 2009; Hara et al., 2011).

1.9.1.3 Molecular and structural aspects of human G-CSF

Human G-CSF was purified in 1983-1984 from the human bladder carcinoma cell line 5637 and cloned a few years later (Welte et al., 1985; Nagata et al., 1986). A single human G-CSF gene is localized on chromosome 17 at the q21-17q22 (Kanda et al., 1987). The full-length gene consists of about 2500 nucleotides and comprises five exons separated by four introns (Tsuchiya et al., 1987; Shannon et al., 1990). Four different mRNA isoforms resulting due differential splicing have been reported for G-CSF: transcript variants 1, 2, 3, 4. Transcript variant 1 encodes G-CSF isoform A composed of 177 amino acids, transcript variant 2 encodes the major biologically active G-CSF isoform B composed of 174 amino acids (Nagata et al., 1986; Toghraie et al., 2019). The activity of 174 amino acid form is 50-fold higher than that of the longer isoform (Arakawa et al., 1995). The two other G-CSF isoforms, transcript variants 3 and 4 encode 141 amino acid isoform C and 138 amino acid isoform D, respectively.

The G-CSF isoform B is the most studied and is the basis for commercial pharmaceutical G-CSF products. The secreted form of the protein was found to be O-glycosylated and 19600 Da in molecular weight (Souza et al., 1986). A single O-glycosylated site at Thr^{133} protects the G-CSF from aggregation but does not appear to influence receptor binding directly or is not crucial for biological activity (Kubota et al., 1990). *E. coli* produced recombinant human G-CSF (rhG-CSF) has identical biological activity as endogenous G-CSF, but contains an additional N-terminal methionine and is not glycosylated (Frampton et al., 1994; Lu et al., 1989). This protein contains 175 residues and has a molecular mass of 18798 Da (Souza et al., 1986).

As shown in Figure 1.7., the G-CSF protein contains five cysteines; one free cysteine thiol at position 17 and two intramolecular disulfide bonds, between residues Cys36-Cys42 and Cys64-Cys74 (Lu et al., 1989, Leon et al., 1999). The disulfide bonds play an important role in maintaining the biological functions of G-CSF.

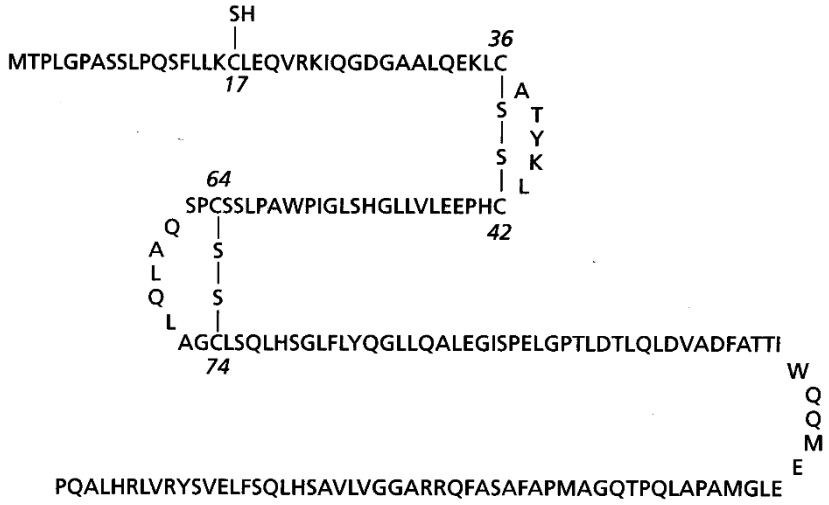

Figure 1.7. Amino acid sequence of rhG-CSF (Leon et al., 1999)**.**

The folding and oxidation process of rhG-CSF solubilized from *E. coli* inclusion bodies was investigated in Lu et al., 1992. The study demonstrated that the folding process of completely reduced rhG-CSF proceeds through intermediates I_1 and I_2 that are partially oxidized and final oxidized forms, respectively. The completely reduced G-CSF form exists temporarily and disappears quickly with the concomitant formation of partially oxidized species containing a single Cys36-Cys42 disulfide bond. Meanwhile the partially oxidized form requires a longer time to fold into the final oxidized species, having two disulfide bonds and this folding is a rate-limiting. The disulfide bond formation is crucial for maintaining G-CSF in properly folded tertiary structure and biologically active form (Lu et al., 1992).

The X-ray crystallographic structure of rhG-CSF expressed in *E.coli* has been solved to 3Å resolution (Hill et al., 1993). The protein has also been studied by 2D and 3D NMR spectroscopy (Zink et al., 1994). As shown in Figure 1.8., the structure of G-CSF is predominantly helical, with 104 of the 175 residues forming an antiparallel four-helix bundle with a left-handed twist. The helices of G-CSF are defined by residues 11-39 (helix A), 71-91 (helix B), 100-123 (helix C), and 143-172 (helix D). Another short helical element, mini-helix E, is comprised of residues 44-53. Despite little sequence similarity, G-CSF is structurally similar to the other five cytokines: four-helix bundle with up-up-down-down connectivity and two long crossover connections have been also observed for growth hormone, GM-CSF, IFN-β, IL-2, and IL-4 (Hill et al., 1993).

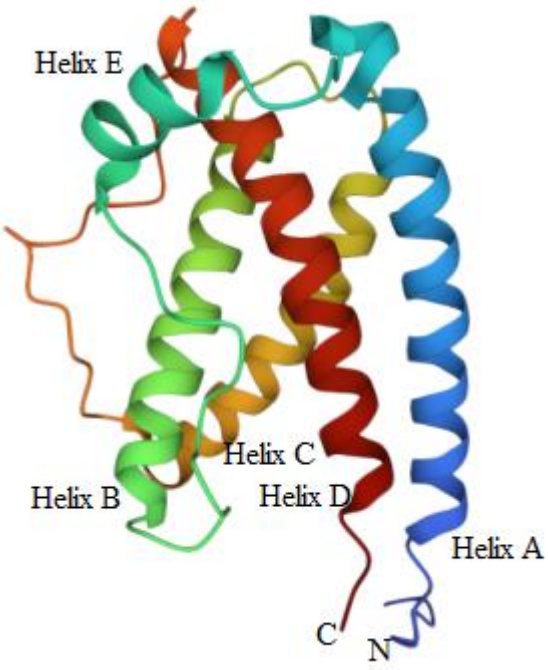

Figure 1.8. Structure of rhG-CSF monomer. The monomer representation is colored as a rainbow gradient, from blue (N terminus) to red (C terminus) PDB ID: 1GNC.

1.9.1.4 Human recombinant G-CSF as a drug

rhG-CSF has become the most widely used hematopoietic growth factor due to its efficacy against various forms of neutropenia, a blood condition characterized by low levels of neutrophils. Neutropenia is one of the most common side effects of chemotherapy and/or bone marrow transplantation. During anticancer chemotherapy, it is diagnosed in 20-40% and in 50-70% of patients with solid tumors and hematological malignancies, respectively (Bolis et al., 2013). The duration and severity of neutropenia are strongly related to the incidence of infections (Bolis et al., 2013).

Repeated administration of rhG-CSF has been determined to increase neutrophil production by ~10-fold (Lord et al., 1989; Price et al., 1996). In many countries, rhG-CSF has been approved for use in the prevention and/or treatment of chemotherapy-induced and severe chronic neutropenia, acute myeloid leukemia-related, and AIDS-related neutropenia. Administration of rhG-CSF in patients causes enhancement of functions such as phagocytosis, superoxide anion generation, chemiluminescence, bacterial killing, and antibody-dependent complement-mediated cytotoxicity (Gerber et al., 2000). Thus, the use of G-CSF may decrease morbidity and mortality related to

infectious complications and leads to safe exploitation of more intensive chemotherapy (Bolis et al., 2013). rhG-CSF is also often used in chemotherapy to induce leucopenia and mobilize progenitor cells for the purpose of autologous or allogeneic transplantation (Frampton et al., 1994; Welte et al., 1996).

Several different forms of rhG-CSF are available commercially for clinical use throughout the world:

- non-glycosylated, methionyl human G-CSF, expressed in *E. coli* (Filgrastim);
- a glycosylated form (possesses a sugar chain on Thr133) prepared in Chinese hamster ovary (CHO) cells (Lenograstim);
- n-terminal mutated filgrastim (Nartograstim);
- long-acting pegylated filgrastim (Pegfilgrastim);
- lipegfilgrastim.

Filgrastim (Neupogen; Amgen) was the first approved rhG-CSF that appeared on the biopharmaceutical market and launched to the American and European market. It was approved by FDA in February 1991 and originally was used to treat cancer patients receiving myelosuppressive chemotherapy. Unlike the endogenous G-CSF, which is O-glycosylated at the Thr^{133} position (Kubota et al., 1990), it contains no sugar moiety, but is otherwise very similar in its amino acid sequence and steric conformation; filgrastim contains only one an extra N-terminal methionine, which is needed for expression in *E. coli* and gives the stability to the molecule (Molineux, 2004). Although differs slightly, the potency of both filgrastim and naturally occurring G-CSF has been reported to be precisely the same (Souza et al., 1986). Currently, it is widely used in clinics and is effective in a number of treatment settings (Frampton et al., 1994; Welte et al., 1996).

Lenograstim is the second form of rhG-CSF that reached the market. Firstly, it appeared on the Asian market as Neutrogin (Chagai Pharmaceuticals); was approved by the Pharmaceuticals and Medicals Devices Agency (PMDA) of Japan in October 1991. Three years later it was launched to the European market as Granocyte (Chugai-Rhone-Poulenc) (Zielinska and Bialik, 2016). As filgrastim, lenograstim belongs to the first generation of G-CSF pharmaceuticals. It is expressed in a mammalian host cell system and is chemically identical to the natural human G-CSF. It consists of the same 174 amino acids and approximately 4% carbohydrate (molecular weight of 20.0 kDa). The sugar chain in lenograstim confers some benefits:
(1) provides the resistance to proteolysis or other inactivating factors present in serum (Kishita et al., 1992; Mire-Sluis et al., 1995);

(2) results in higher stability: lenograstim is stable at both room temperature and physiological pH versus filgrastim, which should be stored in a temperature between 2-8°C and at an acidic pH level (Oheda et al., 1988; Gervais et al., 1997).

On the other hand, the glycosylation does not seem to affect the biological activity of rhG-CSF: filgrastim and lenograstim were almost equivalent in terms of increasing neutrophils *in vivo* (Tanaka et al., 1997). However, the structural differences of these forms of rhG-CSF result in different G-CSF receptor stimulation: lenograstim and endogenous G-CSF have almost identical affinity for G-CSF receptors, meanwhile, filgrastim has shown an irregular binding to the receptor (Mendoza and Campo, 1996; Martin-Christin, 2001).

In vivo, lenograstim and filgrastim are eliminated strongly by the kidneys and via neutrophils/neutrophil precursors (Kuwabara et al., 1996; Roskos et al., 1998); the latter presumably involves binding of the molecule to the G-CSF receptor on the cell surface, internalization via endocytosis, and subsequent degradation inside the cells (Yang and Kido, 2011). This results in a short half-life (3.5 hours) and requires daily injections of pharmaceuticals to stimulate neutrophil recovery (e.g. 5 μg/kg/day of filgrastim/lenograstim for up to 2 weeks following chemotherapy). Although the competitive G-CSF products appeared on the market at a similar time and their therapeutic indications are much the same, filgrastim is dominated on the market. This may be due to marketing strategy, the higher production price of lenograstim based on mammalian cells, and mainly because that lenograstim was not introduced on the American market, which has the largest share of biopharmaceutics sales (Zielinska and Bialik, 2016).

Nartograstim was approved by PMDA of Japan in April 1994. It was originally developed by Kyowa Hakko Kiri, then marketed as Neu-up by Yakult Honsha. Nartograstim is the mutant growth factor by gene mutagenic techniques, in which amino acids were replaced at five positions of N-terminal region of rhG-CSF as follows: Thr^{1}, Leu^{3}, Gly^{4}, Pro^{5} and Cys^{17} to Ala^{1}, Thr^{3}, Tyr^{4}, Arg^{5} and Ser^{17}, respectively (Maruyama et al., 1998). It possesses greater potency (Okabe et al., 1990; Suzuki et al., 1992) and stability (Kuwabara et al., 1991) compared with filgrastim.

As next-generation G-CSF derivative, a pegylated form of G-CSF was developed in order to improve the pharmaceutical properties of filgrastim. Pegfilgrastim (Neulasta; Amgen) was approved by FDA for medical use in the USA in January 2002 and by the EMA in the European Union (EU) in August 2002, meanwhile, in Australia, it was introduced in September 2002. Pegfilgrastim is a pegylated form of filgrastim, where a 20 kDa linear PEG

has been covalently attached to the N-terminal residue of the filgrastim resulting in a molecule of 39 kDa (Figure 1.9.).

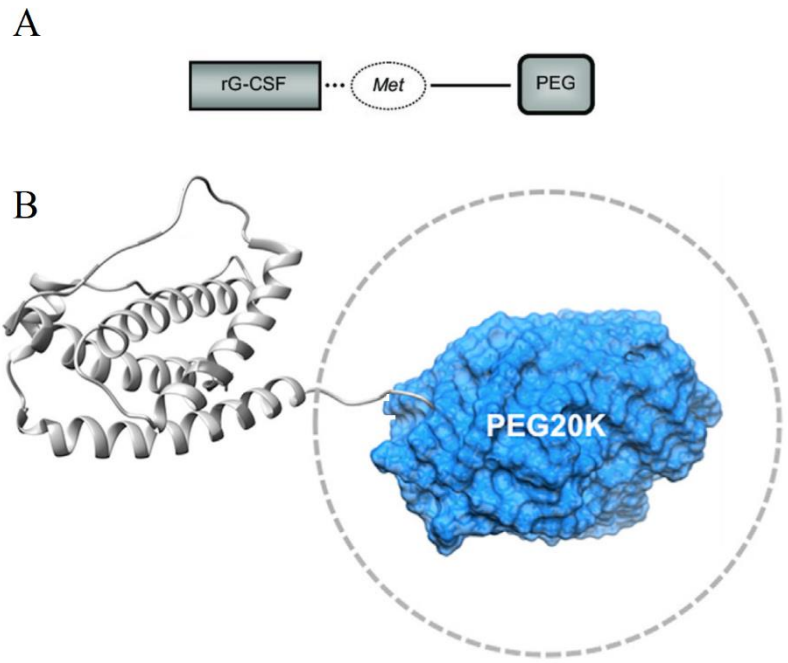

Figure 1.9. (A) Schematic structure and (B) model of Pegfilgrastim (N-terminus hidden in blue PEG model). Hatched lines indicate the size of water-containing PEG 20K (Abdolzade-Bavil et al., 2016, Musto et al., 2016).

However, unlike filgrastim, the pegfilgrastim molecule is too large to undergo glomerular filtration and therefore has minimal renal clearance. A sustained duration of action of pegfilgrastim (serum half-life approximately 42 hours) results in only one injection during one chemotherapy cycle, which is much more convenient for both patients and clinicians. Indeed, due to a neutrophil-mediated mechanism, pegfilgrastim remains in the blood for up to 16 days after a single dose administration: 2 days to reach peak neutrophil counts (Roskos et al., 2006) and at least 14 days from this peak to be eliminated by the same neutrophils (Aapro et al., 2011); this is pegfilgrastim is rapidly cleared as neutrophil counts recover (neutrophil-mediated, self-regulated clearance) (Waladkhani, 2004). Various studies of phase II and phase III clinical trials showed that a single administration of pegfilgrastim of 100 µg/kg is equivalent to 10-11 doses of 5 µg/kg/day of filgrastim in reducing the duration and incidence of severe neutropenia. Also, a single dose of 6 mg in patients (from 46 to 132 kg) is effective as a single dose of 5 µg/kg/day of filgrastim (Holmes et al., 2002; Green et al., 2003; Waladkhani, 2004). Nevertheless, filgrastim, in clinical practice, could be applied more

individually and flexibly, e.g. in dependence on the neutropenic risk of a patient (Ziepert et al., 2008).

Lipegfilgrastim (Lonquex, Teva Ltd), previously known as XM22, is another pegylated form of filgrastim, an alternative to pegfilgrastim, approved by the EMA in July 2013. As shown in Figure 1.10., different from pegfilgrastim, lipegfilgrastim is synthetized using a highly site-specific glyco-PEGylation technology, consisting of conjugation of single 20-kDa PEG to a previously attached glycan moiety; a PEG molecule is covalently attached, via a carbohydrate linker, to filgrastim at Thr^{134} (Abdolzade-Bavil et al., 2016, Musto et al., 2016). The novel pegylation process used in lipegfilgrastim results in different pharmacokinetic and pharmacodynamic profiles than pegfilgrastim (Mahlert et al., 2013; Scheckermann et al., 2013; Ratti et al., 2015). Despite that, the comparative clinical trials showed no significant difference in the efficiency and safety of both competitors (Hoggatt et al., 2015).

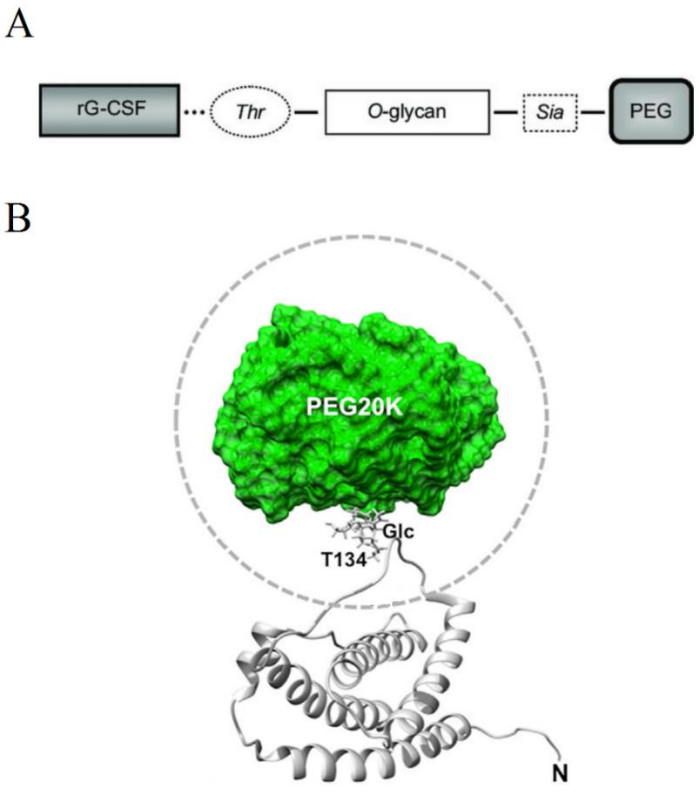

Figure 1.10. (A) Schematic structure and (B) a model of Lipegfilgrastim. Hatched lines indicate the size of water-containing PEG 20 K (Abdolzade-Bavil et al., 2016, Musto et al., 2016). Thr (T134) indicates threonine (threonine-134); O-glycan is the carbohydrate linker; Sia indicates sialic acid; Glc, glucosidic linker.

Currently, biosimilars are the other source of rhG-CSF used on the market along with the originator products. Biosimilars are copies of approved original therapeutic biologics with comparable quality, safety, and efficacy to a reference product whose patent protection has expired. The patent for filgrastim expired in Europe in 2006 and in the US in 2013 (Caselli et al., 2016). In the EU, starting from 2008, 9 filgrastim biosimilars were approved and 7 of them are currently in use, including Ratiograstim, Tevegrastim, Filgrastim Hexal, Zarzio, Nivestim, Grastofil, Accofil. Additionally, two have been approved in the USA: Zarxio (2015) and Nivestym (2018) (Konstantinidou et al., 2019). To date, no Lenograstim biosimilar is currently available on the market (Restelli et al., 2020). Meanwhile, the patent for pegfilgrastim (Neulasta) expired in the US in October 2015 and in Europe in August 2017 (Derbyshire, 2019). In Europe, there are 7 approved pegfilgrastim biosimilars: Pelgraz, Udenyca, Fulphila, Pelmeg and Ziextenzo, Grasustek, Cegfila. In the USA Udenyca, Fulphila, Ziextenzo, and Nyvepria have been approved (Konstantinidou et al., 2019). The introduction of biosimilar rhG-CSF products ensured a high degree of their competition on the market that resulted in a nearly 20% price decrease in all G-CSF products and consequently has expanded patient access to advanced therapies (Zielinska and Bialik, 2016).

1.9.2.Stem cell factor

1.9.2.1 Biology of SCF

Stem cell factor, also called the Steel factor, c-KIT ligand, or mast-cell growth factor, is another essential hematopoietic growth factor that elicits multiple biological effects. It is an important growth factor in normal hematopoiesis (Glaspy et al., 1996). This early acting hematopoietic protein stimulates the proliferation, differentiation, and survival of hematopoietic stem cells and progenitor cells by itself or by synergizing with other cytokines (Ulich et al., 1991; Molineux et al., 1991; McNiece et al., 1991; Brandt et al., 1992; Broudy, 1997). *In vitro,* SCF has direct hematopoietic colony-stimulating activity (Zsebo et al., 1990), can synergize with GM-CSF, G-CSF, IL-3, Epo on human target cells (McNiece et al., 1991), and also with IL-1, IL-3, IL-6, IL-7 on murine bone marrow cells (Zsebo et al., 1990).

In addition to hematopoietic effects, *in vivo* SCF has a major role in the development of melanocytes, germ cells, and intestinal pacemaker cells (Galli et al., 1994; Ali and Ali, 2007). Moreover, SCF promotes mast cell survival by suppressing apoptosis and, under acute conditions, inducing mast cell

hyperplasia (Iemura et al., 1994). The complete absence of SCF leads to embryonic anemia and lethality, so SCF is also identified as a critical regulator of erythropoiesis (Huang et al., 1990; Khodadi et al., 2016).

SCF is expressed throughout the body by stromal cells, fibroblasts, endothelial cells (Heinrich et al., 1993; Mansuroglu et al., 2009). The protein exists in membrane-bound form (mSCF) and is proteolytically released soluble form (sSCF) and both are biologically active. In human serum, the average concentration of sSCF is 3-4 ng/mL (Langley et al., 1993; Hsu et al., 1997).

The biologically active form of SCF is a non-covalently bond homodimer (Hsu et al., 1997). While sSCF is abundantly detected in circulation, sSCF mainly circulates primarily as biologically inactive monomeric molecules. Only 10% represent non-covalently bond dimers mediating the biological function (Hsu et al., 1997). Thus, it is suggested that the SCF receptor (c-KIT) activation primarily occurs through the membrane-associated forms of SCF, which can efficiently cross-link and activate c-KIT (Dastych and Metcalfe, 1994; Miyazawa et al., 1995; Rasky et al., 2020).

1.9.2.2 SCF receptor structure and activation

SCF exerts its multiple effects by interacting with its receptor c-KIT (KIT or CD117). C-KIT is expressed on cells that respond to SCF (Silva et al., 2006). It is expressed on hematopoietic progenitor cells and lymphoid lines (Geissler et al., 1988; Nocka et al., 1989; Aye et al., 1992; Godfrey et al., 1992), melanocytes (Nocka et al., 1989), germinal cells (Mayrhofer et al., 1987), mast cells (Nocka et al., 1989), eosinophils in the peripheral blood (Yuan et al., 1997), and sometimes on basophils (Columbo; 1992).

SCF receptor is a transmembrane glycoprotein, approximately 145-160 kDa in size, which is located at the white spotting (W) locus on chromosome 4q11–q12 in humans. It belongs to the type III receptor tyrosine kinase (RTK) family (Yarden et al., 1987). Similar to other types of RTKs, the SCF receptor is composed of (1) five extracellular immunoglobulin (Ig) like domains, which play a role in the binding of a ligand and receptor dimerization; (2) a single transmembrane domain; (3) and a cytoplasmic domain important for signaling transduction (Figure 1.11.). The cytoplasmic domain is composed of the juxtamembrane region, two subdomains, tyrosine kinase domain 1 and 2, separated by a kinase insert sequence and ends in a carboxy-terminus. Tyrosine phosphorylation of c-KIT mainly occurs either in the juxtamembrane region, the kinase insert, or the carboxy terminus (Lennartsson and Rönnstrand, 2012).

Figure 1.11. depicts activation mechanism of c-KIT by soluble SCF (Lennartsson and Rönnstrand, 2012). (1) In the absence of SCF, c-KIT exists in a monomeric dormant state (Roskoski, 2005). Soluble SCF exists as a non-covalently associated dimer and binds to cell surface c-KIT with a high affinity (Kd approx. 20-300 pM). (2) SCF homodimer binds to two monomeric c-KIT through contacts with the first three Ig-like domains in c-KIT extracellular region. Ligand-binding induces conformational changes that enable homotypic contacts between Ig-like domains 4 and 5 of two neighboring c-KIT molecules (Yuzawa et al., 2007). (3) This conformational change of c-KIT extracellular domain brings the intracellular tyrosine kinase domains into close proximity of each other and leads to their activation and subsequent transphosphorylation of the receptor (Lennartsson and Rönnstrand, 2012). The phosphorylated c-KIT functions as a docking site for signal transduction proteins containing SH2 and phosphotyrosine-binding domains (Roskoski, 2005) and then triggers the initiation of different signal-transduction pathways. These interactions activate the PI3-K, the Src, JAK-STAT, the phospholipase-C (PLC-γ), and MAPK (Cardoso et al., 2017).

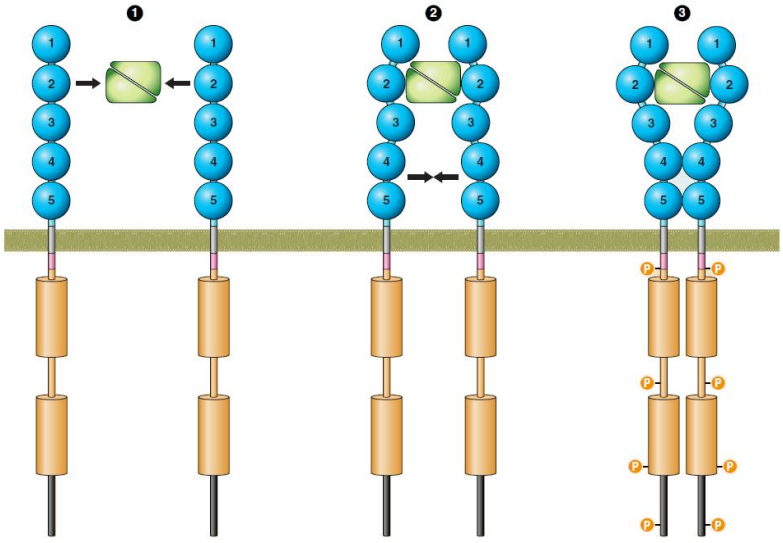

Figure 1.11. Schematic illustration of the SCF-induced c-KIT activation mechanism (Lennartsson and Rönnstrand, 2012)**.**

1.9.2.3 Molecular and structural aspects of human SCF

SCF was first identified and purified by Zsebo and colleagues (1990) and the human gene was first cloned at Amgen, Inc. (Thousand Oaks, Calif., USA). The gene for SCF in humans is located at the Steel (Sl) locus on

chromosome 12 at q22-q24 and has 9 exons (Ropers et al., 1989; Martin et al., 1990; Zsebo et al., 1990; Anderson et al., 1991). Although SCF sequence is highly conserved across different mammalian species (>75% identity), there are significant differences in inter-species receptor activation (Martin et al., 1990; Lev et al., 1992). It is supposed that the receptor-binding domains involve residues that are different between species (Jiang et al., 2000).

SCF is initially expressed as two alternatively spliced membrane-associated forms that include or exclude exon 6 that encodes a proteolytic cleavage site (Figure 1.12.). Membrane-associated forms of SCF contain three distinct domains: (1) extracellular domain responsible for recognizing and binding to c-KIT, (2) a hydrophobic transmembrane domain, (3) and an intracellular domain (Langley et al., 1994). The longer transcript, a 45 kDa, 248 amino acid glycoprotein, is rapidly cleaved to generate 31 kDa, 165-amino acid-soluble SCF (sSCF) that retains the c-KIT recognition domain. The shorter splice form, a 32 kDa, 220 amino acid glycoprotein, lacking exon 6, remains membrane-bound (Anderson et al., 1991; Flanagan et al., 1991; Dehbashi et al., 2017). Both sSCF and mSCF bind and activate c-KIT, however, there are some differences. sSCF induces transient activation and faster internalization and degradation of c-KIT whereas mSCF promotes persistent activity and prolongs the lifespan of the receptor (Miyazawa et al., 1995; Rönnstrand, 2004). The ratio of sSCF and mSCF isoforms varies considerably between tissues, indicating the tissue-specific regulation of SCF expression (Huang et al., 1992). Furthermore, mSCF and sSCF trigger different c-KIT downstream signaling pathways (Kapur et al., 2002).

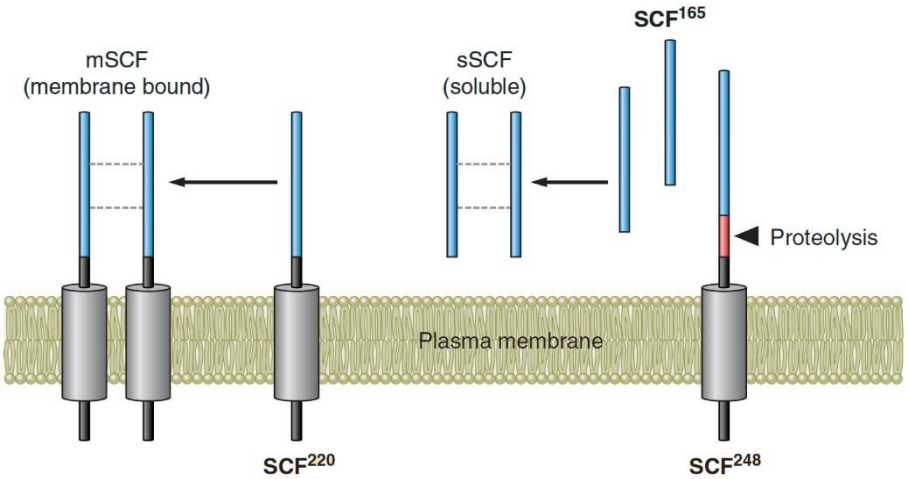

Figure 1.12. Schematic representation of SCF splice forms and protein proteolytic cleavage (Lennartsson and Rönnstrand, 2012)**.**

Each SCF monomer contains four Cys, which form two intra-chain disulfide bridges, Cys4-Cys89 and Cys43-Cys138. Disulfide bridges are required for SCF activity (Langley et al., 1992). The N-terminal 141 residues of SCF, SCF^{1-141}, have been identified as a functional core, which is sufficient for dimerization of SCF, receptor binding, and biologic activity (Langley et al., 1994). The CHO cell-derived recombinant human SCF is heavily glycosylated, about 30% carbohydrate by weight, with both N- linked and O-linked carbohydrates (Arakawa et al., 1991). Three of the four potential N-linked glycosylation sites, Asn^{65}, Asn^{93}, and Asn^{120}, have been identified in CHO-cell-derived human SCF (Lu et al., 1992). Asn^{65} and Asn^{93} are glycosylated in some, but not in all SCF molecules. Glycosylation of human SCF at these residues adversely affects *in vitro* SCF binding to c-KIT and lowers the biological activity. Meanwhile, Asn^{120} is always glycosylated, but this does not affect the binding of SCF to c-KIT (Lu et al., 1992).

The X-ray crystallographic structure of the recombinant human SCF^{1-141} expressed in *E. coli* has been solved at 2.2 A resolution. As shown in Figure 1.13., the SCF monomer presents a core composed of four α-helices (αA, αB, αC, αD) and two β-strands (β1 and β2) (Jiang et al., 2000). According to topologically, the protein belongs to the short-chain helical cytokine family (Rozwarski et al., 1994, Bazan, 1991). The core SCF dimer has its subunits arranged in a head-to-head manner with the opposed four-helix bundle axes nearly coincident. This gives the molecule an elongated shape (Jiang et al., 2000; Zhang et al., 2000).

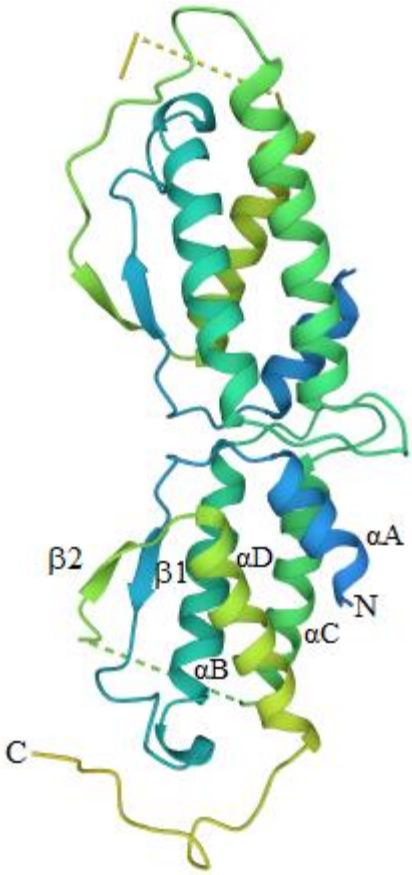

Figure 1.13. Overall structure of SCF dimer. PDB ID: 1SCF.

1.9.2.4 Clinical relevance of SCF alone or in combination with G-CSF

SCF certainly represents the most pleiotropic of the hematopoietic growth factors that have been introduced into the clinic. SCF has an extremely complex biology and multifactorial role to play in the development of several cell systems.

In vivo, recombinant rat SCF (rrSCF) treatment has been reported to stimulate hematopoietic recovery resulting in the survival of mice exposed to otherwise lethal doses of total body irradiation (Zsebo et al., 1992). Similar experiments in dogs receiving recombinant canine SCF (rcSCF) prior to irradiation resulted in protection from hematopoietic death (Schuening et al., 1993). Furthermore, recombinant human SCF (rhSCF) has been shown to improve the survival of human bone marrow progenitor cells after *in vitro* irradiation. Incubation with rhSCF prior to irradiation (0-300 cGy) resulted in an increase in both absolute colony number and surviving fraction for erythroid burst-forming units, granulocyte colony-forming units, and

granulocyte-macrophage colony-forming units as compared to cultures that did not contain SCF (Leigh et al., 1993). The SCF injection resulted in the enhanced cycling of hematopoietic progenitors, suggesting that such cycling may be the basis for the radioprotective effect of SCF (Bodine et al., 1993). The obtained results presume that SCF may be effective in reducing the duration or degree of myelosuppression associated with clinical radiation therapy. Also, the radioprotective effect of SCF allows higher doses of radiation to be delivered without increasing toxicity.

Besides stimulating hematopoietic cell expansion, SCF is a potent antiapoptotic factor for erythroid and megakaryocytic cells (Sui et al., 2000; Endo et al., 2001; Zeuner et al., 2003; Zeuner et al., 2007). It is essential for erythroid homeostasis; mice with loss-of-function mutations in SCF/c-KIT die before or shortly after birth due to severe macrocytic anemia (Chabot et al., 1988; Geissler et al., 1988; Huang et al., 1990; Zsebo et al., 1990). Conversely, gain-of-function c-KIT mutations lead to erythrocytosis compatible with myeloproliferative disorders (Bosbach et al., 2012). *In vitro*, SCF administration prevented chemotherapy-induced apoptosis of immature erythroblasts and megakaryocytes, which were an extremely sensitive target to cytotoxic agents (Zeuner et al., 2003; Zeuner et al., 2007). Also, treatment with this cytokine showed a myeloprotective effect *in vivo*; a constant presence of SCF during and after chemotherapy protected bone marrow erythroid and megakaryocytic precursors from chemotherapy-induced depletion and prevented the occurrence of anemia/thrombocytopenia in the peripheral blood of chemotherapy-treated mice (Bartucci et al., 2011). This indicates a potential use of SCF in the supportive therapy of cancer patients; in preventing drug-induced anemia and thrombocytopenia in cancer patients. Furthermore, it was demonstrated that SCF and G-CSF combined therapy has a clinical benefit on patients with aplastic anemia, who failed to respond to multiple cycles of immunosuppressive treatments (Usuki et al., 2006).

Many studies demonstrated the SCF synergy with G-CSF, which results in important biological responses. The combination of recombinant forms of both SCF and G-CSF has been shown to increase the rate of release of marrow neutrophils into the circulation in rats and causes a dramatic synergistic peripheral neutrophilia (Molineux et al., 1991; Ulich et al., 1991); a marked linear increase in the number of circulating neutrophils occurs between day 4 and 6 after the daily injections of SCF + G-CSF to $41.4 \pm 1.2 \times 10^3$ PMN/mm^3 as compared with $10.6 \pm 3.6 \times 10^3$ PMN/mm^3 in G-CSF-treated rats and $2.4 \pm 1.3 \times 10^3$ PMN/mm^3 in SCF-treated rats (Ulich et al., 1991). Furthermore, the combination of SCF and G-CSF showed beneficial effects in patients with severe congenital neutropenia (SCN). In case of reduced responsiveness of

mature myeloid progenitors to G-CSF in such SCN patients, myeloid progenitors responsive to the combination of SCF and G-CSF showed normal dose-response. SCF + G-CSF induced the formation of neutrophils almost to the same extent compared with cultures of normal bone marrow cells and therefore may prove to be more effective in the treatment of SCN patients, compared with G-CSF alone (Hestdal et al., 1993).

SCF synergy with G-CSF has important implications for *ex vivo* a long-term expansion of human primitive hematopoietic cells and for mobilization of peripheral blood progenitor cells (PBPC) for transplantation. In randomized studies, the combined use of SCF and G-CSF exerts a sustained mobilization effect that the increased number of peripheral blood (PB) CD34+ cells persist longer than does the effect of G-CSF alone (13 days versus 7 days) (Glaspy et al., 1997; Weaver et al., 1998; Facon et al., 1999; Shpall et al., 1999). Ancestim (Stemgen, Amgen) is the only rhSCF that reached the market and was approved for medical use in Australia, Canada, and New Zealand in 1999. It has an amino acid sequence identical to the endogenous SCF except for the addition of an N-terminal methionine (18.5 kDa of weight) retained after expression in *E. coli.*

Ancestim is indicated for use in combination with filgrastim (Neupogen) to affect a sustained mobilization of PBPCs and achieve a reduction in the number of aphereses required to reach the PBPC number target; with or without PBPC-mobilizing chemotherapy. However, its use is hindered by a possible life-threatening anaphylactic/anaphylactoid reaction and the resultant need to closely monitor patients after rhSCF administration. Ancestim is therefore used with filgrastim (Neupogen) to certain cancer patients who are at risk of inadequate PBPC mobilization and prophylactically medicated with H1 and H2 antihistamines and a bronchodilator (Amgen Inc., 2003).

Some studies have suggested that both SCF and G-CSF play roles in the central nervous system. SCF deficient mice showed a deficit in spatial learning and memory (Motro et al., 1996). Meanwhile, G-CSF deficient mice also show cognitive problems, impairments in long-term potentiation, and reductions in dendrites in the hippocampus (Diederich et al. 2009). Many studies have demonstrated that SCF and G-CSF combined therapy has beneficial effects on brain protection/repair and could be suggested as a new therapeutic strategy for stroke. It has been demonstrated that administration of SCF (Zhao et al., 2007) and G-CSF (Schäbitz et al., 2003; Shyu et al., 2004; Zhao et al., 2007) or SCF + G-CSF (Zhao et al., 2007; Toth et al., 2008) during the acute phase of experimental stroke reduces infarct size and ameliorates brain ischemia-induced neurological deficits. Also, SCF + G-CSF treatment during 10-20 days after focal brain ischemia also displays beneficial effects

on reduction in infarct size and improvement of functional outcome in a mouse model of ischemic stroke (Kawada et al., 2006). In addition to neuroprotection, SCF and G-CSF combined treatment has shown synergistic effects in enhancing neurite outgrowth (Su et al., 2007) and neural network reorganization in chronic stroke (Zhao et al., 2007).

2. MATERIALS AND METHODS

2.1. Materials

Table 2.1. The basic reagents

Reagent	Source
NaCl, Urea, EDTA, Acetic acid (glacial), Tris, KH_2PO_4, Na_2HPO_4 x $2H_2O$, $(NH_4)_2SO_4$, $MgSO_4$ x $7H_2O$, D(+)-glucose, $FeCl_3$ x $6H_2O$, $CaCl_2$, $ZnSO_4$ x $7H_2O$, $MnSO_4$ x H_2O, $CuSO_4$ x $5H_2O$, $CuSO_4$ x $5H_2O$, H_3BO_3, $CoCl_2$ x $6H_2O$, Na_2MoO_4 x $2H_2O$, $(NH_4)_2HPO_4$, Na_2HPO_4 x $2H_2O$, NaH_2PO_4 x $2H_2O$, NH_4HCO_3	Merck
ACN, NaOH	Honeywell
TEMED	Acros Organics
APS, Rotiphorese gel 30 (37.5:1), SDS pellets, Phosphate buffered saline (PBS) tablets	Carl Roth
Trifluoracetic acid (TFA)	Acros Organics
Tween 80, Tween 20, $C_6H_8O_7$ x H_2O, L-glutathione oxidized, Na_2SO_4	Sigma-Aldrich
1,4-dithiothreitol (DTT), isopropyl β-D-1-thiogalactopyranoside (IPTG)	Thermo Scientific

Table 2.2. The bacterial strains

***E. coli* strains**	**Genotype**	**Source**
BL21(DE3)	B F^- *ompT gal dcm lon hsd* $S_B(r_B^-m_B^-)$ λ(DE3 [*lacI lacUV5-T7p07 ind1 sam7 nin5*]) $[malB^+]_{K-12}(\lambda^S)$	Novagen/Thermo Fisher Scientific
BL21STAR(DE3)	F^- *ompT hsd*S_B ($r_B^-m_B^-$) *gal dcm rne131* (DE3)	Invitrogen/Thermo Fisher Scientific

Table. 2.3. The plasmid vectors

Plasmids	Properties	Source
pET21b(+)	AmpR, *lacI*, PT7*lac*, 5442 bp	Novagen/Thermo Fischer Scientific
pET28a(+)	KanR, *lacI*, PT7*lac*, 5368 bp	Novagen/Thermo Fischer Scientific
pET21b-GCSF-L2-GCSF	Two copies of the *g-csf* gene interspaced by linker L2 were cloned into pET21b(+) plasmid	This study
pET21b-GCSF-L7-GCSF	Two copies of the *g-csf* gene interspaced by linker L7 were cloned into pET21b(+) plasmid	This study

Table. 2.3. The plasmid vectors

Plasmids	Properties	Source
pET21b-GCSF-Lα-GCSF	Two copies of the *g-csf* gene interspaced by linker Lα were cloned into pET21b(+) plasmid	This study
pET28a-GCSF-Lα-GCSF	Two copies of the *g-csf* gene interspaced by linker Lα were cloned into pET28a(+) plasmid	This study
pET21b-SCF-Lα-GCSF	The *scf* and *g-csf* genes interspaced by linker Lα were cloned into pET21b(+) plasmid	This study
pET21b-GCSF-Lα-SCF	The *g-csf* and *scf* genes interspaced by linker Lα were cloned into pET21b(+) plasmid	This study

Table 2.4. The primers

Primer name	Sequence (5'-3')
GCSF-Nde	CATATGACACCTTTAGGACCTGCT
GCSF-Bam-Kpn	GGATCCGCATCCGGACGGCTGCGCAAGGTGGCGTAG
GCSF-Bam	GGATCCACACCTTTAGGACCT
GCSF-Hind	AAGCTTATTACGGCTGCGCAAGGTGGCG
SCF-Nde	GTGCATATGGAAGGTATCTGTCGT
SCF-Kpn-Bam	GGATCCAAGTCCGGAAGCAGCAACCGGCGGCAGC
SCF-Bam	TGGATCCGAAGGGATCTGCCGTAATCG
SCF-Hind	TAAGCTTAGGCTGCAACAGGGGG

All primers were purchased from Metabion (Germany).

Table 2.5. Resins

Resin	Source
DEAE Sepharose Fast Flow (FF), SP Sepharose FF, CM Sepharose FF, Sephadex G-25 Medium, Q Sepharose FF, Chelating Sepharose FF, Ni-Sepharose FF, Butyl Sepharose FF, Phenyl Sepharose FF	GE Healthcare
CHT ceramic hydroxyapatite, Type II	Bio-Rad Laboratories
Superdex 200	Fisher Scientific

Table 2.6. Recombinant proteins

Protein	Source
rhG-CSF (filgrastim)	Sicor Biotech/ Teva

rhSCF (#ab179506)	Abcam
Albumin standard (Bovine serum albumin, BSA)	Thermo Scientific
rhG-CSF receptor fused with Fc of human IgG1, GCSF-R (#ab83994)	Abcam
rhc-Kit fused with Fc of human IgG1, c-KIT (#ab219878)	Abcam
Protein-G	Sigma-Aldrich
HSA	Baxter Healthcare

Table 2.7. Bacteria culture media

Bacterial culture media	Composition
Luria-Bertani (LB) broth	10g/L peptone, 10g/L yeast extract, 5g/L NaCl
Flask medium	50 mM Na_2HPO_4, 20 mM KH_2PO_4, 20 mM NH_4Cl, 10 mM NaCl (from M9, Minimal Salts, 5x, Sigma-Aldrich), 0.5% (w/v) yeast extract, 0.4% (w/v) glucose (20% (w/v) stock solution is prepared separately and then added to M9 media), 2 mM $MgSO_4$ x $7H_2O$ (added separately from 1 M stock solution)
Preinoculum medium I	100 mM Na_2HPO_4, 40 mM KH_2PO_4, 40 mM NH_4Cl, 20 mM NaCl (from M9, Minimal Salts, 5x), 0.4% (w/v) glucose, 1% (w/v) yeast extract, 0.14 mM $MgSO_4$ x $7H_2O$
Bioreactor medium I	50 mM Na_2HPO_4, 20 mM KH_2PO_4, 20 mM NH_4Cl, 10 mM NaCl (from M9, Minimal Salts), 0.5% (w/v) yeast extract, 7% (w/v) glucose, 8 mM $MgSO_4$ x $7H_2O$
Feed medium I	30% (w/v) glucose, 18% (w/v) yeast extract, 67 mM $MgSO_4$ x $7H_2O$
Preinoculum medium II	15 mM KH_2PO_4, 105 mM Na_2HPO_4 x $2H_2O$, 25 mM $(NH_4)_2SO_4$, 2 mM $MgSO_4$ x $7H_2O$, 1.63% (w/v) glucose
Stock solution of microelements	111 mM $FeCl_3$ x $6H_2O$, 36 mM $CaCl_2$, 23 mM $ZnSO_4$ x $7H_2O$, 9 mM $MnSO_4$ x H_2O, 12 mM $CuSO_4$ x $5H_2O$, 11 mM H_3BO_3, 5 mM $CoCl_2$ x $6H_2O$, 1.2 mM Na_2MoO_4 x $2H_2O$
Bioreactor medium II	114 mM KH_2PO_4, 35 mM $(NH_4)_2HPO_4$, 9 mM $C_6H_8O_7$ x H_2O, 2 mM $MgSO_4$ x $7H_2O$, 3.5% (w/v) glucose
Feed medium II	70% (w/v) glucose, 84 mM $MgSO_4$, 3.4 µL/mL stock solution of microelements (added separately)

Table 2.7. Bacteria culture media

Bacterial culture media	Composition

All media and stock solutions were sterilized for 20 min. at 121ºC.

Laboratory animals

Age-matched healthy female rats (8-12 weeks old) were used in all experimental procedures. The study with laboratory animals was approved by the State Food and Veterinary Service of the Republic of Lithuania (approval no. 0182).

Animal experiments were conducted in accordance with the Lithuanian laws for animal protection or according to institutional guidelines at Vilnius University. All animal care and use protocols adhere to national and European (Directive 2010/63/EU) laws and regulations as well as European Federation of Animal Science Associations (FELASA, http://www.felasa.eu/).

2.2. Methods

2.2.1. Generation of three variants of dimeric G-CSF proteins

All cloning procedures were performed by Dr. M. Plečkaitytė (VU Life Sciences Center (LSC), Institute of Biotechnology). The DNA fragment coding for the mature isoform B with an extra N-terminal methionine of G-CSF protein (Genbank accession no. NM_172219) was amplified using a synthetic cDNA gene of human G-CSF by polymerase chain reaction (PCR) to introduce NdeI at the 5'-end and Kpn2I and BamHI sites at the 3'-end of the PCR fragment using GCSF-Nde and GCSF-Bam-Kpn primers (Table 2.4.). The obtained PCR product was verified by sequencing, then digested with Kpn2I and BamHI restriction enzymes (all enzymes were purchased from Thermo Fisher Scientific, Vilnius, Lithuania) and fused with the Kpn2I/BamHI digested DNA fragment containing the Lα linker coding sequence ($SGLEA(EAAAK)_4ALEA(EAAAK)_4ALEGS$) (Arai et al., 2001). The resulting construct included the first copy of the *gcsf* gene fused with the linker coding sequence. The second copy of the *g-csf* gene was amplified to introduce BamHI and HindIII sites at the 5'- and 3'- ends of the PCR fragment using primers GCSF-Bam and GCSF-Hind, respectively. The construct obtained by fusion of the two copies of the G-CSF coding gene interspaced by the Lα linker was named GCSF-Lα-GCSF. To introduce the L2 linker (coding for $(Ser\text{-}Gly_4)_2$-Ser) and the L7 linker (coding for $(Ser\text{-}Gly_4)_7$-Ser), the DNA coding for GCSF-Lα-GCSF was further digested with Kpn2I and BamHI and

fused with the DNA fragments coding for the respective linker sequences. The constructs obtained by fusion of the two *g-csf* gene copies interspaced by the L2 or L7 linker sequences were named GCSF-L2-GCSF and GCSF-L7-GCSF, respectively. The DNA constructs for GCSF-Lα-GCSF, GCSF-L2-GCSF, and GCSF-L7-GCSF were digested with NdeI and HindIII restriction endonucleases and cloned into expression vectors pET21b(+) and pET28a(+), respectively. The resulting plasmids were transformed into *E. coli* BL21(DE3).

2.2.2. Generation of SCF-Lα-GCSF and GCSF-Lα-SCF heterodimers

Two recombinant proteins SCF-Lα-GCSF and GCSF-Lα-SCF were generated by a covalent fusion of SCF and G-CSF molecules. The DNA fragment coding for a human SCF and Lα linker was synthesized at Integrated DNA Technologies (USA). The *scf* gene having NdeI at the 5′-end and Kpn2I/BamHI sites at the 3′-end was amplified using SCF-Nde and SCF-Kpn-Bam primers (Table 2.4.). All amplified sequences were verified by sequencing. The DNA fragment was fused with the Kpn2I/BamHI digested DNA fragment coding for the Lα linker sequence $SGLEA(EAAAK)_4ALEA(EAAAK)_4ALEGS$ (Arai et al., 2001). The synthetic human *g-csf* gene (Integrated DNA Technologies, Coralville, IA, USA) having the BamHI and HindIII sites at the 5′- and 3′-ends, respectively, was fused to the 3′-end of the linker Lα sequence. The construct obtained by a fusion of the *scf* and *g-csf* genes interspaced by the linker Lα sequence was named SCF-Lα-GCSF.

The *scf* gene was amplified to introduce the BamHI and HindIII sites at the 5′-and 3′-ends of the PCR fragment using primers SCF-Bam and SCF-Hind (Table 2.4.), respectively. The copy of the human *g-scf* gene was cut out with the enzymes BamHI and HindIII from the plasmid bearing two copies of the *g-csf* gene interspaced by the Lα sequence. The BamHI/HindIII digested DNA fragment coding for SCF was fused with the DNA construct bearing the *g-scf* gene and the Lα linker sequence. The resulting construct was named GCSF-Lα-SCF.

The DNA fragments coding for SCF-Lα-GCSF and GCSF-Lα-SCF were cloned into the expression vector pET21b(+). The resulting plasmids pET21-SCF-Lα-GCSF and pET21-GCSF-Lα-SCF were transformed into *E. coli* BL21(DE3) and BL21(DE3)STAR strains, respectively.

The recombinant *E. coli* strains were stored at -70ºC in LB broth supplemented with 15% glycerol.

2.2.3.Expression of recombinant fusion proteins in *E. coli*

A small-scale production

To develop a purification scheme for each protein, a small-scale synthesis was carried out. One-µL of frozen cultures of GCSF-L2-GCSF, GCSF-Lα-GCSF, GCSF-L7-GCSF, SCF-Lα-GCSF or GCSF-Lα-SCF was transferred to 5 mL of LB medium supplemented with 100 µg/mL of ampicillin (Roche). Bacteria were grown overnight at 37°C with shaking at 250 rpm. Four-mL of overnight culture was inoculated into a 1 L flask containing 400 mL medium (Table 2.7.) supplemented with 100 µg/mL of ampicillin. The cells were cultivated for 3 hours at 37ºC with shaking until optical density (OD_{600}) reached 0.8-1.0. The target gene expression was induced by the addition of 1 mM IPTG and then cells were cultivated for 3 hours at 37ºC with shaking. The cells were collected by centrifugation at 4,000 x g at 4ºC. The cell pellet was stored at -20ºC.

A large-scale production of GCSF-Lα-GCSF

Large-scale production of GCSF-Lα-GCSF in a bioreactor was performed by Ž. Dapkūnas (VU LSC, Institute of Biotechnology). The large-scale synthesis of GCSF-Lα-GCSF was carried out in a Biostat B5 L bioreactor (Sartorius Stedim Biotech, Germany) containing a 4 L initial volume in fed-batch mode using two different growth media.

1. Large-scale production of GCSF-Lα-GCSF in M9 minimal media supplemented with yeast extract. Sixty-µL of the frozen culture of GCSF-Lα-GCSF was transferred to a 250 mL flask containing 60 mL of pre-inoculum medium I (Table 2.7.). The culture was incubated for 16-18 hours at 37 ºC. Fifty-mL of the overnight culture was inculated into the 4 L of bioreactor medium I in a 5 L bioreactor. Throughout the fermentation process, temperature and dissolved oxygen tension (DOT) concentration were monitored and maintained at set points of 37ºC and 30%, respectively. The pH was controlled at pH 6.8 by the addition of 25% NH_4OH. The addition of feed medium I was started at a constant rate of 15 g/h when the batch glucose was depleted. When OD_{600} was around 15, the expression of GCSF-Lα-GCSF was induced by the addition of 1 mM IPTG and then cells were cultivated for 3 hours at 37°C. Cells were collected by centrifugation at 4,000 x g at 4ºC and stored frozen at -20 ºC.

2. Large-scale production of GCSF-Lα-GCSF in the chemically defined medium. Sixty-μL of the frozen culture of GCSF-Lα-GCSF was transferred to a 250 mL flask containing 60 mL of pre-inoculum medium II (Table 2.7.) supplemented with microelements (5 μL of stock solution). The culture was incubated for 21-22 hours at 37°C. Fifty-mL of overnight culture was inoculated into the 4 L of bioreactor medium II, supplemented with microelements (1.17 mL of stock solution) in a 5 L bioreactor. Throughout the fermentation process, temperature and DOT concentration were monitored and maintained at set points of 37ºC and 30%, respectively. The pH was controlled at pH 6.8 by the addition of 25% NH_4OH. The addition of feed medium II was started at a constant rate of 15 g/h when the batch glucose was depleted. When OD_{600} reached 20, the expression of GCSF-Lα-GCSF was induced by the addition of 1 mM IPTG and then the cells were cultivated grown for 3 hours at 37°C. Cells were collected by centrifugation at 4,000 x g at 4ºC and stored frozen at -20ºC.

2.2.4.Isolation and purification of inclusion bodies

The harvested biomass was suspended (10 mL/g of biomass) in 0.1 M Tris-HCl buffer (pH 7.0), containing 5 mM EDTA, 1 mM PMSF, 0.1% (w/v) Triton X-100 (Sigma-Aldrich, USA). Prior to cell lysis, β-mercaptoethanol was added to the cells at a final concentration of 100 mM. Two different methods were used for cells lysis. The cells obtained from a small-scale production were disrupted by sonication on ice using ultrasonic homogenizer (Sonopuls Bandelin, Germany) at 70% amplitude and the cycles consisted of 30 s sonication followed by 30 s recovery. The cells obtained from a large-scale production of GCSF-Lα-GCSF were disrupted by three repeated disruption cycles at 4ºC using a high pressure homogenizer (APV 2000; APV homogenizers AS, Denmark) at a pressure of 800 bar. Subsequently, both bacterial lysates were clarified by centrifugation at 30,000 × g and 4ºC for 25 min. The pellets containing of insoluble inclusion bodies (Ibs) washed twice with buffer (20 mM Tris-HCl, pH 8.0, 1 M NaCl), containing 0.1% Tween 80 and once with 20 mM Tris-HCl (pH 8.0) solution.

2.2.5. Purification of recombinant fusion proteins

Purification of recombinant fusion proteins were performed at 2-8ºC using the ÄKTA pure 150 system (GE Healhcare, Uppsala, Sweden).

Purification of the G-CSF homodimers

Various protocols were used to find out the optimal solubilization, refolding and purification conditions for each G-CSF homodimer. A flowchart of the purification steps and tested conditions is presented in Figure 3.3.

The optimized purification scheme for G-CSF homodimers included the following steps:

1. Solubilization. The washed inclusion bodies were solubilized in urea containing buffer (8 M urea, 1 mM EDTA, 50 mM Tris-HCl, pH 8.0). To reduce the disulfide bonds within the proteins, DTT was added to a final concentration of 0.5-5 mM. After centrifugation at 30,000 × g for 25 min at 4°C, the supernatants containing the solubilized Ibs were collected.
2. Refolding. Refolding of recombinant proteins was initiated by a rapid dilution of the denatured-reduced proteins into buffer (50 mM Tris-HCl, 1 mM EDTA, pH 8.0) that contained oxidized glutathione (GSSG), until the concentration of 3 M urea and 0.5 mg/mL protein were reached. The final molar ratio of GSSG to DTT was 5:1 for GCSF-L2-GCSF and 6:1 for GCSF-L7-GCSF and GCSF-Lα-GCSF. Refolding of homodimers was carried out for 24 h at 4°C with gentle stirring. The solution was then centrifuged for 25 min at 30,000 × g at 4ºC.
3. DEAE Sepharose chromatography. The refolded recombinant proteins were loaded onto a DEAE Sepharose Fast Flow column (GE Healthcare, Uppsala, Sweden) that was equilibrated with 10 mM Tris-HCl (pH 7.5) and contained 20 mM NaCl. Two-step elution was performed at NaCl concentrations of 0.08 and 0.45 M. Fractions containing G-CSF homodimers were collected and diluted with 20 mM sodium acetate to reach a pH of 5.4 and a conductivity of 3.2 mS/cm.
4. SP or CM Sepharose chromatography:

   a) SP Sepharose chromatography. The solutions containing GCSF-Lα-GCSF or GCSF-L2-GCSF proteins were applied to the SP Sepharose Fast Flow column, equilibrated with 20 mM sodium acetate (pH 5.4), 20 mM NaCl. The target proteins were eluted with a

NaCl gradient using 20 mM sodium acetate (pH 5.4) that contained 450 mM NaCl.

b) CM Sepharose chromatography. The solution containing GCSF-L7-GCSF was applied onto a CM Sepharose Fast Flow column. The target protein was eluted with a NaCl gradient using 20 mM sodium acetate (pH 5.4) that contained 450 mM NaCl.

5. Sephadex G-25 chromatography. Recombinant proteins were subsequently loaded onto a Sephadex G-25 Medium column that was equilibrated with 10 mM acetic acid/NaOH buffer, pH 4.0.
6. Formulation and storage. Fractions containing the homodimeric G-CSF proteins were subsequently pooled and D-sorbitol and Tween 80 were added to reach a final concentration of 5% and 0.0025%, respectively. The protein solutions were filtered through 0.2 μm Acrodisc Units with Mustang E membrane (Pall Corporation) for endotoxin removal. The purified protein solutions were stored at 4ºC.

Purification of heterodimeric proteins composed of SCF and G-CSF

A set of experiments was done to find out the optimal solubilization, refolding, and purification conditions for SCF-Lα-GCSF protein. A flowchart of the purification steps and tested conditions is presented in Figure 3.16. The same purification scheme was applied for SCF-Lα-GCSF, and GCSF-Lα-SCF proteins.

The optimized purification scheme for heterodimers contains the following steps:

1. Solubilization. The washed pellets of SCF-Lα-GCSF and GCSF-Lα-SCF were solubilized in urea containing buffer (8 M urea, 1 mM EDTA, 50 mM Tris-HCl, pH 8.0). To reduce the disulfide bonds within the proteins, DTT was added to a final concentration of 0.5 mM. The solution was stirred at 4ºC for 2 hours and centrifuged at 30,000 × g for 25 min at 4ºC. The supernatants containing the solubilized Ibs were collected.
2. Refolding. Refolding of the recombinant proteins was initiated by rapid dilution of the denatured-reduced proteins into the 50 mM Tris-HCl (pH 8.0) buffer supplemented with GSSG until the concentration of 2 M urea was reached. The final molar ratio of GSSG to DTT was kept 1:5 in the mixture. The renaturation reaction was carried out for 24 h at 4ºC with gentle stirring. The solution was then centrifuged at 30,000 × g for 25 min.

3. DEAE Sepharose chromatography. The refolded recombinant proteins were loaded onto a DEAE Sepharose FF column equilibrated with 50 mM Tris-HCl (pH 7.5). The proteins were eluted by a step-wise elution steadily increasing the concentration of NaCl from 0 to 0.5 M.
4. Mixed-mode chromatography. The collected fractions containing recombinant proteins were subsequently loaded onto a CHT ceramic hydroxyapatite, Type II column, equilibrated with a 50 mM Tris-HCl buffer (pH 7.2). The column was washed with 5 mM NaH_2PO_4 (pH 7.2) containing 0.1 M NaCl, and the proteins were eluted using a gradient of NaH_2PO_4 (5 to 500 mM). The target protein-containing fractions were pooled and diluted with 20 mM sodium acetate to pH 4.7.
5. SP Sepharose chromatography. Recombinant proteins were subsequently loaded onto an SP Sepharose FF column equilibrated with 20 mM sodium acetate (pH 4.7). The column was washed with the equilibration buffer and the proteins were eluted with the NaCl gradient using the equilibration buffer supplied with 500 mM NaCl.
6. Sephadex G-25 chromatography. Recombinant proteins were subsequently loaded onto a Sephadex G-25 Medium column that was equilibrated with 10 mM acetic acid/NaOH buffer, pH 4.0.
7. Formulation and Storage. The protein solution was filtered through 0.2 μm Acrodisc Units with Mustang E membrane (Pall Corporation) for endotoxin removal. The purified protein solutions were stored at 4ºC.

2.2.6. Analytical methods

Table 2.8. Analytical methods used in this study

Quality attribute	First line-methods	Complementary methods
Protein content	Bradford assay	UV spectroscopy
Purity and impurities	SDS-PAGE and Reverse-phase high-performance chromatography (RP-HPLC)	Bacterial endotoxins and Size-Exclusion HPLC (SEC)
Identity	Western-blot and High-performance liquid chromatography/electrospray ionization mass spectrometry (HPLC/ESI-MS)	Peptide Mapping by RP-HPLC

Table 2.8. Analytical methods used in this study

Quality attribute	First line-methods	Complementary methods
Molecular weight	SE-HPLC	HPLC/ESI-MS
Disulfide bond assignment	RP-HPLC	Fluorescence Spectroscopy

Determination of protein content

The concentration of proteins after each stage of purification was determined by the Bradford assay (Bradford, 1976). After the final purification step, the protein concentration was determined by measuring the absorbance of aromatic amino acids at 280 nm and subtracting the absorbance at 340 nm due to light-scattering. Both Bradford and UV absorbance analysis were determined using a UV-VIS spectrophotometer Specord S 600 (analytic Jena GmbH, Germany).

Methods for assessing the purity of recombinant proteins

The purity of recombinant fusion proteins after each stage of purification was assessed by both SDS-PAGE and RP-HPLC analysis. RP-HPLC was carried out using an Alliance e2695 HPLC system (Waters, USA) with UV absorbance detection at 215 nm. Endotoxins, as process-related impurities, were determined using the Pyrotell Gel-Clot endotoxin testing kit.

SDS-PAGE

SDS-PAGE was performed according to the method of Laemmli (Laemmli, 1970) using the 4% stacking and 15% separating gels. The gels were stained using PageBlue Protein Staining Solution (Thermo Scientific).

RP-HPLC analysis of G-CSF homodimers

The GCSF-Lα-GCSF, GCSF-L2-GCSF, and GCSF-L7-GCSF proteins obtained from Ibs extracts, their folding intermediates, and fractions derived from the chromatography columns were analyzed on a C18 reverse-phase column (Hi-Pore RP-318, 4.6 x 250 mm, Bio-Rad, USA). The column was equilibrated with mobile phase A (0.1% trifluoroacetic acid (TFA) in water), and separation of the proteins was performed via gradient and isocratic elution with mobile phase B (10% water, 89.9% acetonitrile, and 0.1% TFA) at a flow

rate of 1 mL/min, as follows: (1) initial equilibration with 100% A, (2) 5-min gradient to 55% B, (3) 50-min gradient to 80% B, (4) 1-min gradient to 90% B, (5) 4-min isocratic elution at 90% B, (6) 2-min gradient to 0% B, and (7) 12-min isocratic elution at 0% B.

The purified G-CSF homodimers collected after Sephadex G-25 Medium were also analyzed with RP-HPLC using a C18 reverse-phase column (Zorbax SB-C18, 4.6 x 250 mm, Agilent Technologies, USA). Mobile phases A (0.1% TFA in water) and B (0.1% TFA in acetonitrile) were used for gradient and isocratic elution at a flow rate of 0.9 mL/min, as follows: (1) initial equilibration at 100% A, (2) 2-min gradient to 50% B, (3) 3-min gradient to 53% B, (4) 38-min gradient to 67% B, (5) 2-min gradient to 81% B, (6) 3-min isocratic elution at 81% B, (7) 2-min gradient to 0% B, and (8) 5-min isocratic elution at 0% B. For both elution conditions, the temperature of the columns was maintained at 30°C and eluted proteins were detected at 215 nm.

RP-HPLC analysis of heterodimers

The SCF-Lα-GCSF and GCSF-Lα-SCF proteins from Ibs extracts, their folding intermediates, and fractions derived from the chromatography columns were analyzed on a C18 reverse-phase column (Zorbax 300SB-C18, 4.6 × 250 mm; Agilent Technologies, USA). The chromatographic separation of the proteins was performed in acetonitrile gradient (mobile phase A – 0.1% TFA in water, mobile phase B – 9.9% water, 90% acetonitrile, and 0.1% TFA) at a flow rate of 1 mL/min, as follows: (1) initial equilibration at 10% B, (2) a 5-min gradient to 58% B, (3) a 74-min gradient to 81% B, (4) a 3-min gradient to 90% B, (5) a 4-min isocratic elution at 90% B, (6) a 3-min gradient to 10% B, and a final (7) 5-min isocratic elution at 10% B. The temperature of the column was maintained at 30ºC.

Endotoxin quantification

The presence of endotoxins in purified protein preparations was detected using the Pyrotell Gel-Clot endotoxin testing kit (Cape Cod, USA) according to the manufacturer's instructions. The sensitivity of the Limulus amebocyte lysate-based assay was 0.125 EU/mL. The determined endotoxin level in the purified proteins was ≤0.25 EU/mL or ≤0.29 EU/mg.

Protein identification methods

1. Western-blot

The purified recombinant proteins and monomeric G-CSF and SCF resolved by SDS-PAGE were transferred onto the Immobilon-PVDF membranes (Merck Millipore, Tullagreen, Carrigtwohill, Cork, Ireland). The wet protein transfer was done at 150 V for 90 min. After blotting, the membranes were blocked with 5% BLOT-QuickBlocker (Calbiochem, USA) in PBS supplemented with 0.1% Tween 20 (PBS-T) for 2 h. The blocking solution was removed and the membranes were incubated for 1 h either with 1:2,000 PBS-T diluted monoclonal antibody (clone no. 5D7) against human G-CSF (Abcam, UK) or 1:1,000 diluted polyclonal antibody against human SCF (Invitrogen/Thermo Fisher Scientific, USA). The membranes were washed with PBS-T and then incubated for 1 h either with 1:4,000 diluted rabbit anti-mouse IgG conjugated to horseradish peroxidase (Invitrogen/ThermoFisher Scientific) or 1:1,000 diluted goat anti-rabbit IgG conjugated to horseradish peroxidase (Invitrogen/Thermo Fisher Scientific). The enzymatic reaction was developed using a tetramethylbenzidine chromogenic substrate (Sigma-Aldrich, USA).

2. Molecular mass determination

The molecular mass of recombinant fusion proteins was determined by the integrated method of high-performance liquid chromatography/electrospray ionization mass spectrometry (HPLC/ESI-MS). The molecular mass determination experiments were performed by A. Rukšėnaitė (VU LSC, Institute of Biotechnology). The protein samples were diluted with an aqueous solution containing 1% formic acid (FA) and 2% acetonitrile at a concentration of 0.1 μg/μL. The samples were loaded onto a C8 reverse-phase column (Poroshell 300SB-C8, 2.1×75 mm; Agilent Technologies). Chromatographic separation of proteins was performed in an acetonitrile gradient (mobile phase A – 1% FA in water, mobile phase B – 1% FA in acetonitrile) at a flow rate of 0.4 mL/min on an Agilent 1290 Infinity HPLC system coupled to an Agilent Q-TOF 6520 mass spectrometer (Agilent Technologies), as follows: (1) initial equilibration at 2% B, (2) a 5-min gradient to 98% B, (3) a 1-min isocratic elution at 98% B, (4) a 2 min gradient to 2% B, and a final (5) a 1-min isocratic elution at 2% B. The temperature of the column was maintained at 30 ºC. The mass analyzer was set to 100-3,200 m/z range in a positive ionization mode. The data were analyzed with Agilent MassHunter Workstation Software.

3. Peptide mapping by RP-HPLC

Peptide mapping was done according to a slightly modified method described previously (Council of Europe, European Pharmacopea, 2009). Purified GCSF-Lα-GCSF and G-CSF monomer were dissolved in 50 mM Na_2HPO_4 (pH 8.0) buffer at a concentration of 25 µg/mL. Endoproteinase Glu-C (Sigma-Aldrich) was added to the protein solution at a concentration of 2.5 µg/mL and digestion was performed for 18 h at 37°C. The separation of peptides was performed on a Hi-Pore RP-318 column (Bio-Rad) via acetonitrile gradient (mobile phase A – 94.5% water, 5% acetonitrile, and 0.05% TFA, mobile phase B – 5% water, 94.5% acetonitrile, and 0.05% TFA) at a flow rate of 1 mL/min as follows: (1) initial equilibration at 3% B, (2) 12-min gradient to 6% B, (3) 34-min gradient to 34% B, (4) 29-min gradient to 90% B, (5) 8-min isocratic elution at 90% B, (6) 2-min gradient to 3% B, and (7) 12-min isocratic elution at 3% B. The temperature of the column was maintained at 50ºC.

Size-Exclusion HPLC

The purified fusion proteins and monomeric G-CSF and SCF were injected into a TSK-gel G3000 SWXL column (7.8×300 mm, 5 µm, Tosoh Bioscience, Japan) connected to an Alliance e2695 HPLC system (Waters). The proteins were eluted with an isocratic mobile phase of 0.1 M Na_2HPO_4, 0.1 M Na_2SO_4 (pH 7.2) and a flow rate of 0.6 mL/min (22ºC). The molecular weight of G-CSF homodimers was estimated based on the retention time of the Low molecular weight standards (GE Healthcare) and heterodimers using Protein standard mix for SEC (Sigma-Aldrich).

Assignment of disulfide bonds in purified recombinant proteins

1. Fluorescence spectroscopy

The fluorescence emission spectra of GCSF-Lα-GCSF and G-CSF monomer were recorded at 290-420 nm with an excitation at 280 nm on a FluoroMax-4 spectrofluorometer (Horiba Jobin Yvon Inc., USA) using a 1-cm path-length cuvette. The protein samples were diluted with 10 mM sodium citrate (pH 3.2 or 7.5) containing 100 mM NaCl to a concentration of 0.14-0.16 mg/mL. Fluorescence signals were recorded after mixing and standing the solutions for 5 min at room temperature.

2.2.7.Activity of recombinant fusion proteins

The activity of recombinant homo- and heterodimers were assessed using TIRE and *in vivo*, and *in vitro* bioassays (Table 2.9.).

Table 2.9. Activity methods used in this study

First line-methods	Complementary methods
Total internal reflection ellipsometry (TIRE)	
In vitro biological activity	*In vivo* biological activity

Total internal reflection ellipsometry measurements

The binding kinetics assays were performed by total internal reflection ellipsometry. All TIRE procedures were performed at the Center for Physical Sciences and Technology (FTMC) and the binding kinetics were investigated by Prof. Dr. Z. Balevičius (FTMC), Dr. I. Plikusienė (FTMC), Dr. J. Talbot (Sarbonne Universitè, Centre National de la Recherche Scientifique), Dr. A. Stirkė (FTMC) and Dr. L. Tamošaitis (VU, Institute of Chemistry). GCSF-R and c-KIT used for TIRE were chimeric proteins. The extracellular domain of the receptors was fused to the Fc region of human immunoglobulin G1 (IgG1). The experimental setup consisted of a spectral ellipsometer M-2000X, J. A. Woollam (Lincoln, USA) with a rotating compensator, BK7 70° glass prism and 1 mm thick BK7 glass slide covered by a layer of chromium and gold (BK7-glass/Cr-Au, XanTec Bioanalytics GmbH, Germany). During the TIRE measurements, differently modified BK7-glass/Cr-Au were attached to the BK7 70° glass prism by refractive index matching fluid (Cargille, USA) (Figure 2.1.).

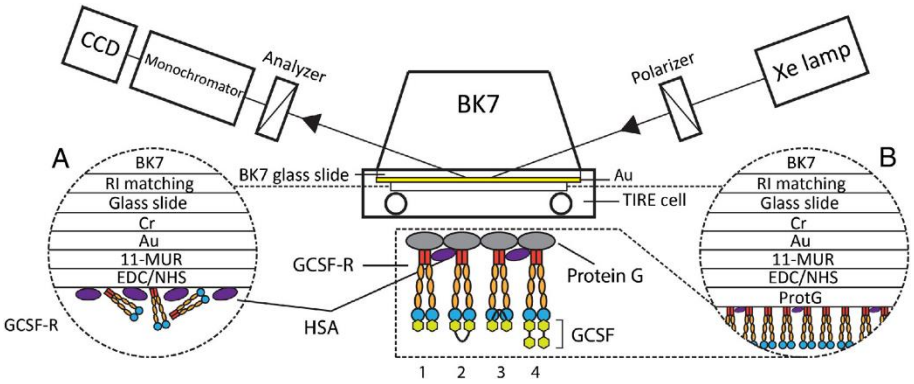

Figure 2.1. The scheme of TIRE experimental setup used for GCSF-L*α*-GCSF and monomeric G-CSF (Balevicius et al., 2014)**.**

In general, the BK7-glass/Cr-Au slides were cleaned using piranha solution (1/3 peroxide, 2/3 sulphuric acid) or with the BAL-TEC SCD 050 Sputter Coater plasma cleaner, washed with ethanol or methanol, and then rinsed with ultrapure water or hexane. The self-assembled monolayer (SAM) was prepared by immersing the surface plasmon resonance (SPR) chips into a 1 mM 11-mercaptoundecanoic acid (11-MUA) solution in ethanol or methanol for 12-18 h. The formed BK7-glass/Cr-Au/MUA structure was rinsed with ethanol or methanol, ultrapure water and dried with argon gas. Then carboxyl groups of 11-MUA were activated using the solution of 0.1 M N-hydroxysuccinimide (NHS) and 0.4 M N-(3-dimethylaminopropyl)-N'-ethyl-carbodiimide hydrochloride (EDC). For this, a fresh solution containing 0.1 M NHS and 0.4 M EDS was injected into TIRE-cell for 5-50 min. TIRE-cell was rinsed with a 10 mM sodium acetate buffer, pH 4.0. From this step, protocols differ for each sample (Balevicius et al., 2014; Balevicius et al., 2019; Mickiene et al., 2020; Plikusiene et al., 2020). An important step was the formation of GCSF-R layer (Figure 2.1.). A non-covalently oriented-bound GCSF-R and c-KIT was established by choosing the formation of the protein G layer. To accomplish this, a solution of 100 μg/mL of protein G in 10 mM sodium acetate buffer, pH 4.0 was added into TIRE cell. When a steady-state TIRE signal was achieved indicating that the structure of BK7-glass/Cr-Au/MUA/Protein-G formed, the latter slide was rinsed with sodium acetate buffer, pH 4.0. Subsequently, the surface was exposed to 1 M ethanolamine, pH 8.5 for 15 min to deactivate the remaining active carboxyl groups. Non-covalently bounded protein G was removed with a 10 mM solution of glycine, pH 3.0 for 5 min. The immobilization of GCSF-R or c-KIT was performed by incubation of BK7-glass/Cr-Au/MUA/Protein-G in PBS (pH 7.4), containing 0.0532 mM of GCSF-R or 0.0602 mM of c-KIT for

33-60 min. The slides BK7-glass/Cr-Au/MUA/Protein-G/GCSF-R or BK7-glass/Cr-Au/MUA/Protein-G/c-KIT were washed with PBS to remove an unbound receptor. Binding kinetics of BK7-glass/Cr-Au/MUA/Protein-G/GCSF-R or BK7-glass/Cr-Au/MUA/Protein-G/c-KIT with purified recombinant proteins were evaluated in PBS. Ten-μg/mL concentration of GCSF-Lα-GCSF was determined as enough to form a ligand-receptor complex (Balevicius et al., 2014), so for the measurements, 10 μg/mL of each protein was applied and added into the TIRE cell. Finally, the cell was flushed with PBS to remove the non-specifically attached protein layer.

The protein-receptor interactions were analyzed using the CompleteEase software (J. A. Woollam Co., USA). The binding kinetics of GCSF-L2-GCSF homodimer, SCF-Lα-GCSF and GCSF-Lα-SCF heterodimers, and monomeric G-CSF and SCF were evaluated by a standard fully reversible Langmuir kinetics model. Unlike, interaction kinetics of both GCSF-L7-GCSF and GCSF-Lα-GCSF homodimers were analyzed using a multi-layer model (Balevicius et al., 2019; Plikusiene et al., 2020).

In vitro biological activity of recombinant proteins

In vitro activity experiments were performed by I. Dalgėdienė (VU LSC, Institute of Biotechnology). The biological activity of fusion proteins was determined using the SCF-dependent human M-07e cell line (Drexler et al., 1997) and G-CSF-dependent mouse G-NFS-60 cell line (Weinstein et al., 1986; Matsuda et al., 1989), respectively. The SCF and G-CSF monomers were used as the reference standards. Briefly, before the assays, the M-07e and G-NFS-60 cells were centrifuged and resuspended at the concentration of 5.0×10^7 cells/mL in the test medium (RPMI 1640 supplemented with a 10% fetal bovine serum, antibiotic gentamicin sulfate and 0.05 mM 2-mercaptoethanol). A total of 50-μL of the test medium was aliquoted into each well of a 96-well tissue culture plate. The purified G-CSF homodimers or heterodimers and standard proteins were serially diluted in the test medium. A volume of 50 μL of the diluted protein was added to the wells to the concentrations of 0.004-7.8 pg/mL in technical triplicate. Each protein was tested in at least three independent assays. After the incubation at 37°C and 5% CO_2 for 48 h, 20 μL of a tetrazolium salt solution (MTS, 5 g/L) (Promega, USA) was added to each well of the plate, and the incubation was continued for 3 h under the same conditions. The absorbance of formazan derived from the MTS cleavage by cellular mitochondrial dehydrogenases was measured using a multi-well scanning spectrofluorometer (FluoroMax-4; Horiba Scientific, USA) at 490 nm. The biological activity of each protein was

calculated from the proliferation curves using OriginLab Origin and Microsoft Excel. The proliferation curves were constructed by plotting the log2 dilution of the proteins or standards against the absorbance value at 490 nm. To calculate the specific biological activity of the fusion recombinant proteins *in vitro*, the following equations were used:

$$A_T = \frac{2^{D_T} \cdot S_T}{2^{D_S} \cdot S_S} \cdot A_S \quad (2.1)$$

$$SA = \frac{A_T}{c_T} \quad (2.2)$$

where A_T and A_S are the activity (IU/mL) of the tested dimeric protein and the standard monomer, respectively; S_T and S_S are the initial dilutions of the dimeric protein and monomer, respectively; D_T is the log2 dilution of the dimeric protein at 50% of the maximum absorbance; D_S is the log2 dilution of the monomer at 50% of the maximum absorbance (these values are obtained from the proliferation curves); c_T is the concentration (mg/mL) of the dimeric protein, and SA is the specific activity (IU/mg) of the dimeric protein.

In vivo biological activity of GCSF-L*α*-GCSF and SCF-L*α*-GCSF

All *in vivo* experiments were performed by Dr. V. Bukelskienė (VU, Institute of Biochemistry). To evaluate the biological activity of purified GCSF-Lα-GCSF *in vivo*, the rats were randomized to 3 different test groups with 3-6 rats in each group. Group 1 received a single subcutaneous injection of 200 μg/kg of GCSF-Lα-GCSF and the group 2 – 200 μg/kg of G-CSF monomer. Group 3 received the sodium acetate buffer.

To evaluate the biological activity of purified SCF-Lα-GCSF *in vivo*, the rats were randomized to different test groups with 3-5 rats in each group. Five groups of rats received a single subcutaneous injection of the protein preparations, as follows: 500 μg/kg of G-CSF monomer (group 1), 500 μg/kg of SCF monomer (group 2), 500 μg/kg of purified SCF-Lα-GCSF (group 3), 1,000 μg/kg of purified SCF-Lα-GCSF (group 4) and a combination of 500 μg/kg of SCF and 500 μg/kg of G-CSF (group 5). Group 6 received the sodium acetate buffer.

The biological activity of the G-CSF moiety *in vivo* was assessed by measuring an absolute neutrophil count (ANC) in the rats of each group. Blood samples were collected from the tail veins at 0, 24, 48, and 72 h after injection. ANC was determined using a microcell counter (hematology analyzer Exigo EOS, BouleMedical AB, Sweden).

2.2.8. Bioavailability of GCSF-Lα-GCSF *in vivo*

Assays for bioavailability of purified GCSF-Lα-GCSF and G-CSF monomer were determined using two different test groups with 4-5 rats in each group. Group 1 received a single subcutaneous injection of 150 μg/kg of GCSF-Lα-GCSF and the group 2 – 150 μg/kg of G-CSF monomer. Blood samples were drawn at 0, 3, 6, 12, 18, and 24 h after injection. Protein concentrations in the blood serum were determined by a sandwich ELISA using G-CSF ELISA Development Kit according to the manufacturer's instructions (PeproTech, USA). Concentration values of the G-CSF in serum at selected time intervals after protein injection were fitted with an exponential function using GRAFIT software, which obtained a coefficient kappa for every protein function. To determine the circulation half-life ($t_{1/2}$) of the proteins, the following equation was used:

$$t_{1/2} = \frac{\ln(2)}{k_{app}} \qquad (2.3)$$

2.2.9. Thermal stress analysis of GCSF-Lα-GCSF

To evaluate the stability of purified GCSF-Lα-GCSF formulated in a storage buffer composed of 10 mM acetic acid/NaOH and supplemented with 5% D-sorbitol and 0.0025% Tween 80, the thermal stress study by simulating stress storage conditions was performed. The protein samples at a concentration of 0.6 mg/mL were stored in a climatic chamber for 4 weeks at 40ºC/75% relative humidity (RH) and evaluated every 7 days. For analysis, RP-HPLC, SE-HPLC, SDS-PAGE methods, as described in Supplementary File S2, were used. In the final stage of stress storage, the biological activity of GCSF-Lα-GCSF was determined using an *in vitro* bioassay. All experimental results were compared with the GCSF-Lα-GCSF sample stored at 4ºC.

2.2.10. Statistical analysis

The data were evaluated using GraphPad Prism software (version 8.0, GraphPad, San Diego, CA, USA). The data were subjected to analysis using the unpaired t-test, the one-sample t-test, and the one-way analysis of variance (ANOVA) combined with the Tukey's multiple comparison test. Results are presented as mean ± standard error of the mean (SEM) or mean ± standard deviation (SD) of at least 3 independent experiments.

3. RESULTS

3.1. Expression, refolding, purification and characterization of G-CSF homodimers

The novel dimeric G-CSFs composed of two human G-CSF molecules interspaced by a 11-amino-acid (L2), 36-amino-acid (L7) and 54-amino-acid (Lα) linkers were generated (Table 3.1.). GCSF-L2-GCSF, GCSF-L7-GCSF, GCSF-Lα-GCSF were cloned into expression vector pET21b(+) and transformed into *E. coli* BL21(DE3) cells.

Table 3.1. G-CSFs homodimers

Protein	Theoretical Mw (kDa)	Amino acid sequence of linker	Model
GCSF-L2-GCSF	38.17	(SG_4)–(SG_4)–S	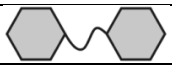
GCSF-L7-GCSF	39.74	(SG_4)–(SG_4)–(SG_4)–(SG_4)–(SG_4)–(SG_4)–(SG_4)–S	
GCSF-Lα-GCSF	42.51	SGLEA–$(EAAAK)_4$–ALEA–$(EAAAK)_4$–ALEGS	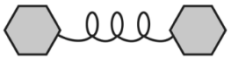

3.1.1. Expression of G-CSF homodimers

Small-scale production of GCSF-L2-GCSF, GCSF-L7-GCSF, and GCSF-Lα-GCSF was carried out in M9 media with supplements (Flask medium, Table 2.7.). IPTG was added at the mid-exponential phase of growth. The expression level of recombinant proteins was approx. 30% of the total cellular protein (Figure 3.1.). SDS-PAGE analysis of soluble and insoluble fractions of *E. coli* lysate revealed that recombinant dimeric G-CSFs were expressed as insoluble proteins that accumulated in Ibs (data not shown).

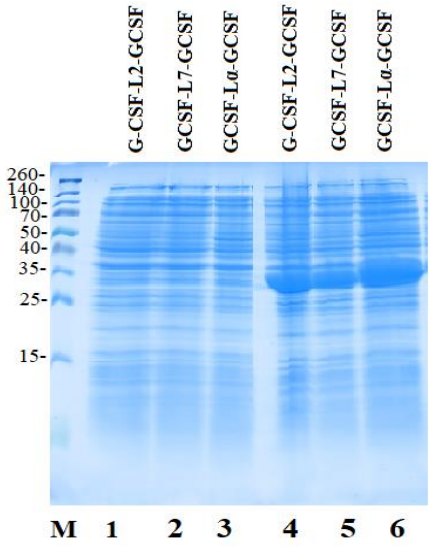

Figure 3.1. Expression of dimeric G-CSFs in *E. coli*. Recombinant proteins-expressing cell lysates before induction (lanes 1-3) and cell lysates after induction (lanes 4-6). *M*, molecular weight market (Thermo Fisher Scientific).

3.1.2. Refolding and two-step purification of G-CSF homodimers

The expression of recombinant G-CSF homodimers leads to the formation of aggregated proteins referred to as inclusion bodies. The main focus of this work was on the selection of appropriate refolding conditions for recombinant proteins. Various tested conditions dedicated to finding out the optimal purification scheme for each recombinant protein are shown in Figure 3.3. A. The final flow-chart of purification steps is presented in Figure 3.3. B.

The RP-HPLC analysis was the main tool throughout the refolding step to monitor the transition of the reduced protein form into an oxidized state and to determine the purity level of the proteins throughout purification. After the selection of optimal refolding conditions for each G-CSF homodimer, RP-HPLC analysis showed that the highest purity after refolding was reached for GCSF-Lα-GCSF (61%) (Table 3.2.). The refolding purity of GCSF-L2-GCSF and GCSF-L7-GCSF were significantly lower (43.2 and 51.2%, respectively) because of the accumulation of protein forms with longer retention times (peak 2, Figure 3.2.). The GCSF-Lα-GCSF protein (37 kDa) was detected as a single band on the SDS-PAGE gel, while some heterogeneity was visible in the GCSF-L2-GCSF and GCSF-L7-GCSF preparations under non-reducing conditions. The proteins migrated as a single band after reduction, indicating the presence of heterogenic disulfide-bonded species in the non-reduced preparations (Figure 3.2. C).

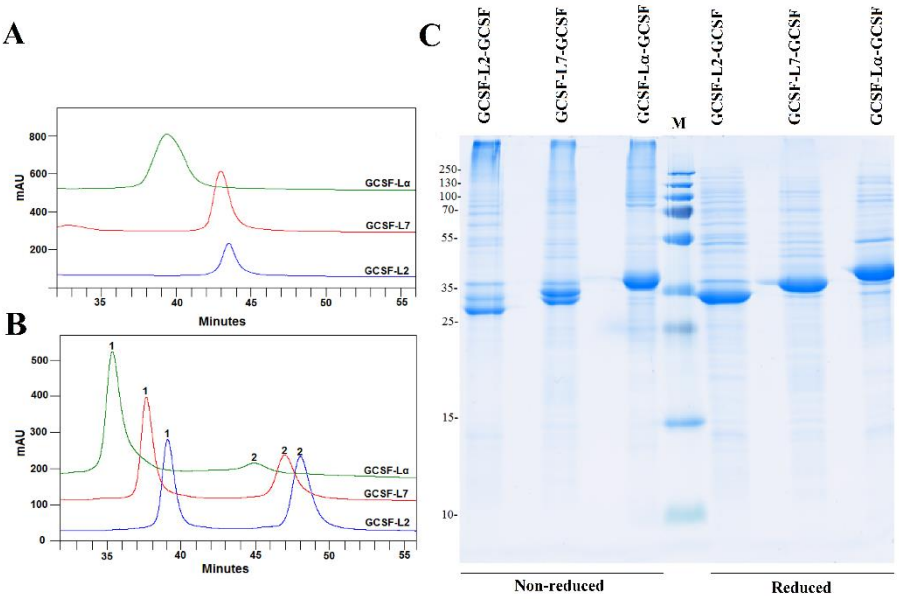

Figure 3.2. (A, B) RP-HPLC and (C) SDS-PAGE profiles of GCSF-L2-GCSF, GCSF-L7-GCSF and GCSF-Lα-GCSF. (A) RP-HPLC analysis of the extracts from inclusion bodies in the presence of DTT. **(B)** The protein samples after refolding in the presence of DTT/GSSG couple. Each protein sample was injected into a Hi-Pore RP-318 octadecyl-silica column and separated via gradient and isocratic elution with mobile phase A (0.1% TFA in water) and mobile phase B (10% water, 89.9% acetonitrile and 0.1% TFA) at 30°C. Absorbance at 215 nm is reported as mAU. **(C)** SDS-PAGE of protein samples after refolding in the presence of DTT/GSSG couple under non-reducing and reducing conditions. *M*, molecular weight marker (Thermo Fisher Scientific).

After refolding, GCSF-L2-GCSF, GCSF-L7-GCSF, and GCSF-Lα-GCSF proteins were subjected to further purification using a combination of different types of chromatography resins, including Sephadex G-25 Medium, DEAE Sepharose FF, CHT ceramic hydroxyapatite, Type II, Cu-IDA Sepharose FF, and others (Figure 3.3. A). Efficient purification of GCSF-Lα-GCSF was achieved with the DEAE Sepharose FF column (the first chromatography step) using a linear salt gradient between 0.02 and 0.08 M NaCl (Table 3.2.). With the same conditions, a considerable amount of the longer, RP-HPLC-retained protein forms were eluted along with the oxidized protein forms of GCSF-L2-GCSF and GCSF-L7-GCSF. To reduce accompanying impurities, all G-CSF derivatives were further loaded onto a cation-exchange chromatography column (the second chromatography step). A strong cation exchange medium, SP Sepharose Fast Flow, was selected for GCSF-L2-GCSF and GCSF-Lα-GCSF, while a weak cation-exchange matrix (CM Sepharose Fast Flow) was applied to the purification of GCSF-L7-

GCSF. Application of CM Sepharose FF facilitated the better separation of the refolded form of GCF-L7-GCSF from impurities (data not shown). Fractions of the purified proteins were applied to Sephadex G-25 Medium for desalting and buffer exchange.

A

Step	Parameter	Material/Resin	GCSF-Lα-GCSF	GCSF-L2-GCSF	GCSF-L7-GCSF
Solubilization	Solubilizing agent	GdnHCl	+	+	-
		Urea	+	+	+
	Reducing agent	No reducing agent	+	+	-
		β-mercaptoethanol	+	-	-
		DTT	+	+	+
Renaturation	Oxidation agent	Air/Cu^{2+}	+	+	-
		GSH/GSSG	+	-	-
		DTT/GSSG	+	+	+
Chromatography	Capturing step	Sephadex G-25 Medium	+	+	-
		DEAE Sepharose FF	+	+	+
	Intermediate purification step	CHT ceramic hydroxyapatite, Type II	-	+	-
		Cu-IDA Sepharose FF	-	-	+
		Resource Q	-	-	+
		Ni Sepharose 6 FF	-	+	+
		Butyl Sepharose FF	-	+	-
	Polishing step	SP Sepharose FF	+	+	+
		CM Sepharose FF	+	+	+
	Formulation step	Sephadex G-25 Medium	+	+	+

B

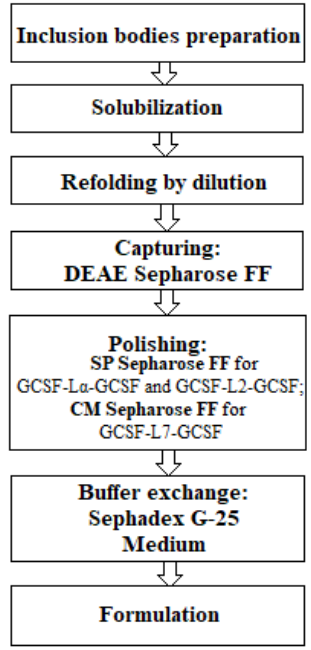

Figure 3.3. Purification scheme for G-CSF homodimers. (**A**) Screening of optimal protein purification conditions. (**B**) A flowchart of the purification steps of GCSF-Lα-GCSF, GCSF-L2-GCSF, and GCSF-L7-GCSF. Abbreviations: + tested; - not tested.

Table 3.2. Yield and purity of G-CSF homodimers after three selected processing step

Protein purification step	Characteristic	GCSF-L2-GCSF	GCSF-L7-GCSF	GCSF-Lα-GCSF
Refolding step	Yield[1]	89.25±2.20	90.33±2.70	90.99±1.51
	Purity[2]	43.24±3.81	51.23±3.45	61.02±2.73
I chromatography step (anion exchange)	Yield[1]	4.56±1.63	7.55±2.12	16.99±2.08
	Purity[2]	55.43±4.21	68.12±3.75	90.21±3.21
II chromatography step (cation exchange)	Yield[1]	1.20±0.52	2.21±1.12	14.10±2.21
	Purity[2]	79.14±2.13	82.41±1.54	95.14±0.99

Each value represents the mean of three independent analyses ± SD.
[1]Protein concentration was determined by the Bradford method (Bradford, 1976) using bovine serum albumin as a standard.
[2]Purity of the protein was determined by RP-HPLC.

3.1.3. Characterization of the purified G-CSF homodimers

The purified G-CSF dimers were characterized by a subset of analytical methods that included HPLC (RP- and size exclusion), SDS-PAGE, Western blotting, and HPLC/ESI-MS. *E. coli*-derived G-CSF monomer was used as a reference.

The RP-HPLC analysis revealed different hydrophobicities and degrees of purity for G-CSFs (Figure 3.4. A). The shortest retention time was observed for monomeric G-CSF, whereas it increased for the dimeric proteins in the order of GCSF-Lα-GCSF<GCSF-L7-GCSF<GCSF-L2-GCSF. The purity of GCSF-Lα-GCSF, GCSF-L7-GCSF, and GCSF-L2-GCSF determined by RP-HPLC were 95, 82, and 79%, respectively (Table 3.2.). The purified G-CSF dimers migrated on SDS-PAGE depending on their molecular weight; however, the corresponding bands were observed at slightly lower positions on the gel than their calculated molecular weight (38.2 kDa for GCSF-L2-GCSF, 39.7 kDa for GCSF-L7-GCSF, and 42.5 kDa for GCSF-Lα-GCF) (Figure 3.4. B). GCSF-Lα-GCSF produced a single major band on the gel, while the bands corresponding to GCSF-L2-GCSF and GCSF-L7-GCSF had an extra, thinner band, which was present throughout the purification process. This extra band was not found under reducing conditions, suggesting that it might correspond to the later eluted protein form detected by RP-HPLC with a retention time between 37 and 42 min (Figure 3.4. A).

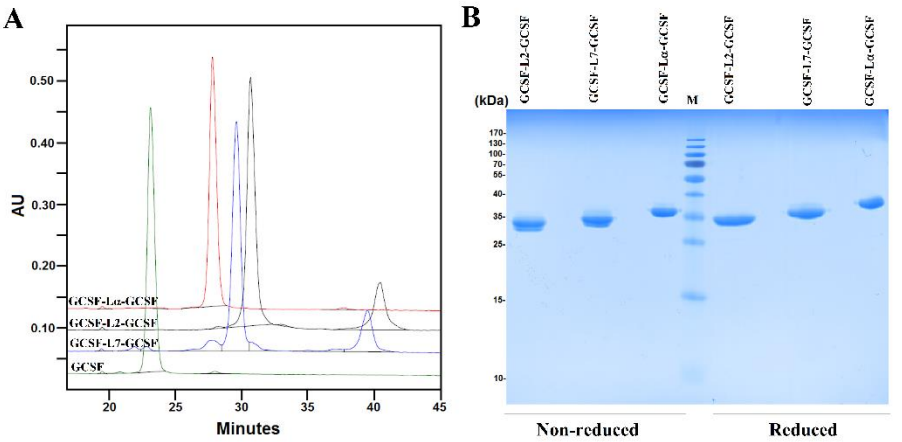

Figure 3.4. Purification characteristics of fusion proteins. (A) The RP-HPLC analysis of the purified dimeric G-CSF proteins collected after Sephadex G-25 Medium and the G-CSF monomer used as a control. Fifteen µg of each protein was loaded onto Zorbax 300SB-C18 column (Agilent Technologies) and separated via gradient and isocratic elution with mobile phase A (0.1% TFA in water) and mobile phase B (0.1% TFA in acetonitrile) at 30°C. Absorbance at 215 nm is reported as AU. **(B)** SDS-PAGE of the purified dimeric proteins under non-reducing and reducing conditions. *M*, molecular weight marker (Thermo Fisher Scientific).

The mobility of the dimers and the G-CSF monomer on a calibrated SE-HPLC column was estimated (Figure 3.5.). The proteins were separated according to their relative molecular weights (55 kDa for GCSF-Lα-GCSF, 49 kDa for GCSF-L7-GCSF, and 42 kDa for GCSF-L2-GCSF), which were higher than those calculated from the corresponding amino acid sequences (Table 3.1.). Such discrepancies resulted from the fact that the SEC column is able to separate proteins by their shape (hydrodynamic radius), as well as their molecular weight (Hagel, 2001). The G-CSF monomer, which has the smallest hydrodynamic radius, was eluted with a relative molecular weight of 17 kDa, which is lower than what was established for filgrastim (18.8 kDa), indicating that G-CSF is a compact molecule. The SE-HPLC profile of GCSF-L2-GCSF showed the presence of a small amount of impurities (approx. 6% of the higher molecular weight forms), whereas GCSF-Lα-GCSF, GCSF-L7-GCSF, and G-CSF protein preparations reached approximately 99% of purity.

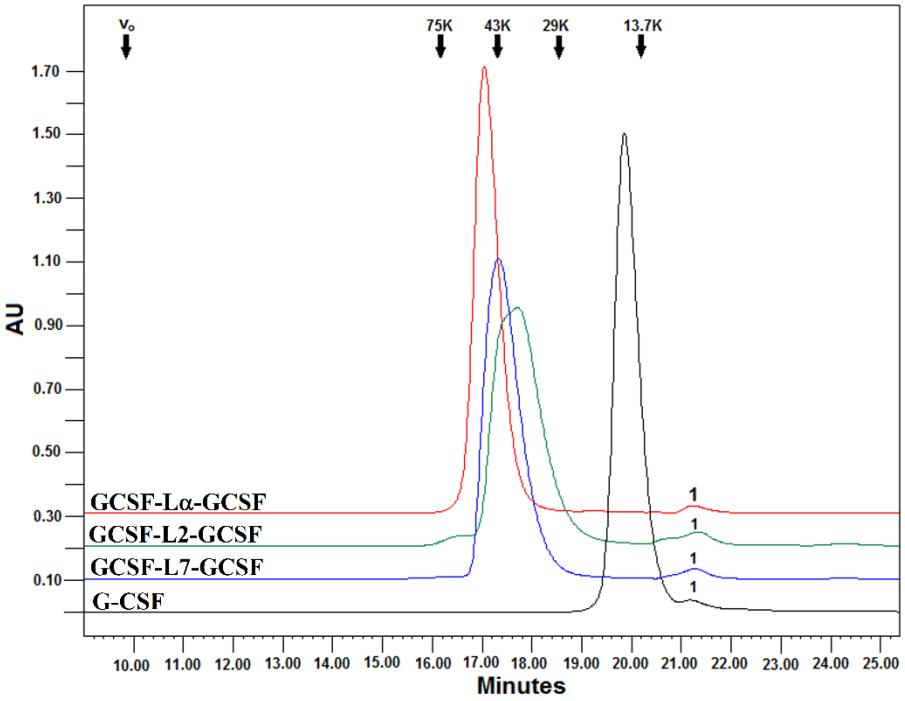

Figure 3.5. Size-exclusion HPLC analysis of the purified dimeric G-CSF proteins collected after Sephadex G-25 medium and the G-CSF monomer used as a control. Twelve µg of each protein was injected into a TSK-gel G3000 SWXL (7.8/300) column and eluted at 0.6 mL/min in 0.1 M Na_2HPO_4 (pH 7.2) buffer, containing 0.1 M Na_2SO_4. Arrows indicate the retention time of molecular weight standards: conalbumin (75 kDa), ovalbumin (43 kDa), carbonic anhydrase (29 kDa), and ribonuclease A (13.7 kDa). Blue dextran was used to determine the void volume (Vo) of the column. Absorbance at 215 nm is reported as AU. Peak 1 obtained at retention time of 21.25 min represents excipients from the storage buffer.

To resolve the question of the molecular weight of proteins, the exact molecular weight was determined by applying HPLC/ESI-MS. The molecular weights of GCSF-L2-GCSF, GCSF-L7-GCSF, and GCSF-Lα-GCSF (38,166.67, 39,742.90, and 42,513.95 Da, respectively) determined by electrospray ionization mass spectrometry were in good agreement with the ones calculated from their amino acid sequences (within a range of 2 Da of the theoretical values) (Supplementary Figure S1.). A high degree of purity and homogeneity of the preparations were confirmed. The G-CSF dimers were detected by Western blot analysis using a mAb specific to the G-CSF monomer (Supplementary Figure S2.). The major bands corresponding to GCSF-L7-GCSF and GCSF-L2-GCSF on the Western blot had an extra lower

molecular weight band that is suggested to be degradation products of the dimeric proteins.

The RP-HPLC peptide mapping of GCSF-Lα-GCSF was used to confirm the identity of this protein sequence and its structural alterations. GCSF-L2-GCSF and GCSF-L7-GCSF, due to insufficient purity (Table 3.2.) were not subjected to this analysis. Peptide mapping of the G-CSF monomer and purified GCSF-Lα-GCSF was performed by digestion with glutamyl endopeptidase endoproteinase Glu-C (Sigma-Aldrich), which cleaves G-CSF at the carboxyl side of glutamyl and/or aspartyl peptide bonds (Drapeau, 1976). The obtained peptide mixture was analyzed by RP-HPLC (Figure 3.6.). The peptide maps of GCSF-Lα-GCSF and G-CSF showed similar profiles; however, several discrepancies were found. The chromatogram of G-CSF showed peptide 2 at 51.8 min (Figure 3.6.), which might indicate a partially digested larger fragment from the peptide mixture. The additional peak (peptide 1, Figure 3.6.), which eluted from the GCSF-Lα-GCSF peptide mixture at 26.5 min, may belong to the linker sequence joining the two G-CSF molecules into a whole polypeptide chain.

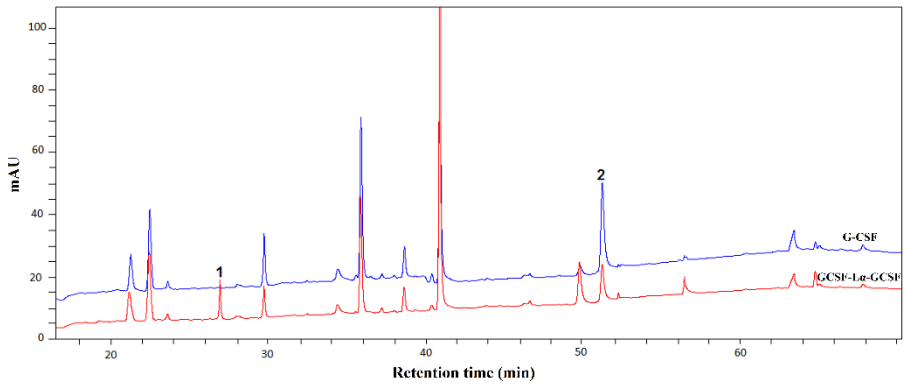

Figure 3.6. The RP-HPLC peptide mapping of GCSF-Lα-GCSF (red line) and the G-CSF monomer (blue line). Eight µg of each protein was used for analysis. The separation of peptides was performed on Hi-Pore RP-318 octadecyl-silica column via acetonitrile gradient elution with mobile phase A (94.5% water, 5% acetonitrile, and 0.05% TFA) and mobile phase B (5% water, 94.5% acetonitrile, and 0.05% TFA) at 50°C. Absorbance at 215 nm is reported as mAU.

To verify that native disulfide bonds were formed, a sample of GCSF-Lα-GCSF was subjected to fluorescence analysis. It was demonstrated that under acidic conditions (pH 3.2) correctly folded active G-CSF exhibits a characteristic Tyr and Trp fluorescence spectrum, which was not observed for any disulfide-reduced intermediates (Lu et al., 1992). At neutral pH, the fluorescence emission spectra of GCSF-Lα-GCSF and G-CSF were

characterized by the tryptophan fluorescence with a maximum at 350 nm. At pH 3.2, the Trp fluorescence decreased and a shoulder with a maximum at 310 nm, attributable to Tyr fluorescence, was present (Figure 3.7.). Such changes are characteristic feature of the native G-CSF molecule, since the disulfide-reduced intermediates as well as the disulfide-unpaired analogs show a decrease in the intensity of the Trp fluorescence, but no change in the Tyr fluorescence (Lu et al., 1992). The obtained data demonstrated (Figure 3.7.) the formation of native disulfide bonds in the dimeric GCSF-Lα-GCSF protein.

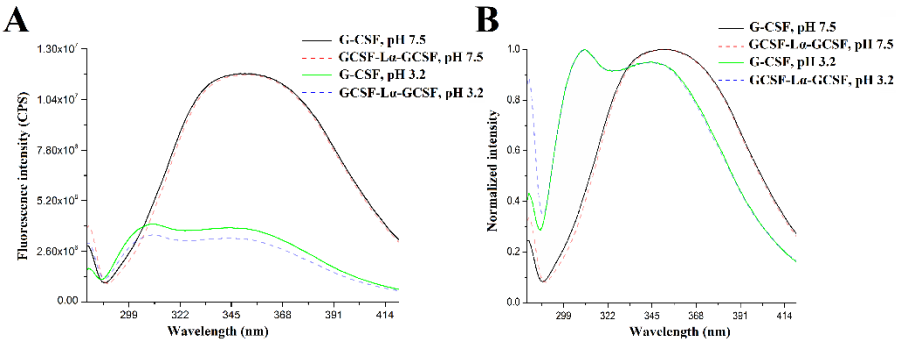

Figure 3.7. (A) Raw and (B) normalized fluorescence emission spectra of the purified GCSF-Lα-GCSF protein and G-CSF monomer at pH 3.2 and 7.5. The spectra were normalized at their maximum.

3.1.4. Binding kinetics of the homodimeric G-CSF proteins to the immobilized receptors

The binding kinetics assay of purified GCSF-L2-GCSF, GCSF-L7-GCSF, and GCSF-Lα-GCSF to the SAM-immobilized receptor GCSF-R was performed by total internal reflection ellipsometry. The obtained binding kinetics were compared to that of monomeric G-CSF. To improve the sensitivity of the ligand-binding platform, the receptors were oriented perpendicular to the sensor's surface. This "site-directed" immobilization was realized by the formation of the G protein-based SAM layer and the receptor layer (GCSF-R) (Balevicius et al., 2014). To reduce possible non-specific binding of G-CSF homodimers on the GCSF-R based layer, dimers were mixed with human serum albumin.

The GCSF-L2-GCSF, GCSF-L7-GCSF, and GCSF-Lα-GCSF proteins showed different binding kinetics. To analyze the binding of GCSF-L2-GCSF to GCSF-R, a standard fully reversible Langmuir kinetic model was used. However, to describe the binding kinetics of GCSF-L7-GCSF and GCSF-Lα-

GCSF the advanced a three-step consecutive kinetics model with irreversible last step of rearrangement was applied (Plikusiene et al., 2020).

The binding kinetics parameters are presented in Table 3.3. and Figure 3.8. The association rate constant *k*a of GCSF-Lα-GCSF and its receptor was 2-fold higher than that of GCSF-L2-GCSF, whereas *k*a was about 2- and 3.5-fold lower than that of monomeric G-CSF and GCSF-L7-GCSF, respectively.

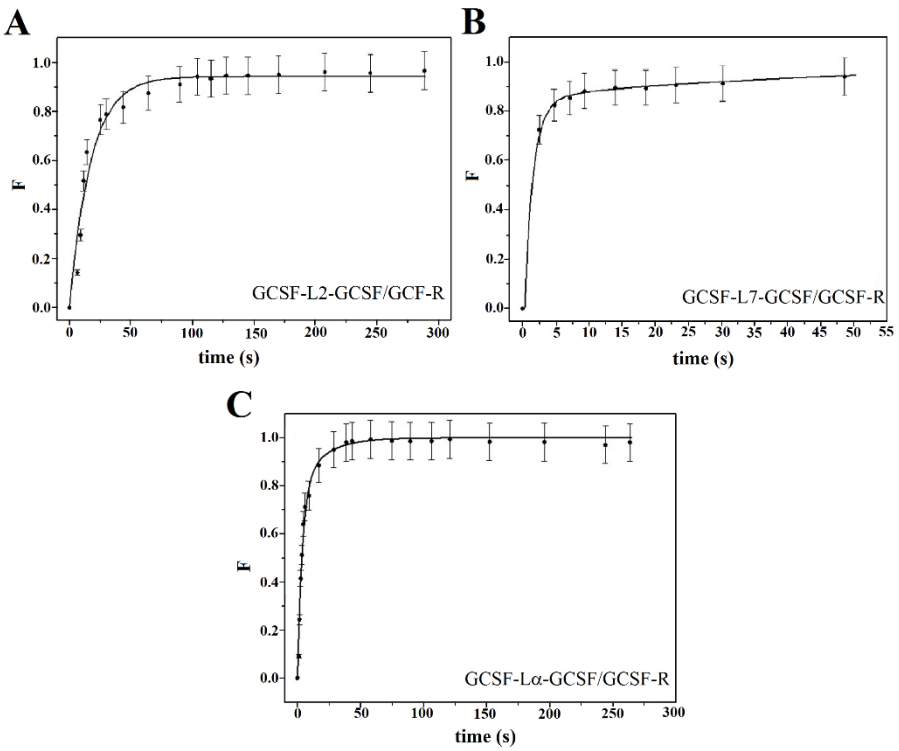

Figure 3.8. Experimental data (points) and fitting results of interaction between the homodimeric G-CSF proteins and the oriented SAM-immobilized receptor GCSF-R. (A) GCSF-L2-GCSF and GCSF-R. **(B)** GCSF-L7-GCSF and GCSF-R. **(C)** GCSF-Lα-GCSF and GCSF-R. The estimated standard deviation of experimental results was calculated as 14%. F, normalized analytical signal.

3.1.5. Biological activities of G-CSF homodimers *in vitro*

In vitro activity of the G-CSF dimers was determined using a cell proliferation assay with the G-CSF dependent cell line M-NFS-60 (Matsuda et al., 1989). The G-CSF monomer was used as a reference. Results were obtained by absorbance readings of the colored formazan product accessed by the cleavage of tetrazolium salt by viable cells (Monsmann, 1983). The proteins induced proliferation of the cells in a dose dependent manner (Figure 3.9.). Calculated *in vitro* activity of GCSF-Lα-GCSF reached 48% of that of

the G-CSF monomer, while GCSF-L2-GCSF and GCSF-L7-GCSF demonstrated relative activities of 22% (Table 3.3.).

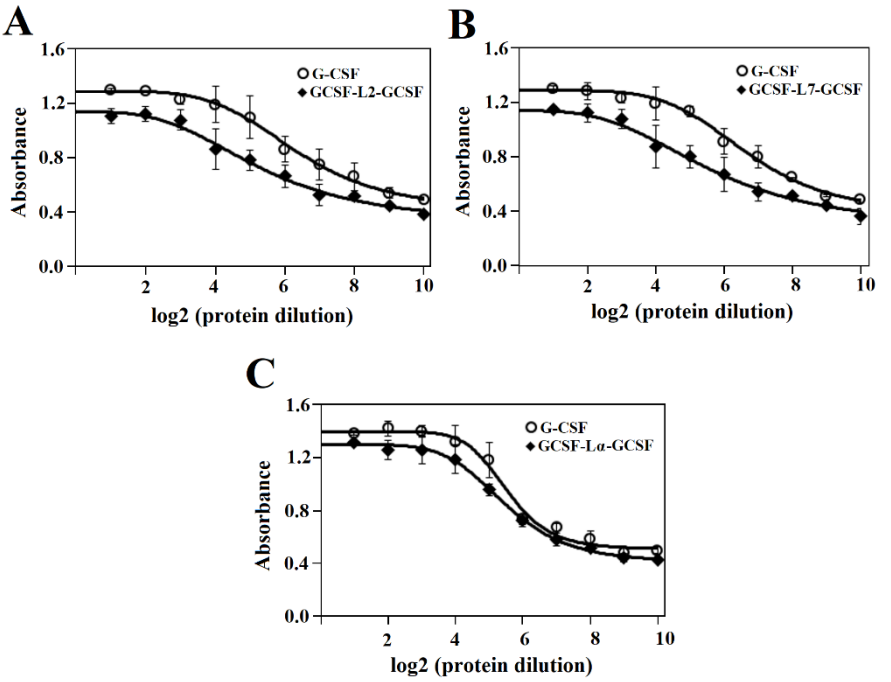

Figure 3.9. *In vitro* proliferation assay profiles for (A) GCSF-L2-GCSF, (B) GCSF-L7-GCSF, (C) GCSF-Lα-GCSF using G-NFS-60 cells. The G-CSF (control) included in each assay. The curves were obtained at two-fold doubling (log 2) serial dilutions of the tested proteins. Error bars represent SD of the absorbance means (490 nm) obtained in triplicate.

Table 3.3. Summary on the activity of homodimeric proteins and the G-CSF monomer

Characteristic	GCSF-L2-GCSF	GCSF-L7-GCSF	GCSF-Lα-GCSF	GCSF monomer
Biological activity on G-NFS-60 cell line[a] (IU/mmol)	$0.84x10^{12}$	$0.86x10^{12}$	$2.02x10^{12}$	$1.88x10^{12}$
Association rate constants of the protein and the G-CSF receptor (TIRE data)				
*k*a (M^{-1} s^{-1})	$2.00x10^{5}$	$14.00x10^{5}$	$4.00x10^{5}$	$7.5x10^{5}$

[a]Cell line expresses the G-CSF receptor.

3.1.6. Bioavailability and biological activity of GCSF-Lα-GCSF *in vivo*

A bioavailability comparison between the G-CSF monomer and GCSF-Lα-GCSF was made using groups of six rats. GCSF-L2-GCSF and GCSF-L7-

GCSF were not included in the assay because of unsatisfactory yield and purity (Table 3.2.). Each rat in the group received a single subcutaneous injection of G-CSF or GCSF-Lα-GCSF at a dose of 150 μg/kg. Protein in the blood serum at selected time intervals after subcutaneous injection was assessed using a human G-CSF ELISA kit. A curve of the protein concentration in the blood serum samples versus time was generated (Figure 3.10. A). Calculated protein circulation half-life ($t_{1/2}$) for G-CSF and GCSF-Lα-GCSF was 1.2 and 8.7 h, respectively. The data indicate that the clearance of GCSF-Lα-GCSF was reduced by more than sevenfold compared to that of the G-CSF monomer.

The biological activity of G-CSF *in vivo* comprises its ability to stimulate neutrophil release from the bone marrow by inducing a transient increase in circulating neutrophils. An increase in ANC in the peripheral blood was detected using three groups of rats. After subcutaneous administration of GCSF-Lα-GCSF, G-CSF, and control buffer, ANCs were determined at selected time intervals after injection (Figure 3.10. B). The ANC peaked at 24 h post-injection of G-CSF and GCSF-Lα-GCSF and decreased at 48 h post-injection. In response to injection of GCSF-Lα-GCSF, rats exhibited a 1.8-fold increase in circulating neutrophils 24 h postinjection.

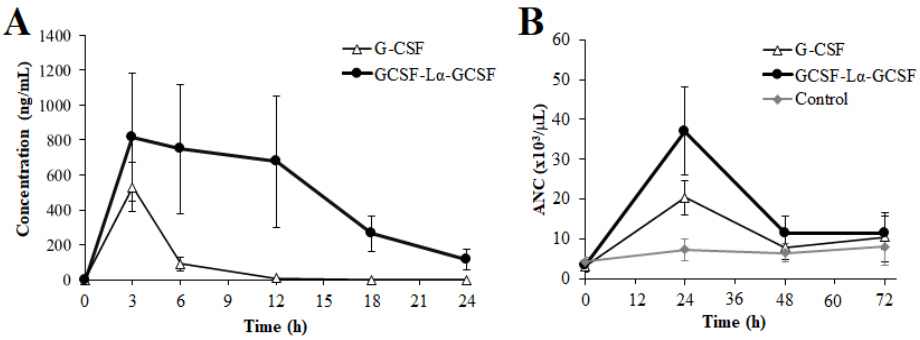

Figure 3.10. (A) Pharmacokinetic and (B) pharmacodynamic profiles obtained by subcutaneously administered recombinant proteins. (A) Pharmacokinetic profile of subcutaneously administered GCSF-Lα-GCSF and the G-CSF monomer. Error bars represent SD of G-CSF serum concentration obtained from four rats per group and GCSF-Lα-GCSF serum concentration obtained from five rats per group. **(B)** The ANC count versus time profiles of subcutaneously administered GCSF-Lα-GCSF, G-CSF, and control buffer. Error bars represent SD of the ANC obtained from blood of five rats per group after injection of G-CSF, blood of six rats per group was used after injection of GCSF-Lα-GCSF, and three rats were in the control group.

3.2. Large-scale purification and quality assessment of GCSF-Lα-GCSF protein

The obtained high-level purity, promising *in vivo* and *in vitro* activity of GCSF-Lα-GCSF compared to other G-CSF homodimers prompted us to select this homodimer as the most potential drug candidate for further studies. For this purpose, a large amount of pure protein should be obtained by scaling up protein production. A prerequisite for the clinical application of protein is the development of formulations where the proteins remain stable and correctly folded.

3.2.1. Large-scale production of GCSF-Lα-GCSF

Large-scale production of GCSF-Lα-GCSF was performed in a bioreactor containing a 4 L initial volume in fed-batch mode. M9 minimal media supplemented with yeast extract and chemically defined media were used for protein expression.

Recombinant *E. coli* cultivated in a chemically defined media yielded the higher biomass (44.5 g/L, expression level of GCSF-Lα-GCSF approx. 30% of total cell protein) than that in M9 media with supplement (24 g/L) over the same fermentation time (data not shown.).

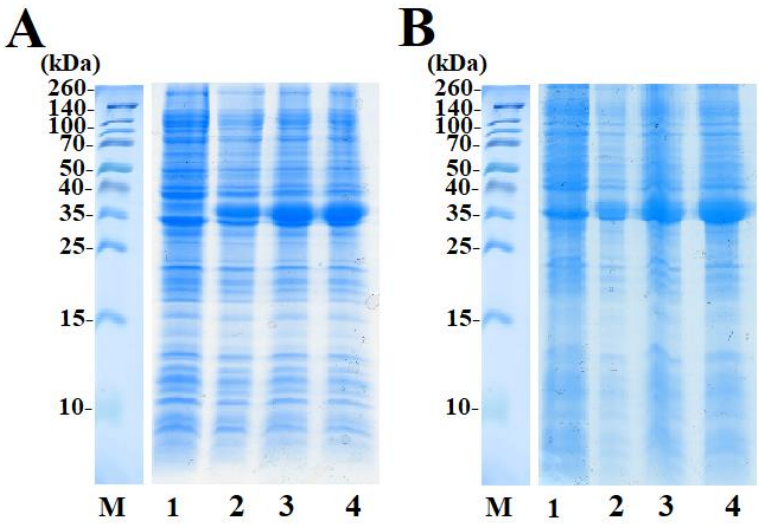

Figure 3.11. SDS-PAGE analysis of GCSF-Lα-GCSF produced in *E. coli*. (A) Recombinant *E. coli* was cultivated in M9 minimal media supplemented with yeast extract or **(B)** in chemically defined media. Lane 1, cell lysates before induction; lanes 2-4, cell lysates after 1, 2, and 3 hours of induction. *M*, molecular weight marker (Thermo Fisher Scientific).

3.2.2. Large scale GCSF-Lα-GCSF purification

About 125 g of wet biomass (44 g/L of the culture media) obtained after cultivation of recombinant *E. coli* in a chemically defined media was disrupted by a high-pressure homogenizer. Ibs were solubilized and refolded as described for a small-scale purification with some modifications (Supplementary File S1). The refolded GCSF-Lα-GCSF was loaded onto a DEAE Sepharose Fast Flow column that was equilibrated with refolding buffer (50 mM Tris-HCl, pH 8.0) containing 3 M urea and chromatography was performed at pH 8.0 instead of 7.5. To reduce analysis time, a segmented gradient instead of a linear one was applied in SP Sepharose FF chromatography step. The summary of the yield and purity level of GCSF-Lα-GCSF after each purification step is presented in Table 3.4. Purification characteristics of the homodimer are shown in Figure 3.12. The final purity of the protein determined by RP-HPLC reached 98.04%. The recovered total amount of 670 mg obtained from 2.8 L of culture media results in a yield of about 17%.

Table 3.4. Yield and purity of GCSF-L*α*-GCSF after four processing steps

Protein purification step	Characteristic	GCSF-L*α*-GCSF
Refolding step	Yield[1]	88.00
	Purity[2]	78.48
I chromatography step (anion exchange)	Yield[1]	19.12
	Purity[2]	97.34
II chromatography step (cation exchange)	Yield[1]	13.05
	Purity[2]	98.03
III chromatography step (buffer exchange)	Yield[3]	17.18
	Purity[2]	98.04

[1]Protein concentration was determined by the Bradford method (Bradford, 1976) using bovine serum albumin as a standard.
[2]Purity of the protein was determined by RP-HPLC.
[3]Protein concentration was determined by using the absorbance at 280 nm and eliminating the impact of light scattering at 340 nm.

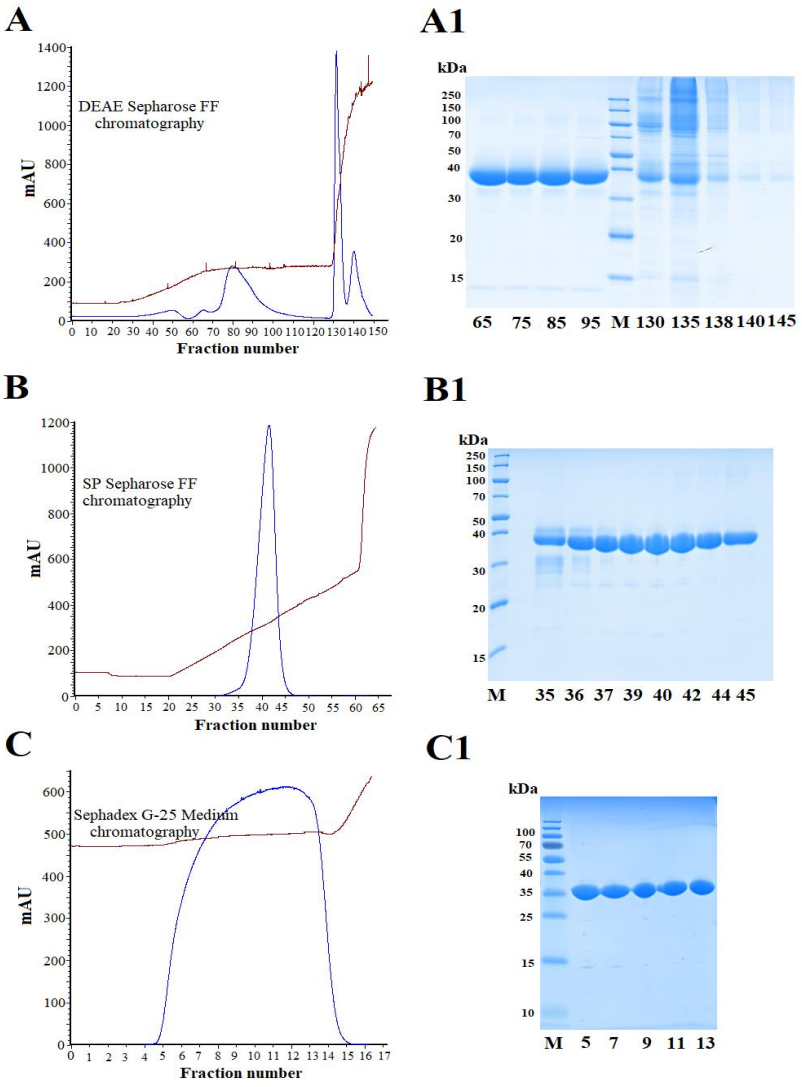

Figure 3.12. (A-C) GCSF-L*α*-GCSF elution profiles of each chromatography step and (A1-C1) SDS-PAGE of the respective protein fractions. Protein fraction numbers are indicated on the bottom of SDS-PAGE. **(A)** Anion exchange chromatography profile of refolded GCSF-Lα-GCSF. **(A1)** SDS-PAGE of protein fractions nos. 65-145. **(B)** Cation exchange chromatography profile of fractions nos. 65-95 obtained from the anion exchange chromatography. **(B1)** SDS-PAGE of fractions nos. 35-45. **(C)** Gel filtration chromatography profile of fractions nos. 37-45 obtained from the cation exchange chromatography. **(C1)** SDS-PAGE of fractions nos. 5-13. *M*, molecular weight marker (Thermo Fisher Scientific). Absorbance at 280 nm is reported as mAU.

3.2.3. Thermal stress analysis of GCSF-Lα-GCSF in a formulation buffer

Stability assays showed that GCSF-Lα-GCSF formulated in a storage buffer composed of 10 mM acetic acid/NaOH (pH 4.0), 5% D-sorbitol, and 0.0025% Tween 80 tend to degrade and to form aggregates under stress conditions (Supplementary Figure S3.). The RP-HPLC showed that the purity of protein solution sampled after incubation at 40ºC/75% RH decreased from 98.0% to 95.7%, whereas SE-HPLC showed a decrease from 99.7% to 94.1% (Figure 3.13. A). The SE-HPLC elution profiles of the samples demonstrated the formation of peaks that corresponded to the higher mol. weight products (Supplementary Figure S3. B). Similar to the SE-HPLC data, GCSF-Lα-GCSF aggregates were detected in the silver-stained SDS-PAGE gel after 2 weeks storage at 40ºC/75% RH (Figure 3.13. B). It was determined that GCSF-Lα-GCSF had a 1.96-fold lower bioactivity than the sample stored at 4°C.

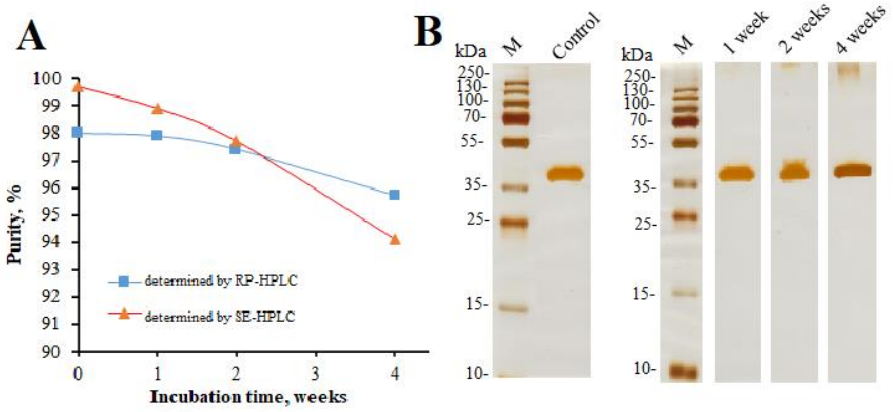

Figure 3.13. Thermal stability analysis of GCSF-Lα-GCSF as a function of time. **(A)** The percentage of GCSF-Lα-GCSF monomer remaining in the formulation buffer was determined by RP-HPLC and SE-HPLC. **(B)** SDS-PAGE of control and treated samples analyzed under reducing conditions. *M*, molecular weight marker (Thermo Fisher Scientific). GCSF-Lα-GCSF was stressed as described in Supplementary File S2.

3.3. Expression, refolding, purification and characterization of heterodimeric proteins composed of SCF and G-CSF

The fact that the α-helix conformation of the linker efficiently separates domains ensuring their functioning in the homodimeric G-CSF molecule and bifunctional fusion proteins (Arai et al., 2001; Chen et al., 2013) prompted us to connect human G-CSF and human SCF via a 54-amino-acid flexible linker (Lα). Two heterodimeric fusion proteins SCF-Lα-GCSF and GCSF-Lα-SCF were generated (Table 3.5.). SCF-Lα-GCSF and GCSF-Lα-SCF were cloned into expression vector pET21b(+) and transformend into *E. coli* BL21(DE3) and BL21STAR(DE3) cells, respectively.

Table 3.5. Characteristics of the heterodimers

Protein	Theoretical mol. Weight (kDa)	Linker sequence	Model
SCF-Lα-GCSF and GCSF-Lα-SCF	42.37	SGLEA–$(EAAAK)_4$–ALEA–$(EAAAK)_4$–ALEGS	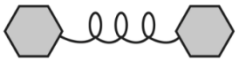

3.3.1. Expression of the heterodimers

Small-scale production of recombinant heterodimers was carried out in M9 media with supplements (Flask medium, Table 2.7.). The expression level of recombinant dimeric proteins was approx. 9-11% of the total cell protein. Both proteins were found in the insoluble fraction of the total cell lysate (Figure 3.14.).

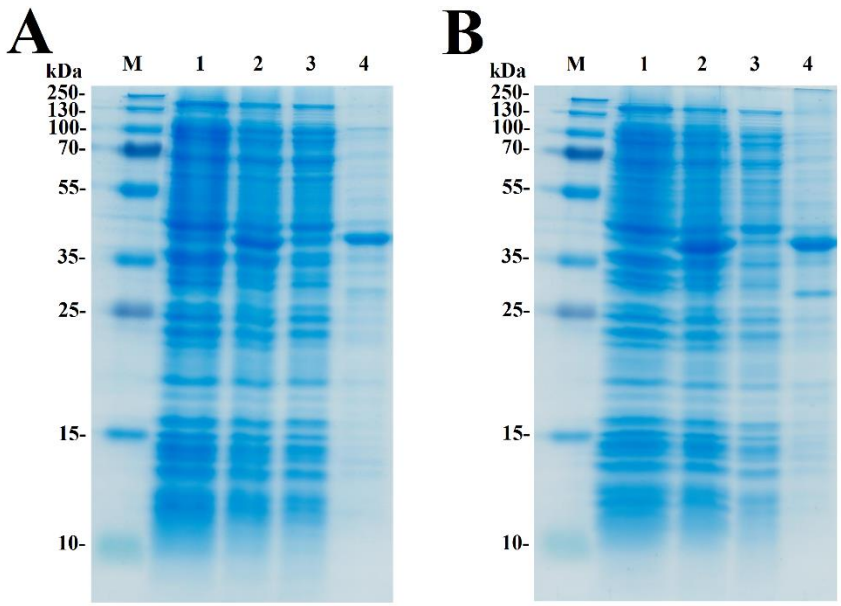

Figure 3.14. SDS-PAGE analysis of recombinant (A) SCF-Lα-GCSF and (B) GCSF-Lα-SCF produced in *E. coli*. Lane 1, total cell lysates before induction; lane 2, cell lysate after induction; lane 3, soluble fraction of cell lysate; lane 4, insoluble fraction of cell lysate; *M*, molecular weight marker (Thermo Fisher Scientific).

3.3.2. Refolding and three-step purification of G-CSF heterodimers

The RP-HPLC analysis was the main tool throughout the purification to monitor the transition of the reduced protein form into an oxidized state. After the solubilization of inclusion bodies, the complete reduction of the disulfide bonds in both proteins was achieved by the addition of 0.5 mM DTT (Figure 3.15. A). The optimized oxidative refolding of SCF-Lα-GCSF and GCSF-Lα-SCF carried out for 24 h resulted in 24.2% and 35.8% pure protein, respectively (Table 3.6.; Figure 3.15. B).

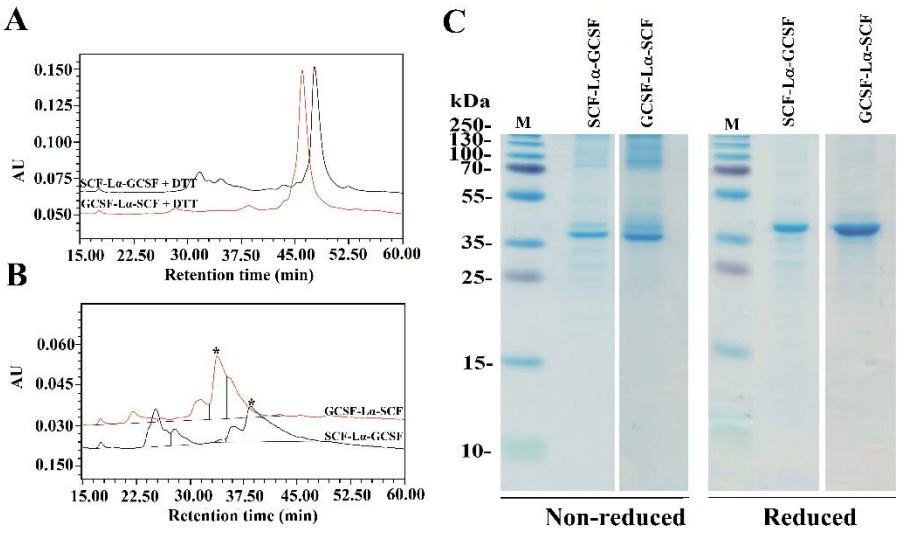

Figure 3.15. (A, B) RP-HPLC and (C) SDS-PAGE profiles of SCF-Lα-GCSF and GCSF-Lα-SCF. (A) RP-HPLC analysis of the extracts from inclusion bodies in the presence of DTT. **(B)** The protein samples after refolding in the presence of DTT/GSSG couple. Each protein sample was loaded onto Zorbax 300SB-C18 column (Agilent Technologies) and separated via gradient and isocratic elution with mobile phase A (0.1% TFA in water) and mobile phase B (9.9% water, 90% acetonitrile, and 0.1% TFA) at 30°C. Absorbance at 215 nm is reported as AU. **(C)** SDS-PAGE analysis of protein samples after refolding in the presence of DTT/GSSG couple under non-reducing and reducing conditions. *M*, molecular weight marker (Thermo Fisher Scientific).

The extensive purification of refolded SCF-Lα-GCSF and GCSF-Lα-SCF proteins were achieved using the DEAE Sepharose FF chromatography column. As a result, most of the nonspecific proteins including the aggregates were removed and the purity of the target proteins reached more than 58% as determined by RP-HPLC (Table 3.6.). To reduce other impurities, there were tested many different types of chromatography media including CM Sepharose FF, SP Sepharose FF, Cu-Ida Sepharose FF, Butyl Sepharose FF, Phenyl Sepharose FF, and Superdex 200 (Figure 3.16. A). Application of CHT Ceramic Hydroxyapatite type II column combined with a sodium phosphate gradient elution demonstrated the best separation of impurities. A strong cation exchanged chromatography on the SP Sepharose FF column was selected for the final purification step of the recombinant proteins. This step allows getting the target protein into the sodium acetate buffer (pH 4.7) suitable for storage. The summary of the yield and purity level of proteins after each purification step is presented in Table 3.6. The recovered total amount of SCF-Lα-GCSF and GCSF-Lα-SCF was 2.8 mg and 2.6 mg, that represents a yield of about 1.4% and 1.2%, respectively (Table 3.6.).

A

Step	Parameter	Material/Resin	SCF-Lα-GCSF	GCSF-Lα-SCF
Solubilization	Solubilizing agent	Urea	+	+
	Reducing agent	No reducing agent	+	-
		DTT	+	+
Renaturation	Oxidation agent	DTT/GSSG	+	+
Chromatography	Capturing step	DEAE Sepharose FF	+	+
		Q Sepharose FF	+	-
	Intermediate purification step	CM Sepharose FF	+	-
		SP Sepharose FF	+	-
		Cu-IDA Sepharose FF	+	-
		Butyl Sepharose FF	+	-
		Phenyl Sepharose FF	+	-
		Superdex 200	+	-
		CHT ceramic hydroxyapatite, Type II	+	+
	Polishing step	SP Sepharose FF	+	+
	Formulation step	Sephadex G-25 Medium	+	+

B

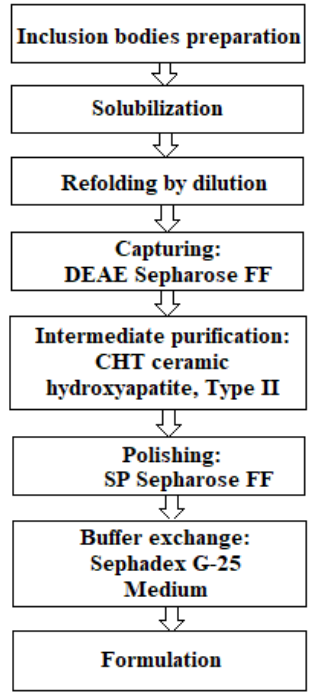

Figure 3.16. Purification scheme for the heterodimers. (**A**) Screening of optimal protein purification conditions. (**B**) A flowchart of the purification steps of SCF-Lα-GCSF and GCSF-Lα-SCF. Abbreviations: + tested; - not tested.

Table 3.6. Yield and purity of heterodimers after three selected processing steps

Protein purification step	Characteristic	SCF-Lα-GCSF	GCSF-Lα-SCF
Refolding step	Yield[1]	93.2±2.9	91.7±2.1
	Purity[2]	24.2±1.0	35.8±2.2
I chromatography step (anion exchange)	Yield[1]	7.3±0.5	6.1±0.3
	Purity[2]	63.5±2.5	58.6±1.4
II chromatography step (mixed-mode)	Yield[1]	1.9±0.4	1.8±0.3
	Purity[2]	77.5±3.0	67.2±2.2
III chromatography step (cation exchange)	Yield[1]	1.4±0.1	1.2±0.2
	Purity[2]	92.2±2.1	90.4±1.6

Each value represents the mean of three independent analyses ± SD.
[1]Protein concentrations were determined by the Bradford method (Bradford, 1976) using bovine serum albumin as a standard.
[2]Purity of the protein was determined by RP-HPLC.

3.3.3. Characterization of the purified heterodimeric proteins

The purified heterodimeric proteins were characterized using a set of analytical methods including SDS-PAGE, Western-blotting, RP-HPLC, SE-HPLC, and HPLC/ESI-MS. The *E. coli* derived G-CSF and SCF monomers were used as the reference standards.

The SDS-PAGE analysis of the reduced and non-reduced heterodimers is shown in Figure 3.17. B. The reduced SCF-Lα-GCSF and GCSF-Lα-SCF proteins were detected as a single band on the gel. The respective bands were observed at the positions that corresponded to the molecular weight of the proteins (42 kDa). The non-reduced SCF-Lα-GCSF and GCSF-Lα-SCF produced the bands that were observed at lower positions (39 and 37 kDa, respectively) on the gel than their calculated molecular weight. Some heterogeneity in the non-reduced protein preparations indicated the presence of minor bands throughout the purification process. Overall, a set of higher molecular weight products in protein preparations were detected both on the SDS-PAGE gel and by Western blotting with polyclonal anti-SCF and monoclonal anti-G-CSF antibodies (Supplementary Figure S4.). The RP-HPLC profiles showed different hydrophobicity of SCF-Lα-GCSF and GCSF-Lα-SCF (Figure 3.17. A), whereas the degree of purity was nearly the same (92.2% and 90.4%, respectively) (Table 3.6.).

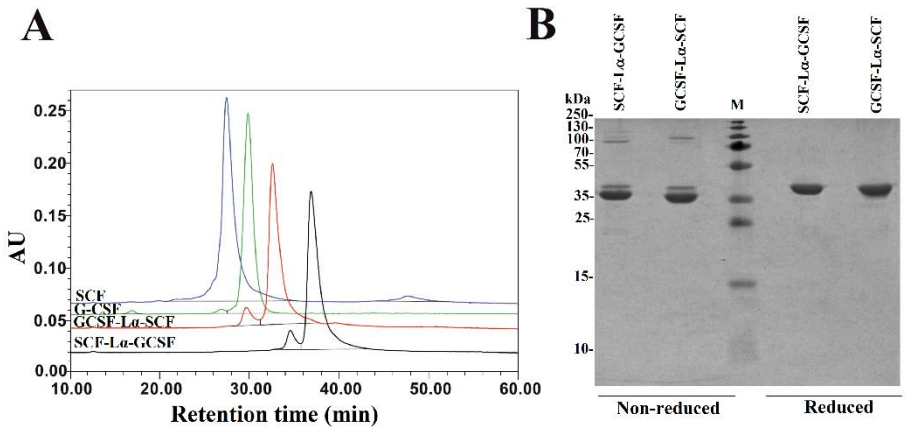

Figure 3.17. Purification characteristics of the fusion proteins. (A) The RP-HPLC analysis of the purified dimeric G-CSF proteins collected after Sephadex G-25 Medium; the G-CSF and SCF monomers used as controls. Fifteen µg of each protein was loaded onto Zorbax 300SB-C18 column (Agilent Technologies) and separated via gradient and isocratic elution with mobile phase A (0.1% TFA in water) and mobile phase B (9.9% water, 90% acetonitrile, and 0.1% TFA) at 30°C. Absorbance at 215 nm is reported as AU. **(B)** SDS-PAGE of the purified dimeric proteins under non-reducing and reducing conditions. *M*, molecular weight marker (Thermo Fisher Scientific).

The oligomeric state and molecular weight of the fusion proteins were analyzed by the calibrated SE-HPLC at pH 7.2 (Figure 3.18.). G-CSF was eluted as a monomer with a molecular weight lower than 13.7 kDa, whereas SCF was detected as a dimeric protein (>44.3 kDa). Both SCF-Lα-GCSF and GCSF-Lα-SCF were found as significantly higher molecular weight (>150 kDa) proteins than predicted (~42 kDa). The SE-HPLC data showed a tendency of heterodimeric proteins to form multimeric structures, presumably elongated non-covalently associated dimers or trimers without a monomeric fraction.

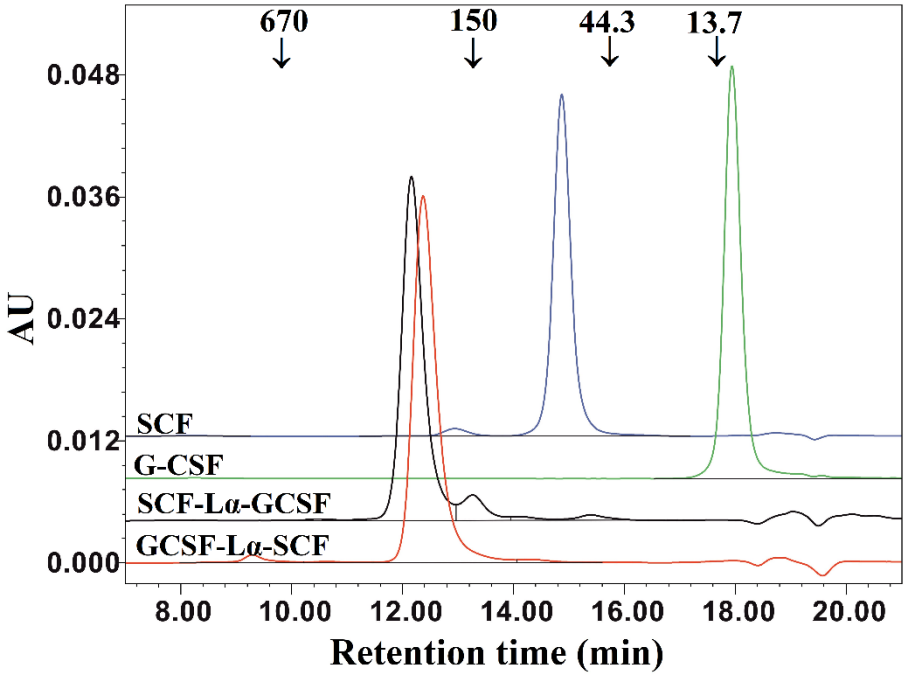

Figure. 3.18. SE-HPLC analysis of purified SCF-Lα-GCSF and GCSF-Lα-SCF. Ten µg of each protein was loaded onto a TSK-gel G3000 SWXL column. The column was calibrated with a protein standard mix (Sigma-Aldrich). The SCF and G-CSF monomers were used as controls. Absorbance at 280 nm is reported as AU.

The HPLC/ESI-MS analysis revealed the composition and molecular mass of purified heterodimers (Supplementary Figure S5.). Some heterogeneity in the monomeric preparations of SCF-Lα-CSF and GCSF-Lα-SCF was observed. The major peaks in the HPLC/ESI-MS chromatograms corresponded to 42,370.48 Da for SCF-Lα-GCSF and 42,370.70 Da for GCSF-Lα-SCF, whereas the minor peaks corresponded to a mass of 42,983.05 and 42,983.27 Da, respectively. The detected molecular mass of both proteins was in good agreement with that of deduced from their amino acid sequences (within a range of 1 Da of the theoretical value).

3.3.4. Binding kinetics of the heterodimeric proteins to the immobilized receptors

Binding of SCF-Lα-GCSF and GCSF-Lα-SCF to the SAM-immobilized receptors, GCSF-R or c-KIT, was analyzed using TIRE. The obtained binding kinetics were compared to that of monomeric SCF and G-CSF. The "site-directed" immobilization was established by the formation of the G protein-based SAM layer and the receptor layer (GCSF-R or c-KIT) (Balevicius et al.,

2014). To analyze the kinetics of the protein-protein interaction, a standard fully reversible Langmuir kinetic model was applied (Balevicius et al., 2014).

The kinetics of the SCF-Lα-CSF, GCSF-Lα-SCF, monomeric G-CSF and SCF binding to the receptors are presented in Table 3.7. and Figure 3.19. Binding kinetics of monomeric G-CSF and SCF-Lα-GCSF to GCSF-R were obtained from our previous study (Balevicius et al., 2019).

The association rate constant *k*a between SCF-Lα-GCSF and c-KIT was about 6-fold higher than that of the SCF monomer, whereas *k*a was 80-fold higher for GCSF-Lα-SCF. The dissociation rate constant k_d for SCF-Lα-CSF was similar to that of the SCF monomer, although it was approximately 45-fold higher for GCSF-Lα-SCF. The *k*a and k_d between SCF-Lα-GCSF and GCSF-R were 10-fold lower than that of monomeric G-CSF. Binding of GCSF-Lα-SCF to GCSF-R was not observed (Figure 3.19.).

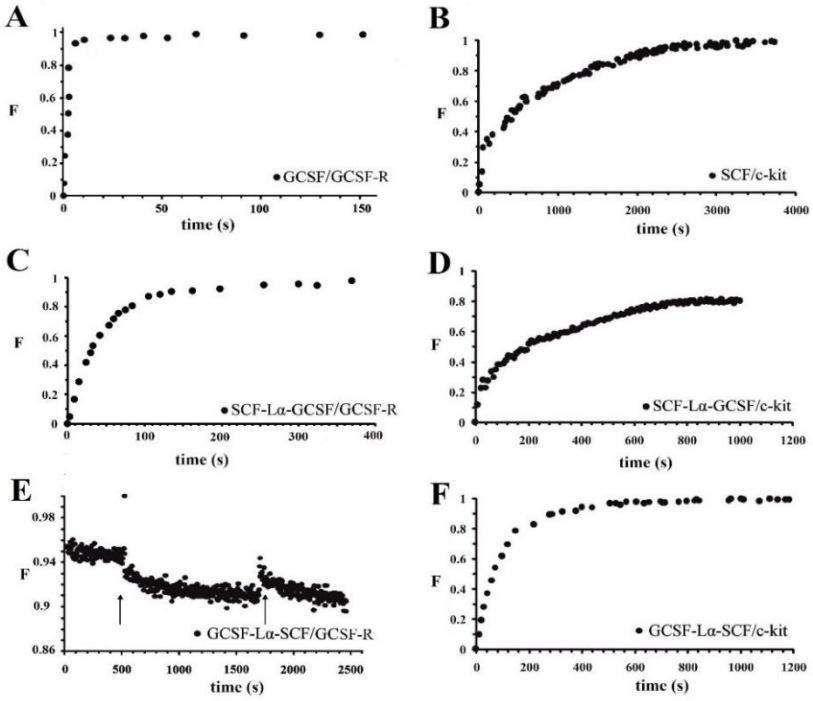

Figure 3.19. Interaction between the monomeric/heterodimeric proteins and the oriented SAM-immobilized receptors. (A) monomeric G-CSF and GCSF-R. **(B)** monomeric SCF and c-KIT. **(C)** SCF-Lα-GCSF and GCSF-R. **(D)** SCF-Lα-GCSF and c-KIT. **(E)** GCSF-Lα-SCF and GCSF-R. **(F)** GCSF-Lα-SCF and c-KIT. The protein-receptor interaction was started to record immediately after protein injection (label by an arrow) into the TIRE cell. After 20 min, the cell was flushed (labeled by an arrow) with the protein-free PBS buffer to remove unbound protein. F, normalized analytical signal.

3.3.5. Biological activity of heterodimers *in vitro*

The *in vitro* biological activity of the SCF and G-CSF moieties in each fusion protein were evaluated by the proliferation assays of M-07e cells expressing the SCF receptor, but not the G-CSF receptor and the G-NFS-60 cells expressing the G-CSF receptor, but not the SCF receptor. The fusion proteins induced a dose-dependent proliferative response on both cell lines (Figure 3.20.). The calculated activity of SCF-Lα-GCSF on the M-07e cells reached 72% ($p \leq 0.01$), whereas GCSF-Lα-SCF showed a relative activity of 137% ($p \leq 0.01$) of that of monomeric SCF at the equimolar amount. The proliferative response of SCF-Lα-GCSF and GCSF-Lα-SCF on the G-NFS-60 cells reached 34% ($p \leq 0.01$) and 13% ($p \leq 0.0001$), respectively, compared to that of the monomeric form of G-CSF at the equimolar amount (Table 3.7.).

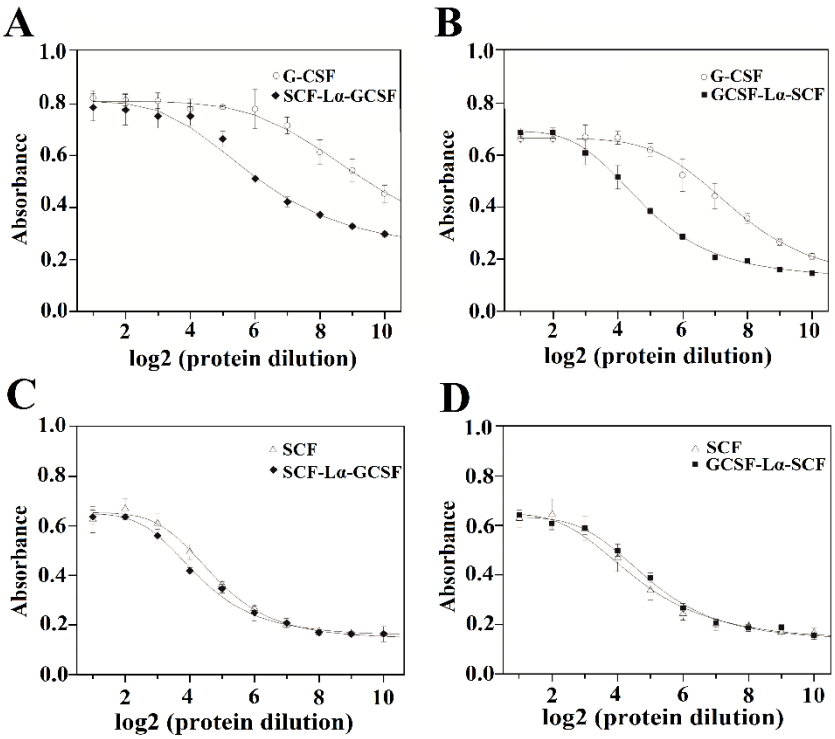

Figure 3.20. Effects of purified SCF-Lα-GCSF and GCSF-Lα-SCF on the proliferation of (A, B) G-NFS-60 and (C, D) M-07e cells, respectively. The G-CSF or SCF monomer (controls) included in each assay. The curves were obtained at two-fold doubling (log 2) serial dilutions of the tested proteins. Error bars represent SD of the absorbance mean obtained from 3-5 independents assays.

Table 3.7. Summary of activity results of heterodimeric proteins and respective monomers

Characteristic	SCF-Lα-GCSF	GCSF-Lα-SCF	G-CSF monomer	SCF monomer
Biological activity on G-NFS-60 cell line[a] (IU/mmol)	$0.64x10^{12}$	$0.25x10^{12}$	$1.88x10^{12}$	ND
Biological activity on M-07e cell line[b] (IU/mmol)	$6.70x10^{9}$	$12.80x10^{9}$	ND	$9.33x10^{9}$
Association and dissociation rate constants of the protein and the SCF receptor (TIRE data)				
*k*a (M^{-1} s^{-1})	$7.77x10^{4}$	$1.14x10^{6}$	ND	$1.37x10^{4}$
$k_d(s^{-1})$	$1.39x10^{-2}$	$6.46x10^{-1}$	ND	$1.43x10^{-2}$
$K_a(M^{-1})$	$5.59x10^{6}$	$1.76x10^{6}$	ND	$9.50x10^{5}$
(K_d) (M)	$1.78x10^{-7}$	$5.67x10^{-7}$	ND	$1.04x10^{-6}$
Association and dissociation rate constants of the protein and the G-CSF receptor (TIRE data)				
*k*a (M^{-1} s^{-1})	$8.5x10^{4}$	−	$7.50x10^{5}$	ND
$k_d(s^{-1})$	$1.25x10^{-3}$	−	$1.05x10^{-2}$	ND
$K_a(M^{-1})$	$6.80x10^{7}$	−	$7.14x10^{7}$	ND
(K_d) (M)	$0.15x10^{-7}$	−	$0.14x10^{-7}$	ND

[a]Cell line expresses the G-CSF receptor.
[b]Cell line expresses the SCF receptor.
−, no interaction detected.
ND, not determined.

3.3.6. Biological activity of SCF-Lα-GCSF *in vivo*

The GCSF-Lα-SCF protein showed a significantly lower activity of the G-CSF moiety *in vitro* than that of SCF-Lα-GCSF, therefore the latter was used for *in vivo* studies. G-CSF stimulates neutrophil release from the bone marrow inducing a transient increase in circulated neutrophils. The biological activity of the G-CSF moiety *in vivo* was tested by the detection of ANC in the peripheral blood of rats in six groups. The ANC peaked 24 h after the subcutaneous administration of SCF-Lα-GCSF (1,000 μg/kg) demonstrating a 7-fold increase ($p \leq 0.01$) compared to ANC before the injection, whereas a mixture of G-CSF and SCF (500 + 500 μg/kg) showed a 6.3-fold increase ($p \leq 0.05$) (Figure 3.21.). The monomeric G-CSF at equimolar concentration showed a 4.4-fold higher ANC count ($p \leq 0.05$), whereas no statistically significant difference was detected after the injection of SCF compared to

ANC before the injection. There is a visible trend that a drop of ANC did not occur immediately at 48 and 72 h post-injection of the heterodimer (a 3-fold ($p< 0.05$) and 5-fold ($p < 0.01$) decrease, respectively compared to ANC at 24 h post-injection) or a mixture of G-CSF and SCF (a 4-fold ($p<0.05$) and 3-fold ($p<0.05$) decrease, respectively compared to ANC at 24 h post-injection) (Figure 3.21.). It was observed a 4-fold decrease in ANC ($p<0.05$) at 48 h post-injection of G-CSF compared to ANC at 24 h post-injection (Figure 3.21.).

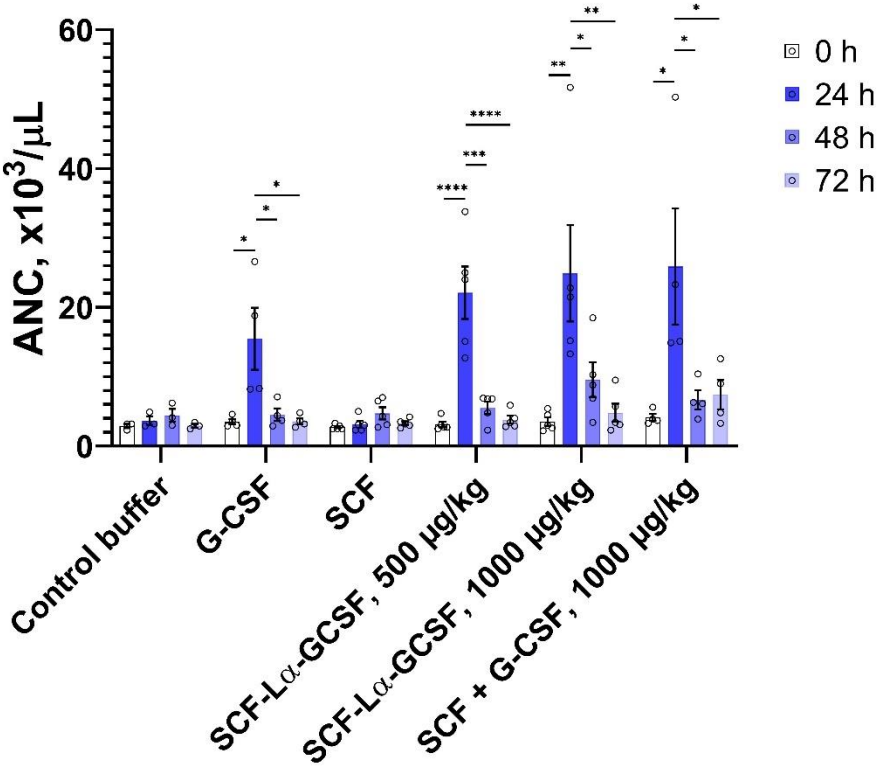

Figure 3.21. The ANC count versus time profiles obtained by subcutaneously administered recombinant proteins. Each rat in the respective group received injections of SCF-Lα-GCSF (500 or 1,000 µg/kg), G-CSF (500 µg/kg), SCF (500 µg/kg), a mixture of SCF and G-CSF (500 + 500 µg/kg), and a control buffer. Results are expressed as the mean ± SEM. Individual values from the independent assays are indicated by the open circles. A one-way ANOVA combined with the Tukey's multiple comparison test was performed to compare the means of ANC values at different time points in each group (buffer or protein). *Values are significantly different between ANC count induced by injection of each protein at different time points (*$p<0.05$; **$p<0.01$; ***$p<0.001$, ****$p<0.0001$).

4. DISCUSSION

The short half-life of biopharmaceuticals is conditioned by a rapid metabolism, proteolytic degradation, and susceptibility of small proteins to renal clearance (Kontermann, 2011). Chemical modification and covalent attachment of PEG are among half-life extension strategies dedicated to increase the hydrodynamic volume of therapeutic proteins. The fusion of the target protein to the Fc region of immunoglobulin and fusion to human serum albumin results in a prolonged circulation time and allows overcoming problems connected with the safety of PEGylated compounds (Baumann et al., 2014). Overall, the multimeric proteins produced by more simple technology than PEGylation have become attractive due to increased biological activity and/or prolonged circulation time (Czajkowsky et al., 2012; Strohl, 2015).

Recombinant forms of human G-CSF are widely used for the treatment of cancer therapy-induced neutropenia. Several second-generation drugs of G-CSF with improved therapeutic properties are already available and the development of new forms is still in progress (Table 4.1.).

In this work, the construction, purification, and characterization of three novel human G-CSF dimers, GCSF-L2-GCSF, GCSF-L7-GCSF, and GCSF-Lα-GCSF, which we developed by genetic fusion of two G-CSF molecules via three specific linkers was described. All proteins were found in the insoluble fraction of the total cell lysate. Active, recombinant human G-CSF contains a free cysteine residue at position 17 and two intramolecular disulfide bonds, Cys36-Cys42 and Cys64-Cys74 (Lu et al., 1989). To recover the biological activity of dimeric G-CSFs accumulated as insoluble proteins, the main focus was laid on the selection of an appropriate refolding procedure for them. The successful refolding of Ibs solubilized in urea in the presence of a sufficient amount of DTT was achieved by a subsequent slow dilution procedure, which gave purities of the refolded proteins of higher than 40%, as determined by RP-HPLC (Table 3.2.).

Two consecutive chromatographic steps were selected for the purification of GCSF-L2-GCSF, GCSF-L7-GCSF, and GCSF-Lα-GCSF. The purity of GCSF-Lα-GCSF determined by RP-HPLC was approximately 95% (Table 3.2.). Complete separation of the oxidized and longer-retained forms of the GCSF-L2-GCSF and GCSF-L7-GCSF proteins was practically infeasible by conventional ion-exchange chromatography methods. The final purity of GCSF-L2-GCSF and GCSF-L7-GCSF was less than 83%, as

determined by RP-HPLC, and the final yield was 6-11 times lower than that of GCSF-Lα-GCSF (Table 3.2.).

Table 4.1. An overview of short- and long-acting G-CSF medications in comparison to GCSF standard filgrastim

Strategy of development	Composition	Expression system	Examples	Advantages	Disadvantages
(A) Short-acting rhG-CSF	GCSF	*E. coli*	Filgrastim	• Biological activity is comparable to endogenous G-CSF • Simple and inexpensive production	• Short plasma half-life • Stability issues • Sensitive to degradation
		CHO cells	Lenograstim	• Glycosylated G-CSF • Resistance to proteolysis • Higher stability	• Higher production price • Short plasma half-life
		E. coli	Nartograstim (N-terminal mutated G-CSF)	• Enhanced biological activity	• Short plasma half-life
(B) PEGylated G-CSF	20PEG-GCSF 20PEG-O-glycan-GCSF 10PEG-GCSF	*E. coli*	Pegfilgrastim Lipegfilgrastim FN10L	• Prolonged half life • Improved stability, resistance to proteolysis	• Lower biological activity • Higher production price
	10PEG-GCSF-GCSF-10PEG	*E. coli*	diPEG-F_{dim}	• Prolonged half life	• Low biological activity • Higher production price
(C) Protein fusion	HSA-GCSF GCSF-3.4PEG-(IgG4)Fc	*S.cerevisiae* *E. coli*	Balugrastim Eflapegrastim	• Prolonged half life • Greater biological activity	• Higher production price

Table 4.1. An overview of short- and long-acting G-CSF medications in comparison to GCSF standard filgrastim

Strategy of development	Composition	Expression system	Examples	Advantages	Disadvantages
	GCSF-(IgG2)Fc-GCSF	CHO cells	F-627[1]	• Prolonged half life • More rapid neutrophil recovery	• Higher production price
	GCSF-L-GCSF[2] SCF-L-GCSF[2]	*E. coli*	GCSF-Lα-GCSF SCF-Lα-GCSF	• Greater biological activity *in vivo* • Prolonged half life • Simple and inexpensive production	• Discrepancy of biological activity *in vivo* and *in vitro*. Further studies needed
	GCSF-GCSF	*E. coli*	F_{dim}	• Simple and inexpensive production	• Short plasma half-life
(D) New formulation	PLGA + GCSF GCSF liposomes	*E. coli*	PLGA + GCSF DPPC/Chol + GCSF	• Controlled sustained release • Long-term circulation *in vivo*	• Different size of particles • Stablity issues • Sterilization challenges • Encapsulation efficiency

Approved G-CSF as therapeutics are underlined, others variants of G-CSF are described in the scientific literature only.
[1]- The first phase III clinical trial was completed.
[2]- G-CSF homo- and heterodimers generated and described in this dissertation work.

The longer RP-HPLC-retained form in the GCSF-L2-GCSF and GCSF-L7-GCSF preparations was detected as an extra band in SDS-PAGE, which was present throughout the purification process. This extra band disappeared in SDS-PAGE under reducing conditions, indicating that this accompanying impurity originated from the formation of extra disulfide bonds within these proteins. This structure could be formed via –S–S– bonds of unpaired cysteine residue that originated from the G-CSF monomer units. This assumption may explain why such protein forms were not completely separated during chromatography steps and confirm the importance of the linker composition and length. The L2 and L7 linkers increased spatial separation between the domains, allowing them to interact with one another (Chen et al., 2013; Chichili et al., 2013), while the Lα linker may rigidly ensure separation and elongation of the two G-CSF monomers to a distance favorable for their independent functioning. GCSF-Lα-GCSF has a significant advantage over the other two dimers, as it is easier to purify and obtain large quantities of high purity protein.

The interaction between the G-CSF molecule and its G-CSF receptor resulted in a stoichiometric ratio of 2:2 (Tamada et al., 2006). In this work, the spectroscopic TIRE method was applied to analyze the binding kinetics between G-CSF homodimers and GCSF-R. G-CSF monomer was used as a reference standard. Although all proteins interacted with the GCSF receptor, their association rate constants were different. The obtained data showed that GCSF-L2-GCSF having a shorter linker sequence act as the G-CSF monomer (1:1 stoichiometry between GCSF-L2-GCSF and GCSF-R) (Figure 4.1. B). L2 linker is short, so it does not allow the second GCSF molecule to find a binding partner if the first is already complexed with the G-CSF receptor. Meanwhile, the length of both L7 and Lα linkers allows spatial separation of the G-CSF molecules in a way that their binding sites become accessible for interaction with their receptors. GCSF-L7-GCSF and GCSF-Lα-GCSF proteins therefore may activate the receptor with higher efficiency supporting the 1:2 stoichiometry between the dimeric G-CSF protein and its G-CSF receptor (Figure 4.1. C). The L7 linker, which consisted of stretches of Gly and Ser residues, implemented greater degrees of freedom in the overall conformation, whereas the Lα linker had a more rigid, helical-alpha, spiral-like structure (Chen et al., 2013; Chichili et al., 2013; Yamasaki et al., 1998).

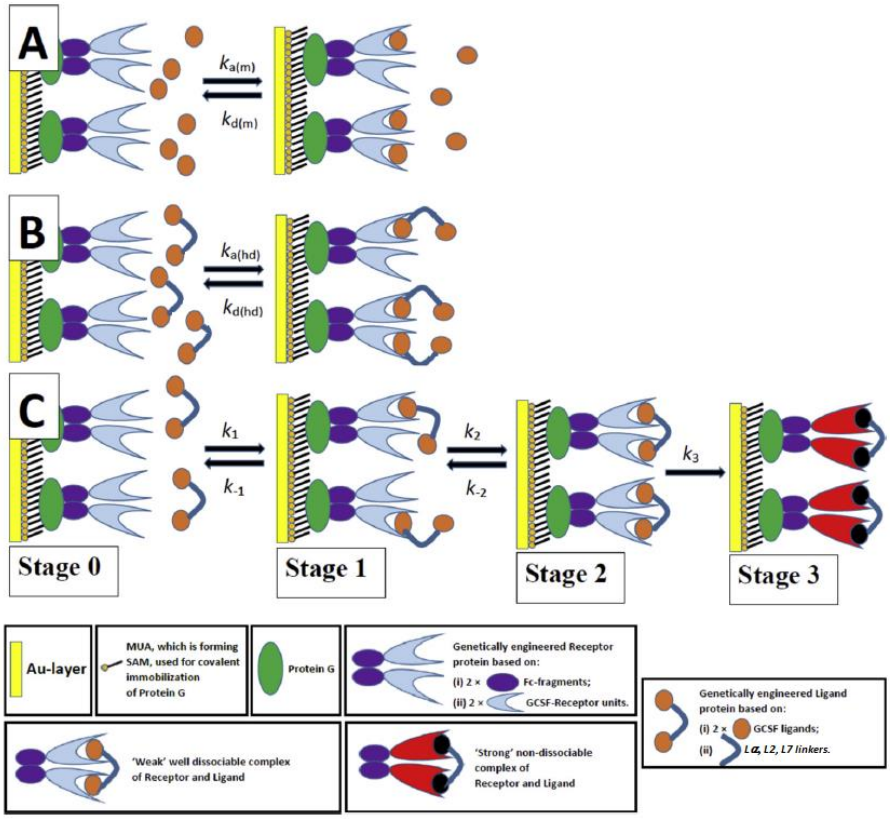

Figure 4.1. Schematic representation of the interaction between immobilized G-CSF receptor and recombinant G-CSF proteins. (A) soluble G-CSF monomer and GCSF-R (interaction described by a standard Langmuir kinetics model); **(B)** GCSF-L2-GCSF and GCSF-R (interaction described by a standard Langmuir kinetics model); **(C)** GCSF-L7-GCSF or GCSF-Lα-GCSF and GCSF-R (interaction described by a three-stage kinetics model).

The ability to stimulate cell proliferation *in vitro* was reduced for all dimeric G-CSF molecules compared to the G-CSF monomer. Retention of about 50% of *in vitro* biological activity by GCSF-Lα-GCSF might indicate that spatial interference has an impact on G-CSF interaction with the receptor as the N- and C-termini of G-CSFs in the dimeric molecule are joined with the linker sequence.

In vitro biological activity of GCSF-Lα-GCSF was comparable to that of PEGylated G-CSF (Pegfilgrastim), whereby PEG is attached to amine groups found at the N-terminus of G-CSF, which retained from 45 to 70% activity relative to the G-CSF monomer (Fidler et al., 2011; Molineux, 2009). The fusion of two G-CSF molecules into a homodimer obviously has an advantage over longer acting forms of G-CSF, as the generation of dimeric proteins was

obtained by more simple technology than PEGylation. Low biological activity of GCSF-L2-GCSF and GCSF-L7-GCSF could be a consequence of the steric hindrance caused by improper linker length and the presence of accompanying impurities.

The biological activity assays in healthy rats demonstrated that the GCSF-Lα-GCSF molecule has advantages over the G-CSF monomer. GCSF-Lα-GCSF showed a circulation half life of 8.7 h, more than seven-fold longer than that of G-CSF. In another study, the dimer (F_{dim}) generated by joining two G-CSF molecules via disulfide bridges between non-paired cysteines had the same circulation half-life as the G-CSF monomer (Fidler et al., 2011). We assume that F_{dim} is a more compact molecule than GCSF-Lα-GCSF; therefore, the prolonged action of GCSF-Lα-GCSF is primarily associated with the hydrodynamic radius of the molecule.

The *in vivo* response, which comprised the ability of G-CSF to stimulate neutrophil release, was more pronounced for GCSF-Lα-GCSF compared to the monomeric protein. After 24 h of a single subcutaneous injection of GCSF-Lα-GCSF, rats exhibited a 1.8-fold increase in circulating neutrophils, albeit with a larger margin of error.

Biological activity studies with healthy rats demonstrated that GCSF-Lα-GCSF had a longer half-life in the blood serum and produced a stronger neutrophil response compared to monomeric G-CSF. Thus, this recombinant fusion protein might be selected for further studies as a potential drug candidate. However, for this purpose the considerable amount of protein is needed by scaling up protein production. A prerequisite for clinical application of protein is the formulations where the protein remains stable and active.

To detect the growth of plasmid-free cells during recombinant *E. coli* cultivation, a resistance marker was habitually added to the plasmid backbone. Resistance to ampicillin is conferred by the *bla* gene whose product is an enzyme β-lactamase that inactivates β-lactam antibiotics. However, degradation of antibiotics ensues and in a couple of hours ampicillin is almost depleted (Korpimäki et al., 2003; Brouwers et al., 2020). Selective agent kanamycin, which is believed to have higher stability during cultivation (Umezava, 1979) might be preferable in laboratories operating in compliance with good manufacturing practice (GMP) standards. Thus, the DNA fragment coding for GCSF-Lα-GCSF was cloned into pET28a(+) plasmid bearing the kanamycin resistance gene. The harvested biomass of recombinant *E. coli* cultivated in a chemically defined media was 1.9-fold higher than that of M9 minimal medium with supplements. However, the protein production yield

was nearly the same in both media. A chemically defined medium offers certain advantages, such as defined nature, reduced risk of batch composition variables, and animal-origin free medium, which is preferable in the manufacturing process (Stramaglia et al., 2009).

The final product purified from 125 g of wet cell mass presented a high purity (>98%) determined by RP-HPLC. The calculated GCSF-Lα-GCSF yield after each purification step was similar to that obtained in small-scale screens (Table 3.2. and Table 3.4., respectively). The recovered total amount was 670 mg of GCSF-Lα-GCSF from a 125 g wet cell mass representing a purification yield of about 17.18%.

The thermal stress conditions applied to GCSF-Lα-GCSF in formulation buffer revealed protein aggregates that also found in stored preparations of monomeric G-CSF (Krishnan et al., 2002). RP-HPLC also detected monomer loss and formation of proteins that differ from the main compound in hydrophobicity.

The Lα linker was used to fuse SCF and G-CSF molecules, based on previous research on G-CSF homodimers. The α-helix conformation of the linker efficiently separates the domains of the bifunctional fusion proteins ensuring that the distance between the monomers is favorable for their independent functioning (Arai et al., 2001; Chen et al., 2013).

Two fusion proteins SCF-Lα-GCSF and GCSF-Lα-SCF were expressed in *E. coli*, recovered from the inclusion bodies with subsequent refolding by dilution, and purified using an anion-exchange, mixed-mode, and cation-exchange chromatography. A purification yield reaching more than 2.6 mg/12 g wet cell mass was obtained for both heterodimers. The purity of proteins was more than 90% as determined by RP-HPLC (Table 3.6.).

The results of SDS-PAGE and Western blot showed that the purified heterodimer preparations represented a homogeneous protein under reducing conditions. Under non-reducing conditions, the amount of monomeric forms of SCF-Lα-CSF and GCSF-Lα-SCF (39 and 37 kDa, respectively) decreased and the higher molecular weight protein bands on the gel were detected. These extra bands found throughout the purification process showed reactions with the monoclonal antibody against G-CSF and the polyclonal antibodies against SCF. It was reported that *E. coli*-derived human SCF produced a major SDS-dissociable form, that is, similar to naturally occurring SCF, whereas a minor form is a non-SDS-dissociable disulfide-linked dimer (Zsebo et al., 1990; Lu et al., 1996; Hsu et al., 1997). The presence of the disulfide-linked multimeric forms (range of 87-120 kDa) in the preparations of heterodimeric proteins corresponded to that of *E. coli*-derived SCF.

The ESI/MS analysis confirmed the calculated molecular mass of the fusion proteins, although additional minor peaks corresponding to the molecular mass of 42,983.05 Da for SCF-Lα-GCSF and 42,983.27 Da for GCSF-Lα-SCF were detected. The molecular mass difference between the minor and major peaks suggests that the impurities may represent a heterodimer with an open disulfide bond (Taniuchi et al., 1977) that results in the association of cysteines with two reduced molecules of glutathione. This assumption might explain the occurrence of the extra minor band with a molecular weight of 47 kDa for SCF-Lα-GCSF and 45 kDa for GCSF-Lα-SCF on SDS-PAGE under non-reducing conditions.

The SE-HPLC analysis showed that both fusion proteins have comparable tertiary structures and the estimated molecular mass was higher than expected. The SCF preparations showed a similar abnormal elution profile (Arakawa et al., 1991). At neutral pH, the apparent molecular weight (57 kDa) of *E. coli*-derived SCFs was related to a relatively large Stoke radius. The lower molecular mass fraction of the heterodimers on the SDS-PAGE gel indicates that the fusion proteins are non-covalent dimers or trimers under native conditions.

The biochemical activity of SCF and G-CSF moieties in each fusion protein was evaluated analyzing the interaction between the heterodimers and their SAM-immobilized receptors. GCSF-Lα-SCF exhibited more efficient binding to the SCF receptor than the SCF-Lα-GCSF protein (Table 3.7.). Thus, the G-CSF moiety on either GCSF-Lα-SCF or SCF-Lα-GCSF did not affect the binding of the SCF moiety to its receptor. The N-terminal SCF moiety of SCF-Lα-GCSF did not impair the C-terminal G-CSF moiety's binding with GCSF-R. However, the C-terminal SCF moiety of GCSF-Lα-SCF blocked the N-terminal G-CSF binding to its receptor.

Each fusion protein promoted the M-07e cell proliferation. The potency of GCSF-Lα-SCF was about 1.4-fold higher than that of monomeric SCF at equimolar concentration, whereas SCF-Lα-GCSF induced cell proliferation at a significantly lower level.

The fusion proteins showed a remarkably reduced proliferative response of the G-CSF moiety on the G-NFS-60 cell line. The structural studies showed that the N-terminal residues and the Cys4-Cys89 disulfide bond of SCF are required for a receptor binding and activity (Zhang et al., 2000; Jiang et al., 2000). However, the N-terminal G-CSF moiety of GCSF-Lα-SCF did not reduce binding of SCF to its receptor. The results indicate that the Lα linker ensured spatial separation between the domains of the fusion protein at a favorable distance for their independent functioning. The reduced G-CSF

activity of two fusion proteins may be due to a steric hindrance caused by the multimeric forms of the SCF moiety.

In vivo, SCF-Lα-GCSF stimulated a 7.0-fold increase of ANC and the effect was similar to that of the mixture of SCF and G-CSF (a 6.3-fold increase), whereas the response induced by the G-CSF monomer was a 4.4-fold higher at equimolar concentration. Human SCF has low bioactivity on rodent hematopoietic cells (Broudy, 1997), therefore the obtained data does not properly reflect the potency of the SCF-Lα-GCSF heterodimer *in vivo*. However, the SCF-Lα-GCSF protein is a promising drug candidate for further studies due to its biological activity *in vitro* and *in vivo* comparable to that of the mixture of SCF and G-CSF.

CONCLUSIONS

1. Compared to other studied homodimeric G-CSFs, the developed purification procedure of dimeric G-CSF with an alpha-helix-forming peptide linker resulted in higher purity (>95%) and yield (>14%). Also, GCSF-Lα-GCSF demonstrated the best performance in term of biological activity *in vitro*.
2. Compared to monomeric G-CSF, GCSF-Lα-GCSF had a 7-fold longer circulation half-life and a 1.8-fold higher biological activity after 24 hours *in vivo*.
3. Developed and optimized protein isolation and purification schemes were applicable for small and large-scale protein production and allowed to achieve more than 79% purity of dimeric proteins, which is suitable for their further characterization.
4. The Lα-type linker ensure a proper distance between G-CSF and SCF molecules favourable for independent functioning of proteins in homo- and heterodimers.
5. The SCF and G-CSF moieties in the fusion protein SCF-Lα-GCSF displayed the *in vitro* receptor binding and *in vivo* neutrophil release ensured by the G-CSF activity.
6. GCSF-Lα-GCSF and SCF-Lα-GCSF proteins might be selected for further studies as potential drugs.

SUMMARY

ĮVADAS

Šiuo metu pasaulyje biologiniai vaistai yra vieni pagrindinių preparatų, skiriamų įvairių ligų gydymui. Jie visuotinai pripažįstami klinikinėje praktikoje ir daugeliu atveju yra nepakeičiami gydant rimtas ir lėtines ligas, tokias kaip cukrinį diabetą, autoimunines ligas ir vėžinius susirgimus (Walsh, 2014). Vis dėlto, biologiniai vaistai, sudaryti iš baltymų ar peptidų, dažnai pasižymi nepakankamomis fizikinėmis, cheminėmis bei farmakokinetinėmis savybėmis: nestabilumu organizme, ribotu tirpumu, santykinai trumpu gyvavimo organizme pusamžiu, imunogeniškumu ar toksiškumu.

Buvo sukurta daug įvairių technologijų, kuriomis siekiama pagerinti biologinių vaistų savybes (Metzner ir kt., 2013; Pasut, 2014; Strohl, 2015; Witteloostuijn ir kt., 2016). Jos apima specifinius aminorūgščių pakeitimus – siekiant sumažinti vaisto imunogeniškumą ir proteolitinį nestabilumą, galutines produkto modifikacijas sujungiant su natūraliais ar sintetiniais polimerais (polietileno glikolio molekule (PEG), polisialo rūgštimi, hidroksietilo krakmolu) bei kitas strategijas (Pasut, 2014; Witteloostuijn ir kt., 2016). Tikslinio baltymo genetinis suliejimas su žmogaus serumo albuminu (pvz. Albiglutidas) prailgina biologinio vaisto cirkuliaciją kraujo plazmoje (Rogers ir kt., 2015). Fc fragmentas, kuris yra imunoglobulino IgG dalis, daugeliu atveju taip pat pagerina prijungto partnerio fizikines savybes, tokias kaip baltymo stabilumas (Czajkowsky ir kt., 2012). Kiti nauji konjugavimo partneriai, kurie gali būti pritaikomi terapeutinių baltymų ir peptidų pusamžio prailginimui, yra žmogaus trasferinas ir sialilintas C-gale peptidas (CTP) (Duijkers ir kt., 2002; Fares ir kt., 2007).

Žmogaus granuliocitų kolonijas stimuliuojantis veiksnys (G-CSF) yra hematopoetinis citokinas, kuris reguliuoja neutrofilinių granuliocitų pirmtakinių ląstelių brendimą, proliferaciją ir diferenciaciją. Rekombinantinės jo vaistinės formos plačiai taikomos gydyti neutropeniją, ypač tą, kurią sukelia citotoksinė chemoterapija. Modifikuotos G-CSF baltymo formos taip pat turi pasisekimą biologinių vaistų tarpe. Be pirmųjų, taip vadinamų pirmosios kartos biologinių vaistų, filgrastimo ir lenograstimo, klinikoje yra naudojami ir pagerinti (angl. *biobetters*) biologiniai vaistai – nartograstimas ir pegfilgrastimas. Nartograstimas dėl pakeistos aminorūgščių sekos pasižymi padidėjusiu granuliopoetiniu aktyvumu (Maruyama ir kt., 1998; Okabe ir kt., 1990; Suzuki ir kt., 1992). Tuo tarpu, filgrastimo pegilinimas padidina molekulės hidrodinaminį spindulį ir prailgina vaisto cirkuliavimą kraujyje, taip sumažindamas jo dozavimo dažnį (Molineux, 2004). Nėra aišku ar PEG molekule modifikuoti baltyminiai vaistai visiškai yra saugūs pacientui, nes

PEG nėra biologiškai skaidomas, todėl gali kauptis organizme, o tai yra ypatingai svarbu vartojant pegilintus vaistus ilgesnį laiką. Be to, kai kuriais atvejais stebimas ir padidintas tokių vaistų imunogeniškumas (Baumann ir kt., 2014). Todėl, siekiant pagerinti terapines G-CSF savybes ir įveikti iššūkius, susijusius su cheminėmis modifikacijomis, naujų G-CSF formų kūrimas vis dar tebevyksta ir yra reikalingas.

G-CSF savo biologinę funkciją atlieka specifiškai sąveikaudamas su G-CSF receptoriumi santykiu 2:2 (Tamada ir kt., 2006), vadinasi G-CSF receptorių homodimerizacijai bei tolimesniam signalo perdavimui reikia dviejų G-CSF molekulių. Dėl šios priežasties, G-CSF dimerai yra patraukli ir daug žadanti technologija kuriant pagerintas G-CSF vaistines formas. Šio tyrimo pradžioje, buvo pranešta apie keletą G-CSF dimerų sukūrimą (Hu ir kt. 2010; Fidler ir kt., 2011). Lyginant su G-CSF monomeru, dimeras, sudarytas iš dviejų žmogaus G-CSF, sujungtų tarpusavyje per Fc fragmentą, sukėlė greitesnį neurofilų skaičiaus padidėjimą (Hu ir kt. 2010). Tuo tarpu kitas G-CSF dimeras (F_{dim}), sukurtas sujungiant dvi G-CSF molekules per disulfidinius tiltelius tarp nesuporuotų cisteinų, nebuvo toks sėkmingas. F_{dim} turėjo mažesnį biologinį aktyvumą bei tą patį cirkuliacijos pusamžį ($t_{1/2}$) kraujyje kaip ir G-CSF monomeras (Fidler ir kt., 2011).

Daugelis tyrimų patvirtino, kad jungiančiosios sekos (angl. *linkers*) yra svarbios kuriant sulietų baltymų technologijas, nes jų sudėtis, ilgis ir lankstumas lemia šių baltymų fizikines, chemines bei biologines savybes. Todėl racionalus jungiančiųjų sekų pasirinkimas lieka sudėtinga, bet labai svarbi užduotis.

Nors yra sukurta ir patvirtinta keletas rekombinantinių G-CSF vaistinių formų, neutropenijai gydyti reikia veiksmingesnių ir pigesnių biologinių vaistų.

Šio darbo tikslas buvo sukurti bei charakterizuoti naujus žmogaus G-CSF homo- ir heterodimerinius baltymus, genetiniu būdu suliejant G-CSF ir SCF molekules per įvairaus ilgio ir struktūros jungiančiąsias sekas.

Pagrindinės šio darbo užduotys buvo:

1. *E. coli* bakterijose susintetinti žmogaus G-CSF homodimerus, turinčius tris skirtingas jungiančiąsias sekas.
2. Išgryninti ir charakterizuoti G-CSF dimerus jautriais analitiniais metodais.
3. Ištirti G-CSF homodimerų biologinį aktyvumą ir jų cirkuliacijos laiką *in vivo*.

4. Nustatyti perspektyviausią G-CSF homodimerinį vaistą-kandidatą ir optimizuoti jo gryninimo protokolą bei įvertinti suformuluoto dimero stabilumą.
5. *E. coli* bakterijose susintetinti heterodimerus, sudarytus iš G-CSF ir SCF bei pasirinktos G-CSF homodimerus jungiančios sekos, kuri užtikrina pagerintas G-CSF homodimero charakteristikas.
6. Išgryninti ir charakterizuoti heterodimerus jautriais analitiniais metodais.

Mokslinis naujumas ir svarba

Įvairios strategijos yra naudojamos siekiant pagerinti biologinių vaistų savybes. Sulieti baltymai, dar vadinami chimeriniais, pasižymi prailginta cirkuliacijos *in vivo* trukme ar didesniu funkciniu aktyvumu. Šiame darbe aprašytas homodimerų, sudarytų iš dviejų G-CSF molekulių, ir heterodimerų, susidedančių iš G-CSF ir SCF, kūrimas. Siekiant išsamiau įvertinti G-CSF monomerus jungiančių sekų ilgio/sudėties įtaką sulieto baltymo fizikinėms bei biologinėms savybėms, pirmą kartą dvi G-CSF molekulės buvo genetiniu būdu sulietos per skirtingas jungiančiąsias sekas. G-CSF homodimeras, turintis struktūrizuotą alfa spiralės seką (Lα), turėjo 7 kartus ilgesnį cirkuliacijos pusamžį ($t_{1/2}$) ir stimuliavo didesnį neutrofilų kiekio išsiskyrimą, palyginus su monomeriniu G-CSF. Visiško vidaus atspindžio elipsometrijos (VVAE) metodu išmatuotos G-CSF homodimerų su G-CSF receptoriumi sąveikos kinetikos parodė, kad tiek GCSF-Lα-GCSF, tiek GCSF-L7-GCSF sąveikavo su receptoriumi GCSF-R efektyviau nei GCSF-L2-GCSF baltymas bei pagrindė 1:2 stechiometriją dimero ir receptoriaus atžvilgiu.

Dviejų G-CSF molekulių suliejimas į homodimerą turi akivaizdų pranašumą, lyginant su kitais G-CSF pagrindu sukurtais antros kartos G-CSF biologiniais vaistais. G-CSF dimerų gamybos technologija yra žymiai paprastesnė ir efektyvesnė nei PEGilinimo procesas. Sukurta GCSF-Lα-GCSF gryninimo schema, susidedanti iš oksidacinės baltymo renatūracijos tirpale bei trijų chromatografinių žingsnių (jonų mainų ir einančios paskui gel-filtracijos), leido gauti didelio grynumo (≥95%) ir didelės išeigos (≥14%) baltymą. Optimizuota dimero išskyrimo ir gryninimo procedūra yra tinkama tiek mažos, tiek didelės skalės mastu, pasižymi santykinai trumpu gamybos laiku ir kaina.

Tolimesnės studijos yra reikalingos, kad GCSF-Lα-GCSF būtų laikomas kaip potencialus G-CSF terapinis vaistas, kuris yra struktūriškai naujas, palyginus su šiuo metu rinkoje esančiais G-CSFs. Be to, Lα

jungiančioji seka galėtų būti taikoma ir kuriant kitas struktūriškai panašias receptorių/ligandų sistemas.

Norėdami įrodyti Lα jungiančiosios sekos gebėjimą efektyviai atskirti domenus ir įveikti iššūkius, susijusius su kombinuota dviejų baltymų terapija, antroje šio darbo dalyje mes sukūrėme sulietus baltymus, sudarytus iš žmogaus G-CSF ir SCF, sujungtus per alfa spiralę formuojančią seką. Daugelyje tyrimų atskleistas SCF ir G-CSF sinergetinis veikimas, sukeliantis svarbius biologinius atsakus. Sinergetiškai veikiančių citokinų suliejimo technologija yra patraukli terapiniais tikslais, norint sustiprinti atskirų baltymų poveikį ir suteikti naujų baltymo savybių. Be to, dimero vartojimas sumažintų ir neigiamą pakartotinį baltyminių injekcijų poveikį.

VVAE duomenys bei biologinio aktyvumo tyrimai *in vitro* su išgrynintais SCF-Lα-GCSF ir GCSF-Lα-SCF parodė, kad Lα jungiančioji seka užtikrina jų atskirų domenų atskyrimą ir funkcines savybes. Heterodimerai sąveikavo su SCF ir G-CSF receptoriais, taip skatindami tiek G-NFS-60, tiek M-07e ląstelių proliferaciją. SCF-Lα-GCSF biologinio aktyvumas *in vivo* buvo panašus į SCF ir G-CSF monomerų mišinio aktyvumą, todėl šis sulietas baltymas gali būti toliau tiriamas kaip perspektyvus vaistas-kandidatas.

Ginamieji teiginiai:

1. Sukurta grynimo procedūra leidžia pasiekti didesnį GCSF-Lα-GCSF dimero grynumo laipsnį bei išeigą, nei kitų darbo metu ištirtų G-CSF homodimerų atvejais.
2. Palyginus su monomeriniu G-CSF, GCSF-Lα-GCSF turi ilgesnį cirkuliacijos laiką ir yra biologiškai aktyvesnis tyrimuose *in vivo*.
3. Sukurtos dimerų išskyrimo ir gryninimo procedūros yra tinkamos tiek mažo, tiek didelio masto baltymų gryninimui.
4. Lanksti Lα tipo jungiančioji seka sulietuose baltymuose užtikrina nepriklausomą monomerų funkcinį veikimą.
5. SCF ir G-CSF monomerai, sudarantys SCF-Lα-GCSF heterodimerą, yra biologiškai aktyvūs.
6. Sulieti homo- ir heterodimeriniai citokinai gali būti plėtojami kaip biofarmacinės paskirties vaistai.

MEDŽIAGOS IR METODAI

Cheminės medžiagos

1 lentelė. Darbe naudoti pagrindiniai reagentai

Reagentas	Šaltinis
NaCl, karbamidas, EDTA, ledinė acto rūgštis, Tris, KH_2PO_4, Na_2HPO_4 x $2H_2O$, $(NH_4)_2SO_4$, $MgSO_4$ x $7H_2O$, D(+)-gliukozė, $FeCl_3$ x $6H_2O$, $CaCl_2$, $ZnSO_4$ x $7H_2O$, $MnSO_4$ x H_2O, $CuSO_4$ x $5H_2O$, $CuSO_4$ x $5H_2O$, H_3BO_3, $CoCl_2$ x $6H_2O$, Na_2MoO_4 x $2H_2O$, $(NH_4)_2HPO_4$, Na_2HPO_4 x $2H_2O$, NaH_2PO_4 x $2H_2O$, NH_4HCO_3	Merck
Acetonitrilas (ACN), NaOH	Honeywell
N,N,N',N'-tetrametiletilendiaminas (TEMED)	Acros Organics
Amonio persulfatas (APS), 30% akrilamido-BIS tirpalas, 37,5:1, natrio dodecilsulfato (SDS) granulės, fosfato buferinio tirpalo (PBS) tabletės	Carl Roth
Trifluoracto rūgštis (TFA)	Acros Organics
Tween 80, Tween 20, $C_6H_8O_7$ x H_2O, L-oksiduotas glutationas (GSSG), Na_2SO_4	Sigma-Aldrich
1,4-ditiotreitolis (DTT), izopropil-β-D-1-tiogalaktopiranozidas (IPTG)	Thermo Scientific

Bakterijų kamienai

2 lentelė. Darbe naudoti bakterijų kamienai

E. coli kamienas	Genotipas	Šaltinis
BL21(DE3)	B F^- *ompT gal dcm lon hsd* $S_B(r_B^-m_B^-)$ λ(DE3 [*lacI lacUV5-T7p07 ind1 sam7 nin5*]) $[malB^+]_{K-12}(\lambda^S)$	Novagen/Thermo Fisher Scientific
BL21STAR(DE3)	F^- *ompT hsd*S_B ($r_B^-m_B^-$) *gal dcm rne131* (DE3)	Invitrogen/Thermo Fisher Scientific

Plazmidiniai vektoriai

3 lentelė. Darbe naudoti plazmidiniai vektoriai

Plasmidinis vektorius	Savybės	Šaltinis
pET21(b)+	AmpR, *lacI*, PT7*lac*, 5442 bp	Novagen/Thermo Fischer Scientific
pET28(a)+	KanR, *lacI*, PT7*lac*, 5368 bp	Novagen/Thermo Fischer Scientific

3 lentelė. Darbe naudoti plazmidiniai vektoriai

Plasmidinis vektorius	Savybės	Šaltinis
pET21b-GCSF-L2-GCSF	Dvi *g-csf* geno kopijos sujungtos per L2 jungiančiąja seką ir įterptos į pET21b(+) plazmidę	Šis darbas
pET21b-GCSF-L7-GCSF	Dvi *g-csf* geno kopijos sujungtos per L7 jungiančiąja seką ir įterptos į pET21b(+) plazmidę	Šis darbas
pET21b-GCSF-Lα-GCSF	Dvi *g-csf* geno kopijos sujungtos per Lα jungiančiąja seką ir įterptos į pET21b(+) plazmidę	Šis darbas
pET28a-GCSF-Lα-GCSF	Dvi *g-csf* geno kopijos sujungtos per Lα jungiančiąja seką ir įterptos į pET28a(+) plazmidę	Šis darbas
pET21b-SCF-Lα-GCSF	*scf* ir *g-csf* genai sujungti per Lα jungiančiąja seką ir įterpti į pET21b(+) plazmidę	Šis darbas
pET21b-GCSF-Lα-SCF	*g-csf* ir *scf* genai sujungti per Lα jungiančiąja seką ir įterpti į pET21b(+) plazmidę	Šis darbas

Oligonukleotidų pradmenys

4 lentelė. Darbe naudoti oligonukleotidų pradmenys

Primer name	Sequence (5'-3')
GCSF-Nde	CATATGACACCTTTAGGACCTGCT
GCSF-Bam-Kpn	GGATCCGCATCCGGACGGCTGCGCAAGGTGG CGTAG
GCSF-Bam	GGATCCACACCTTTAGGACCT
GCSF-Hind	AAGCTTATTACGGCTGCGCAAGGTGGCG
SCF-Nde	GTGCATATGGAAGGTATCTGTCGT
SCF-Kpn-Bam	GGATCCAAGTCCGGAAGCAGCAACCGGCGGC AGC
SCF-Bam	TGGATCCGAAGGGATCTGCCGTAATCG
SCF-Hind	TAAGCTTAGGCTGCAACAGGGGG

Sorbentai

5 lentelė. Darbe naudoti sorbentai

Sorbentas	Šaltinis
DEAE Sepharose Fast Flow (FF), SP Sepharose FF, CM Sepharose FF, Sephadex G-25 Medium, Q Sepharose FF, Chelating Sepharose FF, Ni-	GE Healthcare

5 lentelė. Darbe naudoti sorbentai

Sorbentas	Šaltinis
Sepharose FF, Butyl Sepharose FF, Phenyl Sepharose FF,	
CHT ceramic hydroxyapatite, Type II	Bio-Rad Laboratories
Superdex 200	Fisher Scientific

Rekombinantiniai baltymai

6 lentelė. Recombinantiniai baltymai naudoti šiame darbe

Baltymas	Šaltinis
rhG-CSF (filgrastimas)	Sicor Biotech/ Teva
rhSCF, ab179506	Abcam
Albumino standartas (Jaučio serumo albuminas (BSA))	Thermo Scientific
rhG-CSF receptorius sulietas su žmogaus IgG1 Fc (GCSF-R), ab83994	Abcam
rhc-Kit sulietas su žmogaus IgG1 Fc (c-KIT), ab219878	Abcam
Baltymas-G	Sigma Aldrich
Žmogaus serumo albuminas (HSA)	Baxter Healthcare

Bakterijų auginimo terpės

7 lentelė. Bakterijų auginimo terpės naudotos šiame darbe

Bakterijų auginimo terpės	Sudėtis
Luria-Bertani (LB) mitybinė terpė	10g/L peptonas, 10g/L mielių ekstraktas, 5g/L NaCl
Kolbos mitybinė terpė	50 mM Na_2HPO_4, 20 mM KH_2PO_4, 20 mM NH_4Cl, 10 mM NaCl (tirpalas ruošiamas iš „5 x M9 druskos“, Sigma-Aldrich), 0,5% (w/v) mielių ekstraktas, 0,4% (w/v) gliukozė (20% (w/v) tirpalas ruošiamas atskirai), 2 mM $MgSO_4$ x $7H_2O$ (1 M tirpalas ruošiamas atskirai)
Inokuliato auginimo terpė I	100 mM Na_2HPO_4, 40 mM KH_2PO_4, 40 mM NH_4Cl, 20 mM NaCl (tirpalas ruošiamas iš „5 x M9 druskos“), 0,4% (w/v) gliukozė, 1% (w/v) mielių ekstraktas, 0,14 mM $MgSO_4$ x $7H_2O$

7 lentelė. Bakterijų auginimo terpės naudotos šiame darbe

Bakterijų auginimo terpės	Sudėtis
Fermentatoriaus mitybinė terpė I	50 mM Na_2HPO_4, 20 mM KH_2PO_4, 20 mM NH_4Cl, 10 mM NaCl (tirpalas ruošiamas iš „5 x M9 druskos“), 0,5% (w/v) mielių ekstraktas, 7% (w/v) gliukozė, 8 mM $MgSO_4$ x $7H_2O$
Pamaitinimo terpė I	30% (w/v) gliukozė, 18% (w/v) mielių ekstraktas, 67 mM $MgSO_4$ x $7H_2O$
Inokuliato auginimo terpė II	15 mM KH_2PO_4, 105 mM Na_2HPO_4 x $2H_2O$, 25 mM $(NH_4)_2SO_4$, 2 mM $MgSO_4$ x $7H_2O$, 1,63% (w/v) gliukozė
Mikroelementų tirpalas	111 mM $FeCl_3$ x $6H_2O$, 36 mM $CaCl_2$, 23 mM $ZnSO_4$ x $7H_2O$, 9 mM $MnSO_4$ x H_2O, 12 mM $CuSO_4$ x $5H_2O$, 11 mM H_3BO_3, 5 mM $CoCl_2$ x $6H_2O$, 1,2 mM Na_2MoO_4 x $2H_2O$.
Fermentatoriaus mitybinė terpė II	114 mM KH_2PO_4, 35 mM $(NH_4)_2HPO_4$, 9 mM $C_6H_8O_7$ x H_2O, 2 mM $MgSO_4$ x $7H_2O$, 3,5% (w/v) gliukozė
Pamaitinimo terpė II	70% (w/v) gliukozė, 84 mM $MgSO_4$, 3,4 µL/mL mikroelementų tirpalas (įpilamas atskirai)

Visi tirpalai buvo autoklavuoti 20 min. 121°C temperatūroje.

Laboratoriniai gyvūnai

Tyrimai *in vivo* buvo atlikti panaudojant 8-12 savaičių amžiaus moteriškos lyties sveikas laboratorines žiurkes. Tyrimams su laboratoriniais gyvūnais buvo suteiktas LR Valstybinės maisto ir veterinarijos tarnybos veterinarinis leidimas Nr. 0182.

Eksperimentai vykdyti vadovaujantis LR gyvūnų apsaugos įstatymais ir Vilniaus universiteto institucinėmis gairėmis. Visi gyvūnų globos, laikymo ir naudojimo protokolai atitiko nacionalinius ir Europos (Direktyva 2010/63/EU) įstatymus ir reglamentus bei Europos laboratorinių gyvūnų mokslo asociacijų federacijos (FELASA) reikalavimus.

G-CSF homodimerinių genų konstravimas

Visus klonavimo darbus atliko dr. M. Plečkaitytė (Vilniaus universiteto Gyvybės mokslų centro (VU GMC) Biotechnologijos institutas). G-CSF homodimerų konstravimui buvo naudoti sintetiniai DNR fragmentai. Konstruktų kūrimas buvo vykdomas keliais etapais. Pirmiausia, DNR fragmentas, koduojantis žmogaus G-CSF B izoformą su papildomu N-galiniu

metioninu (*Genbank* registracijos Nr. NM_172219), buvo amplifikuotas (polimerazinės grandininės reakcijos (PGR) metodu): naudojant pradmenis, G-CSF geno 5‘-gale įterptas restrikcijos endonukleazės NdeI taikinys, o 3‘-gale įterpti restrikcijos endonukleazių Kpn2I ir BamHI taikiniai. Gauto fragmento nukleotidų seka buvo sekvenuota, karpyta su Kpn2I and BamHI fermentais ir suliguota su Kpn2I ir BamHI karpytu DNR fragmentu, koduojančiu Lα jungiančiąją seką (Arai ir kt., 2001). Taip buvo gautas DNR fragmentas, turintis pirmą *gcsf* geno kopiją su Lα jungiančiąja seka. Tuo tarpu antra *gcsf* geno kopija buvo amplifikuota, įterpiant DNR 5‘ ir 3‘-galuose restrikcijos endonukleazių BamHI ir HindIII taikinius. Fragmentas, turintis dvi *gcsf* geno kopijas ir Lα jungiančiąją seką tarp jų, buvo pavadintas GCSF-Lα-GCSF. Norint turėti GCSF-L2-GCSF ir GCSF-L7-GCSF konstruktus, DNR, koduojanti GCSF-Lα-GCSF, buvo toliau karpyta su Kpn2I and BamHI fermentais ir atitinkamai suliguota su L2 ir L7 koduojančiais DNR fragmentais. GCSF-Lα-GCSF, GCSF-L2-GCSF ir GCSF-L7-GCSF DNR, karpyta su NdeI ir HindIII fermentais, buvo klonuota į pET21b(+) ir pET28a(+) vektorius ir transformuota į BL21(DE3) *E. coli* kamienus.

SCF-Lα-GCSF ir GCSF-Lα-SCF genų konstravimas

SCF-Lα-GCSF ir GCSF-Lα-SCF konstravimui buvo naudoti sintetiniai DNR fragmentai. Pirmiausia buvo sukurtas SCF-Lα-GCSF geno konstruktas, o po to – GCSF-Lα-SCF geno konstruktas. Žmogaus *scf* genas, turintis restriktazių NdeI ir Kpn2I/BamHI taikinius atitinkamai DNR 5‘ ir 3‘-galuose, buvo amplifikuotas. Gauto fragmento nukleotidų seka buvo sekvenuota ir suliguota su Kpn2I ir BamHI karpytu DNR fragmentu, koduojančiu Lα jungiančiąją seką (Arai ir kt., 2001). Toliau, žmogaus *gcsf* genas, turintis restriktazių BamHI and HindIII taikinius atitinkamai DNR 5‘ ir 3‘-galuose, buvo suliguotas su GCSF-Lα DNR fragmento 3‘-gale esančia Lα koduojančia seka. Gautas konstruktas pavadintas SCF-Lα-GCSF.

GCSF-Lα-SCF konstrukto kūrimui, pirmiausia *scf* genas buvo amplifikuotas: naudojant pradmenis, SCF geno 5‘-gale įterptas restrikcijos endonukleazės BamHI taikinys, o 3‘-gale įterptas restrikcijos endonukleazės HindIII taikinys. *gcsf* geno kopija buvo gauta, skaldant GCSF-Lα-GCSF turinčią plazmidę su restrikcijos endonukleazėmis BamHI and HindIII. Toliau, DNR, koduojanti SCF, buvo karpyta su BamHI ir HindIII fermentais ir atitinkamai suliguota su GCSF-Lα koduojančiu DNR fragmentu. Gautas konstruktas pavadintas GCSF-Lα-SCF. SCF-Lα-GCSF ir GCSF-Lα-SCF genai buvo klonuoti į pET21b(+) vektorius ir atitinkamai transformuoti į BL21(DE3) ir BL21(DE3)STAR *E. coli* kamienus.

Bakterijų kultūros, suspenduotos LB terpėje su 15% glicerolio, buvo laikomos -70ºC temperatūroje.

Rekombinantinių baltymų raiška *E. coli* bakterijose

Rekombinantinių baltymų biomasės gamyba mažoje skalėje

Sulietų baltymų gryninimo procedūrų kūrimo tikslams, atitinkamo rekombinantinio baltymo sintezė atlikta nedidelio tūrio skalėje: 1 L tūrio Erlenmejerio kolbose, turinčiose 400 mL kolbos mitybinės terpės (7 lentelė) su ampicilinu (galutinė koncentracija 100 mg/mL). *E. coli* ląstelės buvo auginamos purtyklėje 37°C temperatūroje esant 250 rpm 3 val., kol OD_{600} pasiekia 0,8-1,0. Rekombinantinių baltymų raiška buvo indukuota su IPTG (galutinė koncentracija 1 mM) ir bakterijos tais pačiais parametrais augintos dar 3 val. Ląstelių biomasė buvo surinkta centrifuguojant bei užšaldoma -20ºC temperatūroje.

GCSF-Lα-GCSF biomasės gamyba didelėje skalėje

GCSF-Lα-GCSF biomasės gamybą didelėje skalėje atliko Ž. Dapkūnas (VU GMC Biotechnologijos institutas). Didelės skalės GCSF-Lα-GCSF sintezei su pamaitinimu (ang. *fed-batch fermentation*) buvo panaudotas 5 L darbinio tūrio fermentatorius (Sartorius Stedim Biotech, Vokietija), atitinkamai turintis dvi skirtingas bakterijų auginimo mitybines terpes.

GCSF-Lα-GCSF sintezė M9 minimalioje terpėje, praturtintoje mielių ekstraktu, vykdyta perkeliant 60 µL užšaldytos dimero kultūros į 250 mL tūrio Erlenmejerio kolbą, turinčią 60 mL inokuliato auginimo terpės I (7 lentelė). Po 16-18 val. *E. coli* auginimo purtyklėje esant 37°C temperatūrai, 50 mL naktinės kultūros buvo perkelta į fermentatorių, turintį 4 L fermentatoriaus mitybinės terpės I (7 lentelė). Terpės pH 6,8 buvo palaikomas automatiškai su 25% NH_4OH. Temperatūra bei ištirpęs deguonies kiekis terpėje pO_2 – atitinkamai 37°C ir 30% nuo maksimalaus terpės įsotinimo. Pamaitinimo terpė I (7 lentelė) pradėta tiekti į fermentatorių, kai proceso metu buvo sunaudotas pradinis gliukozės kiekis. OD_{600} pasiekus 15, GCSF-Lα-GCSF raiška buvo indukuota su IPTG (galutinė koncentracija 1 mM) ir bakterijos dar buvo auginamos 3 val. Ląstelių biomasė surinkta centrifuguojant bei užšaldoma -20ºC temperatūroje.

GCSF-Lα-GCSF sintezė chemiškai apibrėžtoje terpėje vykdyta panašiomis sąlygomis kaip ir GCSF-Lα-GCSF sintezė M9 minimalioje terpėje, praturtintoje mielių ekstraktu. 60 µL užšaldytos dimero kultūros buvo perkelta į 250 mL tūrio Erlenmejerio kolbą, turinčią 60 mL inokuliato auginimo terpės II ir 5 µL mikroelementų tirpalo (7 lentelė). Po 21-22 val. *E.*

coli auginimo purtyklėje esant 37°C temperatūrai, 50 mL naktinės kultūros buvo perkelta į fermentatorių, turintį 4 L fermentatoriaus mitybinės terpės II ir 1,17 mL mikrolementų tirpalo (7 lentelė). OD_{600} pasiekus 20, GCSF-Lα-GCSF raiška buvo indukuota su IPTG (galutinė koncentracija 1 mM) ir bakterijos buvo dar paaugintos 3 val. Ląstelių biomasė surinkta centrifuguojant bei užšaldoma -20ºC temperatūroje.

Intarpinių kūnelių išskyrimas ir gryninimas

Surinkta biomasė buvo homogenizuojama 0,1 M Tris-HCl, pH 7,0 (10 mL/g biomasės) buferiniame tirpale, turinčiame 5 mM EDTA, 1 mM PMSF, 0,1% (w/v) Triton X-100. Į gautą suspenciją papildomai buvo pridedamas β-merkaptoetanolis (galutinė koncentracija tirpale 100 mM). Ląstelių lizė atlikta dviems skirtingais metodais: *E. coli* ląstelės, gautos mažos skalės gamybos metu, buvo veikiamos ultragarsu ledo vonioje (Sonopuls Bandelin, Vokietija), tuo tarpu GCSF-Lα-GCSF turinčios ląstelės, gautos didelės skalės gamybos metu, buvo suardytos aukšto slėgio homogenizatoriumi (APV 2000, Vokietija). Bakterijų lizatas surinktas centrifuguojant ir nuosėdos, kartu su intarpiniais kūneliais, du kartus plaunamos su buferiniu tirpalu (20 mM Tris-HCl, pH 8,0, 1 M NaCl), turinčiu 0,1% Tween 80 ir vieną kartą – 20 mM Tris-HCl (pH 8,0) buferiniu tirpalu.

Rekombinantinių baltymų gryninimas

Rekombinantiniai baltymai buvo gryninami 2-8ºC temperatūroje su ÄKTA pure 150 chromatografijos sistema (GE Healthcare, Upsala, Suomija).

G-CSF homodimerų gryninimas

Norint surasti optimalias kiekvienam G-CSF homodimerui gryninimo procedūras, išbandytos įvairios baltymų tirpinimo, renatūravimo ir gryninimo sąlygos (2 pav.).

Po optimizavimo, intarpinių kūnelių tirpinimui pasirinktas buferinis tirpalas, kurio sudėtyje yra karbamido (8 M karbamido, 1 mM EDTA, 50 mM Tris-HCl, pH 8,0). Disulfidiniai tilteliai redukuoti su DTT (0,5-5 mM). Rekombinantinių baltymų renatūravimas atliktas taikant skiedimo renatūracijos buferiniu tirpalu metodą: atitinkamai mažinant karbamido bei baltymo koncentracijas iki 3 M ir 0,5 mg/mL su 50 mM Tris-HCl, 1 mM EDTA, pH 8,0 tirpalu, kurio sudėtyje yra oksiduoto glutationo (GSSG). GCSF-L2-GCSF atveju nustatytas optimalus galutinis DDT:GSSG santykis buvo 1:5, tuo tarpu GCSF-L7-GCSF ir GCSF-Lα-GCSF atvejais – 1:6. Gautas renatūracijos tirpalas maišytas 24 val. 4ºC temperatūroje.

Pirmai gryninimo stadijai parinkta DEAE Sepharose užpildyta kolonėlė, nulygsvarinta 10 mM Tris-HCl (pH 7,5), 20 mM NaCl tirpalu. Baltymai desorbuoti taikant laiptinį NaCl gradientą: nuo 0,02 M iki 0,08 M ir nuo 0,08 M iki 0,45 M. Tikslinį baltymą turinčios eliuato frakcijos buvo apjungiamos ir skiedžiamos su 20 mM natrio acetato buferiniu tirpalu iki pH 5,4 ir laidumo 3,2 mS/cm.

GCSF-Lα-GCSF ir GCSF-L2-GCSF atvejais, antrai gryninimo stadijai parinkta SP Sepharose užpildyta kolonėlė, nulygsvarinta 20 mM natrio acetato (pH 5,4), 20 mM NaCl tirpalu. Tiksliniai baltymai buvo desorbuoti laipsniškai didinant NaCl koncentraciją: nuo 20 mM iki 450 mM. Tuo tarpu GCSF-L7-GCSF baltymui, kaip antra gryninimo stadija, parinkta CM Sepharose užpildyta kolonėlė ir pastarojo baltymo gryninimas atliktas pagal aukščiau aprašytas GCSF-Lα-GCSF ir GCSF-L2-GCSF gryninimo sąlygas.

Buferinio tirpalo pakeitimui, apjungtos išgryninto tikslinio baltymo frakcijos buvo suleidžiamos į Sephadex G-25 Medium užpildytą kolonėlę, nulygsvarintą 10 mM acto rūgšties/NaOH (pH 4,0) buferiniu tirpalu. Baltyminis tirpalas buvo formuluojamas pridedant D-sorbitolio ir Tween 80 atitinkamai iki galutinės 5% ir 0,0025% koncentracijos. Suformuluotas baltymas filtruotas per 0,2 μm MustangE filtrą, sulaikantį endotoksinus, ir saugotas 4ºC temperatūroje.

G-CSF ir SCF heterodimerų gryninimas

Norint surasti optimalią heterodimerų gryninimo procedūrą, išbandytos įvairios SCF-Lα-GCSF tirpinimo, renatūravimo ir gryninimo sąlygos (9 pav.). Optimizuota galutinė SCF-Lα-GCSF gryninimo metodika buvo pritaikyta ir GCSF-Lα-SCF baltymo gryninimui.

Intarpiniams kūneliams tirpinti pasirinktas karbamido turintis buferinis tirpalas (8 M karbamido, 1 mM EDTA, 50 mM Tris-HCl, pH 8,0). Disulfidiniai tilteliai buvo redukuoti su DTT (galutinė koncentracija tirpale 0,5 mM). Rekombinantinių baltymų renatūravimas atliktas taikant skiedimo renatūracijos buferiniu tirpalu metodą: mažinant karbamido koncentraciją iki 2 M su 50 mM Tris-HCl, pH 8,0 tirpalu, kurio sudėtyje yra GSSG (galutinis nustatytas optimalus molinis DDT:GSSG santykis buvo 1:5). Gautas baltyminis tirpalas maišytas 24 val. 4ºC temperatūroje.

Pirmai gryninimo stadijai parinkta DEAE Sepharose užpildyta kolonėlė, nulygsvarinta 50 mM Tris-HCl (pH 7,5) tirpalu. Baltymai desorbuoti taikant tiesinį NaCl gradientą: nuo 0 M iki 0,5 M. Tikslinį baltymą turinčios eliuato frakcijos buvo apjungiamos.

Antrai gryninimo stadijai parinkta CHT ceramic hydroxyapatite, Type II užpildyta kolonėlė, nulygsvarinta 50 mM Tris-HCl (pH 7,2) buferiniu

tirpalu. Kolonėlė buvo plaunama 5 mM NaH_2PO_4 (pH 7,2), 0,1 M NaCl tirpalu ir baltymai desorbuoti laipsniškai didinant NaH_2PO_4 koncentraciją: nuo 5 mM iki 500 mM. Tikslinį baltymą turinčios eliuato frakcijos buvo apjungiamos ir skiedžiamos su 20 mM natrio acetato buferiniu tirpalu iki pH 4,7.

Trečiai gryninimo stadijai parinkta SP Sepharose užpildyta kolonėlė, nulygsvarinta 20 mM natrio acetato (pH 4,7) tirpalu ir kolonėlė buvo toliau plaunama tuo pačiu pradiniu buferiniu tirpalu. Baltymai buvo desorbuoti laipsniškai didinant NaCl koncentraciją iki 500 mM.

Buferinio tirpalo pakeitimui, apjungtos išgryninto tikslinio baltymo frakcijos buvo suleidžiamos į Sephadex G-25 Medium užpildytą kolonėlę, kuri buvo nulygsvarinta 10 mM acto rūgšties/NaOH (pH 4,0) tirpalu. Išgrynintas SCF-Lα-GCSF ir GCSF-Lα-SCF filtruotas per 0,2 μm MustangE filtrą ir saugotas 4ºC temperatūroje.

Analitiniai metodai

8 lentelė. Analitiniai metodai naudoti šiame darbe

Baltymo charakteristikos	Pagrindiniai metodai	Papildomi metodai
Baltymo kiekis	Bradfordo metodas	UV spektroskopija
Grynumas ir priemaišos	Natrio dodecilsulfato poliakrilamidinio gelio elektroforezė (SDS-PAGE) ir Atvirkščių fazių didelio slėgio skysčių chromatografija (RP-HPLC)	Bakterinių endotoksinų nustatatymo metodas ir Gel-filtracija, atliekama didelio slėgio skysčio chomatografijos būdu (SE-HPLC)
Identiškumas	Western imunoblotingas ir Didelio slėgio skysčių chromatografija/ elektros purškimo jonizacijos masių spektrometrija (HPLC/ESI-MS)	RP-HPLC peptidinis žemėlapis
Molekulinis svoris	SE-HPLC	HPLC/ESI-MS
Taisyklingas disulfidinių tiltelių susidarymas	RP-HPLC	Fluorescencinė spektroskopija

Baltymo kiekio nustatymas

Baltymo koncentracija, po kiekvieno gryninimo etapo, buvo nustatoma Bradfordo metodu (Bradford, 1976). Po galutinio gryninimo etapo, tikslinio baltymo koncentracija nustatyta matuojant ultravioletinės šviesos sugertį ties

280 nm ir atimant (dėl šviesos sklaidos) – ties 340 nm. Abi analizės atliktos su UV-VIS spektrofotometru Specord S 600 (analytic Jena GmbH, Jena, Vokietija).

Baltymo grynumo ir priemaišų nustatymas

Rekombinantinių baltymų grynumas patikrintas SDS-PAGE elektroforezės ir RP-HPLC analizių metu. RP-HPLC buvo atliktas su Alliance e2695 HPLC sistema (Waters, JAV), stebint eliuento absorbciją ties 215 nm.

Bakteriniai endotoksinai patikrinti su Pyrotell Gel-Clot endotoxin rinkiniu, pagal gamintojo rekomendacijas.

G-CSF homodimerų RP-HPLC analizės

GCSF-Lα-GCSF, GCSF-L2-GCSF ir GCSF-L7-GCSF intarpinių kūnelių tirpalų, renatūruotų jų formų ir frakcijų, gautų po chromatografinių gryninimų stadijų, RP-HPLC analizėms atlikti naudota Hi-Pore RP-318 kolonėlė (4,6 x 250 mm, Bio-Rad, JAV). Eliucijai naudoti tirpalai A (0,1% TFA:99,9% vanduo) ir B (0,1% TFA:10% vanduo:89,9% acetonitrilas). Kolonėlės temperatūra buvo palaikoma 30ºC, o tėkmės greitis – 1 mL/min.

Išgrynintų G-CSF homodimerų, surinktų po Sephadex G-25 Medium chromatografinės stadijos, RP-HPLC analizėms atlikti naudota Zorbax SB-C18 kolonėlė (4,6 x 250 mm, Agilent Technologies, JAV). Eliucijai naudoti tirpalai A (0,1% TFA:99,9% vanduo) ir B (0,1% TFA:99,9% acetonitrilas). Kolonėlės temperatūra buvo palaikoma 30ºC, o tėkmės greitis – 0,9 mL/min.

Heterodimerų RP-HPLC analizės

SCF-Lα-GCSF ir GCSF-Lα-SCF intarpinių kūnelių tirpalų, renatūruotų jų formų ir frakcijų, gautų po chromatografinių gryninimo stadijų, RP-HPLC analizėms atlikti naudota Zorbax 300SB-C18 kolonėlė (4,6 × 250 mm; Agilent Technologies). Eliucijai naudoti tirpalai A (0,1% TFA:99,9% vanduo) ir B (0,1% TFA:9,9% vanduo:90% acetonitrilas). Kolonėlės temperatūra buvo palaikoma 30ºC, o tėkmės greitis – 1 mL/min.

Tikslinio baltymo identifikavimas

Po SDS-PAGE elektroforezės, iš poliakrilamidinio gelio rekombinantiniai dimerai bei G-CSF ir SCF monomerai buvo pernešami ant Immobilon-PVDF membranos (Merck Millipore, Airija) blotingo aparatu. Šlapias pernešimas truko 90 min (esant 15 V srovės įtampai). Membranos blokuotos PBS buferiniu tirpalu su 0,1% Tween 20 (PBS-T) ir 5% BLOT-QuickBlocker (Calbiochem, JAV) 2 val. Po to membranos inkubuotos su monokloninių antikūnų tirpalu prieš G-CSF (skiedimas 1:2000) ar

poliklonininių antikūnų tirpalu prieš SCF (skiedimas 1:1000) ir praplautos. Po praplovimo, jos inkubuotos atitinkamai su peroksidaziniu konjugatu prieš pelės IgG (skiedimas 1:4000) arba peroksidaziniu konjugatu prieš triušio IgG (skiedimas 1:1000). Membranos ryškintos su TMB-blotting substratu.

Taip pat, išgryninti rekombinantiniai dimeriniai baltymai buvo identifikuoti bei nustatytas jų molekulinis svoris HPLC/ESI-MS analizių metu. HPLC/ESI-MS procedūras atliko A. Rukšėnaitė (VU GMC Biotechnologijos institutas). Mėginiai buvo tirti naudojant C8 atvirkščių fazių kolonėlę (Poroshell 300SB-C8, 2,1 × 75 mm; Agilent Technologies, JAV), esant 0,4 mL/min tėkmės greičiui bei 30ºC kolonėlės temperatūrai. Eliucijai naudoti tirpalai A (1% skruzdžių rūgšties (FA) vandeninis tirpalas) ir B (1% FA:99% acetonitrilo tirpalas). RP-HPLC analizė atlikta su Agilent 1290 Infinity HPLC sistema, kuri buvo sujungta su Agilent Q-TOF 6520 masių spektrometru (Agilent Technologies) ir duomenys analizuoti naudojant Agilent MassHunter Workstation programinę įrangą.

SE-HPLC analizės

SE-HPLC analizės atliktos naudojant TSK-gel G3000 SWXL kolonėlę (7,8 × 300 mm, 5 μm, Tosoh Bioscience, Japonija), kuri buvo sujungta su Alliance e2695 HPLC sistema (Waters). Kolonėlė nupusiausvyrinta 0,1 M Na_2HPO_4, 0,1 M Na_2SO_4 buferiniu tirpalu (pH 7,2) ir mėginių HPLC chromatografija atlikta esant 0,6 mL/min tekmės greičiui ir 22ºC temperatūrai. G-CSF homodimerų ir G-CSF monomero molekulinis svoris įvertintas remiantis žinomos molekulinės masės baltymų tirpalais (ribonukleaze A, karbonine anhidraze, ovalbuminu, konalbuminu, GE Healthcare), tuo tarpu SCF ir G-CSF heterodimerai, kartu su SCF ir G-CSF monomerais – naudojant standartinį baltymų mišinį (Sigma-Aldrich, JAV).

RP-HPLC peptidinis žemėlapis

Išgryninto GCSF-Lα-GCSF ir G-CSF monomero peptidinis žemėlapis atliktas pagal šiek tiek pakeistą farmakopėjinį metodą (Council of Europe, 2009). Mėginiai buvo skiedžiami su 50 mM Na_2HPO_4 (pH 8,0) buferiniu tirpalu (galutinė baltymo koncentracija 25 μg/mL) ir veikiami glutamilo endopeptidaze (galutinė Glu-C koncentracija 2,5 μg/mL). Po 18 val inkubacijos 37°C temperatūroje, sukarpyti mėginiai buvo analizuoti per Hi-Pore RP-318 kolonėlę (Bio-Rad, JAV), esant 50ºC kolonėlės temperatūrai. Eliucijai naudoti tirpalai A (0,05% TFA:94,5% vanduo:5% acetonitrilas) ir B (0,05% TFA:5% vanduo:94,5% acetonitrilas).

Taisyklingas disuldinių tiltelių susidarymas

GCSF-Lα-GCSF ir G-CSF monomero fluorescensijos emisijos spektrai buvo nustatyti panaudojant fluorescencinį spektrofluorometrą (FluoroMax-4, Horiba Jobin YvonInc., JAV), 1 cm^2 kiuvetėje. Spektrų užrašymui baltyminiai tirpalai skiesti su 10 mM natrio citratiniu (pH 3,2 arba 7,5) buferiniu tirpalu, turinčiu 100 mM NaCl (galutinė baltymo koncentracija 0,14-0,16 mg/mL). Sužadinimo bangos ilgis buvo 280 nm, spektrai užrašyti 290-420 nm intervale.

Rekombinantinių baltymų biologinio aktyvumo nustatymas

9 lentelė. Aktyvumo metodai naudoti šiame darbe

Pagrindiniai metodai	Papildomi metodai
Visiško vidaus atspindžio elipsometrija (VVAE)	
Biologinis aktyvumas *in vitro*	Biologinis aktyvumas *in vivo*

Visiško vidaus atspindžio elipsometrijos matavimai

Išgrynintų rekombinantinių baltymų sąveikos kinetikos tyrimai su receptoriais buvo nustatyti VVAE metodu. VVAE eksperimentai buvo atlikti Fizinių ir technologijos mokslų centre (FTMC) ir baltymų kinetikas tyrinėjo prof. dr. Z. Balevičius (FTMC), dr. I. Plikusienė (FTMC), dr. J. Talbot (Sarbonos universitetas, Nacionalinis mokslo tyrimų centras), dr. A. Stirkė (FTMC) ir dr. L. Tamošaitis (VU Chemijos institutas). Matavimams naudoti chimeriniai GCSF ir c-KIT receptoriai, turintys žmogaus IgG1 antikūno Fc dalį.

VVAE eksperimento struktūra buvo pagrinde sudaryta iš skirtingai modifikuotos 1 mm storio BK7 plokštelės, padengtos chromo (Cr) ir aukso (Au) sluoksniu, pritvirtintos prie BK7 70° stiklo prizmės ir spektrinio elipsometro M-2000X, J. A. Woollam (Lincoln, Dearborn, JAV), turinčio besisukantį kompensatorių. Ant aktyvuotų BK7-stiklo/Cr-Au plokštelių, buvo formuojami GCSF-R ar c-KIT receptoriai. Per prijungtą baltymo G sluoksnį kryptingai imobilizavus receptorius, į celę buvo suleidžiama 10 μg/mL analizuojamo baltymo, skiesto PBS buferiniame tirpale. Visas ligandų jungimosi matavimas buvo atliekamas spektre nuo 300 nm iki 1000 nm. GCSF-L2-GCSF homodimero, SCF-Lα-GCSF ir GCSF-Lα-SCF heterodimerų bei G-CSF ir SCF monomerų jungimosi kinetikos charakterizavimui naudotas standartinis Lengmiūro kinetinis modelis. Tuo tarpu, GCSF-L7-GCSF ir GCSF-Lα-GCSF homodimerų sąveikoms analizuoti su G-CSF receptoriumi buvo pritaikytas iš Lengmiūro modelio išvestas trijų etapų modelis (Balevicius ir kt., 2019; Plikusiene ir kt., 2020).

Rekombinantinių baltymų biologinis aktyvumas *in vitro*

Rekombinantinių baltymų biologinius aktyvumus *in vitro* nustatė I. Dalgėdienė (VU GMC Biotechnologijos institutas). Sulietų baltymų biologinis aktyvumas *in vitro* buvo nustatytas panaudojant jautrias SCF poveikiui žmogaus M-07 ląstelių linijas (Drexler ir kt., 1997) ir jautrias G-CSF poveikiui pelės G-NFS-60 ląstelių linijas (Weinstein ir kt., 1986; Matsuda ir kt., 1989). Ląstelės, praskiestos su RPMI 1640 augimo terpe, turinčia 10% embrioninio jaučio serumo, gentamicino sulfato ir 2-merkaptoetanolio buvo inkubuojamos 96 šulinėlių plokštelėse 48 val, pridėjus į terpę skirtingus standartų ir tiriamųjų mėginių kiekius (galutinė jų koncentracija 0,004-7,8 pg/mL). Kontrolėms naudoti SCF ir G-CSF standartai, kurių biologiniai aktyvumai jau yra žinomi. Gyvybingų ląstelių kiekis buvo nustatytas kolorimetriškai naudojant tirpų MTS dažą, kuris veikiant mitochondrijų dehidrogenazėms, virsta spalvotu produktu – formazanu. Susidariusio formazono kiekis buvo nustatomas spektrofotometriškai (FluoroMax-4; Horiba Scientific, JAV), matuojant terpės optinį tankį ties 490 nm. Proliferacijos kreivės buvo sudarytos brėžiant baltymų ar standartų $\log_2$ praskiedimus pagal absorbcijos vertes ties 490 nm. Dimerų biologinis aktyvumas *in vitro* nustatytas atitinkamai palyginus mėginio praskiedimą, duodantį 50% maksimalios stimuliacijos su analogišką stimuliaciją sukeliančiu standartinio monomero praskiedimu.

GCSF-Lα-GCSF ir SCF-Lα-GCSF biologinis aktyvumas *in vivo*

Visus *in vivo* eksperimentus atliko dr. V. Bukelskienė (VU Biochemijos institutas). Išgrynintų GCSF-Lα-GCSF, SCF-Lα-GCSF bei G-CSF ir SCF monomerų biologinio aktyvumo tyrimai *in vivo* buvo atlikti panaudojant laboratorines žiurkes. Eksperimentiniai gyvūnai suskirstyti į grupes, kiekvienoje iš jų buvo po 3-6 žiurkes. Tiriamieji ir kontroliniai mėginiai atitinkamai buvo po vieną kartą sušvirkšti po oda. GCSF-Lα-GCSF aktyvumo nustatymui naudotos šios rekombinantinių baltymų koncentracijos (µg baltymo/kg gyvūno svorio): pirma žiurkių grupė gavo 200 µg/kg GCSF-Lα-GCSF; antra žiurkių grupė gavo 200 µg/kg G-CSF; trečia grupė – natrio acetato buferinio tirpalo. SCF-Lα-GCSF aktyvumo nustatymui naudotos tokios rekombinantinių baltymų koncentracijos (µg baltymo/kg gyvūno svorio): pirma žiurkių grupė gavo 500 µg/kg G-CSF; antra grupė – 500 µg/kg SCF; trečia grupė – 500 µg/kg SCF-Lα-GCSF; ketvirta grupė – 1000 µg/kg SCF-Lα-GCSF; penkta grupė – 500 µg/kg SCF ir 500 µg/kg G-CSF mišinio; šešta grupė – natrio acetato buferinio tirpalo. Prieš eksperimento pradžią (0 val) bei po 24, 48 ir 72 val. kraujo mėginiai buvo surenkami ir analizuoti

kraujo analizatoriumi (Exigo EOS, BouleMedical AB, Spånga, Švedija), taip nustatant absoliutų neutrofilų kiekį (ANC).

GCSF-Lα-GCSF biologinis prieinamumas *in vivo*

GCSF-Lα-GCSF biologinio prieinamumo *in vivo* tyrimams, laboratorinės žiurkės buvo suskirstytos į dvi grupes (kiekvienoje iš jų buvo po 4-5 gyvūnus). Eksperimentiniams gyvūnams po oda sušvirkštas vienodas kiekis rekombinantinių baltymų: pirmajai grupei – 150 µg/kg išgryninto GCSF-Lα-GCSF, antrajai grupei – 150 µg/kg GCSF monomerinio standarto. Prieš eksperimento pradžią (0 val) bei po 3, 6, 12, 18 ir 24 val. kraujo serumas buvo surenkamas ir analizuotas su G-CSF ELISA Development rinkiniu, pagal gaminto rekomendacijas (PeproTech, Rocky Hill, NJ, USA).

Statistinė analizės

Duomenys buvo įvertinti naudojant GraphPad Prism programinę įrangą (8.0 versija, GraphPad, San Diego, CA, JAV). Skirtumai tarp tiriamųjų grupių analizuoti naudojant nesuporuotą t-testą, vienos imties t-testą bei vienpusę dispersijos analizę (ANOVA) kartu su Tukey daugkartinio palyginimo testu. Darbe rezultatai pateikti kaip nepriklausomų eksperimentų vidurkis ± standartinė matavimo paklaida (SEM) arba vidurkis ± standartinis nuokrypis (SD).

REZULTATAI

G-CSF homodimerinių baltymų raiška, gryninimas ir charakterizavimas

G-CSF homodimerinių baltymų raiška

Darbo metu buvo sukonstruoti G-CSF dimerai, sudaryti iš dviejų žmogaus G-CSF molekulių, sujungtų tarpusavyje per skirtingo ilgio jungiančiąsias sekas: (SG_4)–(SG_4)–S **(L2)**, (SG_4)–(SG_4)–(SG_4)–(SG_4)–(SG_4)–(SG_4)–(SG_4)–S **(L7)** ir SGLEA–$(EAAAK)_4$–ALEA–$(EAAAK)_4$–ALEGS **(Lα)**. GCSF-L7-GCSF, GCSF-L2-GCSF ir GCSF-Lα-GCSF koduojantus genai buvo klonuoti į pET21b(+) plazmides ir transformuoti į *E. coli* BL21(DE3) ląsteles. Transformantai buvo kultivuojami kolbose M9 mitybinėje terpėje (7 lentelė). Ląstelės augintos 37°C temperatūroje, kol kultūros optinis tankis OD_{600} pasiekė 0,8-1,0, ir baltymų sintezė indukuota su IPTG. SDS-PAGE metodu nustatyta, kad tikslinių baltymų raiška siekė ~30% nuo visų ląstelės baltymų.

G-CSF homodimerų renatūracija ir gryninimas

Rekombinantiniai baltymai *E. coli* ląstelėse buvo aptikti netirpioje frakcijoje, intarpinių kūnelių pavidalu. Norint išgauti biologiškai aktyvius G-CSF homodimerus, darbo metu didelis dėmesys buvo skirtas jų renatūracijos sąlygų parinkimui. Taip pat buvo išbandytos įvairios gryninimo sąlygos, siekiant surasti optimalias kiekvieno G-CSF homodimero gryninimo technologijas (2 pav. A). Galutinės jų optimizuotos gryninimo schemos pateiktos 2 pav. B.

RP-HPLC analizė buvo pasirinkta kaip tinkamas proceso kontrolės analitinis metodas, renatūracijos metu efektyviai gebantis atskirti teisingos konformacijos baltymą nuo redukuotos jo formos. Be to, gryninimo proceso metu, parodantis tikslinio baltymo grynumą. Parinkus baltymų GCSF-Lα-GCSF, GCSF-L2-GCSF ir GCSF-L7-GCSF optimalias renatūracijos sąlygas, buvo pasiektas atitinkamai 61%, 43,2% ir 51,2% RP-HPLC grynumas (10 lentelė). Mažesnis tiek GCSF-L2-GCSF, tiek GCSF-L7-GCSF grynumas buvo gautas dėl renatūracijos metu susidariusios priemaišinės baltymo formos, turinčios ilgesnį sulaikymo laiką RP-HPLC kolonėlėje (2 smailė, 1 pav. B). Be to, G-CSF homodimerų heterogeniškumas, buvo matomas ir analizuojant SDS-PAGE elektroforezės gelius neredukuojančiomis sąlygomis (1 pav. C).

Po renatūracijos baltymai toliau buvo gryninami, panaudojant skirtingas savybes turinčius chromatografinius sorbentus, tokius kaip Sephadex G-25 Medium, DEAE Sepharose FF, CHT ceramic hydroxyapatite,

Type II, Cu-IDA Sepharose FF, ir kiti (2 pav. A). Pirmojoje chromatografinio gryninimo stadijoje, didelis GCSF-Lα-GCSF grynumas buvo gautas, panaudojus DEAE Sepharose sorbentu užpildytą kolonėlę. Tuo tarpu šis sorbentas nebuvo toks efektyvus gryninant GCSF-L2-GCSF ir GCSF-L7-GCSF, kadangi nepavyko pilnai atskirti tinkamos konformacijos baltymo nuo kitos baltymo formos, kurios RP-HPLC-sulaikymo laikas ilgesnis. Siekiant turėti kuo grynesnius baltymus, antrajai G-CSF homodimerų gryninimo stadijai parinkta katijonų mainų chromatografija. Stiprus anijonitas (SP Sepharose FF užpildyta chromatografinė kolonėlė) buvo pritaikytas GCSF-Lα-GCSF ir GCSF-L2-GCSF gryninimui. Tuo tarpu, silpnas anijonitas (CM Sepharose FF užpildyta chromatografinė kolonėlė) parodė geresnį GCSF-L7-GCSF atskyrimą nuo jo priemaišinių formų. Norint turėti baltymą tinkamame buferiniame tirpale, po gryninimų apjungtos tinkamos konformacijos baltymo frakcijos, buvo leidžiamos per Sephadex G-25 Medium užpildytą chromatografinę kolonėlę. Apibendrintos galutinės G-CSF homodimerų gryninimo schemos pateiktos 2 pav. B.

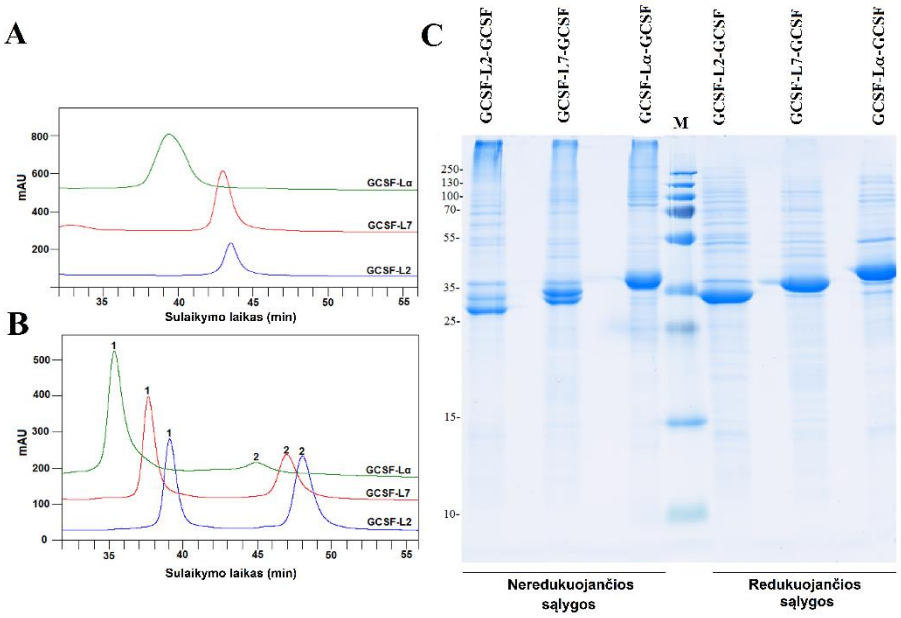

1 pav. GCSF-L2-GCSF, GCSF-L7-GCSF ir GCSF-Lα-GCSF mėginių, parinkus optimalias sąlygas, (A, B) RP-HPLC analizių ir (C) SDS-PAGE elektroforezės vaizdai. (A) Intarpinių kūnelių tirpalų, esant DTT, RP-HPLC analizės vaizdai. **(B)** G-CSF homodimerų, po renatūracijos, esant DTT/GSSG porai, RP-HPLC analizės vaizdai. Eliuentų absorbcija, kai bangos ilgis 215 nm. **(C)** G-CSF homodimerų, po renatūracijos, esant DTT/GSSG porai, prie neredukuojančių ir redukuojančių sąlygų, SDS-PAGE vaizdas. *M* molekulinių masių standartai (Thermo Fisher Scientific).

A

Stadija	Parametras	Medžiaga/ Sorbentas	GCSF-Lα-GCSF	GCSF-L2-GCSF	GCSF-L7-GCSF
Tirpinimas	Tirpinimo agentas	GdnHCl	+	+	-
		Karbamidas	+	+	+
	Redukuojantis agentas	Be reduktoriaus	+	+	-
		β-merkaptoetanolis	+	-	-
		DTT	+	+	+
Renatūracija	Oksiduojantis agentas	Oras/Cu^{2+}	+	+	-
		GSH/GSSG	+	-	-
		DTT/GSSG	+	+	+
Chromatografija	Pirmasis gryninimo žingsnis	Sephadex G-25 Medium	+	+	-
		DEAE Sepharose FF	+	+	+
	Tarpininis gryninimo žingsnis	CHT ceramic hydroxyapatite, Typas II	-	+	-
		Cu-IDA Sepharose FF	-	-	+
		Resource Q	-	-	+
		Ni Sepharose 6 FF	-	+	+
		Butyl Sepharose FF	-	+	-
	Galutinis gryninimo žingsnis	SP Sepharose FF	+	+	+
		CM Sepharose FF	+	+	+
	Formulavimo žingsnis	Sephadex G-25 Medium	+	+	+

B

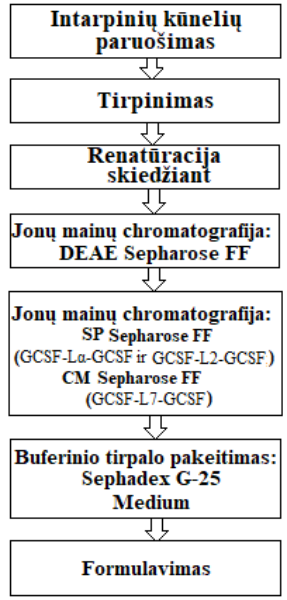

2 pav. G-CSF homodimerų gryninimo charakteristikos. (A) Ištirtos sąlygos, ieškant kiekvienam G-CSF homodimerui tinkamiausios gryninimo procedūros. **(B)** Parinkta GCSF-Lα-GCSF, GCSF-L2-GCSF, GCSF-L7-GCSF gryninimo schema. Santrumpos: + ištirtos; - neištirtos sąlygos.

10 lentelė. G-CSF homodimerų gryninimo eiga

Gryninimo stadija	Charakteristika	GCSF-L2-GCSF	GCSF-L7-GCSF	GCSF-Lα-GCSF
Renatūracija	Išeiga[1]	89,25±2,20	90,33±2,70	90,99±1,51
	Grynumas[2]	43,24±3,81	51,23±3,45	61,02±2,73
I chromatografija (anijonų mainų)	Išeiga [1]	4,56±1,63	7,55±2,12	16,99±2,08
	Grynumas [2]	55,43±4,21	68,12±3,75	90,21±3,21
II chromatografija (katijonų mainų)	Išeiga [1]	1,20±0,52	2,21±1,12	14,10±2,21
	Grynumas [2]	79,14±2,13	82,41±1,54	95,14±0,99

Trijų nepriklausomų eksperimentų vidurkis ± SD.
[1]Baltymo koncentracija nustatyta Bradfordo metodu (Bradford, 1976), naudojant BSA kaip standartinį baltymą.
[2]Baltymo grynumas nustatytas RP-HPLC metodu.

Išgrynintų G-CSF homodimerų charakterizavimas

Išgryninti G-CSF homodimerai buvo charakterizuoti RP- ir SE-HPLC, SDS-PAGE, imunoblotingo bei masių spektrometrijos metodais. G-CSF monomeras buvo naudojamas kaip palyginamasis standartinis baltymas.

G-CSF homodimerų RP-HPLC analizės rezultatai atskleidė skirtingus baltymų grynumo bei hidrofobiško lygius (10 lentelė, 3 pav. A). SDS-PAGE geliuose GCSF-L2-GCSF, GCSF-L7-GCSF ir GCSF-Lα-GCSF skirstėsi šiek tiek žemesnėse pozicijose nei apskaičiuotos jų teorinės molekulinės masės (atitinkamai 38,2 kDa, 39,7 kDa ir 42,5 kDa). Išgrynintas GCSF-Lα-GCSF mėginys gelyje buvo matomas kaip viena juostelė, taigi, pasižymėjo dideliu elektroforetiniu grynumu. Tuo tarpu, GCSF-L2-GCSF ir GCSF-L7-GCSF, be pagrindinės, turėjo papildomas didesnio molekulinio svorio plonas juosteles, kurios buvo stebimos per visą pastarųjų baltymų gryninimo procesą. Mėginius paveikiant reduktoriumi geliuose nebuvo randama papildoma juostelė, kuri, tikėtina, atitinkamai atspindėjo 37-42 min intervale sulaikytą RP-HPLC kolonėlėje priemaišinę baltymo formą (3 pav. A).

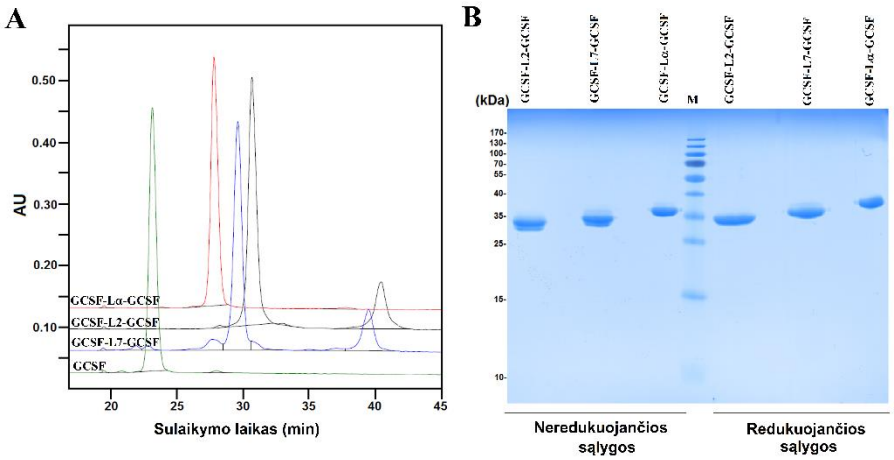

3 pav. G-CSF homodimerų (A) RP-HPLC analizių ir (B) SDS-PAGE elektroforezės vaizdai. (**A**) Išgrynintų G-CSF homodimerų ir standartinio baltymo G-CSF RP-HPLC analizės vaizdai. Eliuentų absorbcijos stebimos ties 215 nm. (**B**) Išgrynintų G-CSF homodimerų, esant neredukuojančiomis bei redukuojančiomis sąlygomis, SDS-PAGE elektroforezės vaizdas. *M* molekulinių masių standartai (Thermo Fisher Scientific).

SE-HPLC analizės būdu buvo įvertintas G-CSF dimerų ir G-CSF monomero molekulinis svoris, oligomerinė būsena tirpale ir grynumas. Nustatytos GCSF-L2-GCSF, GCSF-L7-GCSF ir GCSF-Lα-GCSF molekulių masių reikšmės (atitinkamai 42 kDa, 49 kDa ir 55 kDa) buvo šiek tiek didesnės nei jų teorinės molekulinės masės. Šis skirtumas galėjo atsirasti dėl SE-HPLC kolonėlės ypatybių, t. y., baltymai gelfiltracinėje kolonėlėje skirstosi ne tik pagal molekulinę masę, bet ir pagal baltymo molekulės formą (Hagel, 2001). G-CSF atveju, gautos (17 kDa) ir paskaičiuotos (18,8 kDa) molekulinės masės reikšmių skirtumas parodė, kad monomeras yra santykinai kompaktiška molekulė. GCSF-L7-GCSF ir GCSF-Lα-GCSF SE-HPLC grynumas siekė 99%, tuo tarpu GCSF-L2-GCSF atveju buvo 94%. Didelio slėgio skysčių chromatografijos ir masių spektrometrijos (HPLC/ESI-MS) metodu nustatytos išgrynintų baltymų molekulinių masių reikšmės gerai atitiko teoriškai paskaičiuotas jų reikšmes. Imunoblotingo duomenys parodė, kad visi G-CSF dimerai, kartu su G-CSF monomeru, sąveikauja su specifiniais rhG-CSF antikūnais.

Norint patvirtinti GCSF-Lα-GCSF seką, įvertini jo atitikimą komerciniam G-CSF standartui bei galimus struktūrinius pokyčius, išgrynintam dimerui buvo nustatytas RP-HPLC peptidinis žemėlapis. GCSF-L2-GCSF ir GCSF-L7-GCSF, dėl nepakankamo jų grynumo, nebuvo analizuoti pastaruoju metodu. GCSF-Lα-GCSF ir G-CSF monomero,

paveiktų glutamilo endopeptidaze (Glu-C) ir praleistų per RP-HPLC kolonėlę, chromatografiniai profiliai nežymiai skyrėsi. G-CSF atveju buvo matomas tik vienas santykinai aukštesnis pikas, kuris galėjo būti sietinas su dalinai sukarpytu fragmentu. Tuo tarpu GCSF-Lα-GCSF chromatogramoje esantis papildomas pikas, tikėtina, priklausė dvi G-CSF molekules jungiančiai Lα sekai.

Taisyklingas GCSF-Lα-GCCSF disulfidinių tiltelių susiformavimas buvo įvertintas fluorescensijos emisijos tyrimų metu (4 pav.). Triptofano fluorescencijos emisijos spektrų analizė rodo, jog baltymų GCSF-Lα-GCCSF ir G-CSF esant pH 7,0, bangos ilgio maksimumas buvo ~350 nm. Tuo tarpu rekombinantiniams baltymams esant rūgštinėje aplinkoje (pH 3,2), buvo matomas Trp fluorescencijos intensyvumo sumažėjimas bei atsiradęs fluorescencijos juostos petys trumpesnių bangų pusėje. Pastaroji dominuojanti smailė, turinti bangos ilgio maksimumą ~310 nm yra priskirtina tyrozino (Tyr) fluorescencijai. Šie virsmai yra būdingi tik natyviam G-CSF, tuo tarpu G-CSF monomerai, turintys redukuotus ar nesusiformavusius disulfidinius tiltelius, kai pH 3,2, demonstruoja Trp fluorescencijos intensyvumo sumažėjimą, bet juose nėra stebima Tyr fluorescencija (Lu ir kt., 1992). Taigi, remiantis išgryninto dimero ir rhG-CSF standarto fluorescencijos emisijos spektrų panašumais galima tvirtinti, kad GCSF-Lα-GCCSF atgauna natyvią baltymo konformaciją, t. y., dimeruose susiformuoja taisyklingi disulfidiniai tilteliai.

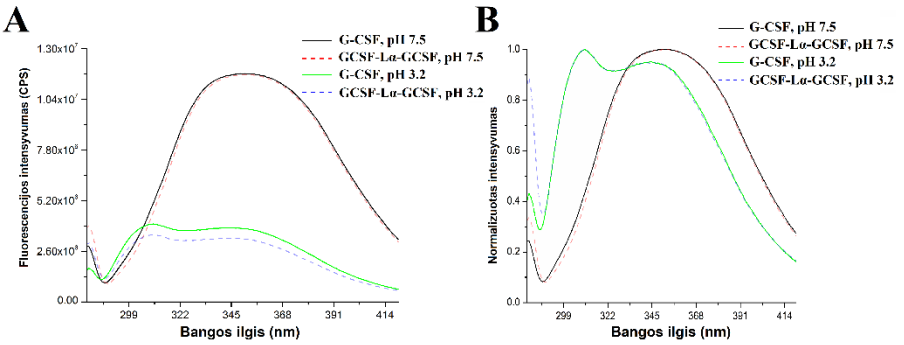

4 pav. Išgryninto GCSF-Lα-GCCSF ir G-CSF monomero (A) neapdoroti ir (B) normalizuoti fluorescencijos emisijos spektrai esant pH 3,2 ir pH 7,5.

G-CSF homodimerų su imobilizuotais receptoriais sąveikos tyrimas

Išgrynintų baltymų GCSF-L2-GCSF, GCSF-L7-GCSF ir GCSF-Lα-GCSF sąveikos su G-CSF receptoriumi (GCSF-R) kinetika buvo tyrinėjama taikant VVAE metodą. Pastaruoju metodu taip pat buvo matuotas ir G-CSF monomero jungimasis prie GCSF-R.

Sąveikoms analizuoti buvo sukurtas imuninis jutiklis, kuriame, siekiant pagerinti ligandų jungimosi platformos jautrumą, per baltymą G buvo kryptingai imobilizuojami receptoriai (Balevicius ir kt., 2014). Norint sumažinti galimą nespecifinį G-CSF homodimerų prisijungimą prie GCSF-R sluoksnio, dimerai buvo maišomi su žmogaus serumo albuminu.

GCSF-L2-GCSF sąveikos su GCSF-R kinetika buvo analizuota taikant standartinę grįžtamą Lengmiūro lygtį. Tuo tarpu GCSF-L7-GCSF ir GCSF-Lα-GCSF atvejais buvo taikytas kiek sudėtingesnis, iš trijų etapų sudarytas kinetinis modelis. Gauti tyrimų rezultatai atskleidė skirtingus dimerų saveikos su receptoriumi reakcijos mechanizmus (11 lentelė). Apskaičiuota GCSF-Lα-GCSF ir GCSF-R asociacijos greičio konstanta (*k*a) buvo 2 kartus didesnė lyginant su GCSF-L2-GCSF ir GCSF-R kompleksu, kai tuo tarpu ji atitinkamai 2 ir 3,5 kartus mažesnė lyginant su G-CSF monomeru ir GCSF-L7-GCSF.

G-CSF homodimerų biologinis aktyvumas *in vitro*

G-CSF dimerų biologinis aktyvumas *in vitro* buvo nustatytas pagal jų gebėjimą stimuliuoti G-NFS ląstelių dauginimąsi (Matsuda ir kt., 1989). Tyrimų metu rhG-CSF buvo naudojamas kaip palyginamasis standartinis baltymas.

Gauti rezultatai parodė, kad baltymai stimuliavo nuo jų koncentracijos priklausomą ląstelių proliferaciją. GCSF-Lα-GCSF biologinis aktyvumas siekė apie 50% monomerinio G-CSF baltymo biologinio aktyvumo reikšmės, kai tuo tarpu GCSF-L2-GCSF ir GCSF-L7-GCSF turėjo iki 22% G-CSF monomero aktyvumo (11 lentelė).

11 lentele. Homodimerinių G-CSF ir G-CSF monomero aktyvumo suvestinė

Charakteristika	**GCSF-L2-GCSF**	**GCSF-L7-GCSF**	**GCSF-Lα-GCSF**	**GCSF monomeras**
Biologinis aktyvumas ant G-NFS-60 ląstelių linijos[a] (IU/mmol)	$0{,}84 \times 10^{12}$	$0{,}86 \times 10^{12}$	$2{,}02 \times 10^{12}$	$1{,}88 \times 10^{12}$
Baltymo ir G-CSF receptoriaus asociacijos greičio konstantos (nustatyti VVAE metodu)				
*k*a ($M^{-1}\ s^{-1}$)	$2{,}00 \times 10^{5}$	$14{,}00 \times 10^{5}$	$4{,}00 \times 10^{5}$	$7{,}5 \times 10^{5}$

[a]Ląstelių linija, kuri vykdo G-CSF receptorių raišką.

GCSF-Lα-GCSF biologinis prieinamumas ir aktyvumas *in vivo*

Atlikus palyginamąsias GCSF-Lα-GCSF ir G-CSF monomero *in vivo* studijas, įvertintas dimero biologinis prieinamumas (5 pav. A) ir jo aktyvumas

(5.B pav.). GCSF-L2-GCSF ir GCSF-L7-GCSF, dėl nepakankamo jų gauto grynumo ir kiekio, nebuvo įtraukti į šiuos tyrimus (10 lentelė). Kiekvienai žiurkių grupei buvo sušvirkštas vienodas GCSF-Lα-GCSF ar G-CSF kiekis po oda (150 µg baltymo/kg gyvūno kūno svorio).

Biologinio prieinamumo tyrime nustatyta, kad G-CSF monomero cirkuliacijos pusamžis ($t_{1/2}$) kraujyje yra 1,2 val. Tuo tarpu GCSF-Lα-GCSF atveju, $t_{1/2}$ siekė 8,7 val., t. y., dimeras pasižymėjo bent 7 kartus ilgesne cirkuliacijos *in vivo* trukme lyginant su monomeru.

G-CSF biologinis aktyvumas *in vivo* apima jo gebėjimą stimuliuoti neutrofilų išsiskyrimą iš kaulų čiulpų, sukeldamas trumpalaikį cirkuliuojančių neutrofilų padidėjimą. Iš 5 pav. B pateiktų duomenų matyti, kad tiek GCSF-Lα-GCSF, tiek G-CSF monomero atvejais, absoliutus neutrofilų kiekis (ANC) buvo didžiausias praėjus 24 val. po injekcijos ir ženkliai sumažėjo praėjus 48 val. po injekcijos. Žiurkėms praėjus 24 val. po GCSF-Lα-GCSF injekcijos, ANC kiekis padidėjo 1,8 karto lyginant su monomeriniu G-CSF.

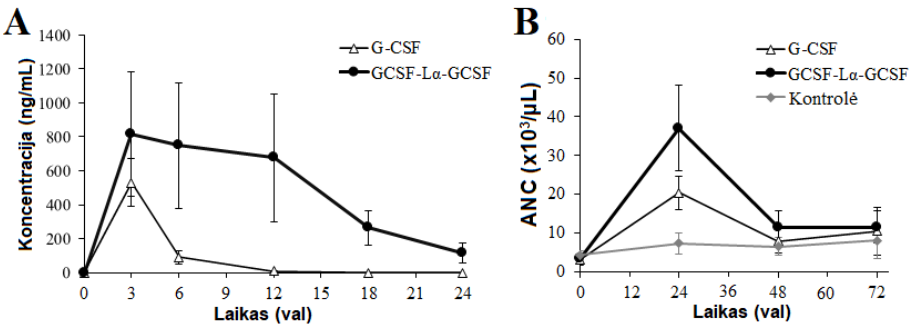

5 pav. (A) Biologinio prieinamumo ir (B) biologinio aktyvumo tyrimo rezultatai, gauti, tiriant žiurkių kraują po GCSF-Lα-GCSF ir G-CSF injekcijos. (A) G-CSF koncentracijos kitimo laike grafikas, po GCSF-Lα-GCSF ir G-CSF injekcijos. Rezultatai pateikti kaip vidurkiai (G-CSF grupėje n = 4, GCSF-Lα-GCSF grupėje n=5) ± SD. **(B)** Absoliutaus neutrofilų skaičiaus kitimo laike grafikas, po GCSF-Lα-GCSF, G-CSF ir kontrolinio buferinio tirpalo injekcijos. Rezultatai pateikti kaip vidurkiai (G-CSF grupėje n = 5; GCSF-Lα-GCSF grupėje n = 6; kontrolinio buferinio tirpalo grupėje n = 3) ± SD.

GCSF-Lα-GCSF didelės skalės gamybos technologijos kūrimas bei kokybės įvertinimas

GCSF-Lα-GCSF, lyginant su kitais G-CSF homodimerais, pasižymėjo didžiausiu grynumu bei aktyvumu (*in vitro* ir *in vivo*), todėl buvo pasirinktas tolimesniems tyrimams kaip potencialus vaistas-kandidatas. Norint turėti daugiau tikslinio baltymo, buvo sukurta didelės skalės GCSF-Lα-GCSF

gamybos technologija, t. y., tiek biosintezės, tiek gryninimo procesas. Be to, siekiant užtikrinti baltymo kokybę, įvertintas ir jo vaistinėje formoje stabilumas.

Didelės skalės GCSF-Lα-GCSF gamyba

Didelės skalės GCSF-Lα-GCSF biomasės auginimas buvo vykdytas 5 L bioreaktoriuje, turinčiame 4 L mitybinės terpės. Rekombinantinio baltymo sintezė įvertinta M9 minimalioje terpėje, praturtintoje mielių ekstraktu, ir chemiškai apibrėžtoje terpėje. Rezultatai parodė, kad daugiau *E. coli* biomasės buvo gauta vykdant baltymų sintezę chemiškai apibrėžtoje terpėje (44,4 g/L) nei M9 minimalioje terpėje, praturtintoje mielių ekstraktu (24 g/L). Abiem atvejais, GCSF-Lα-GCSF raiška siekė ~30% nuo visų netirpių ląstelės baltymų.

Gryninimo proceso kūrimui, buvo paimta 125 g. *E. coli* biomasės (arba 2,8 L ląstelių kultūros, gautos chemiškai apibrėžtoje terpėje), kurios suardymui naudotas didelio slėgio homogenizatorius. Intarpiniai kūneliai tirpininti, renatūruoti bei gryninimo procesas atliktas kiek pakeitus mažos skalės GCSF-Lα-GCSF gryninimo metodiką. Renatūruotas tikslinis baltymas buvo įvestas į DEAE Sepharose FF sorbentu užpildytą kolonėlę, nupusiausvyrintą renatūracijos buferiniu tirpalu (50 mM Tris-HCl, pH 8,0), turinčiu 3 M karbamido, o chromatografinis gryninimas atliktas esant pH 8,0, o ne pH 7,5. Norint sumažinti proceso trukmę, tolimesniame gryninimo žingsnyje per SP Sepharose FF sorbentą, baltymas desorbuotas taikant pakopinį gradientą (vietoj tiesinio). GCSF-Lα-GCSF chromatografijos bei atitinkamų frakcijų SDS-PAGE elektroforezės vaizdai pateikti 6 pav. Išgryninto GCSF-Lα-GCSF kiekis siekė 670 mg ir tai sudarė 17,18% nuo baltymo kiekio pradiniame intarpinių kūnelių tirpale. Tuo tarpu galutinis RP-HPLC grynumas siekė 98,04%.

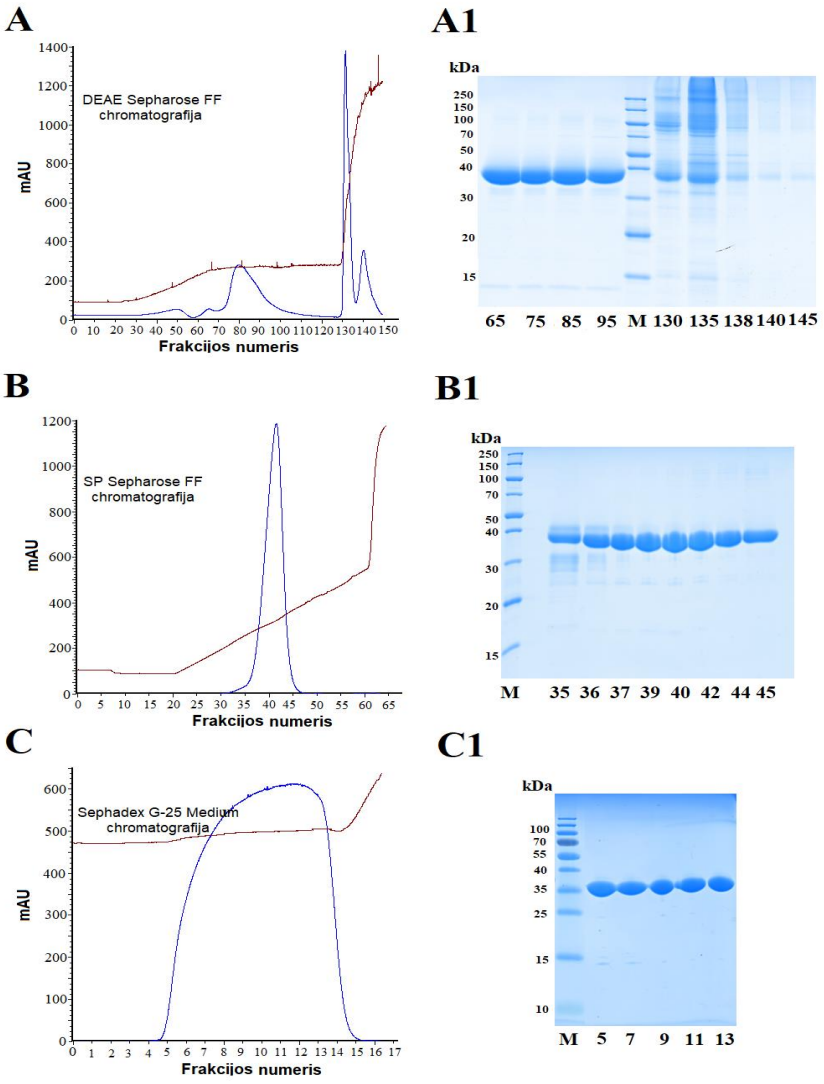

6 pav. Kiekvieno GCSF-Lα-GCSF gryninimo žingsnio eliucijos chromatogramos ir atitinkamų chromatografinių frakcijų SDS-PAGE elektroforezės vaizdai, esant neredukuojančiomis sąlygomis. (A) Renatūruoto GCSF-Lα-GCSF mėginio chromatografija DEAE Sepharose sorbentu užpildytoje kolonėlėje. **(A1)** 65-145 frakcijų, pavaizduotų A pav., analizė SDS-PAGE. **(B)** Apjungtų frakcijų (65-95 fr. gautų per anijonų-mainų chromatografinę stadiją) chromatografija SP Sepharose sorbentu užpildytoje kolonėlėje. **(B1)** 35-45 frakcijų, pavaizduotų B pav., analizė SDS-PAGE. **(C)** Apjungtų frakcijų (37-45 fr. gautų per katijonų-mainų chromatografinę stadiją) chromatografija Sephadex G-25 Medium sorbentu užpildytoje kolonėlėje. **(C1)** 5-13 frakcijų, pavaizduotų C pav., analizė SDS-PAGE. *M* molekulinių masių standartai (Thermo Fisher Scientific). Eliuentų absorbcijos stebimos ties 280 nm.

Suformuluoto GCSF-Lα-GCSF stabilumas, esant stresinėms sąlygoms

Stabilumo tyrimai parodė, kad esant stresinėms sąlygoms, suformuluotas GCSF-Lα-GCSF (10 mM natrio acetato, 5% D-sorbitolio, 0,0025% Tween 80, pH 4,0 tirpale) yra linkęs degraduoti ir formuoti agregatus. Baltymo RP-HPLC grynumas, laikant mėginius 4 savaites 40ºC temperatūroje bei esant 75% santykinei drėgmei (RH), nukrito nuo 98,0% (pradinis) iki 95,7%. Tuo tarpu, SE-HPLC duomenys parodė ženklesnius pokyčius: buvo matomas didesnės molekulinės masės agregatų susidarymas bei SE-HPC grynumas atitinkamai sumažėjo nuo 99,7% iki 94,1% (7 pav. A). Agregatų susidarymas buvo stebimas ir tiriant stresuotus mėginius SDS-PAGE metodu. GCSF-Lα-GCSF biologinio aktyvumo *in vitro* reikšmė, po 4 savaičių, sumažėjo 1,96 karto, lyginant su baltyminiu mėginiu laikytu 4°C.

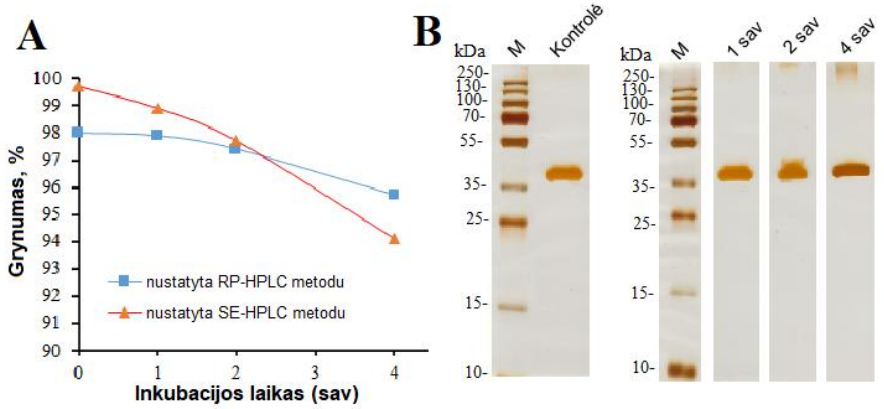

7 pav. Suformuluoto GCSF-Lα-GCSF stabilumo tyrimas. Baltyminiai mėginiai buvo laikomi 4 savaites 40ºC temperatūroje esant 75% RH ir kas savaitę buvo analizuojami pasirinktais metodais. **(A)** GCSF-Lα-GCSF grynumo kitimas (%), nustatytas RP- ir SE-HPLC metodais. **(B)** Pradinio ir stresuotų GCSF-Lα-GCSF mėginių, esant redukuojančioms sąlygoms, SDS-PAGE elektrotroforezės vaizdai. *M* molekulinių masių standartai (Thermo Fisher Scientific).

SCF ir G-CSF heterodimerinių baltymų raiška, gryninimas ir charakterizavimas

SCF ir G-CSF heterodimerų raiška

Aptikus, kad alfa spiralę formuojanti jungiančioji seka Lα geba efektyviai atskirti domenus bei užtikrina jų veikimą homodimerinėje G-CSF molekulėje bei kituose sulietuose baltymuose (Arai ir kt., 2001; Chen ir kt., 2013), buvo nutarta per Lα seką sujungti du sinergetiškai veikiančius baltymus.

Darbo metu buvo sukonstruoti nauji SCF ir G-CSF heterodimerai, susidedantys iš žmogaus SCF ir G-CSF ir sujungtų tarpusavyję per Lα jungiančiąją seką (SGLEA–(EAAAK)$_4$–ALEA–(EAAAK)$_4$–ALEGS). SCF-Lα-GCSF ir GCSF-Lα-SCF genai buvo sėkmingai klonuoti į pET21b(+) raiškos vektorius ir gautos plazmidės transformuotos į *E. coli* BL21(DE3) ir BL21STAR(DE3) kamienus. Transformantai buvo kultivuojami mažame kultūros kiekyje praturtintoje M9 terpėje. SDS-PAGE metodu nustatyta, kad tikslinių baltymų raiška siekė 9-11% nuo visų netirpių ląstelės baltymų. Abu baltymai *E. coli* ląstelėse sudarė intarpinius kūnelius, todėl norint išgauti biologiškai aktyvų tikslinį baltymą, buvo būtina abiems baltymams sukurti renatūracijos procedūrą.

SCF ir G-CSF heterodimerų renatūracija ir gryninimas per tris chromatografines stadijas

Kuriant heterodimerų gryninimo technologiją, RP-HPLC analizė, kaip ir G-CSF homodimerų atveju, buvo pasirinkta kaip tinkamas analitinis metodas, gebantis atskirti teisingos konformacijos baltymą nuo redukuotos jo formos. Po intarpinių kūnelių tirpinimo, visiškas abiejų heterodimerų disulfidinių tiltelių redukavimas buvo pasiektas pridėjus 0,5 mM DTT (8 pav. A). Optimizuota oksidacinė SCF-Lα-GCSF ir GCSF-Lα-SCF renatūracija tirpale po 24 val. davė atitinkamai 24,2% ir 35,8% baltymų grynumą, nustatytą RP-HPLC metodu (12 lentelė; 8 pav. B).

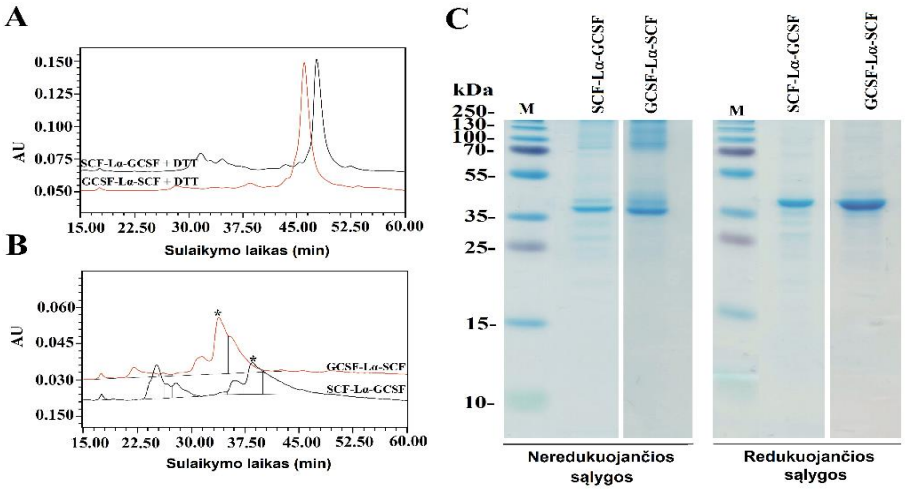

8 pav. SCF-Lα-GCSF ir GCSF-Lα-SCF mėginių, parinkus optimaliais sąlygas, (A, B) RP-HPLC analizių ir (C) SDS-PAGE elektroforezės vaizdai. (A) Intarpinių kūnelių tirpalų, esant DTT, RP-HPLC analizės vaizdai. **(B)** Heterodimerų, po renatūracijos, esant DTT/GSSG porai, RP-HPLC analizės vaizdai. Eliuentų absorbcijos stebimos ties 215 nm. **(C)** Heterodimerų, po renatūracijos, esant DTT/GSSG porai, esant neredukuojančiomis bei redukuojančiomis sąlygomis, SDS-PAGE elektroforezės vaizdai. *M* molekulinių masių standartai (Thermo Fisher Scientific).

Renatūruotų baltymų SCF-Lα-GCSF ir GCSF-Lα-SCF žymus grynumas buvo pasiektas per pirmąją DEAE Sepharose FF sorbentu užpildytą chromatografinę kolonėlę. Daugelis nespecifinių baltymų, įskaitant ir agregatus, buvo pašalinti šios stadijos metu, ir tikslinio baltymo RP-HPLC grynumas siekė daugiau nei 58% (12 lentelė). Siekiant sumažinti likusias priemaišas, buvo išbandyta ir daugiau skirtingų savybių turinčių chromatografinių sorbentų, įskaitant CM Sepharose FF, SP Sepharose FF, Cu-Ida Sepharose FF, Butyl Sepharose FF, Phenyl Sepharose FF ir Superdex 200 (9 pav. A). Rezultatai parodė, kad CHT ceramic hydroxyapatite II tipo sorbentu užpildyta kolonėlė, heterodimerus desorbuojant linijiniu gradientu didinant NaH_2PO_4 koncentraciją, efektyviausiai atskiria tikslinį baltymą nuo pašalinių jo formų. Paskutinei gryninimo stadijai parinktas stiprus katijonitas, t. y., SP Sepharose FF sorbentu užpildyta kolonėlė, kuri leido heterodimerams patekti į natrio acetato buferinį tirpalą, tinkamą baltymų formulavimui. Taip, parinkus atitinkamas renatūracijos ir gryninimo sąlygas, SCF-Lα-GCSF ir GCSF-Lα-SCF kiekis atitinkamai siekė 2,8 mg and 2,6 mg (~1,4% ir 1,2% pradinių intarpinių kūnelių atžvilgiu). Tuo tarpu galutinis abiejų heterodimerų RP-HPLC grynumas buvo >90% (12 lentelė). 9 pav. A pavaizduotos išbandytos gryninimo sąlygos, siekiant surasti optimalią SCF-Lα-GCSF

gryninimo technologiją, kuri toliau buvo taikyta GCSF-Lα-SCF gryninimui. Galutinė abiejų heterodimerų gryninimo schema pateikta 9 pav. B.

A

Stadija	Parametras	Medžiaga/ Sorbentas	SCF-Lα-GCSF	GCSF-Lα-SCF
Tirpinimas	Tirpinimo agentas	Karbamidas	+	+
	Redukuojantis agentas	Be reduktoriaus	+	-
		DTT	+	+
Renatūracija	Oksiduojantis agentas	DTT/GSSG	+	+
Chromatografija	Pirmasis gryninimo žingsnis	DEAE Sepharose FF	+	+
		Q Sepharose FF	+	-
	Tarpininis gryninimo žingsnis	CM Sepharose FF	+	-
		SP Sepharose FF	+	-
		Cu-IDA Sepharose FF	+	-
		Butyl Sepharose FF	+	-
		Phenyl Sepharose FF	+	-
		Superdex 200	+	-
		CHT ceramic hydroxyapatite,Tipas II	+	+
	Galutinis gryninimo žingsnis	SP Sepharose FF	+	+
	Formulavimo žingsnis	Sephadex G-25 Medium	+	+

B

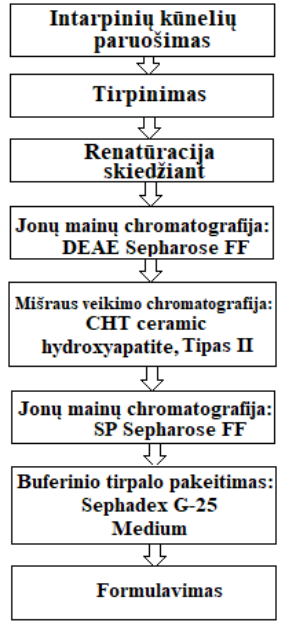

9 pav. SCF ir G-CSF heterodimerų gryninimo charakteristikos. (A) Ištirtos sąlygos, ieškant tinkamiausios heterodimerų gryninimo procedūros. **(B)** Tinkamiausia SCF-Lα-GCSF ir GCSF-Lα-SCF gryninimo schema. Santrumpos: + ištirtos; - neištirtos sąlygos.

12 lentelė. SCF ir GCSF heterodimerų gryninimo eiga

Gryninimo stadija	Charakteristika	SCF-Lα-GCSF	GCSF-Lα-SCF
Renatūracija	Išeiga[1]	93,2±2,9	91,7±2,1
	Grynumas[2]	24,2±1,0	35,8±2,2
I chromatografija (anijų-mainų)	Išeiga[1]	7,3±0,5	6,1±0,3
	Grynumas[2]	63,5±2,5	58,6±1,4
II chromatografija (mišraus veikimo)	Išeiga[1]	1,9±0,4	1,8±0,3
	Grynumas[2]	77,5±3,0	67,2±2,2
III chromatografija (katijonų-mainų)	Išeiga[1]	1,4±0,1	1,2±0,2
	Grynumas[2]	92,2±2,1	90,4±1,6

Rezultatai pateikti kaip trijų nepriklausomų eksperimentų vidurkis ± SD.
[1]Baltymo koncentracija nustatyta Bradfordo metodu (Bradford, 1976), panaudojant BSA kaip standartą.
[2]Baltymo grynumas nustatytas RP-HPLC metodu.

Išgrynintų heterodimerų charakterizavimas

Išgryninti heterodimerai buvo charakterizuoti SDS-PAGE, imunoblotingo, RP- ir SE-HPLC bei masių spektrometrijos metodais. rhG-CSF ir rhSCF buvo naudojami kaip palyginamieji standartiniai baltymai.

Išgrynintų SCF-Lα-GCSF ir GCSF-Lα-SCF SDS-PAGE elektroforezės vaizdas, tiek neredukuojančiomis, tiek redukuojančiomis sąlygomis yra pateiktas 10 pav. B. Redukuoti baltymai takeliuose matomi kaip viena juostelė, atitinkanti apskaičiuotas heterodimerų teorines molekulines mases (42 kDa). Tuo tarpu neredukuotus SCF-Lα-GCSF ir GCSF-Lα-SCF baltymus atitinkančios juostelės gelyje stebimos šiek tiek žemiau nei pagal jų molekulines mases (atitinkamai 39 kDa ir 37 kDa). Nesant reduktoriui, šalia pagrindinės, rasta ir papildoma juostelė, atitinkanti didesnio molekulinio svorio baltymą, kuri buvo aptinkama per visą pastarųjų heterodimerų gryninimo procesą. Tolesni imunoblotingo tyrimų rezultatai parodė, kad visi pastarieji baltymai (pagrindinė ir didesnio molekulinio svorio priemaišinė baltymo forma) sąveikavo tiek su poliklonineis anti-SCF, tiek su monokloniniais anti-G-CSF antikūnais. RP-HPLC metu buvo nustatytas SCF-Lα-GCSF ir GCSF-Lα-SCF grynumas, kuris atitinkamai siekė 92,2% ir 90,4% (12 lentelė). Taip pat, šios RP-HPLC analizės metu stebimas skirtingas baltymų sulaikymo laikas kolonėlėje atskleidė ir skirtingus jų hidrofobiškumo lygius (10 pav. A). Trumpiausias sulaikymo laikas kolonėlėje buvo nustatytas SCF monomerui, tuo tarpu hidrobiškumo lygis atitinkami didėjo G-CSF<GCSF-Lα-SCF<SCF-Lα-GCSF.

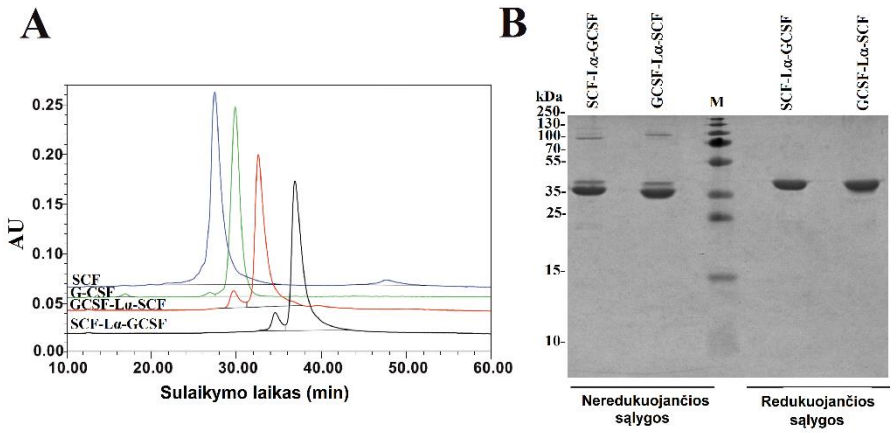

10 pav. Heterodimerų (A) RP-HPLC analizių ir (B) SDS-PAGE elektroforezės vaizdas. (**A**) Išgrynintų heterodimerų ir standartinių baltymų SCF ir G-CSF RP-HPLC analizės vaizdai. Eliuentų absorbcijos stebimos ties 215 nm. (**B**) Išgrynintų heterodimerų, esant neredukuojančiomis bei redukuojančiomis sąlygomis, SDS-PAGE elektroforezės vaizdas. *M* molekulinių masių standartai (Thermo Fisher Scientific).

G-CSF ir SCF monomerinių standartų bei heterodimerų oligomerinės būsenos tirpale bei molekuliniai svoriai buvo įvertinti SE-HPLC metodu. Nustatyta G-CSF molekulinio svorio reikšmė buvo mažesnė nei 13,7 kDa (teorinė 18,8 kDa), o SCF monomeras gelfiltracinėje kolonėlėje aptiktas kaip dimerinis baltymas (>44,3 kDa). Tuo tarpu gauti heterodimerų molekuliniai svoriai buvo gerokai didesni (>150 kDa) nei tikėtasi (teorinė ~42 kDa). Iš pastarųjų rezultatų galima daryti prielaidą, kad SCF ir GCSF heterodimerai tirpaluose yra linkę formuoti multimerines struktūras, t. y., heterodimerai greičiausiai sudaro pailgos formos nekovalentinius dimerus ar trimerus. HPLC/ESI-MS metu nustatytos išgrynintų SCF-Lα-GCSF ir GCSF-Lα-SCF molekulinių masių reikšmės gerai atitiko teoriškai paskaičiuotas jų reikšmes. Be to, atskleidė ir pastarųjų heterodimerų heterogeniškumą: tiek SCF-Lα-GCSF, tiek GCSF-Lα-SCF atvejais, šalia pagrindinės smailės buvo stebima ir nedidelė dalis didesnės molekulinės masės baltymo forma (atitinkamai 42983,05 Da ir 42983,27 Da dydžio).

SCF ir GCSF heterodimerų su imobilizuotais receptoriais sąveikos tyrimas

Išgrynintų SCF-Lα-GCSF ir GCSF-Lα-SCF su kryptingai imobilizuotais receptoriais, GCSF-R ir c-KIT, sąveikos kinetikos buvo analizuotos VVAE metodu. Tuo pačiu principu buvo tirtos ir SCF ir G-CSF monomerų sąveikos. Baltymų jungimosi kinetikos charakterizavimui taikytas

standartinis grįžtamas Lengmiūro modelis (Balevicius ir kt., 2014). Gautų tyrimo rezultatų suvestinė yra pateikta 13 lentelėje.

Visi baltymai sąveikavo su receptoriais, išskyrus GCSF-Lα-SCF, kuris, nors ir jungėsi prie c-KIT, su GCSF-R nesąveikavo. Apskaičiuota SCF-Lα-GCSF ir c-KIT asociacijos greičio konstanta *k*a buvo 6 kartus didesnė lyginant su SCF monomeru. Tuo tarpu GCSF-Lα-SCF atveju *k*a buvo 80 kartų didesnė už SCF monomero. Apskaičiuota SCF-Lα-CSF disociacijos greičio konstanta k_d buvo panaši į SCF monomero, nors GCSF-Lα-SCF ji buvo 45 kartus didesnė. SCF-Lα-GCSF su GCSF-R sąveikos atveju, reakcijos greičio konstantos *k*a ir *k*d buvo 10 kartų mažesnės lyginant su G-CSF monomeru.

Heterodimerų biologinis aktyvumas *in vitro*

Heterodimerų biologinis aktyvumas *in vitro* buvo nustatytas su M-07e bei G-NFS-60 ląstelių linijomis atitinkamai turinčiomis SCF ir G-CSF receptorius. SCF-Lα-GCSF santykinis aktyvumas M-07e ląstelėse siekė 72%, o GCSF-Lα-SCF atveju 137% monomerinio SCF aktyvumo. Tuo tarpu dimerų stimuliavimas G-NFS-60 ląstelių dauginimąsi buvo ženkliai sumažėjęs lyginant su G-CSF monomeru. SCF-Lα-GCSF atveju jis siekė 34%, o GCSF-Lα-SCF turėjo tik 13% G-CSF monomero aktyvumo.

13 lentelė. Heterodimerų ir G-CSF ir SCF monomerų aktyvumo suvestinė

Characteristika	**SCF-Lα-GCSF**	**GCSF-Lα-SCF**	**G-CSF monomeras**	**SCF monomeras**
Biologinis aktyvumas ant G-NFS-60 ląstelių linijos[a] (IU/mmol)	$0{,}64\times10^{12}$	$0{,}25\times10^{12}$	$1{,}88\times10^{12}$	NA
Biologinis aktyvumas ant M-07e ląstelių linijos[b] (IU/mmol)	$6{,}70\times10^{9}$	$12{,}80\times10^{9}$	NA	$9{,}33\times10^{9}$
Baltymo ir SCF receptoriaus asociacijos ir disociacijos greičio konstantos (nustatytos VVAE metodu)				
*k*a (M^{-1} s^{-1})	$7{,}77\times10^{4}$	$1{,}14\times10^{6}$	NA	$1{,}37\times10^{4}$
$k_d(s^{-1})$	$1{,}39\times10^{-2}$	$6{,}46\times10^{-1}$	NA	$1{,}43\times10^{-2}$
$K_a(M^{-1})$	$5{,}59\times10^{6}$	$1{,}76\times10^{6}$	NA	$9{,}50\times10^{5}$
(K_d) (M)	$1{,}78\times10^{-7}$	$5{,}67\times10^{-7}$	NA	$1{,}04\times10^{-6}$
Baltymo ir G-CSF receptoriaus asociacijos ir disociacijos greičio konstantos (nustatytos VVAE metodu)				
*k*a (M^{-1} s^{-1})	$8{,}5\times10^{4}$	–	$7{,}50\times10^{5}$	NA
$k_d(s^{-1})$	$1{,}25\times10^{-3}$	–	$1{,}05\times10^{-2}$	NA
$K_a(M^{-1})$	$6{,}80\times10^{7}$	–	$7{,}14\times10^{7}$	NA
(K_d) (M)	$0{,}15\times10^{-7}$	–	$0{,}14\times10^{-7}$	NA

13 lentelė. Heterodimerų ir G-CSF ir SCF monomerų aktyvumo suvestinė

Characteristika	SCF-Lα-GCSF	GCSF-Lα-SCF	G-CSF monomeras	SCF monomeras

[a]Ląstelių linija, kuri vykdo G-CSF receptorių raišką.
[b]Ląstelių linija, kuri vykdo SCF receptorių raišką.
−, sąveika nebuvo nustatyta.
NA, netaikoma, tyrimas nereikalingas.

SCF-Lα-GCSF biologinis aktyvumas *in vivo*

GCSF-Lα-SCF baltymas parodė žymiai mažesnį G-CSF aktyvumą *in vitro* lyginant su SCF-Lα-GCSF, todėl pastarasis baltymas buvo pasirinktas *in vivo* studijoms. SCF-Lα-GCSF biologinio aktyvumo tyrimai atlikti su žiurkėmis, tiriamuosius ir kontrolinius baltymus sušvirkščiant po oda (500 ar 1000 μg baltymo/kg gyvūno kūno svorio) bei tiriant cirkuliuojančių neutrofilų kiekį laike (11 pav.).

Tiek heterodimero, tiek ir monomerinių baltymų atveju, didžiausias ANC kiekis buvo stebimas praėjus 24 val. po injekcijos. Kaip ir tikėtasi, SCF bei kontrolinis buferinis tirpalas nestimuliavo neutrofilų išsiskyrimo (11 pav.). Žiurkėms, praėjus 24 val. po SCF-Lα-GCSF (1000 μg/kg) injekcijos, absoliutus neutrofilų kiekis padidėjo 7 kartus, o po G-CSF ir SCF monomerų mišinio (500 + 500 μg/kg) injekcijos, ANC kiekis padidėjo 6,3 karto atitinkamai lyginant su jų pradiniais kiekiais (0 val.). Tuo tarpu G-CSF monomero (500 μg/kg) biologinis aktyvumas pasireiškė 4,4 karto didesniu cirkuliuojančių neutrofilų kiekiu. Taip pat, tarp rekombinantinių baltymų nustatyti ir ANC kitimo skirtumai. Būtent heterodimero atveju nebuvo tokio ženklaus neutrofilų skaičiaus kritimo laike lyginant su monomerais.

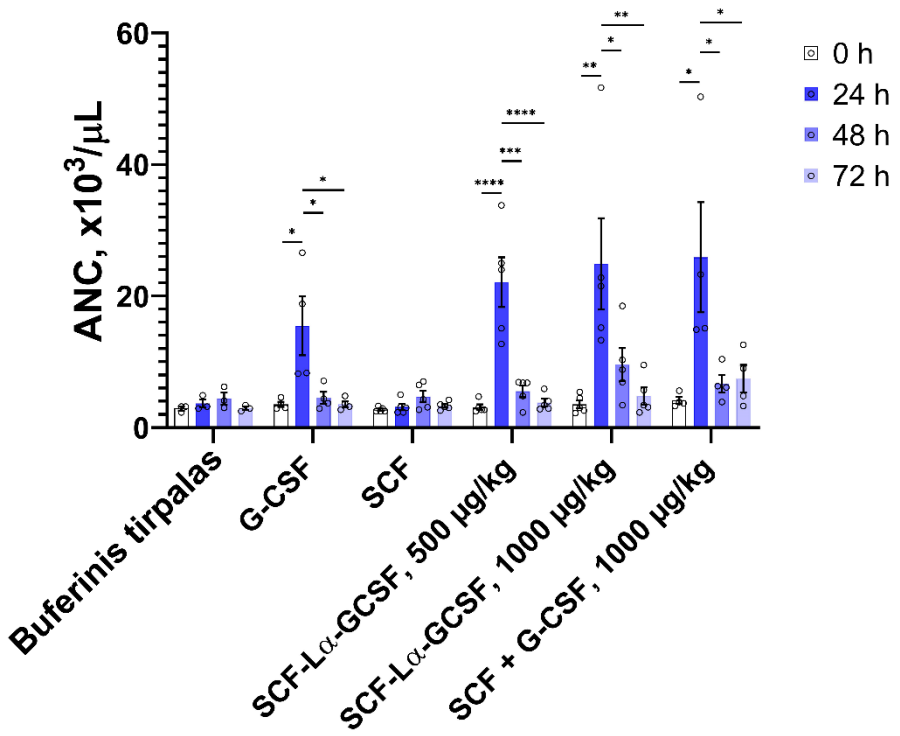

11 pav. Absoliutaus neutrofilų skaičiaus kitimo laike grafikas, tiriant žiurkių kraują po tiriamųjų rekombinantinių baltymų injekcijos. Rezultatai pateikti kaip vidurkiai ± SEM. Tušti apskritimai nurodo atskiras nepriklausomų tyrimų vertes. ANC skirtumai tarp tiriamųjų grupių analizuoti naudojant ANOVA kartu su Tukey daugkartinio palyginimo testu. Žvaigždutės žymi grupes, tarp kurių yra statistiškai reikšmingi skirtumai (*p < 0,05; **p < 0,01; ***p < 0,001, ****p < 0,0001).

REZULTATŲ APTARIMAS

Žmogaus G-CSF rekombinantinės vaistinės formos yra plačiai naudojamos gydyti neutropeniją, ypač tą, kurią sukelia citotoksinė chemoterapija. Keletas antros kartos G-CSF vaistų, pasižyminčių prailginta cirkuliacijos *in vivo* trukme, jau yra patvirtini ir naudojami gydymui, o naujų jų formų kūrimas vis dar tebevyksta (14 lentelė).

Šiame darbe aprašytas trijų naujų G-CSF dimerų, sudarytų iš dviejų žmogaus G-CSF molekulių, genetiniu būdu sujungtų per tam tikro ilgio aminorūgščių sekas, konstravimas, gryninimas ir charakterizavimas. Homodimeriniai rekombinantiniai baltymai kaupėsi *E. coli* ląstelėse netirpioje frakcijoje. Biologiškai aktyvus, rekombinantinis žmogaus G-CSF turi du disulfidinius tiltelius Cys36-Cys42 ir Cys64-Cys74, bei nesuporuotą Cys17 (Lu ir kt., 1989). Todėl norint išgauti biologiškai aktyvius dimerinius G-CSF baltymus, besikaupiančius intarpinių kūnelių pavidalu, didelis dėmesys darbo metu buvo skiriamas kiekvieno G-CSF dimero renatūracijos sąlygų parinkimui. Efektyvi renatūracija buvo pasiekta intarpinius kūnelius tirpinant karbamido tirpale, esant pakankam kiekiui DTT (suredukuoti disulfidinius tiltelius), bei toliau baltymą skiedžiant renatūracijos buferiniu tirpalu. Optimizavus renatūracijos procedūras, buvo gautas didesnis nei 40% RP-HPLC atitinkamo renatūruoto baltymo grynumas.

Tolesniam G-CSF homodimerų gryninimui buvo parinktos dvi chromatografinio gryninimo stadijos. Galutinis GCSF-Lα-GCSF grynumas, nustatytas RP-HPLC metodu, siekė daugiau nei 95% (10 lentelė). Tuo tarpu, GCSF-L2-GCSF ir GCSF-L7-GCSF atvejais, baltymų gryninimas per jonų mainų chromatografines kolonėles nebuvo toks sėkmingas. Abiems atvejais nepavyko gauti didelio grynumo baltymų, kadangi jų tirpaluose, be pagrindinės, dominavo ir netaisyklinga baltymo forma, turinti ilgesnį sulaikymo laiką RP-HPLC kolonėlėje nei natyvus baltymas. To pasekoje, galutinis GCSF-L2-GCSF ir GCSF-L7-GCSF RP-HPLC grynumas siekė mažiau nei 83%, o išeiga buvo 6-11 kartų mažesnė lyginant su GCSF-Lα-GCSF išgautu kiekiu (10 lentelė).

14 lentelė. Trumpo ir prailginto veikimo G-CSF vaistų apžvalga, lyginant su G-CSF standartu filgrastimu

Strategijos	Sudėtis	Raiškos sistema	Pavyzdžiai	Privalumai	Trūkumai
(A) Trumpo veikimo rhG-CSF	GCSF	*E. coli*	Filgrastimas	• Biologinis aktyvumas panašus į endogeninio G-CSF • Paprasta ir nebrangi gamyba	• Trumpas gyvavimo laikas • Mažai stabilus • Jautrus degradacijai
		Kinijos žiurkėno kiaušidžių (CHO) ląstelės	Lenograstimas	• Glikozilintas G-CSF • Didesnis atsparumas proteolizei	• Brangesnė gamyba • Trumpas gyvavimo laikas
		E. coli	Nartograstimas (GCSF N-galinė seka yra mutuota)	• Didesnis biologinis aktyvumas	• Trumpas gyvavimo laikas
(B) PEGilinti rhG-CSF	20PEG-GCSF 20PEG-O-glycan-GCSF 10PEG-GCSF	*E. coli*	Pegfilgrastimas Lipegfilgrastimas FN10L	• Prailgintas gyvavimo laikas • Didesnis stabilumas, atsparumas proteolizei	• Sumažėjęs biologinis aktyvumas • Brangesnė gamyba
	10PEG-GCSF-GCSF-10PEG	*E. coli*	diPEG-F_{dim}	• Prailgintas gyvavimo laikas	• Mažas biologinis aktyvumas • Brangesnė gamyba
(C) Baltymų suliejimas	GCSF-(IgG2)Fc-GCSF	CHO ląstelės	F-627[1] Balugrastimas	• Prailgintas gyvavimo laikas	• Brangesnė gamyba

14 lentelė. Trumpo ir prailginto veikimo G-CSF vaistų apžvalga, lyginant su G-CSF standartu filgrastimu

Strategijos	Sudėtis	Raiškos sistema	Pavyzdžiai	Privalumai	Trūkumai
	HSA-GCSF	*S.cerevisiae*		• Didesnis biologinis aktyvumas	
	GCSF-3.4PEG-(IgG4)Fc	*E. coli*	Eflapegrastimas	• Prailgintas gyvavimo laikas • Greitesnė neutrofilų gamyba	• Brangesnė gamyba
	GCSF-L-GCSF[2] SCF-L-GCSF[2]	*E. coli*	GCSF-Lα-GCSF SCF-Lα-GCSF	• Didesnis biologinis aktyvumas *in vivo* • Prailgintas gyvavimo laikas • Paprasta ir nebrangi gamyba	• Biologinio aktyvumo *in vitro* ir *in vivo* neatitikimas • Reikalingi tolesni tyrimai
	GCSF-GCSF	*E. coli*	F_{dim}	• Paprasta ir nebrangi gamyba	• Trumpas gyvavimo laikas
(D) Naujos formuluotės	PLGA + GCSF GCSF esantis liposomose	*E. coli*	PLGA + GCSF DPPC/Chol + GCSF	• Kontroliuojamas baltymo atpalaidavimas • Prailgintas gyvavimo laikas	• Skirtingo dydžio dalelės • Su sterilinimu susiję iššūkiai • Mažas inkapsuliavimo efektyvumas

Patvirtinti ir rinkoje naudojami G-CSF vaistai yra pažymėti pabraukimo brūkšniu (_), o visi kiti G-CSF variantai yra aprašyti tik mokslinėje literatūroje.
[1]- Pirmasis III fazės klinikinis tyrimas yra baigtas.
[2]- Šio darbo metu sukurti ir aprašyti G-CSF homo- ir heterodimerai.

Tiriant GCSF-L2-GCSF ir GCSF-L7-GCSF mėginius SDS-PAGE metodu, ši ilgesnė RP-HPLC-sulaikyta baltymo forma buvo matoma geliuose kaip papildoma juostelė, kuri buvo stebima viso dimerų gryninimo procesų metu. Pastaroji juostelė išnykdavo esant redukuojančioms sąlygoms, todėl daroma prielaida, kad ši priemaiša galėjo atsirasti susidarant papildomiems disulfidiniams tilteliams baltymo viduje, tikėtina, per nesuporuotus cysteinus, esančius homodimero G-CSF. Tai paaiškintų, kodėl ši priemaiša buvo taip sunkiai atskiriama chromatografinių procesų metu bei pagrįstų G-CSF monomerus jungiančiosios sekos ilgio bei sudėties svarbą. Sprendžiant iš literatūros apžvalgoje pateiktų duomenų, L2 ir L7 jungiančios sekos didina erdvinį domenų atskyrimą ir taip leidžia monomerams sąveikauti vienas su kitu (Chen ir kt., 2013; Chichili ir kt., 2013). Tuo tarpu Lα jungiančioji seka gali užtikrinti dviejų G-CSF molekulių atskyrimą bei atstumą, palankų jų nepriklausomam veikimui. Tokiu būdu, GCSF-Lα-GCSF baltymas turi didelį pranašumą prieš kitus du G-CSF homodimerus, kadangi jį lengviau išgryninti bei gauti didesnę baltymo išeigą.

2006 m. Tamada ir kt. išsprendė G-CSF:G-CSF receptoriaus komplekso kristalinę struktūrą, kuri parodė, kad monomero ir jo receptoriaus jungimosi stechiometrija yra 2:2 (Tamada ir kt., 2006). Darbo metu, G-CSF homodimerų ir GCSF-R sąveikos analizei buvo pritaikytas VVAE metodas, kuriuo matuotas dimerų jungimasis prie imobilizuoto ant aukso paviršiaus receptoriaus. Lygiai taip pat buvo stebimas ir G-CSF monomero, kaip palyginamojo standartinio baltymo, veikimas. Nors visi baltymai sąveikavo, jų asociacijos greičiai su GCSF-R skyrėsi. Rezultatai parodė, kad GCSF-L2-GCSF, turintis trumpiausią G-CSF monomerus jungiančiąją seką, veikia kaip natyvus G-CSF monomeras (nustatyta GCSF-L2-GCSF:GCSF-R stechiometrija buvo 1:1). Taip gali nutikti dėl L2 jungiančiosios sekos ilgio – pastaroji yra pakankamai trumpa, tokiu būdu neleidžianti antram G-CSF monomerui sąveikauti su kitu GCSF-R, jei pirmasis jau yra G-CSF:GCSF-R komplekse. Prielaida, kad tiek L7, tiek Lα jungiančiųjų sekų ilgiai turėtų būti pakankami erdviškai atskirti G-CSF molekules ir leistų abiems dimero dalims sąveikauti su receptoriais buvo patvirtinta mūsų eksperimentais. GCSF-L7-GCSF ir GCSF-Lα-GCSF sąveikavo su G-CSF receptoriumi efektyviau nei GCSF-L2-GCSF baltymas bei pagrindė 1:2 stechiometriją dimero ir receptoriaus atžvilgiu.

Tolesni išgrynintų baltymų biologinio aktyvumo tyrimai *in vitro* parodė, kad G-CSF homodimerų gebėjimas stimuliuoti G-NFS-60 ląstelių dauginimąsi yra sumažėjęs lyginant su standartiniu G-CSF monomeru. GCSF-Lα-GCSF biologinis aktyvumas siekė iki 50% monomerinio G-CSF baltymo

aktyvumo. Šis mažesnis biologinis aktyvumas galėtų būti siejamas su erdviniais trukdžiais, atsiradusiais suliejant G-CSF molekules per jungiančiąją seką, tokiu būdu modifikuojant vieno G-CSF domeno C-galą bei kito N-galą. Tuo tarpu žymiai sumažėjęs GCSF-L2-GCSF ir GCSF-L7-GCSF biologinis aktyvumas *in vitro* galėjo atsirasti ne tik dėl atitinkamo G-CSF monomero N- ir C-galo modifikavimo, bet ir dėl netinkamos jungiančios sekos ilgio/sudėties bei kartu lydinčių priemaišų. Nustatytas GCSF-Lα-GCSF biologinis aktyvumas *in vitro* buvo panašus į PEGilinto G-CSF (Pegfilgrastimo) aktyvumą, kuriame PEG molekulė yra prijungta prie amino grupių, esančių G-CSF molekulės N-gale (Fidler ir kt., 2011; Molineux, 2009).

Palyginus išgryninto GCSF-Lα-GCSF ir G-CSF monomerinio standarto biologines funkcijas *in vivo*, t. y., panaudojant sveikas žiurkes, paaiškėjo, kad dimerinis baltymas turi pranašumų: GCSF-Lα-GCSF atveju nustatytas $t_{1/2}$ siekė 8,7 val., vadinasi, dimero išsilaikymas kraujyje pailgėjo net 7 kartus lyginant su G-CSF monomeru. Reikia pastebėti, kad skirtingai nuo GCSF-Lα-GCSF, kitose studijose tirtas dimerinis G-CSF (F_{dim}), sudarytas iš dviejų G-CSF molekulių, sujungtų per disulfidinius tiltelius tarp nesuporuotų cisteinų, turėjo analogišką $t_{1/2}$ kaip ir G-CSF monomeras (Fidler ir kt., 2011). Gali būti, kad F_{dim} yra žymiai kompatiškesnis baltymas nei GCSF-Lα-GCSF, todėl ilgesnis GCSF-Lα-GCSF cirkuliacijos laikas pirmiausia turi būti siejamas su molekulės didesniu hidrodinaminiu spinduliu.

Biologinio aktyvumo tyrimuose *in vivo*, kurie apėmė G-CSF gebėjimą stimuliuoti neutrofilų išsiskyrimą, GCSF-Lα-GCSF parodė didesnį funkcinį aktyvumą nei G-CSF monomeras. Praėjus 24 val po GCSF-Lα-GCSF injekcijos, cirkuliuojančių neutrofilų kiekis padidėjo 1,8 karto lyginant su G-CSF.

Gauti GCSF-Lα-GCSF *in vivo* rezultatai leidžia daryti išvadą, kad šis sulietas baltymas yra perspektyvus vaistas-kandidatas. Tolesniems dimero charakterizavimo tyrimams būtina turėti didesnius baltymo kiekius bei formulavimo buferinį tirpalą, kuriame GCSF-Lα-GCSF ilgą laiką išliktų aktyvus bei stabilus.

Siekiant turėti daugiau tikslinio baltymo, darbo metu buvo sukurta didelės skalės GCSF-Lα-GCSF gamybos technologija, kuri apėmė tiek biosintezės, tiek gryninimo procesus. Plazmidėje su GCSF-Lα-GCSF koduojančiu genu parinktas atsparumo antibiotikui kanamicinui genas, kuris bakterijų auginimo metu, yra stabilesnis nei atsparumo ampicilinui bla genas (Korpimäki ir kt., 2003; Brouwers ir kt., 2020; Umezava, 1979). Kuriant biosintezės procesą, nauji *E. coli* trasformantai buvo auginti bioreaktoriuje, esant skirtingoms mitybinėms terpėms. Nustatyta, kad *E. coli* biomasės kiekis,

auginant bakterijas chemiškai apibrėžtoje terpėje yra 1,9 karto didesnis nei auginant M9 minimalioje terpėje su papildais. Tuo tarpu didelės skalės gryninimo procesas leido gauti didelius kiekius bei didelio grynumo laipsnio GCSF-Lα-GCSF. Galutinė produkto išeiga sudarė 17,18% nuo baltymo kiekio pradiniame intarpinių kūnelių tirpale, t. y., iš 125 drėgnos biomasės buvo gauta 670 mg išgryninto tikslinio baltymo, kurio RP-HPLC grynumas siekė >98%.

Norint įvertinti pirminį baltymo vaistinėje formoje stabilumą, suformuluotam GCSF-Lα-GCSF buvo atliktas trumpalaikis stabilumo tyrimas esant stresinėms sąlygoms. Keturias savaites laikant tiriamuosius mėginius 40ºC temperatūroje, tiek SE-HPLC, tiek SDS-PAGE metodais buvo stebimas didesnės molekulinės masės tirpių baltymų-agregatų susidarymas, kuris būdingas ir vaistiniams monomeriniams G-CSF preparatams (Krishnan ir kt., 2002). Tuo tarpu, nedidelis GCSF-Lα-GCSF grynumo mažėjimas buvo nustatytas RP-HPLC metodu: be tikslinės baltymo formos kiekio sumažėjimo, buvo stebimas nedidelis priemaišinių baltymo formų augimas.

Sprendžiant iš darbo metu gautų gryninimo, biologinio aktyvumo rezultatų, galima padaryti išvadą, kad dviejų G-CSF molekulių suliejimas į homodimerą turi pranašumą, lyginant su kitomis ilgiau veikiančiomis modifikuotomis G-CSF formomis. Sukurta G-CSF dimerinių baltymų gamybos technologija yra žymiai paprastesnė nei PEGilinimo procesas ir tolesnis pastarojo baltymo gryninimas yra efektyvesnis bei pasižymi santykinai trumpu gamybos laiku ir kaina.

Lα tipo jungiančioji seka, kaip tinkamiausia dviem G-CSF molekulėms sujungti, buvo pritaikyta ir kuriant heterodimerinius baltymus sudarytus iš žmogaus G-CSF ir SCF. Šios heterodimerinės baltymų formos buvo sukurtos kaip alternatyva kombinuotai SCF ir G-CSF terapijai, žinomai dėl sinergetinio jų veikimo.Taip pat, norint turėti ilgesnio veikimo baltymą nei monomerinės jų formos.

Baltymų SCF-Lα-GCSF ir GCSF-Lα-SCF raiška buvo gauta *E. coli* ląstelėse, kuriose tiksliniai baltymai kaupėsi intarpinių kūnelių pavidalu. Norint išgauti atitinkamai biologiškai aktyvų baltymą, darbo metu sukurta heterodimerinių baltymų renatūracijos bei chromatografinio gryninimo procedūra. Abiems atvejais, iš 12 g drėgnos *E. coli* biomasės buvo gauta apie 2,6-2,8 mg išgryninto baltymo. Heterodimerų RP-HPLC grynumas siekė daugiau nei 90% (12 lentelė).

SDS-PAGE bei imunolotingo eksperimetų duomenys parodė, kad esant redukuojančioms sąlygoms, išgryninti heterodimerai sudaro homogenišką didelio elektroforetinio grynumo baltymą. Neredukuojančiose sąlygose, be pagrindinės formos buvo stebima ir didesnio molekulinio svorio baltymą

atitinkanti juostelė (10 pav. B). Ši priemaiša buvo matoma viso heterodimerų grynininimo proceso metu bei sąveikavo tiek su monokloniniais antikūnais prieš G-CSF, tiek su poliklonineis antikūnais prieš SCF. Gautos išgrynintų baltymų SCF-Lα-GCSF ir GCSF-Lα-SCF molekulinės masės, nustatytos masių spektometrijos metodu, atitinkamai buvo 42370,48 Da ir 42370,70 Da ir gerai atitiko teorines heterodimerų molekulines mases. Tuo tarpu abiejų dimerų chromatografiniai profiliai parodė nedidelį šių galutinių produktų heterogeniškumą. Šalia pagrindinės formos, buvo nustatyta ir didesnio molekulinio dydžio papildoma baltyminė forma, SCF-Lα-GCSF atveju esanti 42983,05 Da, o GCSF-Lα-SCF atveju – 42983,27 Da dydžio. Abiems baltymams, apkaičiuotas molekulinės masės skirtumas tarp pagrindinės ir papildomos smailių leidžia daryti prielaidą, kad pastaroji priemaiša yra heterodimeras su atviru disulfidiniu tilteliu (Taniuchi ir kt., 1977), kuriame laisvi cisteinai yra prijungę dvi redukuotas glutationo molekules. Ši prielaida paaiškintų ir SDS-PAGE geliuose neredukuojančiose sąlygose nustatytų papildomų juostelių kilmę.

SE-HPLC analizės rezultatai parodė, kad abu heterodimerai turi panašias oligomerines būsenas tirpale ir jų molekulinis svoris žymiai skyrėsi nuo teorinės baltymo molekulinio svorio reikšmės. Reikia pastebėti, kad molekulinių svorių neatitikimas, nustatytas gel-filtracijos metu, buvo gaunamas ir tiriant kitus SCF preparatus. SCF monomero atveju, gautos (57 kDa) ir teorinės reikšmių neatitikimas, esant netraliam pH, yra siejamas su baltymo dimerine būsena tirpale bei jo forma, t. y., santykinai dideliu hidrodinaminiu spinduliu (Arakawa ir kt., 1991). Darbo metu, SDS-PAGE geliuose, nustatytos mažesnės heterodimerų molekulinės masės patvirtina, kad SCF-Lα-GCSF ir GCSF-Lα-SCF sudaro nekovalentinius dimerus ar trimerus esant nedenatūruojančioms sąlygoms.

Kaip buvo aptarta literatūros apžvalgoje, N-galinė seka SCF molekulėje yra atsakinga už sąveiką su jo receptoriumi (Langley ir kt., 1994), todėl heterodimerų konstrukcija yra sėkminga tik tada, kai monomerus jungiančioji seka yra tokio ilgio, kuri yra pakankama pašalinant galimus domenų tarpusavio konformacinius trikdžius laisvai monomerų sąveikai su jų receptoriais. Jungiamosios sekos tinkamumas SCF-Lα-GCSF ir GCSF-Lα-SCF buvo įrodytas VVAE ir biologinio aktyvumo *in vitro* tyrimais, atitinkamai analizuojant išgrynintų heterodimerų ir jų receptorių biocheminius ir biologinius aktyvumus.

VVAE metodu gauti rezultatai atskleidė, kad GCSF-Lα-SCF sąveikavo su SCF receptoriumi efektyviau nei SCF-Lα-GCSF baltymas bei abiejų dimerų SCF domenai parodė didesnį aktyvumą nei SCF monomeras (13

lentelė). Remiantis šiais rezultatais, galime padaryti išvadą, kad G-CSF monomero prijungimas nei GCSF-Lα-SCF, nei SCF-Lα-GCSF atveju netrukdė SCF baltymo sąveikai su receptoriumi. N-galinis SCF monomeras SCF-Lα-GCSF baltyme leido C-gale esančiam G-CSF domenui sąveikauti su G-CSF receptoriumi. Vis dėlto, GCSF-Lα-SCF baltymo, C-gale esantis SCF monomeras blokavo N-gale esančio G-CSF domeno jungimąsi su G-CSF receptoriumi (13 lentelė).

Biologinio aktyvumo *in vitro* tyrimuose, abu heterodimeriniai sulieti baltymai stimuliavo M-07e ląstelių proliferaciją. GCSF-Lα-SCF biologinis aktyvumas buvo maždaug 1,4 karto didesnis nei standartinio SCF monomero. Tuo tarpu SCF-Lα-GCSF skatino M-07e ląstelių proliferaciją mažesniu lygiu, t. y., buvo 0,7 karto mažesnis lyginant su SCF. GCSF-Lα-SCF baltyme esantis N-galinis G-CSF monomeras nesumažino SCF domeno sąveikos su SCF receptoriumi. Taigi, sulietame baltyme, Lα jungiančioji seka užtikrina erdvinį atskirų domenų atskyrimą bei netrukdo nepriklausomam jų veikimui. Heterodimeruose mažas G-CSF domeno aktyvumas gali būti susijęs su sterinėmis kliūtimis, kurias sukelia SCF domenų multimerinės formos.

Žmogaus SCF turi mažą biologinį aktyvumą graužikų homopoetinėms ląstelėms (Broudy, 1997), todėl biologinio aktyvumo *in vivo* tyrimams, panaudojant žiurkes, buvo pasirinktas didesnį G-CSF aktyvumą *in vitro* turintis heterodimeras, t. y., išgrynintas SCF-Lα-GCSF. Gauti rezultatai parodė, kad graužikams, praėjus 24 val. po SCF-Lα-GCSF injekcijos, neutrofilų skaičius padidėjo 7 kartus, kai tuo tarpu G-CSF monomero atveju tik 4,4 karto. Pastarojo sulieto baltymo aktyvumas buvo panašus į SCF ir G-CSF monomerų mišinio aktyvumą (neutrofilų skaičius padidėjo 6,3 kartus). Gauti *in vivo* gauti rezultatai tinkamai neatspindėjo SCF-Lα-GCSF baltymo aktyvumo, todėl reikalinga surasti modelines sistemas, gebančias įrodyti heterodimere esančių SCF ir G-CSF molekulių sinergetinį efektą. Vis dėlto, tiek gautas *in vitro*, tiek *in vivo* biologinis aktyvumas, atitinkantis SCF ir G-CSF mišinio aktyvumą, rodo SCF-Lα-GCSF baltymą kaip perspektyvų vaistą-kandidatą.

IŠVADOS

1. Sukurta gryninimo procedūra G-CSF dimerui su alfa spiralę formuojančia jungiamąja seka, lyginant su kitais G-CSF homodimerais, buvo efektyvesnė: gautas didesnio grynumo (>95%) bei išeigos (>14%) dimeras. Be to, GCSF-Lα-GCSF pasižymėjo didesniu biologiniu aktyvumu *in vitro*.
2. GCSF-Lα-GCSF, palyginus su monomeriniu G-CSF, turėjo 7 kartus ilgesnį cirkuliacijos pusamžį kraujyje ir 1,8 kartų didesnį biologinį aktyvumą po 24 val *in vivo*.
3. Sukurtos ir optimizuotos baltymų išskyrimo ir gryninimo schemos buvo tinkamos baltymų gryninimui tiek mažu, tiek dideliu mastu ir leido išgryninti dimerus iki didesnio nei 79% RP-HPLC grynumo, kuris buvo pakankamas tolimesniam jų charakterizavimui.
4. Lα jungiančioji seka užtikrino erdvinį GCSF ir SCF monomerų atskyrimą bei netrukdė nepriklausomam jų veikimui tiek homo-, tiek heterodimeruose.
5. SCF-Lα-GCSF baltymą sudarantys SCF ir G-CSF monomerai sąveikavo su savo receptoriais biologinio aktyvumo *in vitro* tyrimuose bei stimuliavo neutrofilų išsiskyrimą G-CSF biologinio aktyvumo *in vivo* tyrime.
6. GCSF-Lα-GCSF ir SCF-Lα-GCSF gali būti pasirenkami tolimesnėms studijoms kaip potencialūs vaistai-kandidatai.

CURRICULUM VITAE

Name, Surname:	Gitana Mickienė (Žvirblytė)
Date and place of birth:	29th of September, 1986, Pasvalys, Lithuania
Current work place:	UAB Thermo Fisher Scientific Baltics, V. A. Graičiūno g. 8, LT-02241 Vilnius, Lithuania
Contact details:	Phone: +370 648 98070 E-mail: gitana.mickiene@gmail.com

Education:

2012 – 2019	PhD studies in Chemical Engineering, Institute of Biotechnology, Life Sciences Center, Vilnius University
2009 – 2011	Master of Science in Biochemistry, Faculty of Chemistry, Vilnius University
2005 – 2009	Bachelor of Science in Bioengineering, Faculty of Fundamental Sciences, Vilnius Gediminas Technical University

Work experience:

From 2022	Sr. Manufacturing Scientist, UAB Thermo Fisher Scientific Baltics, Vilnius
2011 – 2021	Researcher, UAB Profarma, Vilnius
2013 – 2015	Biological Researcher, Institute of Biotechnology, Vilnius University, Vilnius
2011 – 2012	Bioengineer, Institute of Biotechnology, Vilnius University, Vilnius
2010 – 2011	Laborant, Institute of Biotechnology, Vilnius University, Vilnius

LIST OF PUBLICATIONS

- **Mickiene, G.**, Dalgediene, I., Dapkunas, Z., Zvirblis, G., Pesliakas, H., Kaupinis, A., Valius, M., Mistiniene, E., Pleckaityte, M. (2017) Construction, Purification, and Characterization of a Homodimeric Granulocyte Colony-Stimulating Factor. *Mol Biotechnol* 59: 374-384. doi: 10.1007/s12033-017-0026-7.

  G. Mickiene's contribution. Experimental part: small-scale synthesis of recombinant GCSF-L2, GCSF-L7, GCSF-Lα proteins in *E. coli* cells. Isolation of inclusion bodies. Purification of G-CSF homodimers and analytical characterization: SDS-PAGE, RP-HPLC, western blotting, RP-HPLC, peptiding mapping, fluorescence spectroscopy. Analysis of data and visualization of results. Writing: original draft preparation and article editing at different stages.

- **Mickiene, G.**, Dalgediene, I., Zvirblis, G., Dapkunas, Z., Plikusiene, I., Buzavaite-Verteliene, E., Balevicius, Z., Ruksenaite, A., Pleckaityte, M. (2020) Human granulocyte-colony stimulating factor (G-CSF)/stem cell factor (SCF) fusion proteins: design, characterization and activity. *PeerJ* 8: 1-23. doi: 10.7717/peerj.9788.

  G. Mickiene's contribution. Experimental part: small-scale synthesis of recombinant SCF-Lα-GCSF and GCSF-Lα-SCF proteins in *E. coli* cells. Isolation of inclusion bodies. Purification of heterodimers and analytical characterization: SDS-PAGE, RP-HPLC, western blotting, RP-HPLC, endotoxin quantification. Analysis of data and visualization of results. Writing: original draft preparation and article editing at different stages.

- Balevicius, Z., Talbot, J., Tamosaitis, L., Plikusiene, I., Stirke, A., **Mickiene, G.,** Balevicius, S., Paulauskas, A., Ramanavicius, A. (2019) Modelling of immunosensor response: the evaluation of binding kinetics between an immobilized receptor and structurally-different genetically engineered ligands. *Sensors and Actuators B: Chemical* 297: 1-8. doi:10.1016/j.snb.2019.126770.

  G. Mickiene's contribution. Experimental part: preparation, purification and analytical characterization of recombinant dimers $(GCSF)_2$Lα and SCF-Lα-GCSF. The assistance with methodology.

- Plikusiene, I., Balevicius, Z., Ramanaviciene, A., Talbot, J., **Mickiene, G.**, Balevicius, S., Stirke, A., Tereshchenko, A., Tamosaitis, L., Zvirblis, G., Ramanavicius, A. (2020) Evaluation of affinity sensor response kinetics

towards dimeric ligands linked with spacers of different rigidity: Immobilized recombinant granulocyte colony-stimulating factor based synthetic receptor binding with genetically engineered dimeric analyte derivatives. *Biosens Bioelectron* 156: 1-8. doi: 10.1016/j.bios.2020.112112.

G. Mickiene's contribution. Experimental part: preparation, purification and analytical characterization of recombinant G-CSF homodimers $(GCSF)_2L\alpha$, $(GCSF)_2L2$ and $(GCSF)_2L7$. The assistance with methodology. Writing: contribution in responce to reviewer comments.

PATENT APPLICATION

- Pesliakas, J. H., Pleckaityte, M., Mistiniene, E., **Zvirblyte, G.**, Petreikyte, I., Leiva, A., Stirke, A., Zvirblis, G. Fused proteins of granulocyte colony-stimulating factor with other partners of growth factor, preferably with stem cell factor, and method of preparation thereof. WO2015047062A4. European patent granted 2018-11-07 EP3049433B1.

CONFERENCE PRESENTATIONS

Poster presentations:

- **Zvirblyte, G.**, Pleckaityte, M., Mistiniene, E., Zvirblis, G. Pesliakas, H. ProMer™ technology – extended plasma half life of biopharmaceuticals, „The XIIIth International Conference of Lithuanian Biochemical Society", June 17-20, 2014, Birztonas, Lithuania.

- **Zvirblyte, G.**, Pleckaityte, M., Mistiniene, E., Zvirblis, G. Pesliakas, H. ProMer™ technology – extended plasma half life of biopharmaceuticals, „The second Life Sciences Baltics 2014 forum", September 10-12, 2014, Vilnius, Lithuania.

Oral presentations:

- **Zvirblyte, G.** Citokininių dimerinių baltymų, su prailgintu gyvavimo laiku, gavimo būdai bei charakterizavimas,"BIOATEITIS: gamtos ir gyvybės mokslų perspektyvos, LMA jaunųjų mokslininkų konferencija", December 11, 2013, Vilnius, Lithuania.

- **Zvirblyte, G.** Homo- ir hetero- oligomerinių citokinų gryninimas ir charakterizavimas, „Thermo Fisher Scientific Day of Science“, October 9, 2019, Vilnius, Lithuania.

FINANCIAL SUPPORT

This work was supported by the Lithuanian Science and Studies Foundation (Grant No. N-07006).

ACKNOWLEDGEMENTS

This work would not have been possible without the collaboration and support of many people inside and outside the lab and I am thankful to everybody who contributed to the completion of this thesis.

First, I would like to express my deepest gratitude to my scientific supervisor Dr. Milda Plečkaitytė for her invaluable scientific outstanding guidance, support, and constructive feedback, which greatly helped me to evolve the Ph.D. theses.

I wish also to express my deep gratitude to Dr. Gintautas Žvirblis for his important professional assistance and advice. Thank you for being always approachable and accessible.

I would like to thank Dr. Henrikas Pesliakas who has brought up the idea of fused G-CSF and SCF dimeric constructs for a long time and for his scientific outstanding guidance.

I would like to thank Dr. Edita Mištinienė for the opportunity to perform this work in UAB Profarma and to use the laboratory equipment.

I wish to extend my gratitude to Indrė Dalgėdienė for *in vitro* experiments.

Many thanks to Dr. Ieva Plikusienė, Prof. Zigmas Balevičius, and Dr. Arūnas Stirkė for smooth collaboration and help with TIRE experiments.

I would like to express my appreciation to Dr. Virginija Bukelskienė for her kind assistance with the *in vivo* experiments.

Thanks to all the researchers that I shared with the lab for providing a great work environment. I want to especially thank my colleagues: Žilvinas Dapkūnas and Aurimas Baranauskas – you were the best laboratory neighbors. Thank you for all the laugher and discussions, for invaluable comradeship, amusements, and scientific knowledge sharing.

A special thanks to my great husband Darius for his support, understanding, and belief in me and my decisions. I would like to thank my parents, Lidija and Almundas, and sister Egle. All of you encouraged me to seek more. Thank you for your love and support.

Finally, Gabrielius, my dearest son! This PhD, this one is for you!

REFERENCES

1. Aapro, M. S., Bohlius, J., Cameron, D. A, Dal Lago, L., Donnelly, J. P., Kearney, N., Lyman, G. H. et al. (2011) European Organisation for Research and Treatment of Cancer. 2010 update of EORTC guidelines for the use of granulocyte-colony stimulating factor to reduce the incidence of chemotherapy induced febrile neutropenia in adult patients with lymphoproliferative disorders and solid tumours. *Eur J Cancer* 47: 8-32. doi: 10.1016/j.ejca.2010.10.013.
2. Abdolzade-Bavil, A., Kerczek, A., Cooksey, B. A., Kaufman, T., Philip A Krasney, P. A., Pukac, L., Görlach, M., Lammerich, A., Scheckermann, C., Allgaier, H., Shen, W. D., Liu, P. M. (2016) Differential sensitivity of lipegfilgrastim and pegfilgrastim to neutrophil elastase correlates with differences in clinical pharmacokinetic profile. *J Clin Pharmacol* 56: 186-194. doi: 10.1002/jcph.578.
3. Alarcon, L. H., Fink, M. P. (2008) Mediators of the Inflammatory Response. In: Townsend, C. M., Beauchamp, R. D., Evers, B. M. (ed.), Sabiston Textbook of Surgery. The Biological Basis of Modern Surgical Practice, vol. 18. Saunders Elsevier, Philadelphia.
4. Ali S, Ali S. (2007) Role of c-kit/SCF in cause and treatment of gastrointestinal stromal tumors (GIST). *Gene* 401: 38-45. doi: 10.1016/j.gene.2007.06.017.
5. Amgen Inc. (2003) Stemgen (ancestim) Product Information.
6. Anderlini, P., Przepiorka, D., Champlin, R., Körbling, M. (1996) Biologic and clinical effects of granulocyte colony-stimulating factor in normal individuals. *Blood* 88: 2819-2825.
7. Anderson, C. L., Chaudhury, C., Kim, J., Bronson, C. L., Wani, M. A., Mohanty, S. (2006) Perspective - - FcRn transports albumin: relevance to immunology and medicine. *Trends Immunol* 27: 343-348. doi: 10.1016/j.it.2006.05.004.
8. Anderson, D. M., Williams, D. E., Tushinski, R., Gimpel, S., Eisenman, J., Cannizzaro, L. A., Aronson, M. et al. (1991) Alternate splicing of mRNA encoding human mast cell growth factor and localization of the gene to chromosome 12q22-q24. *Cell Growth Differ* 2: 373-378.
9. Andreakos, E. T. H., Foxwell, B. M. J., Brennan, F. M., Feldman, M. (2004) Role of Cytokines, p. 134-149. In: William St. Clair, E., Pisetsky, D. S., Haynes, B. F. (ed.), Rheumatoid Arthritis, Lippincott Williams & Wilkins, Walnut Street, Philadelphia, USA.

10. Arai, R., Ueda, H., Kitayama, A., Kamiya, N., Nagamune, T (2001) Design of the linkers which effectively separate domains of a bifunctional fusion protein. *Protein Eng* 14: 529-532. doi: 10.1093/protein/14.8.529.
11. Arakawa, T., Yphantis, D. A., Lary, J. W., Narhi, L. O., Lu, H. S., Prestrelski, S. J., Clogston, C. L. et al. (1991) Glycosylated and unglycosylated recombinant-derived human stem cell factors are dimeric and have extensive regular secondary structure. *J Biol Chem* 266: 18942-18948.
12. Arakawa, T., Horan, T. P., Leong, K., Prestrelski, S. J., Narhi, L. O., Hu, S. (1995) Structure and activity of granulocyte colony-stimulating factor derived from CHO cells containing cDNA coding for alternatively spliced sequences. *Arch Biochem Biophys* 316: 285-289. doi: 10.1006/abbi.1995.1039.
13. Avalos, B. R. (1996) Molecular analysis of the granulocyte colony-stimulating factor receptor. *Blood* 88: 761-777. doi: 10.1182/blood.V88.3.761.761.
14. Aye, M. T., Hashemi, S., Leclair B., Zeibdawi, A., Trudel, E., Halpenny, M.,Fuller, V., Cheng, G. (1992) Expression of stem cellfactor and c-kit mRNA in cultured endothelial cells, monocytes and cloned human bone marrow stromal cells (CFU-RF). *Exp Hematol* 20: 523-527.
15. Azari, P. R., Feeney, R. E. (1958) Resistance of metalcomplexes of conalbumin and transferring to proteolysis and to thermal denaturation. *J Biol Chem* 232: 293-302.
16. Baldo, B. A. (2014) Side Effects of Cytokines Approved for Therapy. *Drug Saf* 37: 921-943. doi: 10.1007/s40264-014-0226-z.
17. Baldo, B. A. (2016) Cytokines, p. 217-261. In: Baldo, B. A., Safety of Biologics. Monoclonal Antibodies, Cytokines, Fusion Proteins, Hormones, Enzymes, Coagulation Proteins, Vaccines, Botulinum Toxins. Springer International Publishing, Switzerland.
18. Balevicius, Z., Baleviciute, I., Tumenas, S., Tamosaitis, L., Stirke, A., Makaraviciute, A., Ramanaviciene, A., Ramanavicius, A. (2014) In situ study of ligand-receptor interaction by total internal reflection ellipsometry. *Thin solid Films* 571: 744-748. doi: 10.1016/j.tsf.2013.10.090.
19. Balevicius, Z., Talbot, J., Tamosaitis, L., Plikusiene, I., Stirke, A., Mickiene, G., Balevicius, S., Paulauskas, A., Ramanavicius, A. (2019) Modelling of immunosensor response: the evaluation of binding kinetics between an immobilized receptor and structurally-different

genetically engineered ligands. *Sensors and Actuators B: Chemical* 297 :1-8. doi: 10.1016/j.snb.2019.126770.

20. Banerjee, D., Flanagan, P. R., Cluett, J., Valberg, L.S. (1986) Transferrin receptors in the human gastrointestinal tract. Relationship to body iron stores. *Gastroenterology* 91: 861-869. doi: 10.1016/0016-5085(86)90687-6.
21. Bartucci, M., Dattilo, R., Martinetti, D., Todaro, M., Zapparelli, G., Virgilio, A. Di., Biffoni, M. (2011) Prevention of Chemotherapy-Induced Anemia and Thrombocytopenia by Constant Administration of Stem Cell Factor. *Clin Cancer Res* 17: 6185-6191. doi: 10.1158/1078-0432.CCR-11-1232.
22. Basu, S., Dunn, A., Ward, A. (2002) G-CSF: function and modes of action (review) *Int J Mol Med* 10: 3-10.
23. Baumann, A., Tuerck, D., Prabhu, S., Dickmann, L., Sims, J. (2014) Pharmacokinetics, metabolism and distribution of PEGs and PEGylated proteins: quo vadis? *Drug Discov Today* 19: 1623-1631. doi: 10.1016/j.drudis.2014.06.002.
24. Bazan, J. F. (1991) Genetic and structural homology of stem cell factor and macrophage colony-stimulating factor. *Cell* 65: 9-10. doi: 10.1016/0092-8674(91)90401-j.
25. Berry, M. A., Hargadon, B., Shelley, M., Parker, D., Shaw, D. E., Green, R. H., Bradding, P. et. al. (2006) Evidence of a role of tumor necrosis factor alpha in refractory asthma. *N Engl J Med* 354: 697-708. doi: 10.1056/NEJMoa050580.
26. Beschin, A., Bilej, M., Magez, S., Lucas, R., De Baetselier, P. (2004) Functional convergence of invertebrate and vertebrate cytokine-like molecules based on a similar lectin-like activity. *Prog Mol Subcell Biol* 34: 145-163. doi: 10.1007/978-3-642-18670-7_6.
27. Beschin, A., Bilej, M., Torreele, E., De Baetselier, P. (2001) On the existence of cytokines in invertebrates. *Cell Mol Life Sc*i 58: 801-814. doi: 10.1007/pl00000901.
28. Bienvenu, J., Monneret, G., Fabien, N., Revillard, J. P. (2000) The clinical usefulness of the measurement of cytokines. *Clin Chem and Lab Med* 38: 267-285. doi: 10.1515/CCLM.2000.040.
29. Bodine, D. M., Seidel, N. E., Zsebo, K. M., Orlic, D. (1993) *In vivo* administration of stem cell factor to mice increases the absolute number of pluripotent hematopoietic stem cells. *Blood* 82: 445-455.
30. Bolis, S., Cocorocchio, E., Corti, C., Ferreri, A. J. M., Frungillo, N., Grillo, G., Omodeo, E. et al. (2013) Clinical implications, safety, efficacy of recombinant human Granulocyte Colony-Stimulating

Factors and pegylated equivalent. *Epidemiology Biostatistics and Publich Health* 10: e8845-1-16. doi:10.2427/8845.

31. Bosbach, B., Deshpande, S., Rossi, F., Shieh, J. H., Sommer, G., de Stanchina, E., Veach, D. R. (2012) Imatinib resistance and microcytic erythrocytosis in a KitV558Delta;T669I/+ gatekeeper-mutant mouse model of gastrointestinal stromal tumor. *Proc Natl Acad Sci U S A* 109: E2276-E2283. doi: 10.1073/pnas.1115240109.
32. Bozza F. A., Salluh, J. I., Japiassu, A. M., Soares, M., Assis, E. F., Gomes, R. N., Bozza, M. T. et al. (2007) Cytokine profiles as markers of disease severity in sepsis: a multiplex analysis. *Crit Care* 11: 1-8. doi: 10.1186/cc5783.
33. Bradford, M. M. (1976) A rapid and sensitive method for the quantitation of microgram quantities of protein utilizing the principle of protein-dye binding. *Anal Biochem* 72: 248-254. doi: 10.1006/abio.1976.9999.
34. Brambilla, F., Bellodi, L., Perna, G., Bertani, A., Panerai, A., Sacerdote, P. (1994) Plasma interleukin-1 beta concentrations in panic disorder. *Psychiatry Res* 54: 135-142. doi: 10.1016/0165-1781(94)90002-7.
35. Brambilla, F., Perna, G., Bellodi, L., Arancio, C., Bertani, A., Perini, G., Carraro, C., Gava, F. (1997) Plasma interleukin-1 beta and tumor necrosis factor concentrations in obsessive-compulsive disorders. *Biol Psychiatry* 42: 976-981. doi: 10.1016/s0006-3223(96)00495-7.
36. Brandt, J., Briddell, R. A., Srour, E. F., Leemhuis, T. B., Hoffman, R. (1992) Role of c-kit ligand in the expansion of human hematopoietic progenitor cells. *Blood* 79: 634-641.
37. Brockman, M. A., Kwon, D. S., Tighe, D. P., Pavlik, D. F., Rosato, P. C., Sela, J., Porichis, F. et al. (2009) IL-10 is up-regulated in multiple cell types during viremic HIV infection and reversibly inhibits virus-specific T cells. *Blood* 114: 346-356. doi: 10.1182/blood-2008-12-191296.
38. Broudy, V. C. (1997) Stem cell factor and hematopoiesis. *Blood* 90: 1345-1364.
39. Brouwers, R., Vass, H., Dawson, A., Squires, T., Tavaddod, S., Allen, R. J. (2020) Stability of β-lactam antibiotics in bacterial growth media. *PLoS One* 15: 1-17. doi: 10.1371/journal.pone.0236198.
40. Bussolino, F., Wang, J. M., Defilippi, P., Turrini, F., Sanavio, F., Edgell, Aglietta, M. (1989) Granulocyte- and granulocyte-macrophage-colony stimulating factors induce human endothelial cells to migrate and proliferate. *Nature* 337: 471-473. doi: 10.1038/337471a0.

41. Cardoso, H. J., Figueira, M. I., Socorro, S. (2017) The stem cell factor (SCF)/c-KIT signalling in testis and prostate cancer. *J Cell Commun Signal* 11: 297-307. doi: 10.1007/s12079-017-0399-1.
42. Caselli, D., Cesaro, S., Aricò, M. (2016) Biosimilars in the management of neutropenia: focus on filgrastim. *Biologics* 10: 17-22. doi: 10.2147/BTT.S73580.
43. Chabot, B., Stephenson, D. A., Chapman, V. M., Besmer, P., Bernstein, A. (1988) The proto-oncogene c-kit encoding a transmembrane tyrosine kinase receptor maps to the mouse W locus. *Nature* 335: 88-89. doi: 10.1038/335088a0.
44. Chakraborty, A., White, S. M., Schaefer, T. S., Ball, E. D., Dyer, K. F., Tweardy, D. J. (1996) Granulocyte colony stimulating factor activation of Stat3 alpha and Stat3 beta in immature normal and leukemic human myeloid cells. *Blood* 88: 2442-2449.
45. Chang, C. H., Gupta, P., Goldenberg, D. M. (2009) Advances and challenges indeveloping cytokine fusion proteinsas improved therapeutics. *Expert Opin Drug Discov* 4: 181-194. doi: 10.1517/17460440802702023.
46. Cheers, C., Haigh, A. M., Kelso, A., Metcalf, D., Stanley, E. R., Young, A. M. (1988) Production of colony-stimulating factors (CSFs) during infection: separate determinations of macrophage-, granulocyte-, granulocyte-macrophage-, and multi-CSFs. *Infect Immun* 56: 247-251. doi: 10.1128/IAI.56.1.247-251.1988.
47. Chen, X., Zaro, J. L., Shen, W. C. (2013) Fusion protein linkers: property, design and functionality. *Adv Drug Deliv Rev* 65: 1357-1369. doi: 10.1016/j.addr.2012.09.039.
48. Cheung, L. S., Fu, J., Kumar, P., Kumar, A., Urbanowski, M. E., Elizabeth A. Ihms, E. A. et al. (2019) Second-generation IL-2 receptor-targeted diphtheria fusion toxin exhibits antitumor activity and synergy with anti–PD-1 in melanoma. *Proc Natl Acad Sci U S A* 116: 3100-3105. doi: 10.1073/pnas.1815087116.
49. Chichili, V. P. R., Kumar, V., Sivaraman, J. (2013) Linkers in the structural biology of protein-protein interactions. *Protein Sci* 22: 153-167. doi: 10.1002/pro.2206.
50. Columbo, M., Horowitz, E. M., Botana, L. M., MacGlashan, D. W., Jr., Bochner, B. S., Gillis, S., Zsebo, K. M. et al. (1992) The human recombinant c-kit receptor ligand, rhSCF, induces mediator release from human cutaneous mast cells and enhances IgE-dependent mediator release from both skin mast cells and peripheral blood basophils. *J Immunol* 149: 599-608.

51. Corey, S. J., Burkhardt, A. L., Bolen, J. B., Geahlen, R. L.,Tkatch, L. S., Tweardy, D. J. (1994) Granulocyte colony-stimulating factor receptor signaling involves the formation of a three-component complex with Lyn and Syk protein-tyrosine kinases. *Proc Natl Acad Sci U S A* 91: 4683-4687. doi: 10.1073/pnas.91.11.4683.
52. Council of Europe (2009) Supplement 6.3. Filgrastim concentrated solution, p. 4142-4144. In: European pharmacopoeia. Strasbourg.
53. Croxford, J. L., Triantaphyllopoulos, K., Podhajcer, O. L., Feldmann, M., Baker, D., Chernajovsky Y. (1998) Cytokine gene therapy in experimental allergic encephalomyelitis by injection of plasmid DNA-cationic liposome complex into the central nervous system. *J Immunol* 160: 5181-5187.
54. Cuenca, J. S., Martín, J. C., Pellicer, A., Simón, C. (1999) Cytokine pleiotropy and redundancy – gp130 cytokines in human implantation. *Immunol Today* 20: 57-59. doi: 10.1016/s0167-5699(98)01374-7.
55. Cusabio, What Cells Release Cytokines? https://www.cusabio.com/cytokines/What-Cells-Release-Cytokines.html.
56. Czajkowsky, D. M., Hu, J., Shao, Z., Pleass, R. J. (2012) Fc fusion proteins: New developments and future perspectives. *EMBO Mol Med* 4: 1015-1028. doi: 10.1002/emmm.201201379.
57. Daniels, T. R., Delgado, T., Helguera, G., Penichet, M. L. (2006) The transferrin receptor part II: targeted delivery of therapeutic agents into cancer cells. *Clin Immunol* 121: 159-176. doi: 10.1016/j.clim.2006.06.006.
58. Dastych, J., Metcalfe, D. D. (1994) Stem cell factor induces mast cell adhesion to fibronectin. *J Immunol* 152: 213-219.
59. Dehbashi, M., Kamali, E., Vallian, S. (2017) Comparative genomics of human stem cell factor (SCF). *Mol Biol Res Commun* 6 :1-11.
60. Derbyshire M. (2019) Patent expiry dates for biologicals: 2018 update. *GaBI Journal* 8: 24-31. doi:10.5639/gabij.2019.0801.003.
61. Dhama, K., Chakraborty, S., Wani, M. Y., Tiwari, R., Barathidasan, R. (2013) Cytokine therapy for combating animal and human diseases – A review. *Res Opin Anim Ve*t *Sci* 3: 195-208.
62. Diederich, K., Sevimli, S., Dörr, H., Kösters, E., Hoppen, M., Lewejohann, L., Klocke, R. et al. (2009) The role of granulocyte-colony stimulating factor (G-CSF) in the healthy brain: a characterization of G-CSF-deficient mice. *J Neurosci* 29: 11572-11581. doi: 10.1523/JNEUROSCI.0453-09.2009.

63. Dinarello, C. A. (2000) Proinflammatory cytokines. *Chest* 118: 503-508.doi: 10.1378/chest.118.2.503.
64. Dinarello, C. A. (2011) Historical review of cytokines. *Eur J Immunol* 37: S34-45. doi: 10.1002/eji.200737772.
65. Dong, F., Gutkind, J. S., Larner, A. C. (2001) Granulocyte colony-stimulating factor induces ERK5 activation, which is differentially regulated by protein-tyrosine kinases and protein kinase C. Regulation of cell proliferation and survival. *J Biol Chem* 276: 10811-10816. doi: 10.1074/jbc.M008748200.
66. Dong, F., Larner, A. C. (2000) Activation of Akt kinase by granulocyte colony-stimulating factor (G-CSF): evidence for the role of a tyrosine kinase activity distinct from the Janus kinases. *Blood* 95: 1656-1662.
67. Donnelly, R. P., Young, H. A., Rosenberg, A. S. (2009) An overview of cytokines and cytokine antagonists as therapeutic agents. *Ann N Y Acad Sci* 1182 :1-13. doi: 10.1111/j.1749-6632.2009.05382.x.
68. Dowlati, Y., Herrmann, N., Swardfager, W., Liu, H., Sham, L., Reim, E. K., Lanctôt, K. L. (2010) A meta-analysis of cytokines in major depression. *Biol Psychiatry* 67: 446-457. doi: 10.1016/j.biopsych.2009.09.033.
69. Drapeau, G. R. (1976) Protease from Staphylococcus aureus. *Methods Enzymol* 45: 469-475. doi: 10.1016/s0076-6879(76)45041-3.
70. Drexler, H. G., Zaborski, M., Quentmeier, H. (1997) Cytokine response profiles of human myeloid factor-dependent leukemia cell lines. *Leukemia* 11: 701-708. doi: 10.1038/sj.leu.2400633.
71. Duijkers, I. J., Klipping, C., Boerrigter, P. J., Machielsen, C. S. M., De Bie, J. J., Voortman, G. (2002) Single dose pharmacokinetics and effects on follicular growth and serum hormones of a long acting recombinant FSH preparation (FSH-CTP) in healthy pituitary-suppressed females. *Hum Reprod* 17: 1987-1993. doi: 10.1093/humrep/17.8.1987.
72. Dwivedi, P., Greis, K. D. (2017) Granulocyte colony-stimulating factor receptor signaling in severe congenital neutropenia, chronic neutrophilic leukemia, and related malignancies. *Exp Hematol* 46: 9-20. doi: 10.1016/j.exphem.2016.10.008.
73. Endo, T., Odb, A., Satoh, I., Haseyama, Y., Nishio, M., Koizumi, K., Takashima, H. et al. (2001) Stem cell factor protects c-kitþ human primary erythroid cells from apoptosis. *Exp Hematol* 29: 833-841. 10.1016/s0301-472x(01)00660-9.
74. Facon, T., Harousseau, J. L., Maloisel, F., Attal, M., Odriozola, J., Alegre, A, Schroyens,W. et al. (1999) Stem cell factor in combination

with filgrastim after chemotherapy improves peripheral blood progenitor cell yield and reduces apheresis requirements in multiple myeloma patients: a randomized, controlled trial. *Blood* 94: 1218-1225.
75. Fares, F., Ganem, S., Hajouj, T., Agai, E. (2007) Development of a long-acting erythropoietin by fusing the carboxyl-terminal peptide of human chorionic gonadotropin beta-subunit to the coding sequence of human erythropoietin. *Endocrinology* 148: 5081-5087. doi: 10.1210/en.2007-0026 .
76. Feldmann, M. (2008) Many cytokines are very useful therapeutic targets in disease. *J Clin Invest* 118: 3533-3536. doi: 10.1172/JCI37346.
77. Fibbe, W. E., van Damme, J., Billiau, A., Duinkerken, N., Lurvink, E., Ralph, P., Altrock, B. W. et al. (1988) Human fibroblasts produce granulocyte-CSF, macrophage-CSF, and granulocyte-macrophage-CSF following stimulation by interleukin-1 and poly (rI). poly (rC). *Blood* 72: 860-866.
78. Fidler, K., Jevsevar, S., Milunovic, T., Skrajnar, S., Premzl, A., Kunstelj, M., Zore, I., Podobnik, B., Kusterle, M. et al. (2011) The characterization and potential use of G-CSF dimers and their pegylated conjugates. *Acta Chim Slov* 58: 1-8.
79. Flanagan, J. G., Chan, D. C., Leder, P. (1991) Transmembrane form of the kit ligandgrowth factor is determined by alternative splicing and is missing in the Sld mutant. *Cell* 64: 1025-1035. doi: 10.1016/0092-8674(91)90326-t.
80. Floss, D. M., Scheller, J. (2019) Naturally occurring and synthetic constitutive-active cytokine receptors in disease and therapy. *Cytokine Growth Factor Rev* 47: 1-20. doi: 10.1016/j.cytogfr.2019.05.007.
81. Frampton, J. E., Lee, C. R., Faulds, D. (1994) Filgrastim. A review of its pharmacological properties and therapeutic efficacy in neutropenia. *Drugs* 48: 731-760. doi: 10.2165/00003495-199448050-00007.
82. Franzke, A., Piao, W., Lauber, J., Gatzlaff, P., Könecke, C., Hansen, W.,Schmitt-Thomsen, A. et al. (2003) G-CSF asimmune regulator in T cells expressing the G-CSF receptor: implications for transplantation and autoimmune diseases. *Blood* 102: 734-739. doi: 10.1182/blood-2002-04-1200.
83. Fukunaga, R., Ishizaka-Ikeda, E., Pan, C. X., Seto, Y., Nagata, S. (1991) Functional domains of the granulocyte colony stimulating factor receptor. *EMBO J* 10: 2855-2865.
84. Furst, D. E., Wallis, R., Broder, M., Beenhouwer, D. O. (2006) Tumor necrosis factor antagonists: different kinetics and/or mechanisms of

action may explain differences in the risk for developing granulomatous infection. *Semin Arthritis Rheum* 36: 159-167. doi: 10.1016/j.semarthrit.2006.02.001.

85. Galli, S. J., Zsebo, K. M., Geissler, E. N. (1994) The kit ligand, stem cell factor. *Adv Immunol* 55: 1-96. doi: 10.1016/s0065-2776(08)60508-8.
86. Ganguli, R., Yang, Z., Shurin, G., Chengappa, K. N. R., Brar, J. S., Gubbi, A. V., Bruce S., Rabin, B. S. (1994) Serum interleukin-6 concentration in schizophrenia: Elevation associated with duration of illness. *Psychiatry Research* 51: 1-10. doi: 10.1016/0165-1781(94)90042-6.
87. Geissler, E. N., Ryan, M. A., Housman, D. E. (1988) The dominant-white spotting (W) locus of the mouse encodes the c-kit protooncogene. *Cell* 55: 185-192. doi: 10.1016/0092-8674(88)90020-7.
88. Gerber, A., Struy, H., Weiss, G., Lippert, H., Ansorge, S., Schulz, H. U. (2000) Effect of Granulocyte Colony-Stimulating Factor Treatment on Ex Vivo Neutrophil Functions in Nonneutropenic Surgical Intensive Care Patients. *J Interferon Cytokine Res* 20: 1083-1090. doi: 10.1089/107999000750053753.
89. Gervais, V., Zerial, A., Oschkinat, H. (1997) NMR investigations of the role of the sugar moiety in glycosylated recombinant human granulocyte-colony-stimulating factor. *Eur J Biochem* 247: 386-395. doi: 10.1111/j.1432-1033.1997.00386.x.
90. Gillies, S. D., Lan, Y., Wesolowski, J. S., Qian, X., Reisfeld, R. A., Holden, S., Super, M., Lo, K. M. (1998) Antibody-IL-12 fusion proteins areeffective in SCID mouse models of prostate and colon carcinoma metastases. *J Immunol* 160: 6195-6203.
91. Glaspy, J., Davis, M. W., Parker, W. R., Foote, M., McNiece, I. (1996) Biology and clinical potential of stem-cell factor. *Cancer Chemother Pharmacol* 38: S53-S57. doi: 10.1007/s002800051039.
92. Glaspy, J. A., Shpall, E. J., LeMaistre, C. F., Briddell, R. A., Menchaca, D. M., Turner, S. A., Lill, M. et al. (1997) Peripheral blood progenitor cell mobilization using stem cell factor in combination with filgrastim in breast cancer patients. *Blood* 90: 2939-2951.
93. Godfrey, D. I., Zlotnik, A., Suda, T. (1992) Phenotypic and functional characterization of c-kit expression during intrathymic T cell development. *J Immunol* 149: 2281-2285.
94. Green, M. D., Koebl, H., Baselga, J. Galid, A., Guillem,V., Gascon, P., Siena, S. et al. (2003) A randomized double-blind, multicenter, phase 3 study of fixed-dose single-administration pegfilgrastim versus daily

filgrastim in Patients receiving myelosuppressive chemotherapy. *Ann Oncol* 14: 29-35. doi: 10.1093/annonc/mdg019.

95. Greenbaum, A. M., Link, D. C. (2011) Mechanisms of G-CSF-mediated hematopoietic stem and progenitor mobilization. *Leukemia* 25: 211-217. doi: 10.1038/leu.2010.248.
96. Guilherme L., Cury, P., Demarchi, L. M. F., Coelho, V., Abel, L., Lopez, A. P., Oshiro, S. E. et al. (2004) Rheumatic heart disease: proinflammatory cytokines play a role in the progression and maintenance of valvular lesions. *Am J Pathol* 165: 1583-1591. doi: 10.1016/S0002-9440(10)63415-3.
97. Gulati, K., Guhathakurta, S., Joshi, J., Rai, N., Ray, A. (2016) Cytokines and their Role in Health and Disease: A Brief Overview. *MOJ Immunol* 4: 1-9. doi: 10.15406/moji.2016.04.00121.
98. Gupta, V., Bhavanasi, S., Quadir, M., Singh, K., Ghosh, G., Vasamreddy, K., Ghosh, A. et al. (2019) Protein PEGylation for cancer therapy: bench to bedside. *J Cell Commun Signal* 13: 319-330. doi: 10.1007/s12079-018-0492-0.
99. Hagel, L. (2001) Gel-filtration chromatography. *Curr Protocol Protein Sci* 8: 8.3.1. doi: 10.1002/0471140864.ps0803s14.
100. Hara M., Yuasa S., Shimoji K., Onizuka, T., Hayashiji, N., Ohno, Y., Arai, T. et al. (2011) G-CSF influences mouse skeletal muscle development and regeneration by stimulating myoblast proliferation. *J Exp Med* 208: 715-727. doi: 10.1084/jem.20101059.
101. Heinrich, M. C., Dooley, D. C., Freed, A. C., Band, L., Hoatlin, M. E., Keeble, W. W., Peters, S. T. et al. (1993) Constitutive expression of steel factor gene by human stromal cells. *Blood* 82: 771-783.
102. Hestdal, K., Welte, K., Lie, S. O., Keller, J. R., Ruscetti, F. W., Abrahamsen, T. G. (1993) Severe congenital neutropenia: abnormal growth and differentiation of myeloid progenitors to granulocyte colony-stimulating factor (G-CSF) but normal response to G-CSF plus stem cell factor. *Blood* 82: 2991-2997.
103. Hill, C. P., Osslund, T. D., Eisenberg, D. (1993) The structure of granulocyte-colony- stimulating factor and its relationship to other growth factors. *Proc Natl Acad Sci USA* 90: 5167-5171. doi: 10.1073/pnas.90.11.5167.
104. Hirasawa, K., Kitamura, T., Oka, T., Matsushita, H. (2002) Bladder tumor producing granulocyte colony-stimulating factor and parathyroid hormone related protein. *J Urol* 167: 2130. doi: 10.1016/S0022-5347(05)65104-X.

105. Hoge, E. A., Brandstetter, K., Moshier, S., Pollack, M., H., Wong, K. K., Simon, N. M. (2009) Broad spectrum of cytokine abnormalities in panic disorder and posttraumatic stress disorder. *Depress Anxiety* 26: 447-455. doi: 10.1002/da.20564.
106. Hoggatt, J., Tate, T. A., Pelus, L. M. (2015) Role of lipegfilgrastim in the management of chemotherapy-induced neutropenia. *Int J Nanomedicine* 10: 2647-2652. doi:10.2147/IJN.S55796.
107. Holmes, F. A., Jones, S. E., O'Shaughnessy, J., Vukelja, S., George, T., Savin, M., Richards, D., et al. (2002) Comparable efficacy and safety profiles of once-per-cycle pegfilgrastim and daily injection filgrastim in chemotherapy-induced neutropenia: a multicenter dose-finding study in women with breast cancer. *Ann Oncol* 13: 903-909. doi: 10.1093/annonc/mdf130.
108. Horan, T. P., Martin, F., Simonet, L., Arakawa, T., Philo, J. S. (1996) Dimerization of Granulocyte-Colony Stimulating Factor Receptor: The Ig Plus CRH Construct of Granulocyte-Colony Stimulating Factor Receptor Forms a 2:2 Complex with a Ligand. *J Biochem* 121: 370-375. doi: 10.1093/oxfordjournals.jbchem.a021597.
109. Hsu, Y. R., Wu, G. M., Mendiaz, E. A., Syed, R., Wypych, J., Toso, R., Mann, M. B. et al. (1997) The majority of stem cell factor exists as a monomer under physiological conditions: implications for dimerization mediating biological activity. *J Biol Chem* 272: 6406-6415. doi: 10.1074/jbc.272.10.6406.
110. Hu, Z. T., Huang, Z. H., Cen, X. B., Wang, T., Zhuangm K., Yang, Z., Zhang, D. P. et al. (2010) F-627, a G-CSF Dimer, Stimulated a More Rapid Neutrophil Recovery In Cyclophosphamide-Treated Monkeys Compared to Monomer Rhg-CSFs. *Granulocytes, Monocytes and Macrophages* 116: 1485. doi: 10.1182/blood.V116.21.1485.1485.
111. Huang, E. J., Nocka, K. H., Buck, J., Besmer, P. (1992) Differential expression and processing of two cell associated forms of the kit-ligand: KL-1 and KL-2. *Mol Biol Cell* 3: 349-362. doi:10.1091/mbc.3.3.349.
112. Huang, E., Nocka, K., Beier, D. R., Chu, T. Y., Buck, J., Lahm, H. W., Wellner, D. et al. (1990) The hematopoietic growth factor KL is encoded by the Sl locus and is the ligand of the c-kit receptor, the gene product of the W locus. *Cell* 63: 225-233. doi: 10.1016/0092-8674(90)90303-v.
113. Humpel, C., Hochstrasser, T. (2011) Cerebrospinal fluid and blood biomarkers in Alzheimer's disease *World J Psychiatry* 1: 8-18. doi: 10.5498/wjp.v1.i1.8.

114. Iemura, A., Tsai, M., Ando, A., Wershil, B. K., Galli, S. J. (1994) The c-kit ligand, stem cell factor, promotes mast cell survival by suppressing apoptosis. *Am J Pathol* 144: 321-328.
115. Jason, J., Archibald, L. K., Nwanyanwu, O. C., Byrd, M. G., Kazembe, P. N., Dobbie, H., Jarvis, W. R. (2001) Comparison of serum and cell-specific cytokines in humans. *Clin Diagn Lab Immunol* 8: 1097-1103. doi: 10.1128/CDLI.8.6.1097-1103.2001.
116. Jazayeri, J. A., Carroll, G. J. (2008) Fc-based cytokines: prospects for engineering superior therapeutics. *BioDrugs* 22: 11-26. doi: 10.2165/00063030-200822010-00002.
117. Jiang, X., Gurel, O., Mendiaz, E. A., Stearns, G. W., Clogston, C. L., Lu, H. S., Osslund,T. D. et al. (2000) Structure of the active core of human stem cell factor and analysis of binding to its receptor kit. *EMBO J* 19: 3192-3203. doi: 10.1093/emboj/19.13.3192.
118. Jones, S. A., Rose-John, S. (2002) The role of soluble receptors in cytokine biology: The agonistic properties of the sIL-6R/IL-6 complex. *Biochim Biophys Acta* 1592: 251-263. doi: 10.1016/s0167-4889(02)00319-1.
119. Kanda, N., Fukushige, S., Murotsu, T., Yoshida, M. C., Tsuchiya, M., Asano, S., Kaziro, Y., Nagata, S. (1987) Human gene coding for granulocyte-colony stimulating factor is assigned to the q21-q22 region of chromosome 17. *Somat Cell Mol Genet* 13: 679-684. doi: 10.1007/BF01534488.
120. Kapur, R., Chandra, S., Cooper, R., Mccarthy, J., Williams, D. A. (2002) Role of p38 and ERK MAP kinase in proliferation of erythroid progenitors in response to stimulation by soluble and membrane isoforms of stem cell factor. *Blood* 100: 1287-293.
121. Kawada, H., Takizawa, S., Takanashi, T., Morita, Y., Fujita, J., Fukuda, K., Takagi, S. et al. (2006) Administration of hematopoietic cytokines in the subacute phase after cerebral infarction is effective for functional recovery facilitating proliferation of intrinsic neural stem/progenitor cells and transition of bone marrow-derived neuronal cells. *Circulation* 113: 701-710. doi: 10.1161/CIRCULATIONAHA.105.563668.
122. Khodadi, E., Shahrabi, S., Shahjahani, M., Azandeh, S., Saki, N. (2016) Role of stem cell factor in the placental niche. *Cell Tissue Res* 366: 523-531. doi:10.1007/s00441-016-2429-3.
123. Kim, B. J., Zhou, J., Martin, B., Carlson, O. D., Maudsley, S., Greig, N. H., Mattson, M. P. et al. (2010) Transferrin fusion technology: a novel approach to prolonging biological half-life of insulinotropic

peptides. *J Pharmacol Exp Ther* 334: 682-692. doi: 10.1124/jpet.110.166470.

124. Kim, S. O., Sheikh, H. I., Ha, S. D., Martins, A., Reid, G. (2006) G-CSF-mediated inhibition of JNK is a key mechanism for Lactobacillus rhamnosus-induced suppression of TNF production in macrophages. *Cell Microbiol* 8: 1958-1971. doi: 10.1111/j.1462-5822.2006.00763.x.
125. Kishita, M., Motojima, M., Oh-eda, M. (1992) Stability of granulocyte-colony stimulating factor (rHuG-CSF) in serum *Clin Rep* 26: 221.
126. Kitade, H., Yanagida, H., Yamada, M., Satoi, S., Yoshioka, K., Shikata, N., Kon, M. (2015) Granulocyte-colony stimulating factor producing anaplastic carcinoma of the pancreas treated by distal pancreatectomy and chemotherapy: report of a case. *Surg Case Rep* 1: 46. doi: 10.1186/s40792-015-0048-y.
127. Koeffler, H. P, Gasson, J., Ranyard, J., Souza, L., Shepard, M., Munker, R. (1987) Recombinant human TNF alpha stimulates production of granulocyte colony-stimulating factor. *Blood* 70: 55-59.
128. Konstantinidou, S., Papaspiliou, A., Kokkotou, E. (2019) Current and future roles of biosimilars in oncology practice. *Oncol Lett* 19: 45-51. doi: 10.3892/ol.2019.11105.
129. Kontermann, R. E. (2009) Strategies to extend plasma half-lives of recombinant antibodies. *BioDrugs* 23: 93-109. doi: 10.2165/00063030-200923020-00003.
130. Kontermann, R. E. (2011) Strategies for extended serum half-life of protein therapeutics. *Curr Opin Biotechnol* 22: 868-876. doi: 10.1016/j.copbio.2011.06.012.
131. Korpimäki, T., Kurittu, J., Karp, M. (2003) Surprisingly fast disappearance of beta-lactam selection pressure in cultivation as detected with novel biosensing approaches. *J Microbiol Methods* 53: 37-42. doi: 10.1016/s0167-7012(02)00213-0.
132. Kowanetz, M., Wu, X, Lee, J., Tan, M., Hagenbeek, T., Qu, X., Yu, L. et al. (2010) Granulocyte-colony stimulating factor promotes lung metastasis through mobilization of Ly6G+Ly6C+ granulocytes. *Proc Natl Acad Sci U S A* 107: 21248-21255. doi: 10.1073/pnas.1015855107.
133. Krishnan, S., Chi, E. Y., Webb, J. N., Chang, B. S., Shan, D., Goldenberg, Manning, M. C., Randolph, T. W., Carpenter, J. F. (2002) Aggregation of granulocyte colony stimulating factor under physiological conditions: characterization and thermodynamic inhibition. *Biochemistry* 41: 6422–6431. doi: 10.1021/bi012006m.
134. Kubota, N., Orita, T., Hattori, K., Oh-eda, M., Ochi, N., Yamazaki, T. (1990) Structural characterization of natural and recombinant human

granulocyte colony-stimulating factors. *J Biochem* 107: 486-492. doi: 10.1093/oxfordjournals.jbchem.a123072.

135. Kuwabara, T., Kato, Y., Okumura, S., Kobayashi, S., Yamamoto, M., Ikenaga, T., Deguchi, T. et al. (1991) *Drug Metab Pharmacokinet* 6: 887-897. doi:10.2133/dmpk.6.887.
136. Kuwabara, T., Kobayashi, S., Sugiyama, Y. (1996) Pharmacokinetics and pharmacodynamics of a recombinant human granulocyte colony-stimulating factor. *Drug Metab Rev* 28: 625-658. doi: 10.3109/03602539608994020.
137. Laemmli, U. K. (1970) Cleavage of structural proteins during the assembly of the head of bacteriophage T4. *Nature* 227: 680-685. doi: 10.1038/227680a0.
138. Langley, K. E, Mendiaz, E. A, Liu, N., Narhi, L. O, Zeni, L., Parseghian, C. M., Clogston, C. L. et al. (1994) Properties of variant forms of human stem cell factor recombinantly expressed in *Escherichia coli*. *Arch Biochem Biophys* 311: 55-61. doi: 10.1006/abbi.1994.1208.
139. Langley, K. E., Bennett, L. G., Wypych, J., Yancik, S. A., Liu, X. D., Westcott, K. R., Chang, D. G. et al. (1993) Soluble stem cell factor in human serum. *Blood* 81: 656-660.
140. Langley, K. E.,Wypych, J., Mendiaz, E. A., Clogston, C. L., Parker, V. P., Farrar, D. H., Brothers, M. O. et al. (1992) Purification and characterization of soluble forms of human and rat stem cell factor recombinantly expressed by Eschericia coli and by Chinese hamster ovary cells. *Arch Biochem Biophys* 295: 21-28. doi: 10.1016/0003-9861(92)90482-c.
141. Layton, J. E., Shimanoto, G., Osslund, T., Hammacher, A., Smith, D. K., Treutlein, H. R., Boone, T. (1999) Interaction of granulocyte colony-stimulating factor (G-CSF) with its receptor. Evidence that Glu19 of G-CSF interacts with Arg288 of the receptor. *J Biol Chem* 274: 17445-17451. doi: 10.1074/jbc.274.25.17445.
142. Lee, M. T., Kaushansky, K., Ralph, P., Ladner, M. (1990) Differential expression of M-CSF, G-CSF, and GM-CSF by human monocytes. *J Leukoc Biol* 47: 275-282. doi: 10.1002/jlb.47.3.275.
143. Lefkowitz, D. L., Lefkowitz, S. S. (2001) Macrophage-neutrophil interaction: paradigm for chronic inflammation revisited. *Immunol Cell Biol* 79: 502-506. doi:10.1046/j.14401711.2001.01020.x.
144. Leigh, B. R., Hancock, S. L., Knox. S. J. (1993) The Effect of Stem Cell Factor on Irradiated Human Bone Marrow. *Cancer Res* 53: 3857-3859.

145. Lennartsson, J., Rönnstrand, L. (2012) Stem cell factor receptor/c-Kit: from basic science to clinical implications. *Physiol Rev* 92: 1619-1649. doi: 10.1152/physrev.00046.2011.
146. Leon, J., Reubsaet, E., Beijnen, J. H., van Bennekom, W. P., Bult, A., Hoekstra, A. J., Hop, E. et al. (1999) Reduction of Cys36-Cys42 and Cys64-Cys74 disulfide bonds in recombinant human granulocyte colony stimulating factor. *J Pharm Biomed Anal* 19: 837-845. doi: 10.1016/s0731-7085(98)00253-2.
147. Leonard, W. J. (1994) The defective gene in X-linked severe combined immunodeficiency encodes a shared interleukin receptor subunit: implications for cytokine pleiotropy and redundancy. *Curr Opin Immunol* 6: 631-635. doi: 10.1016/0952-7915(94)90152-x.
148. Lev, S., Yarden, Y., Givol, D. (1992) Dimerization and activation of the Kit receptor by monovalent and bivalent binding of the stem cell factor. *J Biol Chem* 267: 15970-15977.
149. Lieschke, G. J., Grail, D., Hodgson, G., Metcalf, D., Stanley, E., Cheers, C., Fowler, K. J. et al. (1994) Mice lacking granulocyte colony-stimulating factor have chronic neutropenia, granulocyte and macrophage progenitor cell deficiency, and impaired neutrophil mobilization. *Blood* 84: 1737-1746. doi: 10.1182/blood.V84.6.1737.bloodjournal8461737.
150. Lindqvist, D., Wolkowitz, O. M., Mellon, S., Yehuda, R., Flory, J. D., Henn-Haase, C, Bierer, L. M. et al. (2014) Proinflammatory milieu in combat-related PTSD is independent of depression and early life stress. *Brain Behav Immun* 42: 81-88. doi: 10.1016/j.bbi.2014.06.003.
151. Liongue C., Wright C., Russell A. P., Ward A. C. (2009) Granulocyte colony-stimulating factor receptor: stimulating granulopoiesis and much more. *Int J Biochem Cell Biol* 41: 2372-2375. doi: 10.1016/j.biocel.2009.08.011.
152. List, T., Neri, D. (2013) Immunocytokines: a review of molecules in clinical development for cancer therapy. *Clin Pharmacol* 5: 29-45. doi: 10.2147/CPAA.S49231.
153. Liu, C, Chu, D, Kalantar-Zadeh, K., George, J., Young, H. A., Liu, G. (2021) Cytokines: From Clinical Significance to Quantification. *Adv Sci* 8: 1-29. doi: 10.1002/advs.202004433.
154. Liu, F., Wu, H. Y., Wesselschmidt, R., Kornaga, T., Link, D. C. (1996) Impaired production and increased apoptosis of neutrophils in granulocytecolony-stimulating factor receptor-deficient mice. *Immunity* 5: 491-501. doi : 10.1016/s1074-7613(00)80504-x.

155. Lord, B. I., Bronchud, M. H., Owens, S., Chang, J., Howell, A., Souza, L., Dexter, T. M. (1989) The kinetics of human granulopoiesis following treatment with granulocyte colony-stimulating factor. *Proc Natl Acad Sci U S A* 86: 9499-9503. doi: 10.1073/pnas.86.23.9499.
156. Lu, H. S, Jones, M. D, Shieh, J. H, Mendiaz, E. A, Feng, D., Watler, P., Narhi, L. O, Langley, K. E. (1996) Isolation and characterization of a disulfide-linked human stem cell factor dimer. *J Biol Chem* 271: 11309-11316. doi: 10.1074/jbc.271.19.11309.
157. Lu, H. S., Clogston, C. L., Wypych, J., Parker, V. P., Lee, T. D., Swiderek, K., R F Baltera, R. F. Jr et al. (1992) Post-translational processing of membrane-associated recombinant human stem cell factor expressed in Chinese hamster ovary cells. *Arch Biochem Biophys* 298: 150-158. doi: 10.1016/0003-9861(92)90106-7.
158. Lu, H. S., Boone, T. C., Souza, L. M., Lai, P. H. (1989) Disulfide and secondary structures of recombinant human granulocyte colony stimulating factor. *Arch Biochem Biophys* 268: 81-92. doi: 10.1016/0003-9861(89)90567-5.
159. Lu, H. S., Clogston, C. L., Narhi, L. O, Merewether, L. A., Pearl, W. R., Boone, T. C. (1992) Folding and oxidation of recombinant human granulocyte colony stimulating factor produced in *Escherichia coli*. Characterization of the disulfide-reduced intermediates and cysteine----serine analogs. *J Biol Chem* 267: 8770-8777.
160. Mahadevan, J., Sundaresh, A., Rajkumar, R. P., Muthuramalingam, A., Menon, V., Negi, V. S., Sridhard, M. G. (2017) An exploratory study of immune markers in acute and transient psychosis. *Asian Journal of Psychiatry* 25: 219-223. doi: 10.1016/j.ajp.2016.11.010.
161. Mahlert, F., Schmidt, K., Allgaier, H., Liu, P., Müller, U., Shen, W. D. (2013) Rational development of lipegfilgrastim, a novel long-acting granulocyte colony-stimulating factor, using glycopegylation technology. *Blood* 122: 4853-4853. doi: 10.1182/blood.V122.21.4853.4853.
162. Mansuroglu, T., Ramadori, P., Dudas, J., Malik, I., Hammerich, K., Fuzesi, L., Ramadori, G. (2009) Expression of stem cell factor and its receptor c-kit during the development of intrahepatic cholangiocarcinoma. *Lab Invest* 89: 562-574. doi: 10.1038/labinvest.2009.15.
163. Martin, F. H., Suggs, S. V., Langley, K. E., Lu, H. S., Ting, J.,Okino, K. H., Morris, C. et al. (1990) Primary structure and functional expression of rat and human stem cell factor DNAs. *Cell* 63: 203-211. doi: 10.1016/0092-8674(90)90301-t.

164. Martin-Christin (2001) Granulocyte colony stimulating factors: how different are they? How to make a decision? *Anticancer Drugs* 12: 185-191. doi: 10.1097/00001813-200103000-00002.
165. Martin-Moe, S., Osslund, T. Wang J. Mahmood, T., Deshpande, R. Hershenson, S. (2010) The structure of biological therapeutics, p. 3-40. In: Jameel, F., Hershenson, S. (ed.) Formulation and Process Development Strategies for Manufacturing Biopharmaceuticals. John Wiley & Son, Inc. Hoboken, New Jersey.
166. Maruyama, K., Tsuji, K., Tanaka, R., Yamada, K., R., Kodera, Y., Nakahata, T. (1998) Characterization of peripheral blood progenitor cells mobilized by nartograstim (N-terminal replaced granulocyte colony-stimulating factor) in normal volunteers. *Bone Marrow Transplant* 22: 313-320. doi: 10.1038/sj.bmt.1701333.
167. Massague, J. (2008) TGFbeta in Cancer. *Cell* 134: 215-230. doi: 10.1016/j.cell.2008.07.001.
168. Matsuda, S., Shirafuji, N., Asano, S. (1989). Human granulocyte colony-stimulating factor specifically binds to murine myeloblastics NFS-60 cells and activates their guanosine triphosphate binding proteins/adenylate cyclase system. *Blood* 74: 343-348.
169. Matsuda, T., Takahashi-Tezuka, M., Fukada, T., Okuyama, Y., Fujitani, Y., Tsukada, S. Mano, H. et al. (1995) Association and activation of Btk and Tec tyrosine kinases by gp130, a signal transducer of the interleukin-6 family of cytokines. Blood 85: 627-633.
170. Mayrhofer, G., Gadd, S. J., Spargo, L. D., Ashman, L. K. (1987) Specificity of a mouse monoclonal antibody raised against acute myeloid leukaemia cells for mast cells in human mucosaland connective tissues. *Immunol Cell Biol* 65: 241-250. doi: 10.1038/icb.1987.27.
171. McInnes, I. B., Schett, G. (2007) Cytokines in the pathogenesis of rheumatoid arthritis. *Nat Rev Immunol* 7: 429-442. doi: 10.1038/nri2094.
172. McNiece, I. K., Briddell, R. A. (1995) Stem cell factor. *J Leukoc Biol* 58: 14-22. doi: 10.1002/jlb.58.1.14.
173. McNiece, I. K., Langley, K. E., Zsebo, K. M. (1991) Recombinant human stem cell factor synergises with GM-CSF, G-CSF, IL-3 and epo to stimulate human progenitor cells of the myeloid and erythroid lineages. *Exp Hematol* 19: 226-231.
174. Mendoza, J. A., Campo, G. D. (1996) Ligand-induced conformational changes of GroEl are dependent on the bound substrate polipeptide. *J Biol Chem* 271: 16344-16349. doi: 10.1074/jbc.271.27.16344.

175. Metcalf, D. (2013) The colony-stimulating factors and cancer. *Cancer Immunol Res* 1: 351-356. doi: 10.1158/2326-6066.CIR-13-0151.
176. Metzner, H. J., Pipe, S. W., Weimer, T., Schulte, S. (2013) Extending the pharmacokinetic half-life of coagulation factors by fusion to recombinant albumin. *Thromb Haemost* 110: 931-939. doi: 10.1160/TH13-03-0213.
177. Mickiene, G., Dalgediene, I., Zvirblis, G., Dapkunas, Z., Plikusiene, I., Buzavaite-Verteliene, E., Balevicius, Z., Ruksenaite, A., Pleckaityte, M. (2020) Human granulocyte-colony stimulating factor (G-CSF)/stem cell factor (SCF) fusion proteins: design, characterization and activity. *PeerJ* 8: 1-23. doi: 10.7717/peerj.9788.
178. Mishra, P., Nayak, B., Dey, R. K. (2016) PEGylation in anti-cancer therapy: An overview. *Asian J Pharm Sci* 11: 337-348. doi: 10.1016/j.ajps.2015.08.011.
179. Miyazawa, K., Williams, D. A., Gotoh, A., Nishimaki, J., Broxmeyer, H. E, Toyama, K. (1995) Membrane-bound Steel factor induces more persistent tyrosine kinase activation and longer life span of c-kit gene-encoded protein than its soluble form. *Blood* 85: 641-649. doi:10.1182/blood.V85.3.641.bloodjournal853641.
180. Moiton, M. P., Richez, C., Dumoulin, C., Mehsen, N., Dehais, J., Schaeverbeke, T. (2006) Role of anti-tumour necrosis factor-alpha therapeutic agents in the emergence of infections. *Clin Microbiol Infect* 12: 1151-1153. doi: 10.1111/j.1469-0691.2006.01546.x.
181. Molineux, G. (2004) The design and development of pegfilgrastim (PEG rmetHuG-CSF, Neulasta). *Curr Pharm Des* 10: 1235-1244. doi: 10.2174/1381612043452613.
182. Molineux, G. (2009) Pegfilgrastim-designing an improved form of rmetHu-GCSF, p. 169-185. In F. M. Veronese (ed.), Pegylated protein drugs: Basic science and clinical applications, Basel: Birkhauser.
183. Molineux, G., Migdalska, A., Szmitkowski, M., Zsebo, K., T.M. Dexter, T. M. (1991) The effects on hematopoiesis of recombinant stem cell factor (ligand for c-kit) administered in vivo to mice either alone or in combination with granulocyte colony-stimulating factor. *Blood* 78: 961-966.
184. Monastero, R. N., Pentyala, S. (2017) Cytokines as biomarkers and their respective clinical cutoff levels. *Int J Inflam* 2017: 1-11. doi: 10.1155/2017/4309485.
185. Monsmann, T. (1983) Rapid colorimetric assay for cellular growth and survival: Application to proliferation and cytotoxicity assays. *J Immunol Methods* 65: 55-63. doi: 10.1016/0022-1759(83)90303-4.

186. Motro, B., Wojtowicz, J. M., Bernstein, A., van der Kooy, D. (1996) Steel mutant mice are deficient in hippocampal learning but not long-term potentiation. *Proc Natl Acad Sci U S A* 93: 1808-1813. doi: 10.1073/pnas.93.5.1808.
187. Mousa, A., Bakhiet, M. (2013) Role of cytokine signaling during nervous system development. *Int J Mol Sci* 14: 13931-13957. doi: 10.3390/ijms140713931.
188. Musto, P., Guariglia, R., Martorelli, M. C., Lerose, R., Telesca, D., Milella, M. R. (2016) Lipegfilgrastim in the management of chemotherapy-induced neutropenia of cancer patients. *Biologics* 10: 1-8. doi: 10.2147/BTT.S58597.
189. Nagata, S., Tsuchiya, M., Asano, S., Kaziro Y., Yamazaki, T., Yamamoto, O., Hirata, Y. et al. (1986) Molecular Cloning and Expression of cDNA for Human Granulocyte Colony-Stimulating Factor. *Nature* 319: 415-418. doi: 10.1038/319415a0.
190. Nagata, S., Tsuchiya, M., Asano, S., Yamamoto, O., Hirata, Y., Kubota, N., Oheda, M. et al. (1986) The chromosomal gene structure and two mRNAs for human granulocyte colony-stimulating factor. *EMBO J* 5: 575-581.
191. Naito T., Goto K., Morioka S., Matsuba, Y., Akema, T., Sugiura, T., Ohira, Y. et al. (2009) Administration of granulocyte colony-stimulating factor facilitates the regenerative process of injured mice skeletal muscle via the activation of Akt/GSK3αβ signals. *Eur J Appl Physiol* 105: 643-651. doi: 10.1007/s00421-008-0946-9.
192. Ng, A., Tam, W. W., Zhang, M. W., Ho, C. S., Husain, S. F., McIntyre, R. S., Ho, R. C. (2018) IL-1β, IL-6, TNF- α and CRP in Elderly Patients with Depression or Alzheimer's disease: Systematic Review and Meta-Analysis. *Sci Rep* 8: 1-12. 10.1038/s41598-018-30487-6.
193. Nguyen-Jackon, H. T., Zhang, H., Watowich, S. S. (2012) G-CSF Receptor Structure, Function, and Intracellular Signal Transduction, p. 83-108. In Molineux, G., Foote, M., Arvedson, T. (ed.) Twenty years of G-CSF: Clinical and Nonclinical Discoveries, vol. 1. Springer, Basel.
194. Nicholson, S. E., Novak, U., Ziegler, S. F., Layton, J. E. (1995) Distinct regions of the granulocyte colony stimulating factor receptor are required for tyrosine phosphorylation of the signaling molecules JAK2, Stat3, and p42, p44MAPK. *Blood* 86: 3698-3704.
195. Nicholson, S. E., Oates, A. C., Harpur, A. G., Ziemiecki,. A., Wilks, A. F., Layton, J. E. (1994) Tyrosine kinase JAK1 is associated with the granulocyte-colony-stimulating factor receptor and both become

tyrosine-phosphorylated after receptor activation. *Proc Natl Acad Sci U S A* 91: 2985-2988. doi:10.1073/pnas.91.8.2985.

196. Nicola, N. A, Metcalf, D. (1985) Binding of 125I-labeled granulocytecolony-stimulating factor to normal murine hemopoietic cells. *J Cell Physiol* 124: 313-321. doi: 10.1002/jcp.1041240222.
197. Nocka, K., Majumder, S., Chabot, B., Ray, P., Cervone, M., Bernstein, A., Besmer, P. (1989) Expression of c-kitgene products in known cellular targets of W mutations innormal and W mutant mice – evidence for an impaired c-kitkinase in mutant mice. *Genes Dev* 3: 816-826. doi: 10.1101/gad.3.6.816.
198. Oganesyan, L. P., Mkrtchyan, G. M., Sukiasyan, S. H., A S Boyajyan, A. S. (2009) Classic and alternative complement cascades in post-traumatic stress disorder. *Bull Exp Biol Med* 148: 859-861. doi: 10.1007/s10517-010-0836-0.
199. Oheda, M., Hase, S., Ono, M., Ikenaka, T. (1988) Structures of the sugar chains of recombinant human granulocyte-colony-stimulating factor produced by Chinese hamster ovary cells. *J Biochem* 103: 544-546. doi: 10.1093/oxfordjournals.jbchem.a122305.
200. Ohta, H., Wada, H., Niwa, T., Kirri, H., Iwamoto, N., Fujii, H., Saito, K., Sekikawa, K., Seishima, M. (2005) Disruption of tumor necrosis factor-alpha gene diminishes the development of atherosclerosis in ApoE-deficient mice. *Atherosclerosis* 180: 11-17. doi: 10.1016/j.atherosclerosis.2004.11.016.
201. Okabe, M., Asano, M., Kuga, T., Komatsu, Y., Yamasaki, M., Yokoo, Y., Itoh, S. et al. (1990) *In vitro* and *in vivo* hematopoietic effect of mutant human granulocyte colony-stimulating factor. *Blood* 75: 1788-1793.
202. O'Shea, J. J., Gadina, M., Siegel, R. M. (2019), Cytokines and Cytokine Receptors, p. 127-155. In: Rich, R. R., Shearer, W. T., Frew, A. J., Fleisher, T. A., Schroeder, H. W., Weyand, C. M. (ed.) Clinical Immunlogy: Principles and Practice, vol. 5. Elsevier.
203. Pasut, G. (2014) Pegylation of biological molecules and potential benefits: pharmacological properties of certolizumab pegol. *BioDrugs* Suppl 1: S15-S23. doi: 10.1007/s40259-013-0064-z.
204. Paul, W. E. (1989) Pleiotropy and redundancy: T cell-derived lymphokines in the immune response. *Cell* 57: 521-524. doi: 10.1016/0092-8674(89)90121-9.
205. Pires, I. S., Hammond, P. T., Irvine, D. J. (2021) Engineering Strategies for Immunomodulatory Cytokine Therapies – Challenges and Clinical Progress. *Adv Ther (Weinh)* 4: 1-29. doi: 10.1002/adtp.202100035.

206. Pixley, F., Stanley, E. R. (2003) Cytokines and Cytokine Receptors Regulating Cell Survival, Proliferation, and Differentiation in Hematopoiesis, p. 615-623. In: Bradshaw, R. A., Dennis, E. (ed.), Handbook of Cell Signalling, vol. 2. Academic Press.
207. Plikusiene, I., Balevicius, Z., Ramanaviciene, A., Talbot, J., Mickiene, G., Balevicius, S., Stirke, A., Tereshchenko, A., Tamosaitis, L., Zvirblis, G., Ramanavicius, A. (2020) Evaluation of affinity sensor response kinetics towards dimeric ligands linked with spacers of different rigidity: Immobilized recombinant granulocyte colony-stimulating factor based synthetic receptor binding with genetically engineered dimeric analyte derivatives. *Biosens Bioelectron* 156: 1-8. doi: 10.1016/j.bios.2020.112112.
208. Price, T. H., Chatta, G. S., Dale, D. C. (1996) Effect of recombinant granulocyte colony-stimulating factor on neutrophil kinetics in normal young and elderly humans. *Blood* 88: 335-340.
209. Rapaport, M. H., Torrey, E. F., McAllister, C. G., Nelson, D. L., Pickar, Paul, S. M. (1993) Increased serum soluble interleukin-2 receptors in schizophrenic monozygotic twins. *Eur Arch Psychiatry Clin Neurosci* 243: 7-10. doi: 10.1007/BF02191517.
210. Rasky, A., Habiel, D. M., Morris, S., Schaller, M., Moore, B. B., Phan, S., Kunkel, S. L. et al. (2020) Inhibition of the stem cell factor 248 isoform attenuates the development of pulmonary remodeling disease. *Am J Physiol Lung Cell Mol Physiol* 318: L200-L211. doi: 10.1152/ajplung.00114.2019.
211. Ratti, M., Tomasello, G. (2015) Lipegfilgrastim for the prophylaxis and treatment of chemotherapy-induced neutropenia. *Expert Rev Clin Pharmacol* 8: 15-24. doi: 10.1586/17512433.2015.984688.
212. Rausch, O., Marshall, C. J. (1997) Tyrosine 763 of the murine granulocyte colony-stimulating factor receptor mediates Ras-dependent activation of the JNK/SAPK mitogen-activated protein kinase pathway. *Mol Cell Biol* 17:1170-1179. doi: 10.1128/MCB.17.3.1170.
213. Restelli, U., Croce, D., Bonizzoni, E., Marzanatti, M., Andreini, A., Sorio, M., Tecchio, C. et al. (2020) Monocentric Analysis of the Effectiveness and Financial Consequences of the Use of Lenograstimversus Filgrastim for Mobilization of Peripheral Blood Progenitor Cells in Patients with Lymphoma and Myeloma Receiving Chemotherapy and Autologous Stem Cell Transplantation. *J Blood Med* 11: 123-130. doi: 10.2147/JBM.S224173.

214. Rider, P., Carmi, Y., Cohen, I. (2016) Biologics for Targeting Inflammatory Cytokines, Clinical Uses, and Limitations. *Int J Cell Biol* 2016: 1-11. doi: 10.1155/2016/9259646.
215. Rogers, B., Dong, D., Li, Z., Li, Z. (2015) Recombinant Human Serum Albumin Fusion Proteins and Novel Applications in Drug Delivery and Therapy. *Curr Pharm Des* 21: 189-1907. doi: 10.2174/1381612821666150302120047.
216. Rönnstrand, L. (2004) Signal transduction via the stem cell factor receptor/c-Kit. *Cell Mol Life Sci* 61: 2535-2548. doi: 10.1007/s00018-004-4189-6.
217. Ropers, H. H., Craig, I. W. (1989) Report of the committee on the genetic constitution of chromosomes 12 and 13. *Cytogenet Cell Genet* 51: 259-279. doi: 10.1159/000132794.
218. Roskos, L. K., Lum, P., Lockbaum, P., Schwab, G., Yang, B. B. (2006) Pharmacokinetic/ Pharmacodynamic Modeling of Pegfilgrastim in Healthy Subjects. *J Clin Pharmacol* 46: 747-757. doi: 10.1177/0091270006288731.
219. Roskos, L., Cheung, E., Vincent, M. (1998) Pharmacokinetics and pharmacodynamics of a recombinant human granulocyte colony-stimulating factor, p. 51-71. In: Morstyn, G., Dexter, M. (ed), Filgrastim (r-metHuG-CSF) in Clinical Practice, ed 2. New York, Marcel Dekker.
220. Roskoski, R. Jr. (2005) Structure and regulation of Kit protein-tyrosine kinase--the stem cell factor receptor. *Biochem Biophys Res Commun* 338: 1307-1315. doi: 10.1016/j.bbrc.2005.09.150.
221. Rozwarski, D. A., Gronenborn, A. M., Clore, G. M., Bazan, J. F., Bohm, A., Wlodawer, A., Hatada, M. et al. (1994) Structural comparisons among the short-chain helical cytokines. *Structure* 2: 159-173. doi: 10.1016/s0969-2126(00)00018-6.
222. Sanz, A. B., Sanchez-Niño, M., Ortiz, A. (2011) TWEAK, a multifunctional cytokine in kidney injury. *Kidney Int* 80: 708-718. doi: 10.1038/ki.2011.180.
223. Schäbitz, W. R., Kollmar, R., Schwaninger, M., Juettler, E., Bardutzky, J., Schölzke, M. N., Sommer, S., Schwab, S. (2003) Neuroprotective effect of granulocyte colony-stimulating factor after focal cerebral ischemia. *Stroke* 34: 745-751. doi: 10.1161/01.STR.0000057814.70180.17.
224. Scheckermann, C., Schmidt, K., Abdolzade-Bavil, A., Allgaier, H., Mueller, U. W., Liu, W. D. S. P. (2013) Lipegfilgrastim: a long-acting, once-per-cycle, glycopegylated recombinant human filgrastim. *J Clin Oncol* 31: e13548-e13548. doi: 10.1200/jco.2013.31.15_suppl.e13548.

225. Schenk, T., Irth, H., Marko-Varga, G., Edholm, L. E., Tjaden, U. R., van der Greef, J. (2001) Potential of on-line micro-LC immunochemical detection in the bioanalysis of cytokines. *J Pharm Biomed Anal* 26: 975-985. doi: 10.1016/s0731-7085(01)00464-2.
226. Schmidt, S. R. (2009) Fusion-proteins as biopharmaceuticals--applications and challenges. *Curr Opin Drug Discov Devel* 12: 284-295.
227. Schuening, F. G., Appelbaum, F. R., Deeg, H. J., Sullivan-Pepe, M., Graham, T., C, Hackman, R., Zsebo. K. M., Storb, R. (1993) Effects of recombinant canine stem cellfactor, a c-kit ligand, and recombinant granulocyte colony-stimulating factor onhematopoietic recovery after otherwise lethal total body irradiation. *Blood* 81: 20-26.
228. Shannon, M. F., Pell, L.M., Lenardo, M. J., Kuczek, E. S., Occhiodoro, F. S., Dunn, S. M.,Vadas, M. A. (1990) A novel tumor necrosis factor-responsive transcription factor which recognizes a regulatory element in hemopoietic growth factor genes. *Mol Cell Biol* 10: 2950-2959. doi: 10.1128/mcb.10.6.2950.
229. Shojaei, F., Wu, X., Qu, X., Kowanetz, M., Yu, L., Tan, M., Meng, Y. G., Ferrara, N. (2009) G-CSF-initiated myeloid cell mobilization and angiogenesis mediate tumor refractoriness to anti-VEGF therapy in mouse models. *Proc Natl Acad Sci U S A* 106: 6742-6747. doi: 10.1073/pnas.0902280106.
230. Shpall, E. J., Wheeler, C.A., Turner, S. A,, Yanovich, S., Brown, R. A., Pecora, A. L., Shea, T. C. et al. (1999) A randomized phase 3 study of peripheral blood progenitor cell mobilization with stem cell factor and filgrastim in high-risk breast cancer patients. *Blood* 93: 2491- 2501.
231. Shyu, W. C., Lin, S. Z., Yang, H. I., Tzeng, Y. S, Pang, C. Y., Yen, P. S., Li, H. (2004) Functional recovery of stroke rats induced by granulocyte colony-stimulating factor-stimulated stem cells. *Circulation* 110: 1847-1854. doi: 10.1161/01.CIR.0000142616.07367.66.
232. Silva, C. A., Reber, L., Frossard, N. (2006) Stem cell factor expression, mast cells and inflammation in asthma. *Fundam Clin Pharmacol* 20: 21-39. doi: 10.1111/j.1472-8206.2005.00390.x.
233. Souza, L. M., Boone, T. C., Gabrilove, J., Lai, P. H., Zsebo, K. M., Murdock, D. C, Chazin, V. R. et al. (1986) Recombinant human granulocyte colony-stimulating factor: effects on normal and leukemic myeloid cells. *Science* 232: 61-65. doi: 10.1126/science.2420009.

234. Sprague, A. H., Khalil, R. A. (2009) Inflammatory cytokines in vascular dysfunction and vascular disease. *Biochem Pharmacol* 78: 539-552. doi: 10.1016/j.bcp.2009.04.029.
235. Stenken, J. A., Poschenrieder, A. J. (2015) Bioanalytical chemistry of cytokines – a review. *Anal Chim Acta* 853: 95-115. doi: 10.1016/j.aca.2014.10.009.
236. Stramaglia, M. J., Nampallim S. S., Donahue-Hjelle, L., Madigan, L. E. (2009) Strategies for Sourcing Animal-Origin Free Cell Culture Media Components. *Biopharm International*.
237. Strohl, W. R. (2015) Fusion Proteins for Half-Life Extension of Biologics as a Strategy to Make Biobetters. *BioDrugs* 29: 215-239. doi: 10.1007/s40259-015-0133-6.
238. Su, Y., Cui, L., Piao, C., Li, B., Zhao, L. R. (2013) The effects of hematopoietic growth factors on neurite outgrowth. *PLoS One* 8:e75562. doi: 10.1371/journal.pone.0075562. eCollection 2013.
239. Sui, X., Krantz, S. B., Zhao, Z. J. (2000) Stem cell factor and erythropoietin inhibit apoptosis of human erythroid progenitor cells through different signalling pathways. *Br J Haematol* 110: 63-70. doi: 10.1046/j.1365-2141.2000.02145.x.
240. Suzuki, T., Tohda, S., Nagata, K., Imai, Y., Murohashi, I., Nara, N. (1992) Enhanced effect of mutant granulocyte-colony-stimulating factor (KW-2228) on the growth of normal and leukemic hemopoietic progenitor cells in comparison with recombinant human granulocyte-colony-stimulating factor (GCSF). *Acta Haematol* 87: 181-189. doi: 10.1159/000204756.
241. Swierczewska, M., Lee, K. C., Lee, S. (2015) What is the future of PEGylated therapies? *Expert Opin Emerg Drugs* 20: 531-536. doi: 10.1517/14728214.2015.1113254.
242. Tabibzadeh, S., Babaknia, A. (1995) The signals and molecular pathways involved in implantation, a symbiotic interaction between blastocyst and endometrium involving adhesion and tissue invasion. *Hum reprod* 10: 1579-602. doi: 10.1093/humrep/10.6.1579.
243. Tamada, T., Honjo, E., Maeda, Y., Okamoto, T., Ishibashi, M., Tokunaga, M., Kuroki, R. (2006) Homodimeric cross-over structure of the human granulocyte colony-stimulating factor (GCSF) receptor signaling complex. *Proc Natl Acad Sci U S A* 103: 3135-3140. doi: 10.1073/pnas.0511264103.
244. Tanaka, H., Tanaka, Y., Shinagawa, K., Yamagishi, Y., , Ohtaki, K., Asano, K. (1997) Three types of recombinant human granulocyte

colony-stimulating factor have equivalent biological activities in monkeys. *Cytokine* 9: 360-369. doi: 10.1006/cyto.1996.0177.

245. Tang, Y., Liu, J., Zhang, D., Xu, Z, Ji, J., Wen, C. (2020) Cytokine Storm in COVID-19: The Current Evidence and Treatment Strategies. *Front Immunol* 11: 1-13. doi:10.3389/fimmu.2020.01708.
246. Taniuchi, H., Acharya, A. S., Andria, G., Parker, D. S. (1977) On the mechanism of renaturation of proteins containing disulfide bonds. *Adv Exp Med Biol* 86A: 51-65. doi: 10.1007/978-1-4684-3282-4_4.
247. Tansey, M. G., Wyss-Coray, T. (2008) Cytokines in CNS inflammation and disease, p. 59-106. In: Lane, T. E., Carson, M. Bergmann, C., Wyss-Coray, T. (ed) Central nervous system diseases anfd inflammation. Springer, New York.
248. Toghraie, F. S., Yazdanpanah-Samani, M., Maymand, E. M.,Hosseini, A., Asgari, A., Ramezani, A., Ghaderi, A. (2019) Molecular Cloning, Expression and Purification of G-CSF Isoform D, an Alternative Splice Variant of Human G-CSF. *Iran J Allergy Asthma Immunol* 18: 419-426. doi: 10.18502/ijaai.v18i4.1420.
249. Toth, Z. E., Leker, R. R., Shahar, T., Pastorino, S., Szalayova, I., Asemenew, B., Key, S. et al. (2008) The combination of granulocyte colony-stimulating factor and stem cell factor significantly increases the number of bone marrow-derived endothelial cells in brains of mice following cerebral ischemia. *Blood* 111: 5544-5552. doi: 10.1182/blood-2007-10-119073.
250. Touw, I. P, van de Geijn, G. M. (2007) Granulocyte colony stimulating factor and its receptor in normal myeloid cell development, leukemia and related blood cell disorders. *Front Biosci* 12: 800-815. doi: 10.2741/2103.
251. Tsuchiya, M., Kaziro, Y., Nagata, S. (1987) The chromosomal gene structure for murine granulocyte colony-stimulating factor. *Eur J Biochem* 165: 7-12. doi: 10.1111/j.1432-1033.1987.tb11187.x.
252. Ulich, T. R., del Castillo, J., McNiece, I. K., Yi, E. S., Alzona, C. P., Yin, S. M., Zsebo, K. M. (1991) Stem cell factor in combination with granulocyte colony-stimulating factor (CSF) or granulocyte-macrophage CSF synergistically increases granulopoiesis *in vivo*. *Blood* 78: 1954-1962.
253. Umezawa, H. (1979) Studies on aminoglycoside antibiotics: enzymic mechanism of resistance and genetics. *Jpn J Antibiot* 32: Suppl: S1-14.
254. Usuki, K., Iki, S., Arai, S., Iijima, K., Takaku, F., Urabe, A. (2006) Stable response after administration of stem cell factor combined with

granulocyte colony-stimulating factor in aplastic anemia. *Int J Hematol* 83: 404-407. doi: 10.1532/ijh97.05098.

255. Van der Meer, J. W. M., Popa, C., Netea, M. G. (2005) Side Effects of Anticytokine Strategies. *Neth J Med* 63: 78-80.
256. Vazquez-Lombardi, R., Roome, B., Christ, D. (2013) Molecular Engineering of Therapeutic Cytokines. *Antibodies* 2: 426-451. doi: 10.3390/antib2030426.
257. Waight, J. D., Hu, Q., Miller, A., Liu, S., Abrams, S. I. (2011) Tumor-derived G-CSF facilitates neoplastic growth through a granulocytic myeloid-derived suppressor cell-dependent mechanism. *PLoS ONE* 6: e27690. doi: 10.1371/journal.pone.0027690.
258. Waladkhani, A. R. (2004) Pegfilgrastim: a recent advance in the prophylaxis of chemotherapy-induced neutropenia. *Eur J Cancer Care* 13: 371-379. doi: 10.1111/j.1365-2354.2004.00503.x.
259. Walsh, G. (2014) Biopharmaceutical benchmarks 2014. *Nat Biotechnol* 32: 992-1000. doi: 10.1038/nbt.3040.
260. Ward, A. C., Hermans, M. H., Smith, L., van Aesch, Y. M., Schelen, A. M., Antonissen, C., Touw, I. P. (1999) Tyrosine-dependent and -independent mechanisms of STAT3 activation by the human granulocyte colony-stimulating factor (G-CSF) receptor are differentially utilized depending on G-CSF concentration. *Blood* 93: 113-124.
261. Ward, A. C., Monkhouse, J. L., Csar, X. C., Touw, I. P., Bello, P. A. (1998) The Src-like tyrosine kinase Hck is activated by granulocyte colony-stimulating factor (G-CSF) and docks to the activated G-CSF receptor. *Biochem Biophys Res Commun* 251: 117-123. doi: 10.1006/bbrc.1998.9441.
262. Watari, K., Asano, S., Shirafuji, N., Kodo, H., Ozawa, K., Takaku, F., Kamachi, S. (1989) Serum granulocyte colony-stimulating factor levels in healthy volunteers and patients with various disorders as estimated by enzyme immunoassay. *Blood* 73: 117-122.
263. Weaver, A., Chang, J., Wrigley, E., de Wynter, E., Woll, P.J., Lind, M., Jenkins, B. et al. (1998) Randomized comparison of progenitor-cell mobilization using chemotherapy, stem-cell factor, and filgrastim or chemotherapy plus filgrastim alone in patients with ovarian cancer. *J Clin Oncol* 16: 2601-2612. doi: 10.1200/JCO.1998.16.8.2601.
264. Weide, B., Eigentler, T., Catania, C., Ascierto, P. A., Cascinu, S., Becker, J. C., Hauschild, A. et al. (2019) A phase II study of the L19IL2 immunocytokine in combination with dacarbazine in advanced

metastatic melanoma patients. *Cancer Immunol Immunother* 68: 1547-1559. doi: 10.1007/s00262-019-02383-z.

265. Weinstein, Y., Ihle, J. N., Lavu, S., Reddy, E. P. (1986) Truncation of the c-myb gene by a retroviral integration in an interleukin 3-dependent myeloid leukemia cell line. *Proc Natl Acad Sci U S A* 83: 5010-5014. doi: 10.1073/pnas.83.14.5010.
266. Welte, K., Gabrilove, J., Bronchud, M.H., Platzer, E., Morstyn, G. (1996) Filgrastim (r-metHuG-CSF): the first 10 years. *Blood* 88: 1907-1929.
267. Welte, K., Platzer, E., Lu, I.,Gabrilove, J. L., Levi, E., Mertelsmann, R., Moore, M. A. (1985) Purification and biochemical characterization of human pluripotent hematopoietic colony-stimulating factor. *Proc Natl Acad Sci USA* 82: 1526-1530. doi: 10.1073/pnas.82.5.1526.
268. Witteloostuijn, S. B., Pedersen, S. L., Jensen, K. J. (2016) Half-life extension of biopharmaceuticals using chemical methods: Alternatives to PEGylation. *ChemMedChem* 11: 2474-2495. doi: 10.1002/cmdc.201600374.
269. Yamasaki, M., Konishi, N., Yamaguchi, K., Itoh, S., Yokoo, Y. (1998) Purification and characterization of recombinant human granulocyte colony-stimulating factor (rhG-CSF) derivatives: KW-2228 and other derivatives. *Biosci Biotechnol Biochem* 62: 1528-1534. doi: 10.1271/bbb.62.1528.
270. Yarden, Y., Kuang, W. J., Yang-Feng, T., Coussens, L., Munemitsu, S., Dull, T. J., Chen E. et al. (1987) Human proto-oncogene c-kit: a new cell surface receptor tyrosine kinase for an unidentified ligand. *EMBO J* 6: 3341-3351.
271. Yoshikawa, A., Murakami, H., Nagata, S. (1995) Distinct signal transduction through the tyrosine-containing domains of the granulocyte colony-stimulating factor receptor. *EMBO J* 14: 5288-5296.
272. Yuan, Q., Austen, K. F., Friend, D. S., Heidtman, M., Boyce, J. A. (1997) Human peripheral blood eosinophils express a functional c-kitreceptor for stem cell factor that stimulates very late antigen 4 (VLA-4)-mediated cell adhesion to fibronectin and vascularcell adhesion molecule 1 (VCAM-1). *J Exp Med* 186: 313-323. doi: 10.1084/jem.186.2.313.
273. Yuzawa, S., Opatowsky, Y., Zhang, Z., Mandiyan, V., Lax, I., Schlessinger, J. (2007) Structural basis for activation of the receptor tyrosine kinase KIT by stem cell factor. *Cell* 130: 323-334. doi: 10.1016/j.cell.2007.05.055.

274. Zeuner, A., Pedini, F., Signore, M., Testa, U., Pelosi, E., Peschle, C., De Maria, R. (2003) Stem cell factor protects erythroid precursor cells from chemotherapeutic agents via up-regulation of BCL-2 family proteins. *Blood* 102: 87-93. doi: 10.1182/blood-2002-08-2369.
275. Zeuner, A., Signore, M., Martinetti, D., Bartucci, M., Peschle, C.,De Maria, R. (2007) Chemotherapy-induced thrombocytopenia derives from the selective death of megakaryocyte progenitors and can be rescued by stem cell factor. *Cancer Res* 67: 4767-4773. doi: 10.1158/0008-5472.CAN-06-4303.
276. Zhang, C. (2021) Flare-up of cytokines in rheumatoid arthritis and their role in triggering depression: Shared common function and their possible applications in treatment (Review). *Biomed Rep* 14: 1-8. doi: 10.3892/br.2020.1392.
277. Zhang, J. M., An, J. (2007) Cytokines, inflammation, and pain. *Int Anesthesiol Clin* 45: 27-37. doi: 10.1097/AIA.0b013e318034194e.
278. Zhang, M., Yao, Z., Dubois, S., Ju, W.,Müller, J. R., Waldmann, T. A. (2009) Interleukin-15 combined with an anti-CD40 antibody provides enhanced therapeutic efficacy for murine models of colon cancer. *Proc Natl Acad Sci USA* 106: 7513-7518.doi: 10.1073/pnas.0902637106.
279. Zhang, Z., Zhang, R., Joachimiak, A., Schlessinger, J., Kong, X. P. (2000) Crystal structure of human stem cell factor: implication for stem cell factor receptor dimerization and activation. *Proc Natl Acad Sci U S A* 97: 7732-7737. doi: 10.1073/pnas.97.14.7732.
280. Zhao, L. R., Berra, H. H., Duan, W. M., Singhal, S., Mehta, J., Apkarian, A. V., Kessler, J. A. (2007) Beneficial effects of hematopoietic growth factor therapy in chronic ischemic stroke in rats. *Stroke* 38: 2804-2811. doi: 10.1161/STROKEAHA.107.486217.
281. Zhou, X., Fragala, M. S., McElhaney, J. E., Kuchel, G. A. (2010) Conceptual and methodological issues relevant to cytokine and inflammatory marker measurements in clinical research. *Curr Opin Clin Nutr Metab Care* 13: 541-547. doi: 10.1097/mco.0b013e32833cf3bc.
282. Zielinska, J., Bialik, W. (2016) Recent changes on the biopharmaceutical market after the introduction of biosimilar G-CSF products. *Oncol Clin Pract* 12: 144-152. doi: 10.5603/OCP.2016.0006.
283. Ziepert, M., Schmits, R., Trümper, L., Pfreundschuh, M., Loeffler, M. (2008) Prognostic factors for hematotoxicity of chemotherapy in aggressive non-Hodgkin's lymphoma. *Ann Oncol* 19: 752-762. doi: 10.1093/annonc/mdm541.

284. Zink, T., Ross, A., Lueers, K., Cieslar, C., Rudolph, R., Holak T. A. (1994) Structure and Dynamics of the Human Granulocyte Colony-Stimulating Factor Determined by NMR Spectroscopy. Loop Mobility in a Four-Helix-Bundle Protein. *Biochemistry* 33: 8453-8463. doi: 10.1021/bi00194a009.
285. Zou, L., Nock, S. (2020) Immunogenicity assessment of PEGylated proteins, Lonquex, a PEGylated G-CSF case study, p. 125-140. In: Pasut, G., Zalipsky, S. (ed.) Polymer-Protein Conjugates: From PEGylation and Beyond, vol. 1. Cambridge, United Kingdom.
286. Zsebo, K. M, Williams, D. A., Geissler, E. N., Broudy, V. C., Martin, F. H., Atkins, H. L., Hsu, R. Y. et al. (1990) Stem cell factor is encoded at the Sl locus of the mouse and is the ligand for the c-kit tyrosine kinase receptor. *Cell* 63: 213-224. doi: 10.1016/0092-8674(90)90302-u.
287. Zsebo, K. M., Smith, K. A., Hartley, C. A., Greenblatt, M., Cooke, K., Rich,W., McNiece, I. K. (1992) Radioprotection of mice by recombinant rat stem cell factor. *Proc Natl Acad Sci U S A* 89: 9464-9468. doi: 10.1073/pnas.89.20.9464.
288. Zsebo, K. M., Yuschenkoff, V. N., Schiffer, S., Chang, D., McCall, E., Dinarello, C. A., Brown, M. A., Altrock, B., Bagby, G. J. (1988) Vascular endothelial cells and granulopoiesis: interleukin-1 stimulates release of G-CSF and GM-CSF. *Blood* 71: 99-103.
289. Zsebo, K. M., Wypych, J., McNiece, I. K., Lu, H. S., Smith, K. A., Karkare, S. B., Sachdev, R. K. et al. (1990) Identification, purification, and biological characterization of hematopoietic stem cell factor from buffalo rat liver - conditioned medium. *Cell* 63: 195-201. doi: 10.1016/0092-8674(90)90300-4.

SUPPLEMENTARY MATERIAL

File S1: Large scale purification of homodimeric protein GCSF-Lα-GCSF

1. Solubilization. Washed pellets of GCSF-Lα-GCSF were solubilized in urea containing buffer (8 M urea, 1 mM EDTA, 50 mM Tris-HCl, pH 8.0). To reduce the disulfide bonds within the proteins, DTT was added to a final concentration of 1 mM. After centrifugation at 30,000 × g for 25 min at 4°C, the supernatants containing the solubilized IBs were collected.
2. Refolding. Refolding of recombinant proteins was initiated by rapid dilution of the denatured–reduced proteins into buffer (50 mM Tris-HCl, 1 mM EDTA, pH 8.0) that contained GSSG until concentrations of 3 M urea and 0.5 mg/mL protein were reached. The final molar ratio of GSSG to DTT was 6:1. Refolding of GCSF-Lα-GCSF was carried out for 24 h at 4°C with gentle stirring. The solution was then centrifuged for 25 min at 30,000 × g at 4°C.
3. DEAE Sepharose chromatography. The refolded recombinant proteins were loaded onto a DEAE Sepharose FF column that was equilibrated with 50 mM Tris-HCl (pH 8.0) that contained 3 M urea. The column was washed with 10 mM Tris-HCl (pH 8.0), 20 mM NaCl. The proteins were eluted by a two-step elution increasing the concentration of NaCl from 0.02 to 0.08 M and from 0.08 M to 0.45 M, respectively. Fractions containing GCSF-Lα-GCSF were collected and diluted with 20 mM sodium acetate to reach a pH of 5.4 and a conductivity of 4.0 mS/cm.
4. SP Sepharose chromatography. The solution containing GCSF-Lα-GCSF was applied to SP Sepharose FF column, equilibrated with 20 mM sodium acetate (pH 5.4), 20 mM NaCl. The proteins were eluted by a segmented elution increasing the concentration of NaCl from 0.02 to 0.22 M and 0.22 M to 0.50 M, respectively. Fractions containing pure GCSF-Lα-GCSF were collected.
5. Sephadex G-25 chromatography. Target protein was subsequently loaded onto a Sephadex G-25 Medium column that was equilibrated with 10 mM acetic acid/NaOH buffer, pH 4.0.
6. Formulation and storage. Fractions containing GCSF-Lα-GCSF protein were subsequently pooled; D-sorbitol and Tween 80 were added to reach final concentration of 5% and 0.0025%, respectively. The protein solutions were filtered through 0.2 μm Acrodisc Units

with Mustang E membrane (Pall Corporation) for endotoxin removal. The purified protein solutions were stored at 4°C.

File S2: Stress stability study of GCSF-L*α*-GCSF

RP-HPLC analysis. For RP-HPLC, the intact and stressed GCSF-Lα-GCSF samples were analyzed using a C18 reverse-phase column (Zorbax SB-C18, 4.6 x 250 mm, Agilent Technologies, USA). Mobile phases A (0.1% TFA in water) and B (0.1% TFA in acetonitrile) were used for gradient and isocratic elution at a flow rate of 0.9 mL/min, as follows: (1) initial equilibration at 90% A, (2) a 2-min gradient to 50% B, (3) a 5-min gradient to 54% B, (4) a 45-min gradient to 60.8% B, (5) a 15-min gradient to 70% B, (6) a 2.9-min gradient to 81% B, (7) a 3.1-min isocratic elution at 81% B and a final (8) 2-min gradient to 10% B. The temperature of the column was maintained at 30°C and eluted proteins were detected at 215 nm.

SE-HPLC analysis. For SE-HPLC, the intact and stressed GCSF-Lα-GCSF samples were analyzed using TSK-gel G3000 SWXL column (7.8 × 300 mm, 5 μm, Tosoh Bioscience, Japan). The proteins were eluted with an isocratic mobile phase of 50 mM NH_4HCO_3, pH 7.0. The temperature of the columns was maintained at 30°C and eluted proteins were detected at 215 nm.

SDS-PAGE analysis. SDS-PAGE was performed according to the method of Laemmli (Laemmli, 1970). The 4% stacking and 15% separating gels were used. The gels were stained using silver stain kit (Thermo Scientific) according to the manufacturer's protocol.

In vitro biological activity of GCSF-Lα-GCSF. Biological activities of stressed and control GCSF-Lα-GCSF were determined using the G-CSF-dependent mouse G-NFS-60 cell line as described in section 2.2.7.

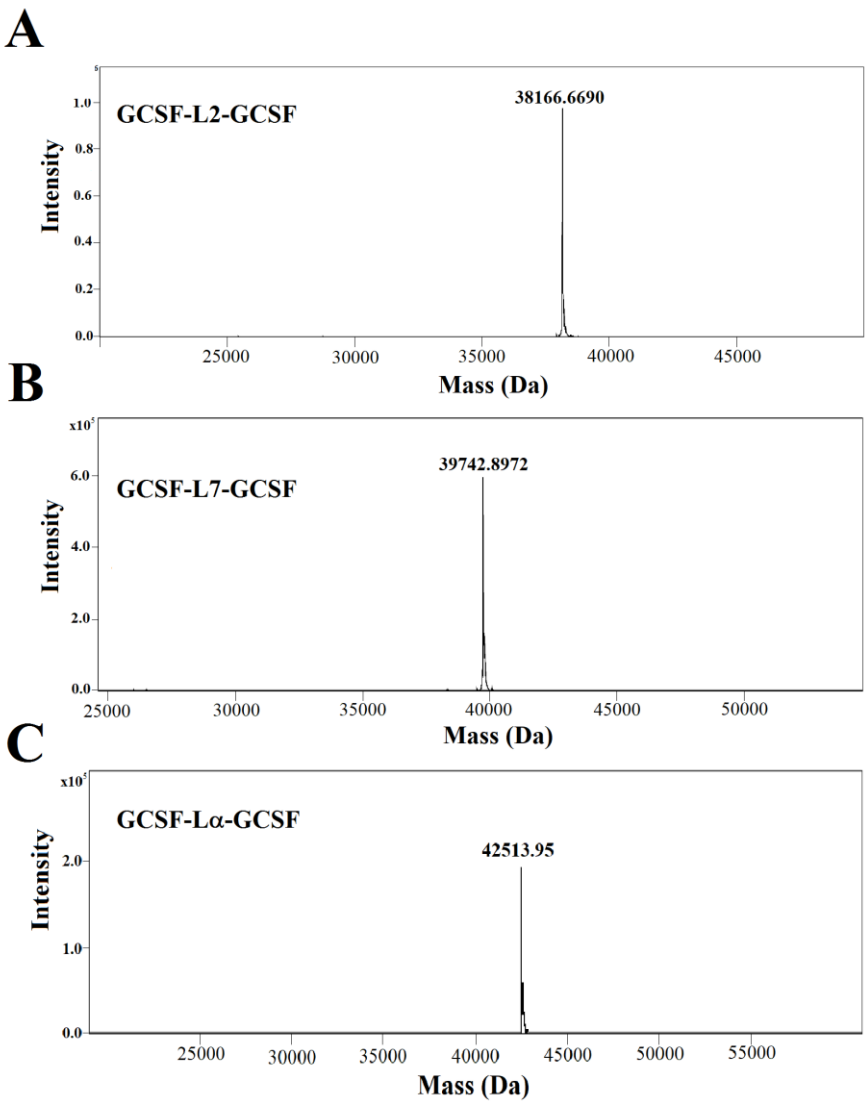

Figure S1. Molecular weight determination of the purified (A) GCSF-L2-GCSF, (B) GCSF-L7-GCSF, (C) GCSF-L*α*-GCSF by mass spectrometry.

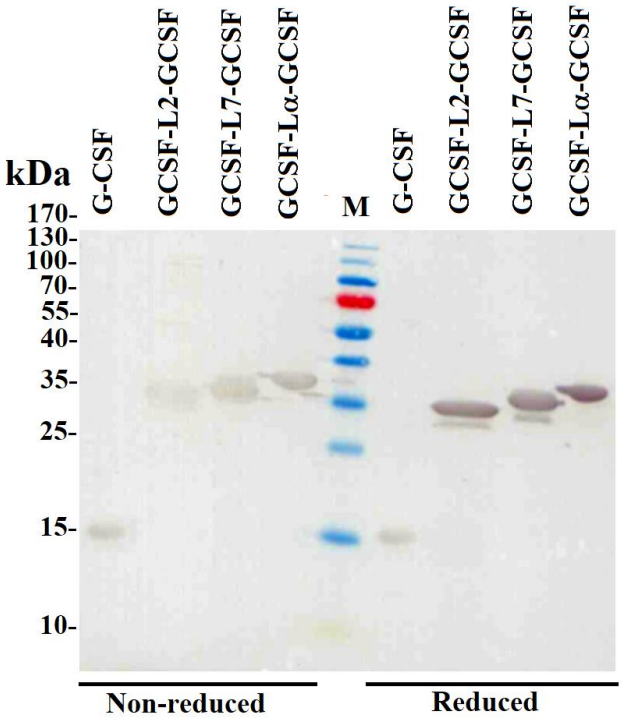

Figure S2. Identification of the purified homodimeric proteins with the monoclonal antibody against G-CSF in Western blot. *M*, molecular weight marker (Thermo Fisher Scientific).

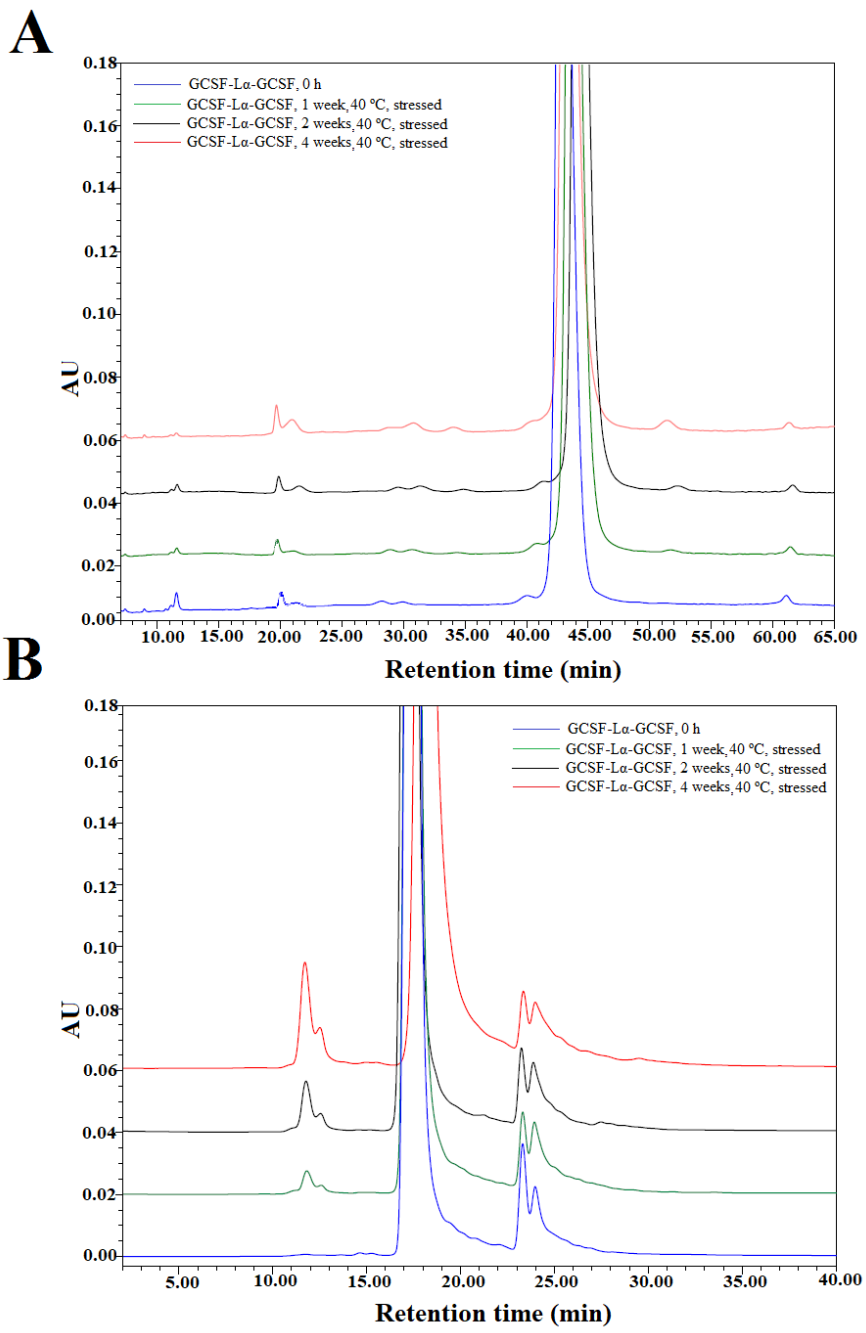

Figure S3. Stability of formulated purified GCSF-Lα-GCSF investigated by (A) RP-HPLC and (B) SE-HPLC under accelerated storage conditions (40 °C for 4 weeks). Formulation: 10 mM acetic acid/NaOH (pH 4.0), containing 5% D-sorbitol, 0.0025% Tween 80. Absorbance at 215 nm is reported as AU.

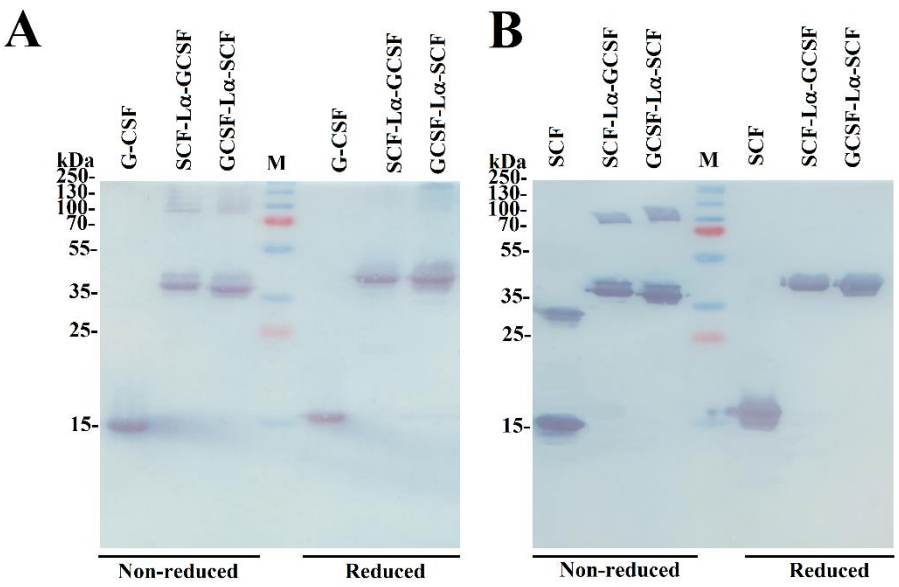

Figure S4. Identification of the purified heterodimeric proteins with the antibodies in Western blot. (A) The Western blot with the monoclonal antibody against G-CSF. **(B)** The Western blot with polyclonal antibodies against SCF. *M*, molecular weight marker (Thermo Fisher Scientific).

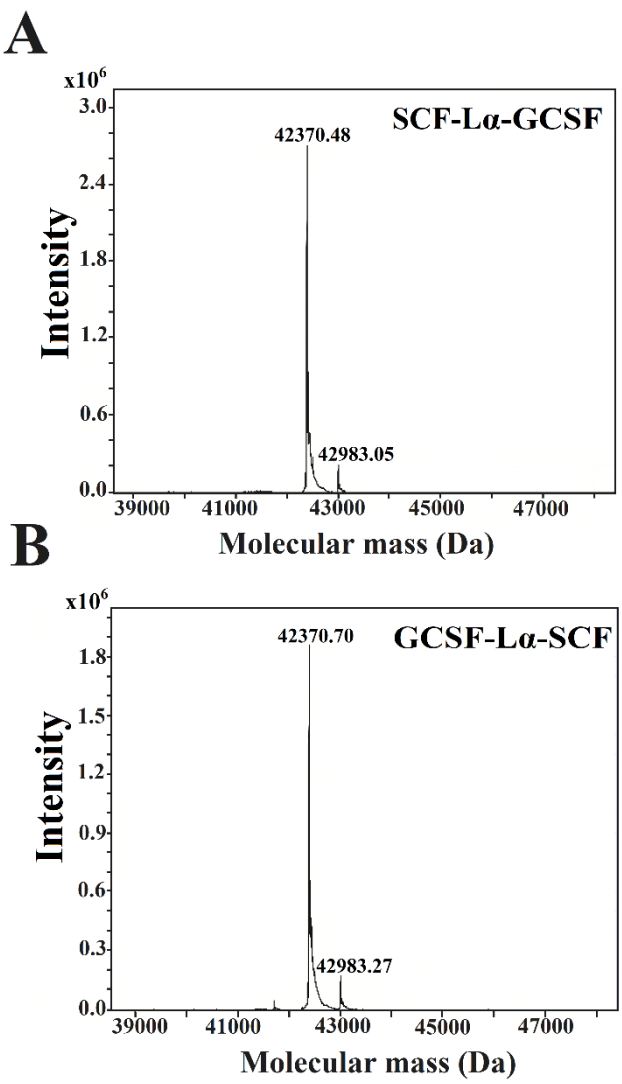

Figure S5. Molecular weight determination of the purified (A) SCF-Lα-GCSF, (B) GCSF-Lα-SCF proteins by mass spectrometry.

NOTES

Vilniaus universiteto leidykla
Saulėtekio al. 9, III rūmai, LT-10222 Vilnius
El. p. info@leidykla.vu.lt, www.leidykla.vu.lt
bookshop.vu.lt, journals.vu.lt
Tiražas 12 egz.